Lev V. Beloussov

Morphomechanics of Development

Springer

Morphomechanics of Development

Lev V. Beloussov

Morphomechanics of Development

With a contribution by Andrei Lipchinsky

Springer

Lev V. Beloussov
Department of Embryology
Moscow State University
Moscow
Russia

ISBN 978-3-319-13989-0 ISBN 978-3-319-13990-6 (eBook)
DOI 10.1007/978-3-319-13990-6

Library of Congress Control Number: 2014957132

Springer Cham Heidelberg New York Dordrecht London

Printed on acid-free paper

Springer International Publishing AG Switzerland is part of Springer Science+Business Media (www.springer.com)

Preface

The aim of this book is to outline the contours of a newly emerging approach to the most complicated and finely regulated successions of events making possible our very existence: the development of organisms. Because of their ubiquity and spontaneity, our primary instinct would be to appreciate these events as given, and simply describe them one after another without asking why they take place at all. On the other hand, since ancient times human beings have not been satisfied by only apprehending any natural events, ranging from movements of celestial bodies to behavior of tiny particles of matter. Instead, people have invented some cognitive approaches, which created the basis for modern civilization, whether for good or evil. Our first aim will be to explore whether any of these approaches can help us to explain the development of organisms. We shall see that in spite of a prolonged history of the science about development (traditionally called embryology, but now named developmental biology) and many important discoveries in this field, this task has still not succeeded. Today, however, due to cooperation between several newly emerged branches of science, some new and unique possibilities allow substantial progress in these directions.

Among the approaches used by natural sciences, we start by outlining the two that have been often regarded as opposites. The first of them is oriented toward searching for components that are kept unchanged (invariant) among events looking quite different from each other. The second, on the opposite, is directed toward outlining reproducible differences between things that are at first glance hardly discernible. The first approach is directed toward formulation of as broad as possible *invariable laws of nature*; this trend dominates in physical sciences since the times of Galileo and Newton. Its unique advantage is the predictive power. It is this approach that provided the tremendous technological progress achieved since then by mankind.

However, not all the sciences followed this path. The second approach, directed toward *classification of events*, emphasizing their specificity and internal differences rather than any common laws that may join them, was long dominant in most of the natural sciences, and remained so in biology. If we are objective, we must admit that practically all the achievements of biology and related applied sciences

(medicine, agriculture, biotechnology) have been reached within the framework of this traditional approach, in the sense of remaining almost unconnected with any general laws. Accordingly, their results continue to be expressed in the form of specific receipts, instructions, drugs, etc. About a century ago, a German philosopher, Windelband defined this approach as ideographic while the law-oriented approach as nomothetic.

The contrast between nomothetic and ideographic approaches becomes most clear when they are applied to more or less prolonged successions of events. For clarifying this, let us use a simple allegory, or better to say, a kind of a caricature (Fig. 1). Frame A illustrates a nomothetic tendency directed toward embracing quite different successions of events by a common law. On the contrary, frame B depicts an old-fashioned postman whose pathway is determined by the addresses of the letters he has to hand. For making this allegory closer to conventional views on the development of organisms, let us assume that by coming to each next address, the postman receives the instructions of where to move further. Under these conditions, each next postman's turn is determined by a specific instruction (which we may call a "cause"). This displays a principle of a so-called uniform determinism which, as related to embryology, will be discussed in the text. Frame C gives an example of a natural periodic process to which a priori any one of the above-mentioned approaches can be applied: it should be a matter of investigation to make a reasonable choice between them.

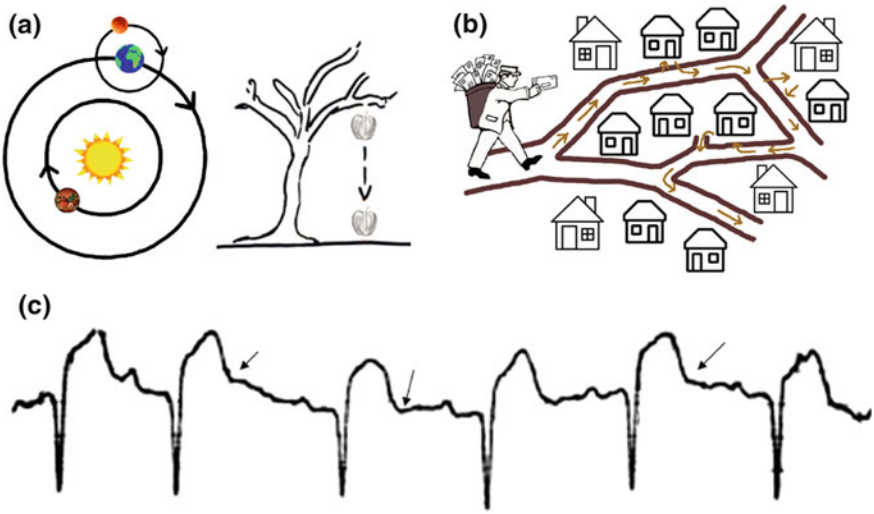

Fig. 1 Movements caused by invariable laws (**a**), by specific causes (**b**), or suggested to be caused by any of these components (**c**). **a** trajectories of the planets and of a falling apple are determined by the same law of gravity. **b** a complicated trajectory of a postman is determined by addresses written on the envelopes. **c** a record of a quasi-periodic movement. It is a matter of investigation to detect whether it may be embraced by a common law or the breaks of trajectories (some of them shown by *arrows*) should be ascribed to specific causes

Initially both the approaches looked mutually exclusive. Since the second half of the previous century, however, a new version of the classificatory approach emerged, formalized within the framework of so-called systems theory (Bertalanffy 1968; Pattee 1973): it arranged the static events according to their characteristic dimensions, and the dynamic events according to their rates.

Briefly speaking, this approach invites us to distinguish small things from large ones and slow processes from fast ones. At first glance, this seems naïve, but is actually very deep. A use of this approach leads to nontrivial conclusions about the stratification of our world, both organic and nonorganic, into a restricted number of *discrete levels*, each of them populated with events of characteristic linear dimensions and characteristic times (i.e., reversed rates). As we shall see in Chap. 1, such stratification is indispensable for applying a law-centered approach to any complex system, whether organic or inorganic. Nevertheless, when taken in isolation, it is but a preparatory step for doing this.

Which of these approaches—or combination of them—has dominated conventional embryology? Because developmental events lie at the very heart of biology, it is in no way surprising that the traditional classification approach dominated throughout the entire history of developmental biology and retained until now the leading positions. This is true not only for so-called descriptive embryology, dealing with normal course of development, but also for experimental research, performing "causal analysis" of developmental mechanisms: this is because the results of such analysis are usually presented as a set of "specific causes," having as a rule nothing in common with each other. Such an approach, seeming at first glance quite safe, will be shown to involve us into a series of principal uncertainties and contradictions.

On the other hand, a classification of developmental events according to their space temporal scale has also been used intuitively for a long time. Already a century or so ago, embryologists actively disputed the relations between a developing "whole" and its parts, thus intuitively using what we call today the interlevel approach. As we shall see later, some of their ideas criticized by contemporaries as being too vague and even nonscientific previewed in fact some firmly accepted notions of the present-day knowledge. However, it remains still uncertain whether it would be reasonable and constructive to transform embryology into a law-centered science. On the one hand, by referring to a classical Maxwell's definition of physics ["Physical science is that department of knowledge which relates to the order of nature, or, in other words, to the regular succession of events" (Maxwell 1871, 1991)], one should immediately regard embryology as but a part of physics: nothing in nature better represents "the regular succession of events" than the development of organisms. However, the successions of events which are really taking place during development of organisms are completely unparalleled in any nonliving systems, both in their duration and complexity. It is not surprising therefore, that in spite of isolated, remarkable attempts by certain authors (to be discussed later), the law-oriented approach in embryology remained marginal, while the majority of researchers could not believe such complicated chains of events to proceed without any specific "instructions."

We suggest that such a situation can be due to a premature use of the law-oriented approach, rather than by its inherent nonadequacy. Until recently, this approach was used in the so-called linear approximation, which did not permit to reproduce unusual dynamic properties of complex multilevel systems; nonlinear approaches (see Chap. 1) emerged much later.

Before coming to these, it would be desirable to find a common category of physical events participating in the main, if not all the activities of developing systems. At first glance, such enterprise looks hopeless. Fortunately, this is not the case. Both superficial observation of the developmental processes and their refined analysis up to the molecular level shows that practically all of them are associated with regular and repeatable *deformations* of material units ranging roughly from 10^{-3} to 10^{-9} m, that is, from cell collectives to single molecules. What is called morphogenesis is actually a succession of such deformations observed at the cellular and supracellular levels. It is but natural to extend this same term to the lower structural levels as well.

By considering the deformations taking place at any structural level to be the leading component of development, we take a crucial step toward what we call *morphomechanics*. Although nobody can deny that organized deformations are essential parts of development, most researchers of even a recent past believed them to be no more than epiphenomena of independent deeply hidden regulatory mechanisms, nonaffected by deformations themselves. Such views are explicable as extrapolations from traditional constructions of common man-made devices, implying a sharp segregation of a macroscopic executive domain from a miniature regulatory mechanism. We shall see however that in living systems this is not the case: executive and regulatory mechanisms are mutually dependent. In other words, we must be ready to accept that morphogenesis can be *self*-regulated.

Meanwhile before doing this, we would like to see at what point the *morphomechanics* deviates from the ordinary mechanics. Such fundamental notions as the deformations and mechanical stresses (MS) are common for both. A basic difference occurs at the next step of our reasoning and is as follows. The ordinary mechanic does not ask, as a rule, what is the origin of the force(s) producing MS, taking it as given (under the name of "initial conditions"): its only concern is in calculating MS as precisely as possible. On the contrary, for morphomechanics the problem of MS origin is central. Moreover, by dealing with such prolonged successions of deformations as those constituting morphogenesis, we cannot be satisfied by discovering the origin of a single force: rather, we must operate with the *chains of forces*, each of them creating a basis for the next one to appear. But for doing this, we have to introduce a distinction between the *passive* and *active* forces. The passive force is that acting to a material element of a biological tissue from outside, while the active one is that generated as a response within this element, certainly by spending some of its internal energy. In these terms, we shall consider morphogenesis as a relay of passive–active forces and corresponding deformations and shall try to construct an embracing law for this relay.

By focusing itself onto this task, morphomechanics follows a way unusual for classical mechanics. True, the gap between both trends of mechanics should not be

considered as impassable: the responses of some nonbiological systems to mechanical forces can be also rather complicated and treated as active ones. However, what takes place in developing organisms has at least two major features going far beyond what can be observed in nonbiological systems. The first of them is the multilevel organization and, the second, a very high diversity and specificity of the morphological structures. Can these properties be adequately and usefully treated within the framework of morphomechanics? These are the questions to be discussed in this book.

The structure of the book is as follows:

In Chap. 1 we start from reviewing the main concepts related to morphogenesis. After doing this, we reformulate developmental events in the language of symmetry theory, so effectively used in physical sciences. This step is necessary for coming toward the realm of the self-organization theory (SOT). We hope to demonstrate that SOT creates an adequate basis for interpreting development but is itself too general for being applied to concrete processes.

Chapter 2 deals with morphomechanical processes related to lower structural levels, ranging from single macromolecules to entire cells. In recent years, this research area has been developed in a really explosive way permitting to reach much more integrated views upon the relations between mechanical events and those treated traditionally as chemical ones. The dynamic processes belonging to these levels are treated in terms of symmetry and mechanically based feedbacks.

In Chap. 3 we pass toward a supracellular level and review the main modes of collective cell behavior separately from each other.

The aim of Chap. 4 is to integrate these modes into natural developmental successions, based on morphomechanical feedbacks.

Chapter 5 comprises a review of plant morphomechanics, written by Dr. Andrei Lipchinsky from the Department of Plant Physiology, St. Petersburg University.

The aim of the "Concluding Remarks" is to generalize the beforehand accounted matters and to outline most important still unsolved problems: the relations between developmental nomothetics and ideography are here discussed again.

One of the main author's problems was to trace a border line between the information to be accounted for reaching the main goal of this book and one that could be left aside. This task was mostly difficult for the adequate solution as related to Chap. 2, due to enormous amount of closely interrelated data; we are far from sure that the optimal balance was achieved. In any case, this monograph in no way can be regarded as a substitution for regular textbooks on the molecular, cell, and developmental biology, which are recommended for the interested reader to be studied beforehand.

To some extent, this book can be considered as an elaborated version of that published almost two decades ago (Beloussov 1998), but the differences between them are substantial. To a considerable part they may be ascribed to existing research progress in related areas, especially in molecular biology of the cell. However, even most important were not always visible, but in fact quite profound recent shifts in scientific paradigms. Among these, the first to be mentioned is extensive penetration of a self-organizing approach in biology accompanied by

increased understanding that so-called "genetic information" is an integral part of more extensive feedbacks rather than a sole master of development.

There are too many people to which the senior author of this book (LB) is obliged by everything. The first part of LB's scientific life which was spent almost without any contacts with the Western authors provided nevertheless a unique possibility to assimilate the traditions of the Russian school of "rational morphology," with its attitude to the rejuvenated idea of the primacy of organic forms. The main person to be mentioned here is Alexander Gurwitsch (1874–1954), who brought toward the midst of the last century a living spiritual memory of Wilhelm Roux and Hans Driesch—his teachers and personal friends—but whose ideology he finally rejected (giving a kind of excuse for making the same with Gurwitsch's "cell field" theory). Remembered should be also other bright persons from the same team: Vladimir Beklemishev, Alexander Liubischev, Sergey Meyen, Pavel Svetlov. His restricted knowledge of SOT and the related parts of physics LB is owed to Prof. Chernavskii and his seminar members from Lebedev Physical Institute. More recently, when a worldwide free exchange became possible, LB got a possibility to establish contacts with many outstanding persons among whom most influential were the talks and a real friendship with Albert Harris and Brian Goodwin. The idea of hyper-restoration emerged in discussions with Jay Mittenthal from Illinois University.

LB had also the privilege to work together with outstanding representatives of the next generation—Boris Belintzev, Vladimir Cherdantzev, Vladimir Mescheryakov, Alexander Stein, and several others. Much of what was taken from them is incorporated in this book. And last but not least—a view of even younger population of researchers, now filling our Lab of Developmental Biophysics—gives the hope that in spite of all the surrounding troubles the great traditions of a fundamental science about development of organisms will never be broken. LB thanks a member of this team, Ilya Volodyaev, for critically reading the manuscript and making valuable remarks.

Moscow Lev V. Beloussov

References

Beloussov LV (1998) The dynamic architecture of a developing organism. Kluwer Academic Publishers, Dordrecht

Maxwell JC (1871, 1991) Matter and motion. Dover, London

Pattee H (1973) Hierarchy theory: the challenge of complex systems. G. Braziller, New York, p 3

von Bertalanffy L (1968) General systems theory: foundations, development, applications (Revised edition). George Braziller, New York

Contents

Abbreviations

AI	Apical index
BM	Belintzev's model
CCP	Contact cell polarization
CIF	Curvature-increasing feedback
EEF, or EE	Extension–extension feedback
GP	Growth pulsations
HR	Hyper-restoration
MS	Mechanical stresses
RAM	Root apical meristem
SAM	Shoot apical meristem
SBA	Suprablastoporal area
SOT	Self-organization theory
TIAE	Tension-induced active extension

Chapter 1
From Strict Determinism to Self-organization

Abstract We start from reviewing several ubiquitous approaches to morphogenesis and argue that for a more adequate presentation of morphogenesis, they should be replaced by explanatory constructions based upon the self-organization theory (SOT). The first step on this way will be in describing morphogenetic events in terms of the symmetry theory, to distinguish the processes driven either toward increase or toward decrease of the symmetry order and to use Curie principle as a clue. We will show that the only way to combine this principle with experimental data is to conclude that morphogenesis passes via a number of instabilities. The latter, in their turn, point to the domination of nonlinear regimes. Accordingly, we come to the realm of SOT and give a survey of the dynamic modes which it provides. By discussing the physical basis of embryonic self-organization, we focus ourselves on the role of mechanical stresses. We suggest that many (although no all) morphogenetic events can be regarded as retarded relaxations of previously accumulated elastic stresses toward a restricted number of metastable energy wells.

1.1 Deterministic Approaches to Development: Expectations and Impediments

1.1.1 Lessons from Embryonic Regulations

Please take a look at Fig. 1.1, displaying development of sea urchin embryo from a non-fertilized egg (Fig. 1.1a) up to a free-swimming larva (Fig. 1.1l, m). This is a textbook example of embryonic development, known for long ago in great details. Let us put a naïve question: Why just such a succession is taking place at all and why it is reproduced for innumerable set of generations? Obviously, our first suggestion will be that within any stage embryo, a certain set of "causes" is embedded providing its transition to the next stage. How large should be such a set? It is easy to see that as the development proceeds, the structure of embryo becomes ever more complicated: some structures not seen before are emerged. So-called

L.V. Beloussov, *Morphomechanics of Development*,
DOI 10.1007/978-3-319-13990-6_1

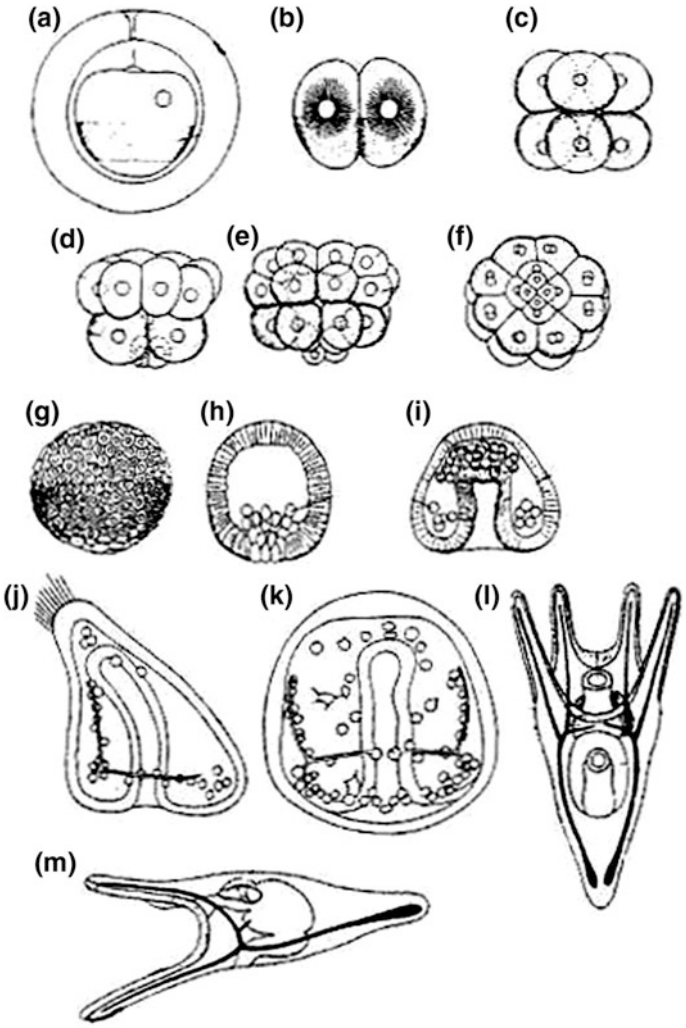

Fig. 1.1 **a**–**m** Successive stages of sea urchin development. **a** An egg within egg membranes; **b**–**f** cleavage; **g**, **h** blastula stage, surface view and sagittal section; **i**–**k** gastrulation in different projections; **l**, **m** pluteus larva in frontal and sagittal projections, correspondingly

arms of free-swimming larvae (Fig. 1.1l, m) are most obvious but not the sole examples of such a complication. Thus, if being consistent, we should suggest that any of the newly arisen structures had its own, individual "cause," settled within an egg in a definite position even before the start of development.

This is a brief exposition of influential ideology of a so-called preformism which dominated in embryology for several centuries and is keeping until now (although in a hidden form) rather strong positions in researchers minds. It is based upon the principles of a so-called Laplacian, or uniform determinism, ascribed (probably, not

at all justifiable) to the great French mathematician Pierre Simon Laplace (1749–1827). By this ideology, the only way for describing and exploring our world is to split it to such a set of cause–effect links that in each of them, a single cause cannot produce more than a single effect (the reverse is permitted: A single effect may require a combination of two or more causes). Until the rise of a quantum physics in the beginning of twentieth century, this ideology was regarded as only one compatible with natural sciences. It is worth mentioning, however, that in physics, it was always more or less shadowed by a law-centered approach (which puts the "causes" to a category of initial conditions and takes them usually as granted). However, in biology and the related sciences, the classical deterministic approach always dominated.

In embryology, it became a basis of one of the most important trends, the so-called Mechanics of Development ("Entwicklungsmechanik" in German) proclaimed by Wilhelm Roux about one and a half century ago (see Moček 1974). By this view, a developing embryo may be simulated by a clockwork which should be experimentally split into minor details in order to understand which one of them "determines" the next part activity; similarly, a task of a researcher would be in dissecting a developing embryo into single parts in order to see which one of them contains the "cause" enforcing another to develop further in a regular way.

By evaluating the role played by "Entwicklungsmechanik" in enlarging and improving our knowledge of development, we come to paradoxical conclusions. On one hand, by using the recommended analytical tools, we recognized a lot about interactions of embryo parts of quite different scales, from whole organs to single cells. But on the other hand—which is often neglected—the conceptual basis of Roux approach (the idea of a strict cause–effect determination) has been undermined already in few years after it was formulated.

This was done by another German embryologist, Hans Driesch, in his experiments on separating from each other two or four blastomeres of sea urchin eggs or on changing their mutual positions. Although Driesch's results have been described virtually in all embryological textbooks, almost never this description was accompanied by conceptual conclusions, forwarded already by Driesch himself and elaborated by recent authors.

As it is widely known, the main result of Driesch's experiments was that fairly normal (although proportionally diminished) larvae with all of their organs properly arranged could be obtained from a single embryonic cell (blastomere) containing no more than ½ (if two first blastomeres were separated) or even ¼ (in the case of four blastomeres separation) of the entire egg's material. Rather soon these effects (defined by Driesch as "embryonic regulations") were numerously confirmed and extended to the species belonging to almost all taxonomic groups of metazoans, from sponges to mammalians. The only noticed difference was the duration of a period of an egg/embryo capacity to regulations: In some groups, such as mollusks or ascidians, this period was rather brief (ending soon after egg's fertilization), while in others (flatworms), it extended over the entire living cycle (interesting, in ascidians, a regulatory capacity is lacking during larva development but restores in adult state). Importantly, after entire embryos lose their regulatory capacities, these

latter are still manifested by their parts: For example, whole limbs or eyes of Vertebrate embryos can be restored from small fragments of these rudiments, or even from dissociated cells. Embryonic regulations took place not only after removal, but also after experimental addition of some excessive amount of embryonic material.

Besides separating blastomeres, Driesch changed their mutual positions by compressing cleaving eggs for some time period. After being released, the eggs also developed in a normal way, although each of the blastomeres became surrounded by abnormal neighbors. Fairly normal embryos, although not in 100 % of cases have been obtained later from dissociated-reaggregated masses of sea urchin blastomeres (Spiegel and Spiegel 1975).

What can these experiments tell us about cause–effect relations? If continuing to apply deterministic approach to embryonic regulations, we have to conclude that complete sets of "causes" required for further development are contained not only within whole eggs/embryos but also in their halves, quarters, etc.; on the other hand, as a rule, the sets are not increased with the addition of embryonic material. Moreover, each time (depending upon the type of a disturbance performed) this hypothetical "set of causes" should change its arrangement for producing the normal pattern. Obviously, under these circumstances, a concept of an individual "cause" (precursor) for any embryonic structure becomes meaningless.

Driesch fully recognized this critical situation. So far as in his time scientific knowledge was in fact identified with strict cause–effect determinism, he concluded that embryonic regulations undermine the very basis of natural sciences. Such a position put this outstanding thinker outside the scientific mainstream, which hampered further study of embryonic regulations for several decades. Driesch formulated his final conclusion from his regulation studies as a law which in slightly simplified form sounds like this: "The fate of an embryo part is a function of its position within a whole" (Driesch 1921). Its idea is in the following. Suggest that both the normal and experimentally disturbed embryos possess a kind of a coordinate grid (including, for example, a polar axis and a set of latitudes) which is each time adjusted to embryo dimensions (being diminished in embryos having a part of their material removed and enlarged in those getting excessive additional amount of material). Each part of the embryo is endowed by a capacity to "read" its own coordinates and to develop accordingly, even if this does not coincide with the normal fate of this part.

Looking at the first glance as an adequate generalization of embryonic regulations and related phenomena, this statement contains nevertheless some hidden contradictions and leaves a number of questions unsolved. The first of them is about the reference points of the postulated coordinate grids. Do they correspond to certain small previously settled structural elements of otherwise homogeneous embryo, to entire embryo geometry and/or topology or to something else? How should the reference points be arranged for providing formation of similar adults out of differently disturbed eggs/embryos?

The second set of questions relates to the notion of "fate." So far as during embryo development any of its parts constantly changes, its position in any system

of coordinates and the notion of "fate" may include developmental periods of quite a different longevity—we are urged to define how long should be the developmental period determined by a given position. This question is closely connected with another, even more important one: What is the nature of the postulated connections between a position and a "fate" of embryonic element, whatever being the latter? Can we point to any universal dynamic component playing a leading role in all the position-fate dependencies or each of them has nothing in common with the others?

The most popular concept pretending to answer these questions is that of "positional information" (PI) (Wolpert 1969, 1996). Appearing after several decades of almost complete oblivion of Driesch's ideas, it aimed to modernize them because the very fact of positional dependencies in embryonic development could not be further ignored. By doing this, Wolpert started from postulating the existence of a few (as a rule two) structural elements of embryo acting as reference points for PI perceived by all the other elements (cells). In more concrete versions of PI concept, the reference points were identified as the source and the sink of a chemical substance (called morphogen) which creates concentration gradient between these points. It is the local morphogen concentration to be "read" and "interpreted" by any embryonic cell (independently of its neighbors) determining thus its fate.

If discussing the problem of reference points, the main trouble for PI concept is lack of robustness to mutual shifts of reference points which inevitably accompany any of experimental disturbances. Let us trace some examples, starting from the so-called French Flag (FF) model, a basic one for PI concept.

According to its name, FF model is dealing with 3-stripe axisymmetric pattern. If putting the "source" and the "sink" to the opposite poles of the main axis and making removals or additions of tissue pieces precisely axisymmetric, such a reference system will be formally suitable for preserving the initial pattern (Fig. 1.2a, b). However, if making tissue removals/additions even slightly asymmetric (which is almost usually the case), the reference points themselves will be shifted asymmetrically, thus distorting the resulting pattern (Fig. 1.2c). Even more important is to remind that axisymmetric eggs/embryos are rare exceptions among those capable of regulations: Rather, most of the eggs already soon after fertilization acquire irreversible differences [called dorso-ventral (DV)] between opposite sides. In these, any removals/additions of embryonic material will shift any pair of points into positions geometrically non-homologous to initial ones (a–a_1, b–b_1, Fig. 1.2d), thus inevitably distorting PI pattern. We can see that any formal way to save PI concept is to suggest that PI is "emanated" from *all* the material points of a given stage embryo, rather than from any previously selected ones. This brings us to the fundamental non-classical idea of *non-locality*, associated with *collective interactions* of a large number of equivalent elements. The both notions, central for a self-organization theory (SOT), will be discussed further in this and the next chapters. Meanwhile, if taken alone, the idea of the multiple PI bearers will be able to interpret embryonic regulations only if the initial shape of the embryo was not significantly changed after experimental perturbations. It will not work, for example, when pretty normal shapes

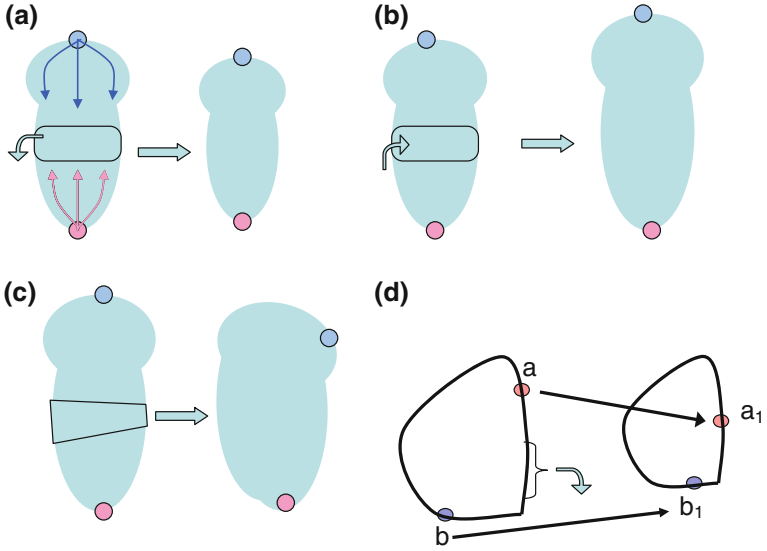

Fig. 1.2 Non-robustness of PI model. Small lilac and *blue circles* depict hypothetical sources of PI, the latter shown by *arrows* at the *upper left* frame. Following PI model embryonic regulations will become possible only if (as in frames **a**, **b**) embryonic body and PI sources are axisymmetric and removals (**a**) or additions (**b**) of embryonic material do not disturb axial symmetry. If, however, the pieces of removed or added material are asymmetric (**c**), or such is the initial shape of the intact embryo (**d**), no restoration of geometric similarity viewpoint is possible within the framework of the PI model

will emerge de novo out of completely chaotic cell arrangement, like in the above-mentioned Spiegel and Spiegel (1975) experiments. Such events belong to a "pure" self-organization and cannot be explained by any concepts demanding a more or less precise initial PI, whether it comes either from single elements or their collectives.

Another problem associated with PI concept is that of relations between cell positions (in any reference system) and their "fates." Actually, PI concept is rather uncertain on the exact meaning of the "fate." Is it identical to the final cell differentiation (which is highly improbable if PI is assumed to be set at initial stages), or just to a next small step of development? In any case, the idea of transformation of cell position (local morphogen concentration) into its fate raises a number of problems. Some of them have been discussed by Furusawa and Kaneko (2006). The authors argue that even in most obvious examples of concentration-dependent action of certain agents (in their case, activin), "the pattern formation… is not predetermined from spatial information, but rather through intracellular dynamics and interaction. Spatial patterns and intracellular states mutually stabilize robust pattern formation…" They present model data showing that PI itself is not enough for establishing order in the population of heterogeneous cells, so that such notions

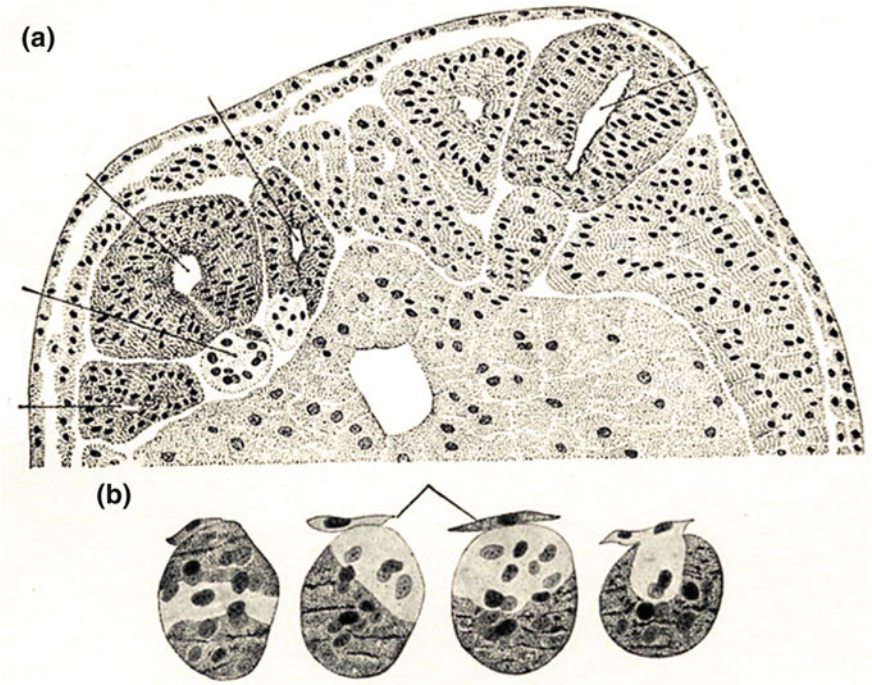

Fig. 1.3 Random mutual arrangement of transplanted inductor's tissue (*light*) and host tissue (*dark*) in the first Spemann and Mangold (1924) experiment on embryonic induction, abolishing the inductor's capacity to be a PI source. **a** Cross-sectional area of the host embryo with its normal axial organs to the right and induced organs to the left. **b** Several cross sections of the chimeric notochord. From Spemann (1936)

as nonlinear intracellular dynamics and attractors are required for getting realistic results. All of these belong to the SOT vocabulary.

By discussing these matters, we come to the most troublesome problem of development—actually going well beyond PI concept—which can be defined as that of *interpretation*.

If we have a certain signal (no matter being located inside of outside of embryonic body) which generates a definite response from the latter, our main interest is to know why such a relation between the signal and the response is taking place. As mentioned in Introduction, we have two epistemological models which can be used for solving this task: Either there is a reason to postulate each time a unique one-to-one cause–effect (signal–response) relation—in this case, our work will consist in compiling a comprehensive list of such relations; or we regard each relation as a particular manifestation of a general law. For example, if we relate velocity of a thrown stone to its position, we do not suggest that a new "specific" force is associated with each next position: Rather, we are searching for a common law embracing all the positions including those never occupied by the stone.

Considered in this context, PI concept resides a strange intermediate place: On the one hand, it ascribes that the leading role in development to a largely non-specific factor of position, which in physical sciences, is always used for constructing an embracing law (as a rule, describing certain field); but, on the other hand, each next position of embryonic elements is claimed to be connected with quite specific response, having no relations with another one.[1] This, by my view, makes the entire PI concept tautological, adding nothing to a mere descriptive approach which takes spatial patterns as given. Let us look now for the situation with interpretation problem in other branches of developmental biology.

1.1.2 Can Embryonic Inductions Be Regarded as Cause–Effect Relations?

The discovery and further exploration of embryonic inductions by Hans Spemann and his followers may look at first glance as a triumph of Wilhelm Roux causal approach: It was shown indeed that one part of embryo can be a crucial factor for the development of another. Does it mean, however, that the inductors can be regarded as a kind of blueprints, or as "PI sources" for induced tissues? It is enough to have a look to the picture from the famous first Spemann and Mangold paper (Fig. 1.3) for seeing how far this is from reality. We can see that the inductor's and host tissues (discerned by their pigmentation as being taken from two different Triton species) are mixed at random, both in the notochord and the neural tube. Nevertheless, the entire structure of the complex of axial organs is perfectly ordered. It means that the inductor tissue cannot serve not only as a spatial template, but even as a source of a hypothetical PI gradient for the reacting tissue: Formation of a proper set of axial organs under the influence of an inductor looks more as embryonic regulation in Driesch sense rather than a kind of a direct causation. Or, if speaking in terms of a SOT (to be later on accounted in this chapter), it was the long-range order, independent from the "micropatterns" of the inductors and host tissues, to be established in the first Spemann and Mangold experiments. At the intuitive level, this was perfectly apprehended by Spemann himself who considered the action of inductor as "abstract," that is, containing no "information" about spatial details (Spemann 1936). This conclusion was later on specified by Waddington as following: "Clearly, the problem [of induction] reduces to that of a complex response to a simple stimulus …somewhere along the line an increase in complexity occurs" (Waddington 1962).

Usually, the problem of complication during embryonic induction is resolved in terms of concentration gradients of inductive substances assumed to be set between

[1] My friend, American biologist Albert Harris, liked to compare PI with a price politics in non-marked economies: The prices (equivalent to local morphologies or cell types) are appointed ad hoc, without being regulated by any mutual feedbacks.

animal and vegetal embryo poles, or between its dorsal and ventral sides (e.g., De Robertis 2009). If accepting the presence of such a macroscopic gradient-like prepattern, the isolated small pieces of embryonic tissue cannot produce more than small parts of it. However, already in the old Holtfreter's (1938) experiment, a miniature copy of entire embryo was obtained from a piece of embryonic tissue extirpated from so-called marginal zone. As commented by Gerhardt (1998) "Holtfreter brought to light an individualistic and anti-authoritarian view of the embryo in which competent responsive cells interact in a self-organizing community, in place of conceptions of the embryo as a collection of naïve passive members dependent for their future on detailed directions from a central organizer."

A modern concept of so-called default induction, reducing the inductors' role to "inhibition of inhibitor" (Hemmati-Brivanloue and Melton 1997) may be regarded as a next step from the cause–effect ideology toward that of self-organization. Indeed, the inductors, instead of being the bearers of the positive "information," become a kind of releasers (triggers) of the potencies already preexisted in reacting tissues. As in the cases of embryonic regulations, this situation cannot be adequately described without using such notions belonging to SOT as a nonlinearity, potential relief (describing a state of embryonic cell), and others. A special question will be whether such a self-organization can be at least partly based upon morphomechanics. Later on, we hope to bring some evidences in favor of such a suggestion.

1.1.3 Genetic Program of Development: Does It Actually Exist?

In not so remote past, a claim that the course of development is "genetically programmed" was accepted as an absolute truth, even in spite of the lack of proper understanding what the "program of development" actually means. So stunned were the successes in deciphering the key roles of genes in "controlling" the development of embryonic rudiments that all the instructions for "making a fly" [a paraphrase of the title of famous Lawrence (1992) book] looked to be in our hands. Only closer to our days, it became realized that our believing to govern the development by switching on or off any genes or signaling pathways is the same as operating an electronic device by pushing its buttons without having even a slight idea on how it actually works.

For clarifying the situation, two main groups of evidences have to be mentioned: one of them related to classical biology and the other recently emerged as a result of unexpected discoveries in modern molecular genetics.

The first group of evidences claims that the factors determining space–time schedule of genes expression are non-genetic in their nature and topography. This statement, which creates the basis of biology for about a century and is supported by experiments on nuclei transplantations and many others, is on its own enough

for concluding that genes themselves should obey outside instructions which are called epigenetic. Meanwhile, recently it was complemented by numerous observations showing that relations between genes and signaling pathways on the one hand and their developmental targets on the other hand turned out to be quite far from being one to one: The products of activity of the same or closely homologous genes and/or of the same signaling pathways were found to be involved in quite different developmental events. Modern textbooks are full of such examples. Here are just a few of them:

- The interactions between msx-1 and msx-2 homeodomain proteins characterize the formation of teeth in the jaw field, the progress zone in the limb field, and the neural retina in the eye (Gilbert 2010).
- The transcription factor Pax-6 is expressed at different times and at different levels in the telencephalon, hindbrain, and spinal cord of the central nervous system; in the lens, cornea, neural and pigmented retina, lacrimal gland, and conjunctiva of the eye; and in the pancreas (Alberts et al. 2003).
- In *Drosophila* embryos, a gene Engrailed is involved in segmentation of a germ band, development of intestine, nervous system, and wings. In mouse, same gene participates in brain and somite development. In Echinodermata, it takes part in skeleton and nervous system development (Alberts et al. 2003).
- Delta–Notch signaling pathway regulates the following: neuro-epithelial differentiation in insects, feather formation in birds, fates of blastomeres in Nematodes, differentiation of T-lymphocytes, etc. (Alberts et al. 2003).
- Hunchback gene is involved at the early stage of Drosophila development as one of so-called gap genes and at the later stages participates in development of neural system.

For the similar conclusions, as related to signaling pathways, see Kupiec (2009). Shrewd remarks on this topic can be found in (Gordon 1999 V. 1, pp. 59–64).

Anyway, our present-day image on genetic regulation of development contains two great negations: (1) even complete knowledge of genome structure cannot tell us what gene will be expressed in a given space/time location; (2) even from exhaustive knowledge of space/temporal schedule of genes expression, one cannot predict what morphological structures will be formed in these definite locations.

Certainly, this is not to claim that the genes play no role in development at all. On the contrary, their role is crucial in permitting or abolishing development of the single structures and their ensembles; in particular, they may affect shapes of entire embryos or their parts. A proper conclusion from the above said is that their action should produce a definite morphological results only if being an integral part of quite extended and ramified regulatory contours, including the feedbacks coming from the upper-level events, such as cell shapes and mechanical forces. Actually, such a situation is in generally acknowledged, but the conclusion is in most cases expressed in an allegoric form, by claiming that genes action is "context-dependent." The urgent aim will be in transforming this vague formulation into a concrete research program.

1.2 Main Notions and Principles of SOT, Applied to Developmental Events

Within one or two last decades, the word "self-organization" became among the most generally used ones, not only in science, but also in politics and every-day life. Meanwhile, for most of the users, it remains to be nothing more than a mere word, or a kind of vague metaphor; only few people knows that it is a designation of a strict theory, being in its essence mathematical but deeply rooted in physics, biology, economy, and even humanitarian sciences. SOT is treated in a number of perfect books ranging from very special to popular ones; among the latter, simplicity and strictness are adequately combined in the book by Capra (1996). For the readers who do not like math, a very qualified and perfectly illustrated account of the main SOT principles by Ball (2001) can be recommended. The aim of this section is more limited: It is in outlining only those notions and concepts of SOT which are necessary for interpreting adequately development of organisms. The first of them has been formulated and widely used well before the emergence of SOT: this is the symmetry theory. In certain sense, the term "symmetry" shares the destiny of a "self-organization": Both are widely used without apprehending their deep meanings. Meanwhile, not only for developmental biology but also for other branches of life sciences, the applications of the main notions of a symmetry theory are quite useful and adequate.

1.2.1 Translating Developmental Events into the Language of Symmetry Theory

A remarkable property of this theory is that it may be regarded as a compact model of any law-oriented science, aiming to search for invariable basis within a set of varying events. In other words, it is dealing with the so-called invariable transformations, keeping constant some properties of a body which in other relations is changing. The transformations used for testing the invariability are the movements in a broad sense, including so-called isometric transformations keeping the form and the dimensions of the object constant as well as the different kinds of deformations. The structural elements taken for testing the invariance may also be qualitatively different, being exemplified either by a macroscopic design (fitting in a particular case with the overall shape of a body), or by the positions of small (point-like) elements of a body. The symmetry evaluated by the first criteria is called geometric, while that using the second criteria is defined as colored (what means that the selected small elements are assumed to be distinguished by different colors). Although the distinctions between geometric and colored symmetry were introduced by persons non-familiar with biology, they luckily correspond to the differences between two main components of development: morphogenesis (overall shape changes) and cell differentiation (changes on the single-cell level).

1.2.1.1 Some Designations Related to Isometric Transformations

In elementary symmetry, three categories of isometric movements are considered: rotations, reflections, and translations (linear shifts). A number of movements of each category which brings a body into coincidence with itself are defined as a symmetry order, and the combination of all such movements for a given body is its symmetry group. Thus, rotational symmetry order of a square is 4 (this is the number of all the rotations—to 90°, 180°, 270° and 360°—matching a square with itself). Accordingly, rotation symmetry order for equidistant triangle is 3 (120°, 240° and 360°); any body (assuming that its shape is not changed during rotation) has at least rotation symmetry of the order 1. The presence of reflection symmetry is defined by letter *m* (the first letter of a French word "miroir" or English "mirror") (Fig. 1.4a, b). Numbers of reflection planes possessed by a given body are not included in the formulas of symmetry groups because it has been proved that if the reflection symmetry takes place at all, its order is equal to that of the rotation symmetry. Thus, symmetry group for a square which has four reflection planes (vertical, horizontal and two diagonal) is written as $4 \cdot m$, and symmetry group of an equidistant triangle as $3 \cdot m$ (reflection planes coincide with three bisectors).

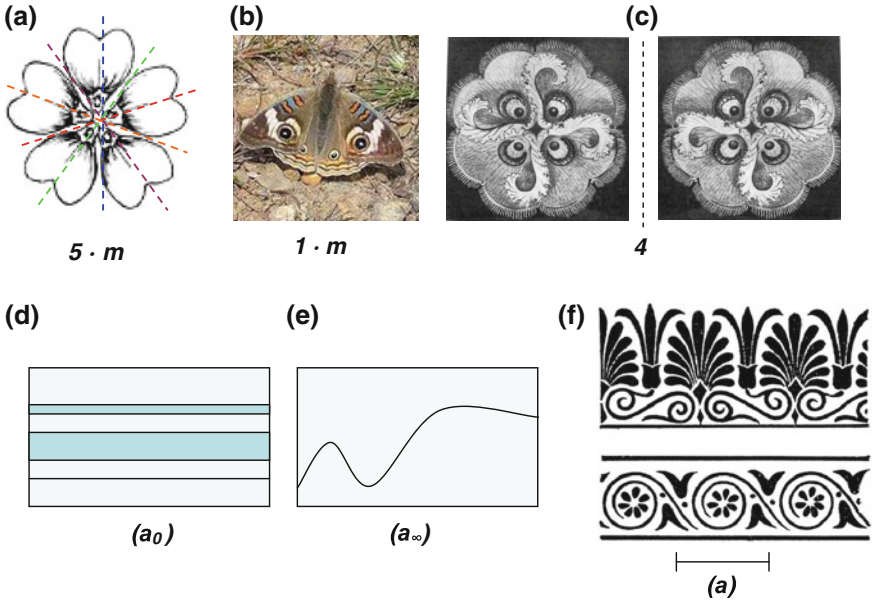

Fig. 1.4 Bodies belonging to different symmetry groups. **a** Rotation symmetry of order 5, combined with the same order mirror symmetry. **b** Mirror symmetry only. **c** A pair of enantiomorphic bodies with fourth-order rotation symmetry reflected to each other by a mirror plane (*vertical dashed line*). **d–f** Translational symmetries of zero, infinite, and finite orders correspondingly. Below each frame symmetry orders are shown. **a–c** and **f** from Shubnikov and Kopzik (1972) with the authors permission

On the other hand, a form depicted in Fig. 1.4c possesses only rotation, but not reflection symmetry. Accordingly, its symmetry group is 4. Any object lacking reflection symmetry has arbitrarily defined left and right configurations matching each other by a reflection. Such objects are called enantiomorphic.

For circles, disks, and cones, the order of rotational symmetry is infinite. So far as these bodies have also infinite number of reflection planes, their complete symmetry group is $\infty \cdot m$. A sphere possesses rotational symmetry around an infinite bundle of its central axes oriented at any angles to each other. Its symmetry group is defined as $\infty/\infty \cdot m$ (a slash means that the angles between rotation axes take arbitrary values). For comparing infinite symmetries, the notion of symmetry power is used. Accordingly, symmetry power of a sphere is greater than that of a disk.

For displaying a reflection plane perpendicular to the axis of rotational symmetry, a sign ":" is used. Thus, symmetry of a bi-cone as well as of a disk of finite thickness is $\infty : m$. Symmetry of a cylinder is $m \cdot \infty : m$.

Translational symmetry is that of linear shifts (transpositions) of a body in relation to its initial position. This kind of symmetry is evaluated by the length of a linear transposition matching a given structure with itself. It is defined as (a). Completely homogeneous bodies or those with a design arranged parallel to the shifts directions are self-coincided under any shifts and have symmetry order (a_0) (Fig. 1.4d). On the other hand, if the design is not at all repeated, the body has the infinite-order symmetry (a_∞) (Fig. 1.4e). An example of design having finite translational symmetry order is given in Fig. 1.4f.

In classical biology (both zoology and botany), the notions of symmetry are used in most cases for comparing static forms belonging to different taxonomic groups. Moreover, the compared symmetries are related as a rule to higher structural levels only. Playing an important role in morphology and taxonomic studies, this approach does not permit to penetrate deeply in developmental problems. Aiming to do just this, we shall compare now the symmetry orders of the different levels processes and the changes of symmetry orders at successive stages of development, using both descriptive and experimental criteria. We hope to show that such an enterprise will promote to clarify our views upon the driving forces of development.

1.2.1.2 Symmetry Orders on the Different Structural Levels

Whereas in ideal crystal bodies, the symmetry order of the crystal lattice is held on all macroscopic levels, in non-crystal bodies to which living beings belong, symmetry orders of different structural levels may be uncoupled. Even without using overtly the notions of symmetry, the researchers of a remote past knew this and believed in its biological importance. One of the most popular generalizations in the century back embryology was that "a whole is more precise than its parts" (e.g., Gurwitsch 1930). In the language of symmetry theory, this means that the symmetry order of a whole body or of its large enough areas is higher than that of its smaller parts (Fig. 1.5a); same are symmetry relations between the induced axial

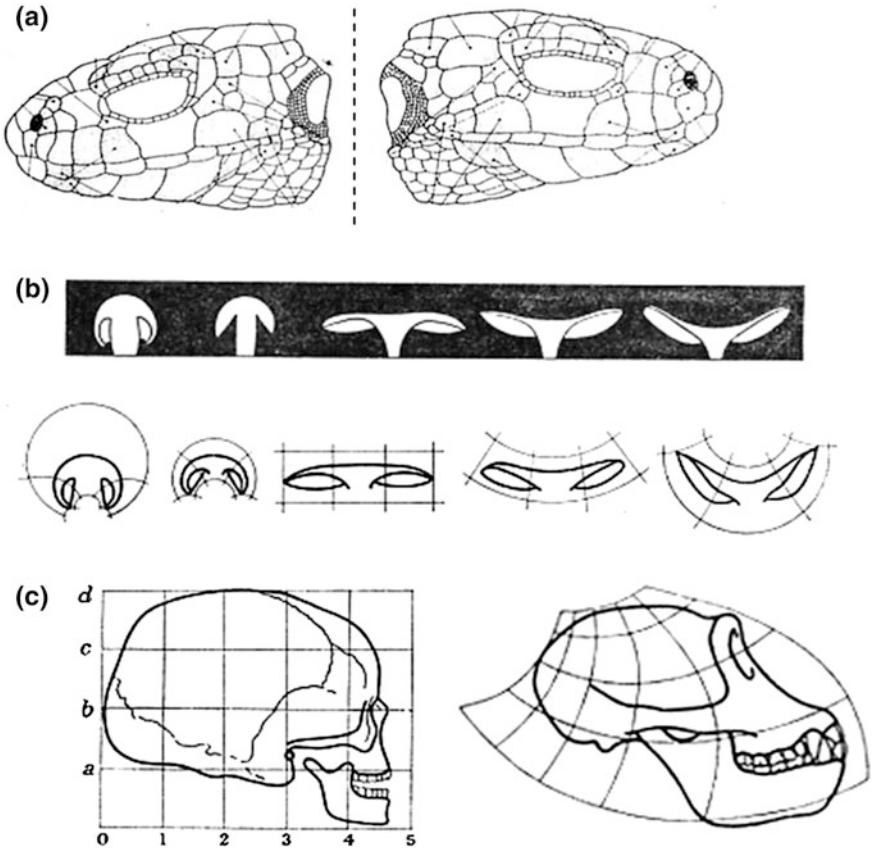

Fig. 1.5 Relations of symmetry orders between different-level structures. **a** A perfect mirror symmetry of *left* and *right* skull parts of the lizard, *Lacerta agilis*, taken as a whole (reflection plane shown by *vertical dotted line*) is combined with the lack of such symmetry at the level of bone plates. **b**, **c** Conformal symmetry transformations, preserving *rectangular shapes* of small parts (symmetry orders 4 m) under substantial deformations taking place at upper levels. **b** Growth of a mushroom fruit body. **c** Comparison of a human and chimpanzee skulls. **a** from Zacharov (1987); **b**, **c** from Petuchov (1981), with the author's permissions

organs taken as wholes and the areas occupied by inductor tissue (see Fig. 1.3). This was considered as a strong argument for holistic regulation of development. More recently, however, the reverse situations have been described (Petuchov 1981). In these cases, described by the so-called conformal symmetry, the shape and the symmetry order of small constituent parts remains invariable, while that of larger areas is extensively distorted (Fig. 1.5b, c).

At the present time, an interest to the symmetry of small body parts, including single cells, was essentially increased owing to discovery of so-called planar cell polarity, most overtly expressed in epithelial cells (Vladar et al. 2009; Eaton and Julicher 2011). This means that in addition to well-known apico-basal polarity

oriented perpendicularly to cell layer plane, a cell possesses also a polarity oriented in the layer's plane. Accordingly, symmetry group of a planarly cell should be reduced from $n \cdot m$ (taking n-edged cell with apico-basal polarity only) to $1 \cdot m$ (in case of the cells with mirror symmetry plane), and even to 1 (if a cell exhibits left–right dissymmetry, as shown by Xu et al. 2007). Although up to now our knowledge of 3-dimensional cell shapes is still rudimentary, there is no doubt that it affects cell differentiation (see Chap. 4 for more details).

What are relations between single-cell symmetries and those of higher structural levels? Does a "whole" dictate symmetry order to its parts? Is true the reverse or even the both levels' symmetries are established independently? The question is far from being solved, but some remarkable examples of a "symmetry orders exchange" between different levels can be traced and will be discussed in more details in Chap. 3. Here, it is worth to emphasize that the relations between the different-level symmetries are closely related to morphomechanics. As argued by Cademartiri et al. (2012), the direct transposition of the constituent parts symmetry to the upper structural levels corresponds to equilibrium state of solid bodies. On the contrary, the increase of a symmetry order at the upper level as compared to those of its constituent parts is typical for the equilibrium state of the liquids. Thus, by comparing the symmetry orders of different levels, we may conclude whether a living body becomes fluidized or instead solidified.

1.2.1.3 Curie Principle and Symmetry Breaks

One of the most important generalizations of symmetry theory is that formulated more than a century ago by a French physicist Pierre Curie (Curie 1894) for the crystal bodies and electromagnetic events. Only recently its applicability to a wider set of events including morphogenesis was acknowledged. Here is the initial formulation of Curie principle (op. cit):

> When certain causes produce certain effects, the elements of symmetry of the causes must be found in the produced effects.
> When certain effects show certain asymmetry, this asymmetry must be found in the causes that gave rise to them.
> The reverse of these propositions is not true, at least in practice that is to say that the produced effects can be more symmetric than the causes.

Thus, Curie principle forbids "spontaneous" (causeless) *decrease* of symmetry order of a given system, but permits its spontaneous *increase*. It is directly related to the second law of thermodynamics. Indeed, the increase of the symmetry order is equivalent to homogenization of a body structure and to enhancement of the freedom degrees of its constituent particles—hence to the entropy increase. Accordingly, the decrease of the symmetry order means establishment of an ordered heterogeneity restricting the particles' degrees of freedom, which corresponds to the decrease of entropy.

Let us trace how the symmetry order of developing organism is changed from the very beginning of egg's development. In our analysis, we shall ignore left–right dissymmetry as being strictly determined by certain supramolecular structures (mictotubules and microfilaments). This issue will be discussed in Chap. 2.

Up to fertilization, the overall shape of oocyte is not changed at all or is changed in an irregular way. This does not permit to use geometric criteria of symmetry. On the contrary, the usage of colored symmetry (addressed to small regions of the body: polar bodies and markers of its future dorsal side) is much more adequate. Indeed, before the extrusion of polar bodies, the polar (future animal–vegetal) axis can take potentially any direction; hence, by these criteria, an egg has the highest possible (spherical) symmetry order ($\infty/\infty \cdot m$) (Fig. 1.6a). [Note that our evaluation is based upon considering an (imaginary) *set* of bodies, rather than a single one; same approach will be used in other cases as well]. When after the second polar body extrusion the position of the polar axis becomes strictly determined, the symmetry order is reduced to $\infty \cdot m$ (Fig. 1.6b). Next, after setting up location of the dorsal side (which is often associated with egg's fertilization) symmetry order becomes $1 \cdot m$ (Fig. 1.6c). Another routine example of the reduction of circular

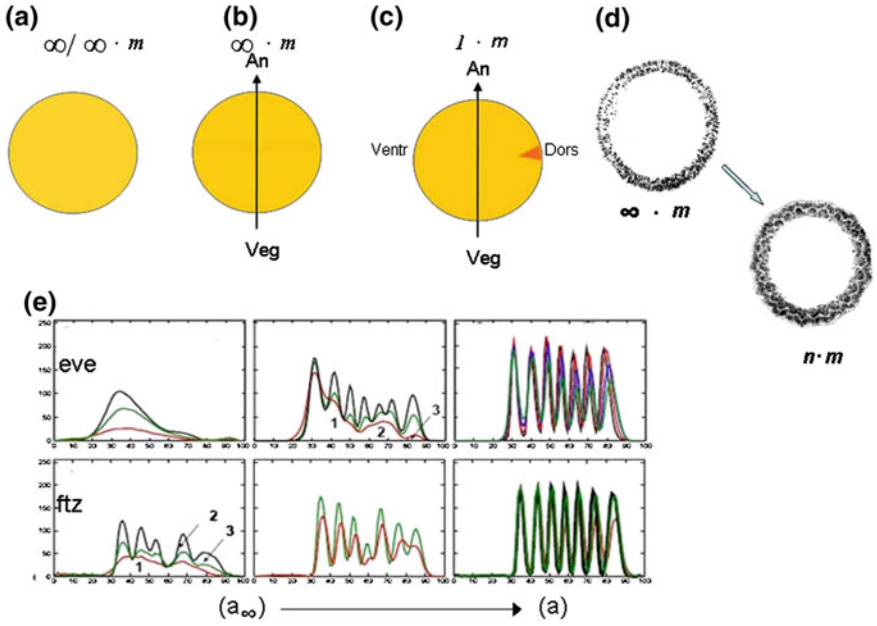

Fig. 1.6 Reductions of symmetry order (symmetry breaks) during development. **a** Non-germinated egg prior to establishment of animal–vegetal polarity. **b** Polarized egg. **c** Egg acquiring dorsoventrality. **d** Formation of tentacles ring in the oral region of hydroid polyp illustrating reduction of rotation symmetry order. **e** Transformation of infinite-to-finite translational symmetry in genes expression patterns of *Drosophila* embryos. *Upper line*: eve, *lower line*: fushi tarazu genes. Frames from left to right correspond to successive periods of development. **e** is from Surkova et al. (2013) with the author's permission, modified

symmetry order is provided by sectioning an initially homogeneous ring into a number of similar angular units, for example, tentacles (Fig. 1.6d).

More advanced stages of development are in many cases associated with acquiring a finite order of translational symmetry. The classical example of such transformation is segmentation of embryonic mesoderm (see Chap. 4 for more details). Recently to this one, the phenomena of the metameric genes expression in *Drosophila* embryos have been added (Alberts et al. 2003). For properly interpreting the finally established symmetries, it is necessary to know the developmental history of the arisen patterns. As shown by Surkova et al. (2013), instead of a previously expected homogeneity or smooth expression gradients, the regular segmented patterns have been emerged from quite variable ones (Fig. 1.6e, frames from the left to the right). This indicates the reduction of the translational symmetry order from infinite to finite and the corresponding entropy decrease.

So by a broadest survey, the general course of development looks as a succession of the reductions in symmetry order, defined also as symmetry breaks. (In no way, this excludes the existence of the periods of symmetry order increases, located between the breaks and/or on the other structural levels: see below for more details). Now the urgent question will be whether it would be possible (as demanded by Curie principle) to find for each symmetry break an external agent having a similarly broken symmetry which can be directly transmitted to a developing organism.

To the credit of experimenters almost surely unfamiliar with Curie principle be it said, they stubbornly looked for the agents which might serve as external "symmetry breakers." To a considerable part, their search was successful: In a number of species, the animal egg pole (the site of polar bodies extrusion) turned out to be determined by the position of the oocyte in relation to follicular cells; similarly, molecular determinants of a future dorsal side of an amphibian egg became located strictly opposite to sperm entrance point (see Chap. 3 for details). In brown algae, the egg pole giving rise to rhizoid became oriented oppositely to the source of light (Jaffe 1969). Thus, Curie principle seemed to be saved at a low price. However, further investigations of similar objects showed that the situation is not so straightforward. The rhizoid of algae eggs was growing in a polarized manner even in the case of isotropic illumination (op. cit); similarly, amphibian eggs underwent dorsalization in the absence of sperm (during parthenogenesis) or when the sperm was inserted exactly in the animal pole being thus unable to break symmetry (Nieuwkoop 1977); moreover, in mammalian eggs, the sperm entrance point is completely unrelated with embryo polarity. It is even more hopeless to find external dissymmetrizers for more advanced structures characterized by translational asymmetry: None of embryonic inductors are able to play this role.

In addition to the observations of intact embryos, the standard experimental procedures associated with changes of mutual positions of body parts can also be taken as adequate criteria of a symmetry order inherent for a given stage embryo. Indeed, if any possible replacements of embryo parts are compatible with its further normal development, we may say that by the criteria of a developmental fate, the given stage embryo has the highest possible symmetry order. Accordingly, if any

single replacement will disturb the entire developmental pathway, the symmetry order estimated by the same criteria should be reduced to 1. So by experimental criteria, similarly to morphological ones, the reduction of symmetry order coincides with the advancement of development.

In some cases, the intermediate steps of such reduction can be traced. One of the best examples is given by classical works of the American embryologist Ross Harrison performed almost a century ago (Harrison 1918). The researcher was interested in tracing the capacity of the limb rudiment to adjust its orientation to the entire body antero-posterior (AP) polarity at the successive stages of development. For this purpose, he turned a still flat limb rudiment (limb disk) of urodelean embryos in such a way that either both AP and DV axes, or only one of them was rotated to 180° in relation to the AP axis of entire body (To rotate just one axis was possible by transplanting a limb disk to the opposite side of embryo) (Fig. 1.7).

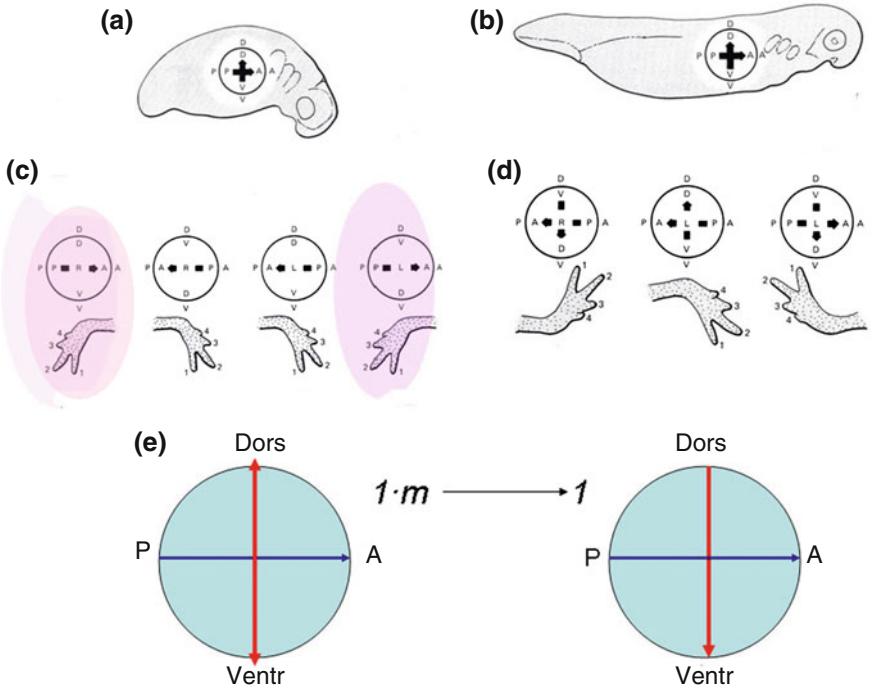

Fig. 1.7 Harrison's experiments on regulations of limb orientation according to body axes. **a**, **b** Ambystoma embryos at two successive stages of development. Shown are dorso-ventral (DV) and antero-posterior (AP) axes of entire bodies and limb buds. **c** A normal limb disk orientation (*left frame*) and results of its rotations at stage A. Only rotations of DV axis keeping AP axis intact (*right rose frame*) are compatible with normal orientation of a limb bud. **d** Results of limb bud rotations at stage **b**. None of these are compatible with normal limb orientation. **e** Harrison's results described in symmetry terms

The results crucially depended upon the stage when the operation has been performed. At the earliest stage, the normal limb orientation was restored after rotation of the both axes of a disk; at the intermediate stage, the restoration could be achieved after rotation of DV, but not AP disk axis (see frames marked by rose color), and at the most advanced stage, none of the axes' rotations were compatible with restoration of the normal orientation. In addition to demonstrate by experimental criteria the successive symmetry breaks, these results show that determination of limb polarity is in each stage essentially holistic: At the intermediate stage, it is AP axis as a whole, rather than any small material element which specifies its final fate. This property permits to describe the results of Harrison experiments in the symmetry terms: By a criteria of the developmental fate, at the initial stage, the limb disk has a rotational symmetry of infinite order ($\infty \cdot m$); at the intermediate stage, it is reduced to $1 \cdot m$ (symmetry axis coinciding with DV axis); and at the final stage the symmetry order becomes 1.

It is important (besides all, for satisfying Popper's falsification criteria) that it is possible not only to imagine but to reproduce experimentally some morphogenetic processes with exactly opposite symmetry dynamics, that is, tending to increase rather than decrease symmetry order. Among those, most important are the so-called cell sorting events described by Townes and Holtfreter (1955) and interpreted in terms of the differential adhesion hypothesis (Steinberg 1978). These experiments start from randomized arrangement of different types of strictly determined cells which become finally segregated into concentric layers (Fig. 1.8). Initial configurations, if evaluated by criteria of color symmetry, cannot be matched with themselves by any kind of movements due to cells heterogeneity: Hence, their symmetry order is 1. On the contrary, the final arrangement is much more symmetric, approaching roughly the symmetry order of a sphere ($\infty/\infty \cdot m$).

Another instructive example is given by Elsdale (1972) observations on the behavior of fibroblast monolayers in the presence of collagenase, destructing collagen fibers. Under these conditions, randomly oriented fibroblasts were grouping into vast domains of parallel oriented cells. Finally, all of the domains have been fused into a single giant one. To what kind of symmetry transformations should we attribute these processes?

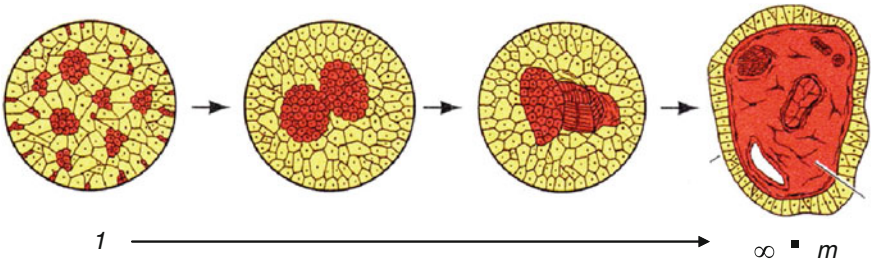

Fig. 1.8 Symmetry transformations under standard cell sorting experiments. For detailed description, see text

The key event here is the axiality ($2 \cdot m$ symmetry order) of each individual cell (lacking in the previous example). If we deliberately neglect it, we have to assume the initial symmetry order to be very high ($\infty \cdot m$ for the case of monolayer) so that the subsequent transformations should be estimated as the reduction of symmetry order down to $1 \cdot m$. This is not so, however, because the formation and fusion of the domains is based upon the inherent axiality of individual cells. Taking this into consideration, the initial symmetry will be of the order 1: a population of the randomly oriented axially symmetric cells would not coincide with itself under any shifts or rotations. Similarly to the previous example, the final stage is characterized by the increase of symmetry order up to $1 \cdot m$. Same is the evolution of the freedom degrees of the individual cells: Their mutual shifts are mostly hampered under random arrangement but facilitated under parallel one. In this respect, the behavior of aligned cells is quite similar to that of the liquid crystals (to be discussed below in this chapter).

> Noteworthy, such a type of behavior is taking place in the absence of long-range interactions, which may be introduced by seeding cells onto elastic substrates or by deposition of extracellular matrix. As we will show in Chap. 3, under the latter conditions, the initial symmetry order will be reduced.

Sometimes, the short-and long-range interactions coexist at different scales. By studying the formation of supramolecular structures (so-called ciliary units) in unicellular Ciliates, Frankel (1989) established a linear threshold (about 1 μm length) subdividing a smaller realm into which the symmetry order of the units' arrangement is "dependent only on the intrinsic properties of the building blocks" (op. cit) from the larger scale one where the units become oriented according to the entire body handedness, rather than their own chirality sign. Thus, the "Frankel's barrier" delimits the domination zones of the short- and long-range interactions.

It is of interest to note that in the most primitive metazoans, the short-range order and the corresponding tendencies to symmetry increase seem to dominate: Thus, in slime molds, the proper mutual positioning of their only two cell types, so-called prestalk and prespore cells, is achieved by a kind of cell sorting (Nicol et al. 1999) rather than according to their positions within a whole. On the other hand, in all the real metazoans developing from macroscopic eggs, the long-range types of order and the associated successions of symmetry reduction dominate from the earlier stages.

Now it will be important to address again to the Curie principle. How should we estimate it after recognizing that most of developmental symmetry breaks look as being proceeded spontaneously? Is this an argument for rejecting the principle? Before doing this, let us explore the situation in more details: This will permit us not only save Curie principle in relation to embryonic development at any price, but make this in a highly constructive way. The matter is that the Curie principle is not bound in any way to exact magnitudes of symmetry breaking agents: in fact, they may be indefinitely small. On the other hand, both whole organisms and their constituent parts are always exposed to some kinds of "noise," that is, to small perturbations of quite different nature coming from somewhere outside. Accordingly, instead of

rejecting Curie principle, one may suggest that for becoming able to symmetry breaks, the embryos should acquire a high sensitivity to some kinds of noise, perceiving them as dissymmetrizing agents; on the other hand during other periods, they should be indifferent to many external disturbances. This idea brings us closely to fundamental notions of SOT, and first of all to those of instability and stability. Let us look now how these notions and principles can help us in comprehending the main property of morphogenesis—regular complication of organic shapes.

1.2.2 Parametric and Dynamic Regulations: Several Basic Models

1.2.2.1 Stratification of Variables According to Characteristic Times

As mentioned in the Introduction, among the main properties of our world is its stratification to a number of more or less discrete levels distinguished from each other not only by characteristic dimensions (Lch) but also by "characteristic times," or Tch (reversed rates) of the events. Although in biology a scale of structural levels has been used for long ago, its real importance could be apprehended only within SOT framework. This is because there are differences in Tch which permit to distinguish two main categories of the variables: the *dynamic* ones characterized by small Tch and the *parameters*, whose Tch should be at least in an order greater.

In the following table, the dimensional and temporal ranges of Lch and Tch belonging to several levels most important for developmental processes are given:

Description of the level	Lch, meters	Tch, seconds
1. Macromolecules transducing chemical energy into mechanical	$\approx 10^{-8}$	$10^{-3} - 10^{0}$ (relaxation time)
2. Supramolecular non-covalently bound structures	$10^{-7} - 10^{-5}$	$\approx 10^{0}$ (assembly−disassembly time)
3. Single cells	10^{-5}	$\approx 10^{2}$ (average time for changing neighbors)
4. Embryonic territories capable of regulations (morphogenetic fields)	$10^{-4} - 10^{-3}$	$10^{2} - 10^{3}$ (time from formation to next step of segregation)
5. Whole organisms	$10^{-3} - 10^{1}$	$10^{5} - 10^{8}$ (duration of life cycle)

1.2.2.2 Linear and Nonlinear Feedbacks: Links to Embryology

Self-organization is impossible if the variable whose changes are a matter of our interest does not act back upon itself, whether positively or negatively. The simplest (but quite far from being the only one) way to explore feedbacks is to take as

examples autocatalytic or autoinhibitory chemical reactions. The first of them display positive and the second negative feedbacks between the amount of synthesized substance and the rate of its synthesis. The both can be described, in the first approximation, by linear differential equations: $dx/dt = kx - C$ for autocatalytic and $dx/dt = -kx + C$ for autoinhibitory reactions. Here, x is a dynamic variable while k and C are the parameters, their Tch being, ex definitio, at least an order greater than Tch for x. Even such simple feedbacks, as depending upon the sign of the parameter, can reproduce two main states of any self-organizing system: a dynamic (Lyapunov's) stability or instability. Indeed, at $k < 0$, a dynamic variable comes to a single stable state, while under $k > 0$, it becomes unstable and diverges toward $\pm\infty$; in practice, that means that it does not exist at all.

The feedback loops can be complicated in different ways: by including positive and negative ones in the same equation, by increasing the number of variables or by passing toward nonlinearity. Let us start from exploring the latter way.

While in the context of linear differential equations, instabilities lead to nothing except destructing the system, if introducing the second (and better a third)-order nonlinearity, they become to play a constructive role by increasing the system's complexity (reducing its symmetry order). In this way, nonlinearities cooperate with Curie principle. Let us also take into mind that nonlinearity (the existence of more than one solution for a given argument value) directly contradicts the classical determinism ("one cause–one effect" paradigm). Endowing the system with the elements of randomness (non-predictability), the nonlinearity provides at the same time its capacity to produce *novelties,* that is, something beforehand non-existed and even non-predictable. As claimed by Prigogine and Stengers (1984): "A novelty is a measure of a causal independence (indefiniteness) of successive states of a developing subject in relation to preceded ones." Neither individual, nor evolutionary development can take place without acquiring novelties, and hence without nonlinearity.

A simplest model illustrating the acquiring of novelties and reduction of symmetry order is described by the following third-order differential equation:

$$dx/dt = kx - k_1x^3 \ (k_1 > 0) \tag{1.1}$$

It combines a first-order positive feedback with a third-order negative one. As can be checked by simple algebraic calculations, at $k < 0$ the equation has only one solution ($x = 0$) which is stable, while at $k > 0$, it has three solutions ($x_1 = 0$; $x_{2,3} = \pm \sqrt{k/k_1}$) among which x_1 becomes unstable and new ones ($x_{2,3}$) are stable (Fig. 1.9a). While passing from $k < 0$ to $k > 0$, the variable x moves toward one of two new stable solutions from any point of the *phase space*,[2] leaving x_1 under any negligibly small perturbation along the x axis (this is so-called soft regime). At the same time, the indefinite-order translational symmetry characterizing $k < 0$ area is

[2] A phase space is a space in which all possible states of a system are represented, with each possible state of the system corresponding to one unique point in the phase space.

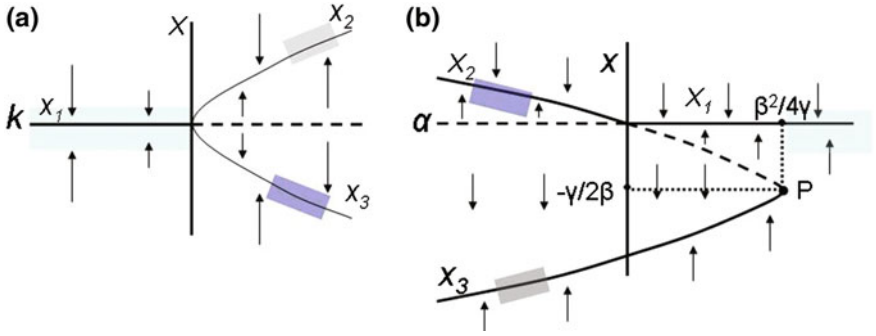

Fig. 1.9 **a**, **b** Soft and hard bifurcation regimes. In the both cases, parameters (k and α, respectively) are plotted along the horizontal and the dynamic variable (x) along the vertical axes. X1 is non-differentiated state (marked by *light blue*) split into alternative differentiation states x2 and x3 (*dark* and *light lilac*) either by infinitesimal perturbations (soft regime: **a**, $k > 0$, B, $\alpha < 0$) or by finite perturbations (hard regime: **b**, $0 < \alpha < \beta 2/4\gamma$)

completely lost. Let us note that variations of the parameter k values (with another parameter, k_1, being constant throughout) and those of the variable x play quite different roles in determining the system's behavior, namely a shift of the k parameter value from negative to positive endows a system by a *possibility to select* any one of the newly emerged stable states (x_2 or x_3), while *the result of selection* will depend upon whether the perturbation of a dynamic variable is shifted toward positive or negative x values. Hence, the first decision is regulated *parametrically*, that is by relatively slow and spatially smoothed evolution, while the second is regulated *dynamically*, due to faster and more local events. Such a strict separation between acquiring the ability to select one of the developmental pathways, and the selection itself is one of the most essential properties of organic development, being noticed by embryologists well before SOT was outlined. In embryological terms, the first (parametrically regulated) property is called *competence,* while the second (dynamically regulated) is defined as *determination* of a given part of embryonic tissue. A possibility to describe these properties in SOT language means that embryonic development obeys universal laws of nonlinear systems behavior.

Let us emphasize that at $k > 0$, initial values of the dynamic variable required for reaching a definite stable state do not need to be set up precisely: It is enough to limit their range either by a positive or by a negative semi-infinity. In mathematical terms, this means that dynamic regulation can be (and as a rule is) highly degenerative. This is in opposition to a widespread opinion that biological systems require very precise regulation. Actually, it is not so: in fact, their extreme reliability is based upon the capacity to produce precise responses to non-precise impulses. This again may take place only in nonlinear regimes.

Even more adequate for representing the universal properties of developing systems is a somewhat complicated version of Eq. (1.1) with an additional quadratic term, describing a new second-order feedback:

$$dx/dt = \alpha x - \beta x^2 - \gamma x^3 \tag{1.2}$$

This equation (Fig. 1.9b) always has one solution ($x = 0$) which is stable at positive and unstable at negative α values. Meanwhile, under $\alpha < \beta^2/4\gamma$ two other solutions appear in a peculiar and biologically relevant asymmetric manner, namely both of them are emerged in a single point P of a phase space as a kind of jump [rather being smoothly branched from a previously existed solution as it took place in Eq. (1.1)]. Among them, the middle one (x_2) is unstable under positive and stable under negative α values while x_1 solution behaves in a reverse manner. The solution x_3 is always stable.

These properties, associated with the appearance of a new feedback very much enrich the developmental potencies and regulatory properties of the imaged system. While that one described by Eq. (1.1) should pass toward new stable states under any infinitesimal perturbations (in a so called soft regime), the transition from x_1 to x_3 at $\alpha > 0$ will go now only under finite perturbations, because in this area of α values the two stable states are separated from each other with the instability barriers. The latter's existence opens new ways for the dynamic regulation of the system's behavior making it more reliable. At the same time, Eq. (1.2) learn us that the state of a competence (which depends upon the parameters values) may itself undergo a qualitative evolution from the area $\alpha > 0$ characterized by requirement of a finite perturbation for reaching x_3 to $\alpha < 0$ when the same transition can be reached in a soft regime.

1.2.2.3 Periodic Regimes and Creation of New Levels

Let us consider now a system of differential equations with two dynamic variables, x and y, having drastically different Tch: y evolving much faster than x. Accordingly, x is defined as a slow variable and y as a fast one. For equalizing the right parts rates, the term dy/dt is multiplied by so-called small parameter ε. A simplest system of this kind to be of interest is called Van der Pol equations. It looks like

$$dx/dt = y \tag{1.3a}$$

$$\varepsilon \cdot dy/dt = -\left(y^3 + ay + x\right) \tag{1.3b}$$

As one can see, the both variables are linked by "+, −" feedback loop: The variable y acts positively to the variable x, while x acts negatively to y. Another new property of the system is its three-level structure (if including the parameter a, assumed to be constant). The system's behavior is characterized by the presence of

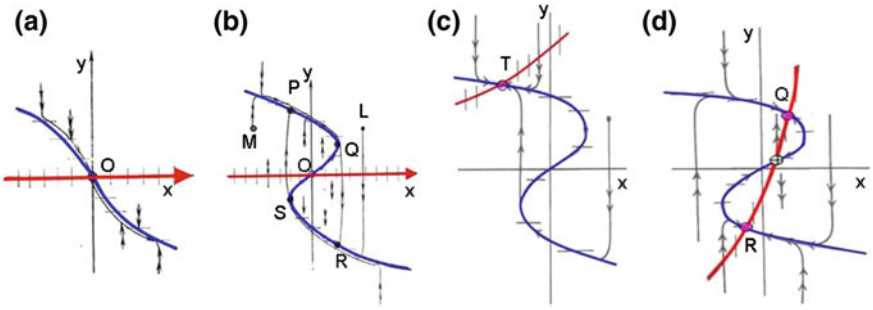

Fig. 1.10 **a**–**d** Phase portraits of auto-oscillations and related regimes. **a** Attraction toward a single stationary point under $a > 0$. In **b**–**d** $a < 0$. **b** Auto-oscillations. **c** Relay regime. **d** Trigger regime. x-zero isoclines are shown in *red* and y-zero isoclines in *blue*. In **a** and **b**, x-zero isoclines coincide with $y = 0$ axis, while in **c** and **d**, they deviate from this axis are inclined and slightly curved

a so-called attractor toward which the dynamic variables trajectories are rapidly (with dy/dt rate) approaching from all the points of a phase space. In its turn, the attractor's configuration crucially depends upon the sign of the parameter a. At $a > 0$, it is a cubic parabola after falling to which the variables are slowly (with dx/dt rate) moving toward a stationary point O which is called the stable nodule (Fig. 1.10a). Much more interesting is the system's behavior under $a < 0$: Now the attractor takes the shape of the so-called limit cycle consisting of two periods of slow movement (along the branches PQ and SR) and two fast "jumps" (QR and SP) (Fig. 1.10b). At the same time, point O becomes unstable. As a result, an entirely new temporal level is born, characterized by a non-damped oscillation period; remarkably, this temporal value depends upon those having no temporal dimensions at all: to these belong a constant parameter a and the entire structure of x, y feedbacks described by Eqs. (1.3a, 1.3b). This is a clear example of generation of a new quality.

The limit cycle is very robust in the sense that that the "phase point" (describing a system's state in the phase space) gets onto it without a possibility to escape from any point of a phase space (e.g., from points L or M, Fig. 1.10b). On the other hand, it principally differs from classical mechanical oscillations driven by external forces (that is, by perturbations alien to the oscillating body itself). Rather, in the case considered, the oscillations are supported by the kinetic properties of the oscillating system itself. Accordingly, such events are defined as *auto*-oscillations, taking place in the *active media*.

Auto-oscillations can be regulated and essentially transformed by including new parameters [mostly in Eq. (1.3a)], e.g., by adding a constant parameter b

$$dx/dt = y - b$$

The movement of the imaging point along the upper branch of the limit cycle is now slowed down compared to the lower branch; under large enough b values a new

stable point T is emerged (Fig. 1.10c) transforming non-damped auto-oscillations to the so-called waiting, or relay regime. Even more extensively, the system will be transformed by sloping x-zero isocline:

$$dx/dt = ky - b$$

If the slope is great enough, x-zero isocline intersects, in addition to the unstable branch QS, also PQ and RS sections of the stable branches (Fig. 1.10d). Under these conditions, two stable nodules, Q and R, are created. A switching from one to another is possible only under finite perturbations of x-variable, shifting it toward the verges of fast jumps. This model exemplifies the so-called trigger regime characterized by the existence of two alternative metastable states. As argued in Chap. 4, this regime plays a first-range role in regulating morphogenesis.

1.2.2.4 From Determinism to Stochasticity

The above-presented models are called deterministic in the sense that they generate predictable and as a rule uniform patterns of behavior even if starting from quite variable (noisy) initial conditions. Certainly, this designation does not mean that they obey the classical "one cause–one effect" determinism: Rather, the latter would always produce different results under different initial conditions which as we could see is not the case. The dynamic stability of the above models is provided by parametric regulation which is quite far from being precisely addressed but is instead essentially smoothed both in time and in space, bearing thus holistic properties.

A similar rise of precision in the course of development (which in a number of cases starts from rather variable initial stages and comes to more uniform results) was known to embryologists for a long time and was called equifinality. One of the greatest embryologists of a remote past, Carl Ernst von Baer, after tracing equifinality in a great set (more than 2,000 samples) of chicken embryos concluded: "it is not any stage by itself which, owing to its own properties, determines the next, but instead, more general and higher relations regulate all of this…" (Baer 1828). Today we may identify these relations with parametric regulation.

Remarkably, the parametric regulation can also bring to opposite results, namely to make a chaos out of order. One of the simplest scenarios of such transformation is based upon so-called logistic equation

$$dx/dt = \lambda x(1-x) \tag{1.4}$$

widely employed for describing the so-called restricted, or S-shaped growth, with its rate firstly increasing and then decreasing in a symmetric fashion. We shall use this expression as a discrete *reflection* written as

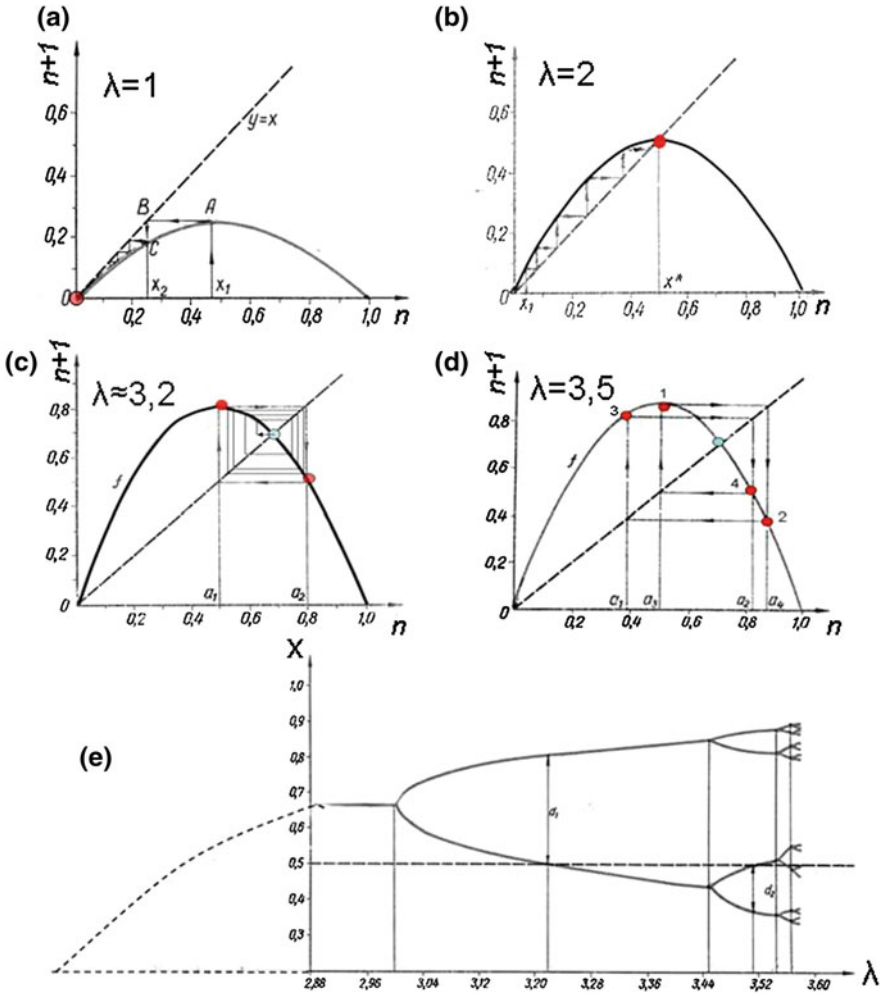

Fig. 1.11 From order to chaos. **a–d** Increase of parameter λ values (shown) transforms single stable point to an increased set of alternated states. **e** Splitting into increased number of alternated states as a function of λ values

$$x_{n+1} = \lambda x_n(1-x_n) \tag{1.4a}$$

where x_n and x_{n+1} are x values at discrete time points n and $n + 1$. The plot of (4a) is bell-shaped, its maximal height proportional to λ value (Fig. 1.11a–d). We have to explore what points at the reflection plot will be immobile and which ones among them will be stable under not too large variations of λ values. Obviously, a condition of immobility is $x_{n+1} = x_n$: The immobile points are always situated at the bisector of the coordinate angle (dashed lines in Fig. 1.11a–d). Also, it can be proved that the condition of stability is $[df(x_{immobile})/dx] < 1$. It is possible to derive

from these results that under the smallest λ values ($\lambda < 1$), there is only one stable point at $x = 0$ (Fig. 1.11a). With λ increase, this point at first shifts to non-zero x values still keeping its stability (Fig. 1.11b), but later on (when the bell-shaped graph becomes steep enough for intersecting the bisector by its descendant branch), the stability is lost. Most important is that in this case, contrary to the above-considered instabilities, the point is not moved toward infinity; rather, it starts to oscillate at first between two discrete points (Fig. 1.11c) and then (with further λ increase) between 4, 8, 16, 32… such points (Fig. 1.11d). In other words, a quasi-stable periodic solution will run through increased numbers of different x values until each next value will become practically unpredictable: a system will come to a state which we shall qualify as chaotic (Fig. 1.11e). Being plotted in the time coordinates, these regimes correspond to chaotic oscillations; if unfolded in space, they give rise to so-called fractal structures, remaining self-similar at quite different scales. A living matter is full of such examples.

The very existence of such structures is fatal for the classical determinism: It would be meaningless to search an individual cause for any single fractal structure—an entire set of these is generated at once by shifting just a single parameter λ. What might be its biological meaning? We can see that λ value determines the interval between two successive x values: If the interval is small, the system behaves in deterministic manner, while at larger intervals, it approaches a chaotic state. On the other hand, the interval between neighboring x values can be regarded as the gap (most probably temporal) between the action and the response or, in other words, as a measure of the feedback rate. Below (see Chap. 4), we shall see that modulations of the feedbacks rates may be among the main tools for regulating morphogenesis. In addition, as being non-spatial, such modulations are easily opened for being directly affected by genetic factors. All of this makes plausible that "playing" with λ values, a biological system employs one of the most effective ways to regulate development, sometimes approaching and sometimes leaving the verge of chaos.

1.2.2.5 Self-organized Criticality

As it was shown during the last few decades, first by theoretists and then by experimenters, the state maintained at the verge of chaos turned out to be, in some sense, rather stable. Consider a sand dune: being from time to time flattened by unpredicted avalanches of various sizes, it restores each time its typical inclination even if moving to some extent from one location to another. This peculiar state is defined as a "self-organized criticality" (see Ball 2001). Being non-equilibrial (a sand dune is created and supported by the energy of the wind), such a system exhibits from time to time large-scale perturbations (avalanches) for which only statistical probability rather than deterministic schedule can be estimated. In double-logarithmic coordinates, the frequency of different size avalanches versus their size obeys a linear slope: small avalanches appear more often than large ones. Events obeying this law are called the scale-free ones: being in a self-criticality state, a system looks as erasing the differences between characteristic times and/or spatial

scales typical for hierarchical systems in the "normal" conditions: Looking again on a sand dune, we can see that it possesses neither characteristic size nor characteristic frequency of the avalanches taking place from time to time. In a sense, this is an ideal case of a holistic, absolutely undivided system.

Many biological systems, from respiration of yeast cultures to electrical records of neural activity, reveal the state of self-criticality. In the next chapter, we shall discuss some similar events related to so-called glassy state of actin networks. However, quite few studies of this kind were performed on the developing organisms. One of the most relevant is that by Gamba et al. (2012) performed on fresh water hydra embryos. By studying the size distribution of gene *ks*1 expression spots, the authors found that it is close to scale-free patterns just at the time of determination of the main body axis. It would be of a great interest to know whether scale-free dynamics is a universal property of developing systems during their transition to a determined state.

1.2.2.6 Spatial Unfolding of Self-organized Regimes

Although nothing in principle forbids to unfold the parameters of the above models not only in time, but also in space, such a possibility is rarely used: To do this would be to consider the space a priori heterogeneous, which contradicts the main SOT demands. A usual way for providing a spatial unfolding by preserving the space homogeneity is to use a notion of diffusion in its broadest sense. It means that if within the active medium (endowed by a proper nonlinear dynamics) the concentration of a certain substance (or the amount of some measurable physical state) X is, due to a perturbation, locally increased, X will be propagated with the rate linearly proportional to the second derivative of X to space coordinate. The basic equation for the diffusion-mediated propagation along one-dimensional reactor is

$$\delta x/\delta t = f(x) + D_x\left(\delta^2 x/\delta r^2\right) \tag{1.5}$$

where *f(x)* describes the kinetics in any point of the active medium (the so-called point kinetics), D_x is the diffusion coefficient and r is the sole spatial coordinate of the reactor. If the point kinetics produces auto-oscillations, its spatial unfolding will look as the so-called autowave of a definite length, moving from the point of initial perturbation to the opposite edge of the reactor. Autowaves are the most remarkable examples of spatial structures created "out of nothing," that is, without any template (the above-described auto-oscillations exemplify temporal structures of similar origin). As claimed by Krinsky and Zhabotinsky (1981), "autowaves exemplify a new type of dynamical processes generating macroscopic linear scale due to local interactions, each of them possessing no linear scale at all." This definition captures the very essence of self-organization and is more precise than qualifying it as emergence of order out of fluctuations: the matter is that the notion of "order" itself requires further explication.

From thermodynamic point of view, autowaves belong to so-called dissipative structures, maintained only under a continuous flow of reagents and energy.

Meanwhile, dissipative structures can well be stationary. Such structures were firstly observed by a French physicist Benard in thin layers of a viscous liquid heated from below: These are so-called Benard cells separated from each other by coherent upward-directed convection flows of the liquid. The importance of these formations has been realized much later, when a British mathematician Alan Turing gave a model of formation of stationary waves of a given length out of a "noise," the latter containing the waves of any lengths (Turing 1952). Although Turing's model had no direct biological parallels, it became extremely influential as revealing some unique and most probably universal properties of spatial self-organization. They are the following.

The 1-dimensional reactor (either tubular or toroidal), if non-perturbed locally, should always contain an integer number of half-waves. Thus, if the reactor's length is gradually changed, it will always contain an integer number of half-waves: Accordingly, the half-wave numbers will be changed abruptly, after passing a certain threshold. Locations of the thresholds depend upon the direction of the length changing: If the length is increased, the thresholds are shifted toward greater values as compared to their positions under reverse movement. In other words, a system possesses a kind of primitive "memory" of its immediate past.

Under progressive shortening of the reactor, we reach the length threshold after crossing which only one half-wave (lacking mirror symmetry) can be formed from the random noise; formation of a complete (mirror symmetric) wave within the same length range is possible only by applying precisely located directed perturbations. The structures of the first class (those formed spontaneously, without requiring special perturbations) are called senior modes, while those of the second class (molded by perturbations) are called the junior modes. Under further shortening, the next threshold is reached marking a "homogeneity border": No structures can be now generated, whatever great would be the initial perturbations. These results belonging to pure mathematics have interesting parallels in the development of organisms. Spontaneous formation of asymmetric structures may explain the absolute domination of unipolar configurations over bipolar ones almost at any structural level of the living matter. The lack of differentiation in very small pieces of embryonic tissue is also a firmly established phenomenon. Thus, the Turing's model, being unrealistic in concrete details, captures several fundamental features of self-organizing systems.

Interestingly, in spite of calling his paper "On the chemical basis of morphogenesis," Turing in no way neglected a possible role of mechanical factors in providing self-organization (see Howard et al. 2011): The main reason for preferring chemokinetic models to mechanical ones was that the first ones were much easier to calculate. However, as we shall see later such a seeming easiness, when applied to morphogenesis has its own shortcomings.

During several decades following publication of a seminal Turing's paper, a great number of models based upon similar ideas appeared mostly known as chemokinetic models of morphogenesis (Meinhardt 1982). Common for all of them is the assumption of "chemical prepatterns," that is, local inequalities in the concentrations of certain substances (morphogenes) serving as precise templates for

morphological structures or/and certain differentiation pathways. Actually, this concept is quite similar to that of PI and is confronted with the same difficulties. Let us look in more details what this model means if being applied to the formation of serial evaginations, such as scales, appendages, and buds. For deriving specific shapes of these rudiments from chemical prepatterns, we have to assume a precise one-to-one dependence of the local curvatures upon the local concentrations of morphogenes. Same dependence should take place within an entire course of development. Thus, we have to accept that the postulated concentration gradients should evolve during development in a regular way, which will be another for any next rudiment: All of these demand separate explanations. Instead of simplifying the entire picture, we come to what is known as an increased multiplication of essences.

In certain cases, the chemical prepatterns, configured like more or less smooth gradients, can play a role of initial conditions, canalyzing somehow the course of morphogenesis, but to consider them as one-to-one morphogenetic templates seems unrealistic. Leaving for the future further elaboration of this important problem, let us ask ourselves, whether morphological structures can be created without any chemical prepatterns. In this chapter, we explore this possibility using in most cases the model examples.

1.2.3 Shaping Without Prepatterns

In this section, we come closer to the realm of mechanics. The reader unfamiliar with its main notions is asked to look for the Sect. 1.2.4, which includes, in addition, the list of recommended readings.

We start from considering a rod to which a compressing axisymmetric force is applied either from one side (the opposite one fixed) or from both sides equally. If the rod consists of a soft (easily deformable, plastic) matter, it will be shortened while remaining rectilinear. However, if it has some elastic resistance, when the compressing force exceeds a certain threshold, the rectilinear shape loses its stability and the rod will be bent to one of the sides. This is the case of the well-known Eulerian instability, described by a great eighteenth-century mathematician Leonard Euler. It obeys Eq. (1.1) and is the simplest case of mechanical instability, leading to the reduction of the symmetry order. On the other hand, it provides the basic model for a large group of morphogenetic processes, driven by increase of internal pressure in cell layers (see Chap. 3 for more details). By furnishing the rod with cross-beams which are also elastic, we may bring the model even closer to biological realities, imitating its cellular structure (Fig. 1.12a). Now, under even infinitesimal deviation of compressing force from the central axis of the rod, the cross-beams will be stretched in asymmetric manner (Fig. 1.12a, hatched lines), increasing elastic energy of transversal surfaces. Being driven toward the minimal elastic energy value, each "cell" tends to return toward rectangular shape which, under continuous action of the pressure force, is possible only by bending the entire

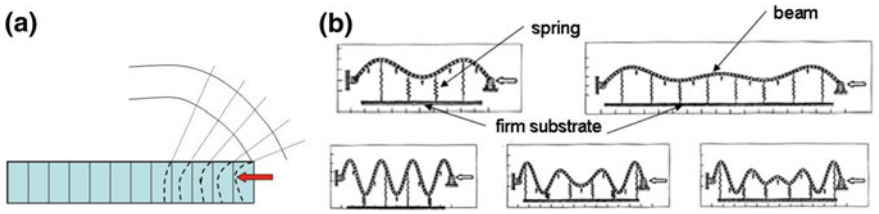

Fig. 1.12 Shape formation via Eulerian instabilities. **a** Bending of a rod split to "cells" with elastic walls (*hatched*) under the action of a slightly eccentric pressure force (*arrow*). The final deformation (*dotted*) is the result of the drift of the bent cell walls toward more relaxed symmetric state. **b** Some examples of bending patterns of laterally compressed elastic rods connected with a number of firmly fixed springs. In each case, the resulted pattern corresponds to the minimal elastic energy state of the entire two-components system and to the maximally homogeneous spread of its energy. Note that in no case, the bending wavelength fits the spring arrangement [From Green et al. (1996), with the authors permission, modified]

rod. It is easy to show that the bending will be directed to the side of the force deviation from the central axis. In this way, we get a two-leveled image of the rod's bending ("cells" first, the whole rod next) which closely imitates some basic epithelial morphogenesis (see Chap. 3 for more details).

As the next example, we take a deformable beam connected with a bundle of elastic springs firmly fixed from the opposite side (Fig. 1.12b). In this case, under the action of lateral pressure the beam will be bent as a rule in several points, always producing an integer number of half-waves. With the beam elongation, the number of half-waves is increased in a threshold manner, imitating thus Turing's behavior without any morphogens! Worth mentioning, in no way the wave pattern fits that of the springs' attachments. If the beam is circular, has finite thickness, and is compressed by its own internal forces (the most natural morphogenetic situation), the resulted half wavelength λ_n can be calculated by the formula

$$\lambda_n = 2\pi(D/k)\exp(1/4) \tag{1.6}$$

where D is the bending rigidity and k is the coefficient of the spring elasticity (Green et al. 1996). Interestingly, if the beam is thick enough, the "conflicts" may arise between its outer and inner perimeters, each one tending to arrange an integer number of half-waves; as a consequence, some irregularities of the resulted pattern will take place.

Now let us address to some examples of shape formation in balloon-like and vesicular bodies, covered with thin elastic shells. We start from considering a flattened puck-like balloon with radius a and height b, inflated through a central pore. As shown by Martynov (1982) if and only if $a > b/\sqrt{2}$, the inflation will stretch the lateral walls of ellipsoid in meridional (vertical) direction and compress it in the equatorial (horizontal) direction (Fig. 1.13a). If the shell is not too thick and rigid the inflation will produce N vertical folds which will be exchanged by the same amount of horizontal folds during deflation. In the both cases, $N \approx 4\sqrt{a}/S$ where S is the thickness of the shell. We can see that the uniformly applied forces within a

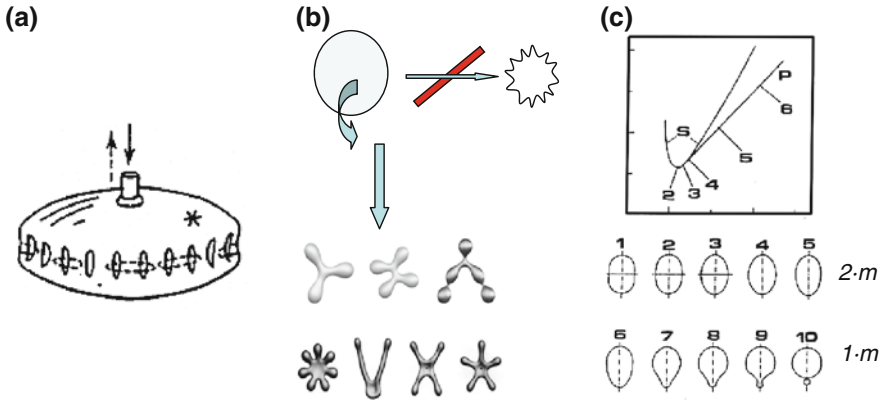

Fig. 1.13 Morphogenesis (symmetry breaks) without chemical prepatterns, driven by energy minimization. **a** Formation of folds under inflation/deflation of a flattened balloon. **b** Formation of "starfish vesicles" from a deflated baloon instead of its uniform shrinkage. **c** Svetina and Zeks (1991) model. Upper frame: a plot of the relative membrane bending energy (*vertical axis*) as a function of the average membrane curvature (*horizontal axis*). The curve denoted S is for shapes with 2 · m symmetry and the curve denoted P for shapes with 1 · m symmetry. Lower frame: numerically obtained axisymmetric shapes with minimum membrane bending energy. After exceeding a certain average curvature threshold, there are 1 · m rather than 2 · m symmetry figures which exhibit local energy minimae. **a** From Martynov (1982), with the author's permission; **b** from Wintz et al. (1996), with the publisher's permission. **c** from Svetina and Zeks (1991), with the authors' permission

restricted but not too small range of initial geometric conditions can produce extensive rotational asymmetry.

A set of the different deformations, each of them decreasing symmetry order, have been obtained in small lipid vesicles (Wintz et al. 1996). The osmotically driven shrinkage of initially spherical vesicles led to formation of peculiar figures with rotational ($n \cdot m$) and mirror-like ($1 \cdot m$) symmetry, some of them called by the authors "star-fish vesicles" (Fig. 1.13b).

So we can see that rather complicated deformations, associated with decrease of the symmetry order, and in some cases biomorphic, can be produced without any outside imposed patterning, including chemical gradients of any origin. What are the basic principles of these events?

The general answer will be quite simple: In full accordance to the second law of thermodynamics, all of the above-described transformations are driven by the tendency of a given body to reach the minimum of its free mechanical energy (which was pumped initially by an external force). Why, however, this tendency brings the bodies toward regular shapes with decreased symmetry order instead of increasing their randomness and homogenization? The response is: those are the geometrical and structural constraints which prevent the described bodies from reaching the "absolute" energy minimum, setting them instead for quite different (up to indefinitely long) time periods into the *metastable energy wells*.

In general terms, this can be achieved, if the system possesses a set of stable states to which it is relaxed with a greater rate than to the homogeneous state, and

which are far enough removed from the latter. Obviously, the first condition making this possible is nonlinearity, providing the multiplicity of stable states. Accordingly, the linear systems possessing only one stable state are incapable of morphogenesis. Next, for enough rapid relaxation to specific stable states, the system should possess a restricted number of *selected degrees of freedom*. The physical mechanisms associated with these tendencies will be discussed in the next chapter.

At the moment let us look how these conditions are fulfilled in the above-described shape-forming systems. First, all of them are nonlinear; the nonlinearity of the laterally compressed beams is expressed by Eq. (1.1). Our next question will be what are the pathways toward metastable states, permitting to avoid thermodynamic averaging?

In case of the compressed beam (Fig. 1.12a), the thermodynamic pathway is that directed toward its continuous rectilinear flattening, accompanied by heat emission. It is quite obvious, that this way is unstable, while just those directed away from it (toward bending which exemplifies elementary morphogenetic events) are stable.

In the second example (Fig. 1.12b), the system has the same fundamental properties although if aggravated by the presence of vertical elastic bonds. Morphogenetic stable states will be now determined by a compromise between the beam resistance to bending and the bonds resistance to stretching: in all the cases, the mechanical energy tends to be maximally equalized throughout the system's components. Under these conditions, the number of bending half-waves produced by the lateral compression will be more than one due to the tendency to equalize the elastic energy between all of the system components (including the beam itself and all the springs). Obviously, at the single half-wave bending, most of the energy will be concentrated in the beam itself and in central springs, contradicting the tendency to overall equalization of mechanical energy.

On the other hand, if the number of half-waves will be too great, the main beam would accumulate too much bending energy. By these ways, the system is working as integrated whole.

In the next two examples (Fig. 1.13a, b), there are not only mechanical, but also geometric constraints which canalize the drive toward free energy minimum along morphogenetic (rather than thermodynamic) pathways. In case of the flattened balloon, the constraints are exemplified by the radius/heights ratio, acting in a threshold-like fashion. Meanwhile, in case of the "star-fish vesicles," the situation is somehow more complicated. Here, the bending energy, which is proportional to the local curvature, plays the main role. Being unable, due to the shell's continuity, to reach the absolute minimum (that is, to flatten all the vesicle's surfaces), the maximal curvatures become concentrated in few small regions connected by tubular bridges (flattened in one dimension at least). Later (Chap. 4), we shall see that a similar tendency although if driven by other mechanisms takes place in real embryos. On the other hand, a great multiplicity of the shapes observed in Wintz et al. models indicates the existence of many metastable states which are not so numerous in biological samples. In any case, however, the thermodynamic minimum (which would correspond to a dense wrinkling of the shrunk shell) is avoided.

Svetina and Zeks (1991) modeled a similar situation imitating the increase of a vesicle's surface with its volume kept constant. They showed that after exceeding a certain threshold of the average curvature, there are $1 \cdot m$ symmetry structures (ovoid vesicle with a small bud) rather than $2 \cdot m$ ones (symmetric ellipsoid) which correspond to the minimal bending energy (Fig. 1.13c). This is another example of inherent drive toward the reduction of the symmetry order.

The second law of thermodynamics tells us that a drive toward the free energy minimum can be realized either by a decrease of enthalpy (which is a measure of the total energy of the system) and/or by an increase of entropy (which is defined as a measure of the number of specific ways in which a system may be arranged, often taken to be a measure of disorder). Which of these two members' contribution is the greatest for the systems we are interested in? According to experts' opinion (Cademarini et al. 2011), "free energy… for hard systems [to which the living matter belongs—LB] is dominated by entropic contributions. This leads to the somewhat surprising observation that ordered, close-packed structures are often more probable (i.e., they have higher entropy) than similar amorphous structures, in which "jamming" limits the mobility of the assembling components."

This suggestion can be adequately illustrated by the behavior of so-called liquid crystals, the highly ordered aggregations of rod-like particles. Usually, three main types of liquid crystals are distinguished: nematic, smectic, and cholesteric. While in cholesteric crystals, the particles, due to their intrinsic geometry, are arranged in spiral fashion, the first two types are characterized by parallel arrangement. Among them, in smectic crystals, the particles create parallel rows, while in nematic crystals, no such alignment is taking place although the parallel arrangement is kept. In the both cases, the particles have more freedom that under disordered arrangement because in nematic crystals, any parallel shifts of the particles are allowed, while in smectic crystals, the particles, although if unable to disturb the row, can incline cooperatively at any angle. Accordingly, the entropy of the liquid crystals in spite of their orderiness is higher than that of a dense population of disordered particles and after passing the density threshold the transition toward crystal state is spontaneous (entropy-driven). These arguments are of a direct interest for biologists because multicellular structures with parallel cells arrangement are widely presented in developing organisms (see Chap. 3).

According to the cited authors, from the thermodynamic view, all the structures arisen due to collective interactions of their components can be divided into three categories:

- equilibrial, that is those corresponding to the absolute (under given conditions) free energy minimum;
- non-equilibrial, trapped in long-living metastable states depending upon the history of the system and non-coinciding with the absolute energy minimum;
- dynamic (dissipative) ones which emerge and persist only under continuous presence of thermodynamic gradients and flows, preventing relaxation even toward metastable energy wells.

The above-described shape-forming systems best of all fit the second category. On the one hand, at the start of their formation, they should be pumped by mechanical energy, and on the other hand, they do not require its continuous flow for being maintained within prolonged time periods. At the first glance, this may be not true for compressed beams which seem to require permanent lateral forces for remaining bent; however, since their elementary structural units will be deformed, the mechanical energy becomes internalized within the system itself and what we qualify as the subsequent bending is an autonomous (independent from any outside forces) relaxation toward the mechanical energy minimum predetermined by the units deformations.

This is not to say that dynamic (dissipative) structures in sensu stricto play no role in morphogenesis. Indeed, their role may be very important, but in relation to morphological structures which we see under the microscope or even by a naked eye, it is mainly preparatory. Dissipative structures are visualized mostly as oscillations, flows, or vortices at supramolecular and sometimes cellular level (see next chapters) which are prerequisites of more stable higher level structures.

In general, the morphogenetic interest of the above-described models is in demonstrating that the relaxation of mechanical stresses established by a single force or by a manifold of symmetrically arranged force(s) can produce less symmetric and in many cases biomorphic macroscopic structures. Obviously, this can take place only if a substantial amount of mechanical energy which deforms a body is not immediately dissipated into heat but is instead stored in the form of elastic stresses to be later slowly relaxed to few metastable states. In the next chapters, we will demonstrate that the elastic stresses are taking place in quite different structural levels and are ultimately indispensable for coordinated morphogenesis.

On the other hand, it is to be emphasized that the relaxations are just single parts of the morphogenetic loops: another parts are associated with generation of new forces required for achieving the next mechanically stressed state. In each of the above-discussed models, the initial force was taken as given: this makes these models incomplete (non-closed). One of the main goals of our further account (see Chaps. 3 and 4) will be to search the ways for creating really closed morphogenetic models in which the both branches—generative and relaxatory—will be included in the common feedback contours.

1.2.4 Brief Biologically Oriented Exposure of Some Notions and Principles of Mechanics

1.2.4.1 Main Definitions

Mechanical stress (MS) **p** is defined as the average force per unit area S that some particle of a given body exerts on adjacent particle across an imaginary surface that separates them. **p** is a vector. More precisely, **p** is a limit of the ratio $\Delta\mathbf{p}/\Delta S$ under

$\Delta S \rightarrow 0$. By another definition, MS is a measure of internal forces arisen in the deformed body under the action of external forces. This expression fits our purposes due to emphasizing that the internal forces may be quite different by their values, directions, and spatial arrangement from the external ones.

When dealing with a single surface passing through a given material point of a body, one should distinguish MS oriented perpendicularly (normally) to the surface from those oriented in-plane. Normal MS can be either *tensile* (exemplified by pulling forces) or *compressive* (pushing forces). On MS plots, the first ones are taken as positive, while the second as negative. In-plane-oriented MS produce the so-called shear stresses. In our subsequent account, we shall be dealing almost always with normal MS.

Meanwhile, for getting a complete description of a *stressed state* of a material point belonging to 3-dimensional continuum (which is what we just want to obtain) to consider a single plane is not enough, in general, we have to introduce an indefinite number (a bundle) of such planes passing through the point and calculate MS within each of them. Usually, such a task is reduced toward evaluation of three mutually perpendicular MS components. In combination, they create a mathematical value called the *tensor*, which gives a full description of the stressed state of a material point. Its basic distinction from vector is a lack of unidirectionality: the simplest tensors are bidirectional. This property is of fundamental importance for biological morphogenesis.

Now we pass to deformations which in the case of linear ones are usually exchanged by the notion of *strain*—ratio of deformation over initial length of a sample. From the physical point of view, the deformations are divided into *elastic* and *inelastic* ones. Elastic deformations are those most closely linked with MS which they produce and vice versa: in the ideal case, the elastic strain/stress relation is linear (Hooke law): Real cases are more or less perfect approximations to Hookean ones. During elastic deformations, the mechanical energy is assumed to be preserved exactly in those inter-particles bonds to which it was directly applied by external force, rather than being dissipated over larger areas. Accordingly, elastic deformations are abolished "immediately" (in fact, with a sound wave speed) after cessation of the force action. Although the concept of elasticity in its strict sense is a kind of idealization (because any natural process is accompanied by energy dissipation), it is of an ultimate importance as a referent state.

Inelastic deformations are those characterized by the dissipation (transformation into a heat) of a considerable part of the pumped mechanical energy. The dissipation is accompanied by various and quite complicated rearrangements of the constituent body particles, driven toward thermodynamic equilibrium. Due to irreversibility of these transformations, at least a part of imposed deformation becomes preserved. In many cases, elastic deformations are transformed to inelastic ones under increase of the amount or of the duration of the force action.

For measuring a resistance of an elastic material to deformation (its stiffness), the so-called Young's modulus is used which is the ratio of the *stress* along *an axis* of deformation over the *strain* along that axis in the range of stress in which *Hooke's law* holds. Young's modulus is expressed in Pascals (Pa) or N/m^2.

Most of the living tissues, being stretched in one direction tend to contract in the directions, transverse to the direction of stretching. This is well-known *Poisson effect* which is measured by a Poisson's ratio υ: the fraction (or percent) of expansion divided by the fraction (or percent) of compression (for small values of these changes). The Poisson's ratio of a stable, *isotropic*, linear *elastic* material cannot be less than −1.0 or greater than 0.5.

A number of morphogenetically important deformations and MS are associated with the events phenomenologically quite similar (although never identical) to those taking place in the interphase borders and usually defined as a *surface tension*. So far as a free energy of the surface layer molecules are greater of those located inside a staff, the surface (interphase border) tends to contract up to a minimal (spherical) area enveloping a given volume. Correspondingly, to deviate a surface layer from a spherical shape (for extending the surface), a certain force should be applied (e.g., a pressure force within the surrounded volume). Similarly to inelastic deformations, those driven by surface tension are always directed toward minimum of free energy under the given initial/border conditions.

The main characteristic of a shape is a *curvature* that is deviation of a line from being straight or of a plane from being flat. A curvature k of an arch of a circle is inversely proportional to the circle's radius: $k = 1/R$. For most of our purposes, it will be enough to dissect in our images the contours of embryonic objects to a number of 1-dimensional circular arches (which in general case will have different radii) and to compare qualitatively their curvatures; the latter are called the local. However, for properly use the Laplace law (see below), a flat (1-dimensional) curvature of a line should be replaced by a 2-dimensional curvature of a surface

$$k = 1/R_x + 1/R_y$$

where R_x and R_y are the local curvature radii, oriented in mutually perpendicular planes. Their sum defines what is called the principal curvature in the intersection point of these two planes.

It is easy to see that the surface tension and local curvatures are inversely related to each other: Increase of surface tension tends to smooth the surface that is to diminish the local curvatures and vice versa. This is expressed by Laplace law describing the dependence of the hydrostatic pressure overfall $\Delta p = p_1 - p_2$ (where p_1 and p_2 are the pressures exerted to the surface from its concave and convex sides correspondingly) upon the interfacial tension σ and the local 2-dimensional curvature $\varepsilon = 1/R_1 + 1/R_2$:

$$\Delta p = \varepsilon\sigma$$

what means that the surface pressure is directly proportional and the surface tension is inversely proportional to the local 2-dimensional curvature.

1.2.4.2 Biological Reservations

For good or for bad when applied to biology, strict notions of mechanics to a great extent lose their preciseness, becoming to some extent vague and arbitrary. Probably the main reason for such a transformation is the appearance of the "activity–passivity" alternative almost unknown in classical mechanics but unavoidable in biological applications. To know whether the given MS (e.g., those demonstrating Poisson's effect) are born by external force or generated inside a given tissue piece is for a biologist in many times more important than to measure them accurately. Another principal difference between inorganic and biological samples is the latter's hierarchic structure leaving far behind that taking place, for example, in crystal bodies. In addition, a number of more particular uncertainties are taking place. For example, determinations of the absolute MS values and of the Young's moduli are largely aggravated by a lack of precise understanding what is the real square to which a given normal force is applied. Suggest that we make such estimations for a stretched bulk of biological tissue. As a first approximation, we can take the square of the entire transverse section through the bulk. Under more precise consideration, we have to conclude that the real square to which the force is applied is a total area of cell contact plaques oriented normally to the force. But this is also far from being the end of the story: Individual cell contact plaques also have complicated structure, and their areas are changed during force application, etc.

This is not to say that mechanics is incompatible with biological realities: our viewpoint is just the opposite. The main thing is to make clear the biological meaning of any mechanical measurement. In many cases, qualitative data will be of a greater importance than precise quantitative ones. Although in no way the latter should be rejected, they will make sense only if becoming the members of homologous sets of data permitting the direct comparison: It should be never forgotten that in biology, the relations are much more important than the absolute values.

1.3 Recommended Readings

For the full papers' titles, see reference list:

Schwarz and Gardel (2012)	Defining the main notions of mechanics
Blanchard and Adams (2011)	Describing techniques for measuring mechanical forces at the different structural levels
Diz-Muñoz et al. (2013)	Describes and explains techniques to measure and manipulate membrane tension
Ladoux and Nicolas (2012)	Gives a list of the cell-generated forces and the external forces used for studying the living cells' mechanics

References

Alberts B, Bray D, Lewis J, Raff M, Roberts K, Watson JD (2003) Molecular biology of the cell. Garland Publishing Inc. New York

Baer KE Von (1828) Ueber Entwicklungsgeschichte der Tiere. Beobachtung und Reflexion. ErsterTheil. Konigsberg

Ball P (2001) The self-made tapestry. Pattern formation in nature. Oxford University Press, Oxford

Blanchard GB, Adams RJ (2011) Measuring the multi-scale integration of mechanical forces during morphogenesis. Curr Opin Genet Dev 21:653–663

Cademartiri L, Bishop KJM, Snyder PW, Ozin GA (2012) Using shape for self-assembly. Philos Trans Roy Soc A 370:2824–2847

Capra F (1996) The web of life. A new scientific understanding of living systems. Anchor Books, New York

Curie P (1894) De symmetriedans les phenomenes physique: symmetrieders champs electriqueet-magnetique. J de Physique Ser 3:393–427

De Robertis EM (2009) Spemann's organizer and the self-regulation of embryonic fields. Mech Dev 126:925–941

Diz-Muñoz A, Fletcher DA, Weiner OD (2013) Use the force: membrane tension as an organizer of cell shape and motility. Trends in Cell Biol 23:47–53

Driesch H (1921) Philosophie des Organischen. Engelmann, Leipzig

Eaton S, Julicher F (2011) Cell flow and tissue polarity patterns. Curr Opin Genet Dev 21:747–752

Elsdale T (1972) Pattern formation in fibroblast cultures: an inherently precise morphogenetic process. In Waddington CH (ed) Towards a theoretical biology 4. Essays, Edinburgh University Press, Edinburgh, pp 95–108

Frankel J (1989) Pattern formation. Ciliates studies and models. Oxford University, New York

Furusawa C, Kaneko K (2006) Morphogenesis, plasticity and irreversibility. Int J Dev Biol 50:223–232

Gamba A, Nicodemi M, Soriano J, Ott A (2012) Critical behavior and axis defining symmetry breaking in Hydra embryonic development. Phys Rev Lett 108:158103

Gerhart J (1998) Johannes holtfreter. National Academic Press, National Academy of Sciences, Washington DC, pp 1–22

Gilbert S-F (2010) Developmental biology. Sinauer Ass, Sunderland

Gordon R (1999) The hierarchical genome and differentiation waves. Novel unification of development, genetics and evolution, V. 1. World Scientific, Singapore

Green P, Steele CS, Rennich SC (1996) Phillotactic patterns: a biophysical mechanism for their origin. Ann Bot 77:515–527

Gurwitsch A (1930) Die histologischenGrundlagen der Biologie. Gustav Fisher, Jena

Harrison RG (1918) Experiments on the development of the forelimb of *Ambystoma*, a self-differentiating equipotential system. J Exp Zool 25:413–461

Hemmati-Brivanloue A, Melton D (1997) Vertebrate neural induction. Annu Rev Neurosci 20:43–60

Holtfreter J (1938) Differenzierungspotenzen isolierter Teile der Urodelengastrula. W.Roux' Arch Bd 138: 657–738

Howard J, Grill SW, Bois JS (2011) Turing's next steps: the mechanochemical basis of morphogenesis. Nat Rev Mol Cell Biol 12:392–398

Jaffe LF (1969) On the centripetal course of development, the Fucus egg, and self-electrophoresis. Dev Biol Suppl 3:83–111

Krinsky VI, Zhabotinsky AM (1981) Autowave structures and the perspectives of their investigations. In: Grechova MT (ed) Autowave processes in diffusional; systems. Gorky, Inst Appl Physics AcadSci USSR: 6–32 (in Russian)

Kupiec J-J (2009) The origins of individuals. World Scientific, London

Ladoux B, Nicolas A (2012) Physically based principles of cell adhesion mechanosensitivity in tissues. Rep Prog Phys 75:116601 (25 pp)

Lawrence PA (1992) The making of a fly. The genetics of animal design. Blackwell Scientific Publications, Hoboken
Martynov LA (1982) The role of macroscopic processes in morphogenesis. In: Zotin AI, Presnov EV (eds) Mathematical biology of development. Nauka, Moskva, pp 135–154 (in Russian)
Meinhardt H (1982) Models of biological pattern formation. Academic Press, New York
Moček, R. (1974) W. Roux–H. Driesch. Zur Geschichte de Entwicklungsphysiologie der Tiere. Jena, Fisher
Nicol A, Rappel W-J, Levine H, Loomis WF (1999) Cell-sorting in aggregates of Dictyostelium discoideum. J Cell Sci 112:3923–3929
Nieuwkoop PD (1977) Origin and establishment of an embryonic polar axis in amphibian development. Curr Top Dev Biol 11:115–117
Petuchov SV (1981) Biomechanics, Bionics and Symmetry. Nauka, Moskva
Prigogine I, Stengers I (1984) Order out of Chaos. Bantham Books, USA
Schwarz US, Gardel ML (2012) United we stand—integrating the actin cytoskeleton and cell-matrix adhesions in cellular mechanotransduction. J Cell Sci 125:1–10
Shubnikov AV, Kopzik VA (1972) Symmetry in science and art. Nauka, Moskva
Spemann H (1936) ExperimentelleBeitragezueinerTheorie der Entwicklung. Fisher, Jena
Spemann H, Mangold H (1924) Uber induktion von embryonalanlagen durch implantation artfremder organizatoren. Arch mikrosk Anat Entwmech 100:599–638
Spiegel M, Spiegel ES (1975) The reaggregation of dissociated embryonic sea urchin cells. Am Zool 15:583–606
Steinberg MS (1978) Cell-cell recognition in multicellular assembly: levels of specificity. In: Curtis ASG (ed) Cell-cell recognition. Cambridge University Press, Cambridge, pp 25–49
Surkova S, Golubkova E, Manu, Panok L, Mamon L, Reinitz J, Samsonova M (2013) Quantitative dynamics and increased variability of segmentation gene expression in the *Drosophila* Kruppel and Knirps mutants. Dev Biol 376:99–112
Svetina S, Zeks B (1991) The mechanical behavior of closed lamellar membranes as a possible physical origin of cell polarity. J Theor Biol 146:115–122
Townes PL, Holtfreter J (1955) Directed movements and selective adhesion of embryonic amphibian cells. J Exp Zool 128:53–120
Turing AM (1952) The chemical basis of morphogenesis. Philos Trans Roy Soc, B 237:37–72
Vladar EK, Antic D, Axelrod JD (2009) Planar cell polarity signaling: the developing cell's compass. Cold Spring Harb Perspect Biol 1:a002964
Waddington CH (1962) New patterns in genetics and development. Columbia University Press, New York
Wintz W, Doebereiner HG, Seifert U (1996) Starfish vesicles. Europhys Lett 33:403–408
Wolpert L (1969) Positional information and the spatial pattern of cellular differentiation. J Theor Biol 25:1–47
Wolpert L (1996) One hundred years of positional information. Trends Genet 12:359–364
Xu J, Van Keymeulen A, Wakida NM, Carlton P, Berns MW, Bourne HR (2007) Polarity reveals intrinsic cell chirality. PNAS 104:9296–9300
Zacharov VM (1987) Asymmetry in Animals. Nauka, Moskva

Chapter 2
From Molecules to Cells: Machines, Symmetries, and Feedbacks

Abstract The first step on the way from chemistry to morphogenesis is the chemo-mechanical transduction that is extensively retarded relaxation of the stored energy onto a small number of selected degrees of freedom. The next level to up is presented by the microtubules and microfilaments-associated supramolecular machines which transform this energy into the dipoles (tensors) of mechanical forces. As a result, the balanced system of tensional and compressive mechanical stresses is created. On the level of isolated supramolecular machines, the processes characterized by the increase of a symmetry order and the drive toward thermo-dynamical equilibrium are dominated. At the upper structural levels, the role of energy-consuming non-equilibrium structures is increased, producing sub- and super-diffusion movements of the particles and a number of temporal and spatial symmetry break—the dynamic elements of still higher levels events. Among them of the most morphogenetic importance is tensile homeostasis of cell membranes and establishment of the polar cell organization.

2.1 Introductory Remarks

It will not be an exaggeration to claim that the main link in the activity of living beings, distinguishing them from non-living ones is what is called chemo-mechanical transduction: This is the transformation of random molecular movements into much more directed ones which we call mechanical. In terms of symmetry theory, it corresponds to enormous decrease of the symmetry order on the molecular level. It is not surprising therefore that even those scientists of the past which did not know Curie principle were intuitively searching for a dissymmetrizer, capable to provide the "information" for such a symmetry break. By a strange coincidence, in the same year of 1944, at the height of WW2 two independent researchers ascribed this property to hereditary substance (which histologists of that time often called the "chromatin"). One of them, the Russian biologist Alexander Gurwitsch postulated the existence of a chromatin-associated anisotropic field which "transforms a part of excitation energy

L.V. Beloussov, *Morphomechanics of Development*,
DOI 10.1007/978-3-319-13990-6_2

of the protein molecules into kinetic energy, oriented along field vectors" (Gurwitsch 1944; reprinted in 1991). This same year Ervin Schroedinger in his famous book (Schroedinger 1944) qualified the hereditary substance as "aperiodic crystal" emphasizing thus the fundamental role of its translational dissymmetry. Subsequent development of molecular and cell biology showed, however ,that it was quite unnecessary to link chemo-mechanical transduction with a single principle, associated with the "hereditary substance": This property appeared to be rooted in the very structure of protein macromolecules and their non-covalently bound multimolecular ensembles, often defined as "molecular machines." The latter can be attributed to the lowest link in the complicated hierarchy of devices coined by the nature for providing the movements of various living structures—from molecules to multicellular formations. In this chapter, we start to review this hierarchy and commence our analysis from describing the physical foundations of chemo-mechanical transduction on the level of single macromolecules.

2.2 Chemo-Mechanical Transduction and Molecular Machines

Among few contributions discussing the physical principles of chemo-mechanical transduction, the most important are those of McClare (1971) and Bluemenfeld (1983). We shall follow mainly the latter author, who elaborated his concepts in greater details. His main idea is that the transduction should be based upon a more or less considerable *reduction of the freedom degrees* of constituent particles of the "working body" (exemplified by either a single macromolecule or an entire supramolecular ensemble) and the *increase of characteristic times* of their deformations (compared to thermal motion). Or, in other formulation, the transduction requires *extremely slow relaxation of the stored energy onto a small number of the so-called distinguished* (*selected*) *degrees of freedom*. The simplest man-made machines, the heat engines, perfectly illustrate this requirement: The rate of thermal movements of single molecules of a gas or a steam are of the order of 10^2–10^3 m/s, while that of the piston should be at least in 2–3 orders less. Protein molecules can be also regarded as machines, which provide even much greater retardations: While the characteristic times (reverse frequencies) of oscillatory, rotational, or translational movements of atoms lay in the range of 10^{-11}–10^{-12} s, the working cycle of the main device for producing movements and deformations at all scales—the actomyosin machine—lasts about 0.2 s exhibiting thus enormous delay.

Such a considerable slowing down of molecular movements can be interpreted as enormous decrease of temperature within the molecular machine. Though it was first proposed by such an outstanding person as Ervin Schroedinger, it was neglected for several decades for being revived recently by several authors (Matsuno 2006; Igamberdiev 2012). By their estimations, a slow conformational

relaxation of actin-activated myosine ATPase releases 5×10^{-13} erg of ATP energy in 10^{-2} s. This corresponds to extremely low temperature of 1.6×10^{-3} K. As a whole, molecular machines performing chemo-mechanical transduction look to be consisting of two parts: The ordinary "heat machine" acting at the room temperature and the "frozen part" performing very much delayed and refined molecular movements on few selected degrees of freedom; the second part is fueled by the energy by the first one. In this, molecular machines differ principally from more familiar to us, man-made ones: So far as the latter are working in the dimensions/timescales very much removed from molecular ones, such a drastic splitting to the heated and frozen parts does not take place (although a much smaller distinction between the heater and the refrigerator remains).

Under more detailed consideration (Chernavskii and Chernavskaia 1999), the following details can be distinguished in the protein machine:

- Reservoir of energy ("springs")—relatively soft elastic elements able to store energy in the form of elastic stresses. Such a role is played by non-spiral parts of the protein molecule and electrically charged groups. Reservoir size is about 5×10^{-9} m.
- Levers, the rigid details which transmit stresses. This role is played by α-spirals.
- Hinges, the flexible joints represented by small amino acids, for example, glycine.
- Fixing points, presented by hydrogen bonds or by S–S bonds.

The energy stored in elastic elements is estimated as ≈0.5 eV per molecule and the lifetimes of metastable (mechanically stressed) states of protein machines ranges from 10^{-6} to 10^{3} s. By comparing these values with the above-presented rates of thermal oscillations of protein molecules, one can see that the relaxation of stressed states is slowed down by about 15 orders of magnitude. That means that macromolecules are spending almost all of their lifetime in mechanically stressed states.

Bluemenfeld emphasized principal importance of such extensive slowing down of the relaxation of the stored mechanical energy. He defined this property as kinetic non-equilibricity (opposed to thermodynamic one, associated with a constant energy inflow) because it prevents a system to reach otherwise available energetic states simply by keeping "frozen" a certain selected state for a long enough time period. This is a property of mechanical, rather than statistical systems, endowing the first ones by memorizing capacities. In other words, molecular machines in Bluemenfeld's sense are *not* dissipative structures: The latter are too vulnerable to the changes in initial/border conditions and have no required amount of memory.

Another peculiar property of molecular machines is that contrary to man-made devices, the regulatory and executing parts are merged together and the amplitude of produced movements is comparable with the dimensions of the entire machine. Next, due to the presence of bound ions and electrically charged parts of protein molecules (negatively charged carbonyls and positively charged amino acids), any mechanical shift is accompanied by changes of electrical field, which contribute to maintaining mechanical stresses within macromolecules. A special role in this

process is played by charged ligands and first of all by ATP molecules, each of them containing three negatively charged phosphate groups. Accordingly, by binding ATP molecules, the proteins should pass to more stressed and rectified configurations which may play an important role in the signaling cascades associated with several rounds of the proteins phosphorylation/dephosphorylation.

Therefore, an essentially mechanical behavior characterized by the presence of long-living stressed conformations which will be shown later to play a crucial role in regulating morphogenesis, can be distinctly traced already on the level of single macromolecules. That does not mean, however, that these properties are directly translated to upper levels, as it takes place in the crystal-like bodies. Rather, they numerously disappear and appear de novo, while moving upwards along the organizational levels scale. Now, we start this way, each time focusing our interests onto morphogenetically relevant properties of the dynamic structures specific for each next level.

2.3 Structures and Actions of Supramolecular Machines, Treated in Symmetry Terms

The above-described mechanochemical transduction on the level of individual macromolecules still cannot provide properly ordered deformations on the large enough scales, required for cells functioning and, the more, morphogenesis. A next step of integration is provided by the so-called supramolecular machines held by weak van der Waals and hydrophobic forces of molecular attraction and combining extremely high efficiency with fast responses to regulatory agents. Without repeating here a detailed description of these machines (see textbooks on the molecular biology of the cell, e.g., Alberts et al. 2003), we shall concentrate ourselves on the rarely discussed topics, directly related to morphogenesis: Those are the structural and functional symmetry transformations of supramolecular machines and the associated energy profiles.

First of all, let us remind that the two main classes of supramolecular machines—microtubules and microfilaments—are self-assembled from tubulin or actin subunits correspondingly into the formations which we shall define in some cases under the common name of filaments. In water solutions under high enough concentration of subunits, the assembly is energetically favorable (directed toward diminishment of a total free energy of the subunits) due to the presence of hydrophobic forces. As mentioned in Chap. 1, the free energy decrease is usually associated with increase of the symmetry order. Just this is taking place in the case considered: Whereas the solution of randomly distributed subunits has a symmetry order 1 (worth mentioning, the symmetry of single subunits is also 1), the assembled supramolecular structure acquires several new symmetry orders, the main of them corresponding to that of a polar vector ($\infty \cdot m$). Polarity is the main property of both kinds of filaments, manifested by the presence of the pole of preferential subunits' assembly (defined as

"+" end) and the opposite pole of preferential disassembly ("−" end). On reverse, the filaments disassembly (corresponding to the decrease of symmetry order back to 1) demands energy spending which comes from splitting of nucleotides (ATP in the case of microfilaments and GTP in the case of microtubules) bound to subunits. More detailed consideration of energy-driven configurations of cytoskeleton will be given in the next sections.

In addition to polarity, actin microfilaments also have translational symmetry with the period $a \approx 13.5$ subunits length and the screw pattern consisting of two left-handed helices. The symmetry order of two latter structures taken together is written as $(a) \cdot 2_1$. Microtubules do not reveal translational symmetry but possess complicated screw patterns with 3, 5, and 8 (members of Fibonacci series) inclining the spiral rows to different angles.

What should be the morphogenetic role of these symmetries? While no data on the role of translational microfilaments symmetry are available, the significance and mutual cooperation of two others is obvious. The main manifestation of the filaments polarity is the exertion of pushing forces deforming cell membrane by "+" end directed growth of either microfilaments or microtubules. These deformations are taking place at the leading edges of migrating cells. They are the elements of the most powerful collective cell events, embraced by the name of cell intercalation which will be discussed in details in the following chapters. "+" end directed growth is accompanied by the chiral component associated, in case of microfilaments, with the activity of membrane-bound proteins, the formins. According to a model suggested (Shemesh et al. 2005), circular formin dimers are periodically rotated in opposite directions around the filament's bulk at the level of its "+" end. During the so-called stair-stepping phase, there are 12 successive turnings of the same direction, each for 14°, producing a torsion stress of the double helical microfilament. Each next turn leaves a space for another actin subunit to be inserted. On the whole, stair-stepping phase takes about a second and spends about 1 eV of energy per actin filament. This energy is taken from ATP and GTP hydrolysis (formins were shown to be associated with GTPases). The stair-stepping phase is followed by the oppositely directed rotation for ≈166° (so-called screw mode) releasing torsion stress. As a result, the forces of several hundreds nanonewtons range are produced by actin polymerization at the leading edge of the crawling cell. Interestingly, up to about 300 nN resistance force, the actin network is growing at the relatively constant rate independently of the applied load (Carey et al. 2011). Such wide-ranging load independence seems to be an inherent and morphogenetically important property of actomyosin machinery.

The chirality (handedness) of the cytoskeletal filaments creates also a molecular basis of the macroscopic handedness of whole organisms. In spite of many blank spots and controversies, there is a growing amount of evidences indicating that the handedness is arisen in early development and is expressed by the chiral organization of tubulin, actin, and actin-bound proteins (Danilchik et al. 2006). For example, in amphibian eggs, the chirality is assumed to be imprinted by the microtubules array grown out of the organizer center brought by the male centriole. Later on, the chirality is amplified up to tissue-level asymmetries by as yet

non-specified ways including asymmetric distributions of potassium channels, proton pumps, and/or some neuromediators like serotonin (Vandenberg and Levine 2013). A peculiar mechanism of establishing left–right asymmetry with the involvement of class I myosins has been discovered in Drosophila (Speder and Noselli 2007). In this case, the so-called unconventional myosin I interacts with a universal regulatory protein, β-catenin and becomes bound with adherent junctions, connecting epithelial cells. Fixed in this location, it provides chiral cell rotations leading to asymmetric looping of intestine rudiment. In general, either right- or left-handed cell rotations, asymmetric inclinations of cell division axes or even of vast cell streams (the latter ones are taking place in chicken embryos: Tsikolia et al. 2012) play a crucial role in establishing handedness and essentially precede asymmetric patterns of genes expression. Thus, the morphological symmetry of a roundworm, *Caenorhabditis elegans*, is broken during the four- to six-cell transition due to inclination of the division spindle in two sister blastomeres called ABa and Abp from the direction orthogonal to antero-posterior embryo axis (Pohl and Bao 2010). Notably, by reversing through micromanipulation the previous division spindle, the body handedness will be also reversed. "…this result suggests that asymmetry in cytoskeletal and spindle mechanics may instruct handedness choice upstream of differential gene expression" (op. cit.).

Leaving now this intriguing and largely non-explored topic, we come to the next step in self-assembly of supramolecular machines. It is the association of the filaments with the so-called motor proteins (briefly "motors"), the ability of the motors to percept the filaments' polarity and to move, by spending energy, toward one of the filaments ends, either "+" or "−". For our purpose, it is enough to remind that motors from the kinesins and dyneins families are associated with microtubules while those from a large myosins family—with microfilaments. Most of kinesins are translocated toward "+" and dyneins to "−" ends of microtubules, while most of myosins (including myosin II) toward "+" ends of microfilaments. Motors are able to transport different molecular loads or cargoes. This ability becomes morphogenetically important when the load is represented by another similar filament, oriented in the same or reverse polarity in relation to the first one. In these cases, the filaments are arranged in doublets; the doublets members may be either identical in the sense that both are pulled by motors in symmetric manner, or nonidentical, one of them (the loading filament) firmly fixing the motor, while another serving as rails for the motor's shifts (a leading filament).

Missing a lot of molecular details of the motors–filaments interactions described in many textbooks and special papers, we will emphasize two main points. The first of them is that so-called motor's working stroke which pulls a load is directed toward relaxation, that is, toward the restoration of de-energized configuration. This step is always preceded by that of energy consumption (provided by ATP or GTP splitting), associated with translocation of the motor's "head" toward one of the poles of the leading filament. The second point is related to a rarely discussed issue of the symmetry of motors–machines associations. Let us consider the following examples:

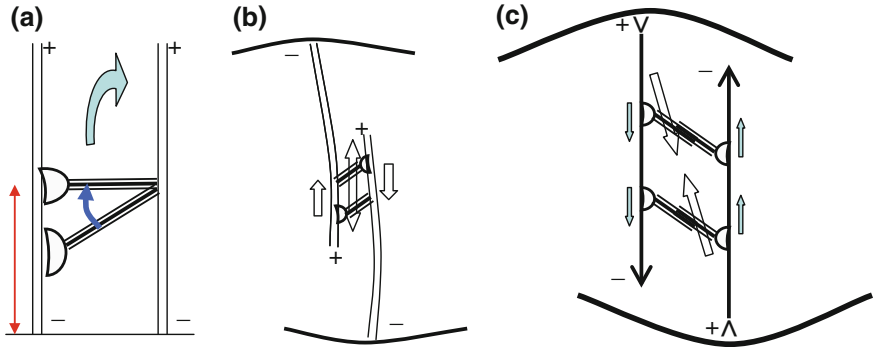

Fig. 2.1 Action symmetry of the double filaments molecular machines. Depicted are working strokes of an eukaryotic flagella (**a**), polar microtubules during cell division (**b**), and actomyosin contraction (**c**). + and − filaments ends are denoted which in the case of microfilaments are also marked as barbed and pointed arrowheads correspondingly. While in (**a**), a static structural symmetry of the microtubules arrangement is broken, in (**b**, **c**) the symmetry order of action is greater than that of the individual filaments. For detailed comments see text

1. Both microtubules creating the doublet have parallel polarities. One of the doublet members is loading and the other leading. This is what takes place in Eukaryotic flagella (recent review: Lindemann and Lesich 2010) where the function of motors is played by "−" oriented dyneins. Under these conditions, if the microtubules poles were not fixed, both microtubules from the same doublet would slide apart, the leading one in the direction of its "+" end, while the loading one in the opposite direction. However, because of the firm fixation of the both microtubules "−" ends, the result will be stretching of the leading microtubule and shrinkage of the loading one, which will make the entire machine bent (Fig. 2.1a).
2. Microtubules doublets consist of antiparallel oriented units. Their "−" ends are fixed at the opposite poles of a cell and both are loading and leading at the same time, each of them translocating kinesins toward their free "+" ends. Such is the activity of the so-called polar microtubules during cell division. In this way, they generate the force pushing apart the microtubules and polar cell areas to which they are attached (Fig. 2.1b). This is the main driving force of cell division translocated on the multicellular level in most powerful pushing forces ever existed in living tissues.
3. Actin microfilaments are oriented to the opposite cell surfaces by their "+" ends so that they are antiparallel and equivalent to each other. The motors (double head myosin II) are translocated toward "+" ends of each filament and pull the filaments in converged directions. This is the most general scheme of actomyosin contraction. It displays the universal mechanism for one-dimensional and circular contractions of cells which producing passive tensional stresses in the surrounding tissues if their outer edges are fixed (Fig. 2.1c).

Let us consider now the static and action symmetries of these machines. So far as in the case of flagella, both microtubules keep the same polarity while only one of them serves as the leading one (the other one being loaded), the action symmetry of the doublet is reduced to $1 \cdot m$ (similarly to an organism possessing both antero-posterior and dorso-ventral polarity). During the working stroke (performed in a coherent way by several dozens of dynein molecules), this dissymmetry is transformed into that of a bending keeping the same symmetry order.

This is not the case, however, for the next two examples (Fig. 2.1b, c): Because of the opposite polarity of the filaments and symmetric attachment of the motors to both of them, the symmetry order of the entire system is *increased* (compared with that of a single filament) by acquiring a reflection plane oriented perpendicularly to the filaments axes. As a result, the symmetry group for these two systems (without considering translational symmetry) becomes $m \cdot 2{:}m$, corresponding to second range *polar tensors*, rather than vectors. Accordingly, they may be called the "force dipoles" (Bishofs and Schwartz 2003). These two kinds of machines produce most substantial elements of morphogenetic forces. In the case of microtubules, they are associated with the post-division moving apart of sister cells and in the case of the microfilaments with various kinds of cell contractions.

2.4 Hierarchy of Stressed Networks and the Condition of Force Balance

By moving up from the isolated supramolecular machines, we enter the world of networks consisting of mechanically stressed (stretched or compressed) cables and the nodules where several such cables are met. Remarkably, such networks create a hierarchy embracing enormous dimensional range. The lowest level of the hierarchy is exemplified by the so-called actin gels—the networks of perplexed actin microfilaments with the nodules (fixed by gel-forming proteins, in most cases filamins) being about 10^{-7} m apart from each other. The upper scale networks belong to cellular and supracellular levels to be described in the next chapter: The greatest distances between the nodules which correspond in these cases to the multicellular clusters are extended up to 10^{-3} m. At the given moment, we have to concentrate ourselves on the most tiny networks for substantiating the important but often missed principle called the condition of the force balance (see, e.g., Odell et al. 1981; Goodwin and Trainor 1985; Forgacs 1995; Kozlov and Mogilner 2007). It claims that all the forces in biological tissues are balanced: Their vector sums are equal to zero (or, more precisely, are equalized within no more than milliseconds) so that the nonzero accelerations take extremely small time periods alternated by much longer periods when they are lacking. Suggest indeed that a mechanical force F which stretches or compresses a cable is generated in point N removed from the closest nodule M to the distance l. As a result, a wave of elastic deformation will move from N to M at the rate close to that of sound waves. When it reaches the

point *M,* the latter will start to move toward *N* with acceleration. This will last, however, only until similar waves of elastic deformations spread from *M* reach the next neighboring nodules *P, Q, R*. From this moment, the vector sum of all the forces applied to *M* turns into zero, and acceleration is abolished. Depending on the resistance of the surrounding medium, point *M* will either stop or continue to move with constant rate. As shown by the corresponding evaluations (Odell et al. 1981) due to high rate of elastic deformation wave and very small distances between the neighboring nodules, the periods of the force imbalance will last no more than 10^{-6}–10^{-7} s. This is negligibly small even compared to the duration of a single actomyosin sliding cycle (2×10^{-1} s). However, this imbalance period is already enough to reach the final velocity of about 3×10^{-5} m/s which largely exceeds typical rates of morphogenetic movements. All the above said permits to conclude that any forces generated within living tissues and providing morphogenetic movements are practically immediately balanced by the opposing ones. The morphogenetic consequences of the force balance are of primary importance. First, it means that the action of a single force is spread toward even far removed regions without considerable damping. Moreover, any changes in a single force value will affect the entire geometry of the network and vice versa: By deforming the web, both the values and the directions of the forces will be also changed: The forces and the geometry are mutually linked.

Under the condition of the force balance, it is enough to know the angular directions of all the forces applied to a given nodule for calculating their relative values and vice versa. This is especially easy if the number of forces is 3, which is the most probable case.[1] Consider indeed a nodule formed by the forces OA, OB, and OC and denote angle AOC as α, COB as β, and AOB as γ. As shown by simple trigonometric calculations, the relations between OA and OC will be

$$\left|\overrightarrow{\mathrm{OA}}\right| = \frac{\left|\overrightarrow{\mathrm{OC}}\right|(\cos\alpha \cdot \cos\gamma - \cos\beta)}{\sin^2\beta} \tag{2.1}$$

In Chap. 3, several examples using Eq. (2.1) will be discussed.

In math terms, the condition of the force balance within each force nodule enforces us to operate with tensors, rather than vectors. This provides some opportunities. First, the dynamic states described by tensors are self-supported, that is, do not require any external foothold demanded by vectors: It is especially important for mass cell movements described in Chaps. 3 and 4. Next, one-dimensional tensors are able to organize two-dimensional spaces, exemplified by cell layers. The best example is the Poisson's deformation (see Chap. 1, Box), widely spread and actively reinforced in morphogenesis. Another process described in terms of tensors is the transformation of oblique cells toward rectangular ones

[1] Because of its robustness: Any higher order nodule can be decomposed into third-order ones just by small shifts.

due to isotropic contraction of actin gel. This process plays the leading role in transformations of so-called cell fans (see Chap. 3).

Meanwhile, the vectors can emerge again on the upper structural level as the combinations of tensors. Suggest that we have an internally stressed conical or ovoid body with uniform density of the force nodules. If isolated from any external forces, such a shape (by the way, rather biomorphic) can be mechanically balanced only if the tensions are reversely proportional to the local diameters (i.e., they are greater in more narrow part). In other words, we get here the *gradient of the stress tensor*, (or briefly, the stress gradient) dictated by geometry (or the other way round). Within the entire body scale, this forms a vector, defining the body polarity. The important morphogenetic role of stress gradients will be discussed in the next chapter.

2.5 Final Remarks on Supramolecular Machines

Now, we return back to molecular level for mentioning some other mechanisms involved in generation and regulation of mechanical stresses.

The first of them is in transforming the fast actomyosin contractions typical for muscle activities to sustained contractions maintaining long-term stresses. The switch from fast to sustained regime is regulated by a family of universal regulators of cytoskeletal activity, RhoA proteins. It is realized by inhibition of phosphatase (associated with light chains of myosin molecule) by RhoA-dependent kinase (Weiser et al. 2007). Myosin II mediated support of sustained tensile stresses non-associated with fast contraction has been shown both for embryonic (Roh-Johnson et al. 2012) and pathologically modified tissues (Samuel et al. 2011).

While these and other data indicate the leading role of actomyosin machinery in supporting long-term stresses, their initiation in early embryos is owed to another mechanism: increase of osmotically driven turgor pressure in primary embryonic cavities (blastocoel and subgerminal cavity of Amniotes). The pressure reaching in amphibian blastula stage embryos ≈325 mosm = 70 N/cm^2 (Wilson et al. 1989) is created due to the inward (blastocoel directed) transport of sodium and chloride ions provided in its turn by predominant location of ionic channels at the apical (external) parts of the blastocoel roof cells and of ionic pumps at the basal (internal) parts (Stern 1984). Although this factor, unique in providing voluminous (three-dimensional) deformations and stretching stresses, is rare for animals (another example related to hydroid polyps will be discussed in Chap. 4), its role should not be underestimated: As shown later, its switching-off leads to grave developmental abnormalities. In plants, it is the dominating stress-producing agent (see Chap. 5).

By concluding this section, in addition to widely accepted and extensively explored supramolecular machines it would be proper to mention a non-conventional hypothesis suggested by Pollack (2001) and Del Guidice with coworkers (2005, 2011) proposing the existence of a quite different class of a similar scale mechanisms which may be called low entropy machines.

The authors assume that supramolecular structures (including cytoskeletal filaments) are surrounded by several layers of a structured water which consist of precisely oriented molecular dipoles, with their positively charged poles directed towards cytoskeletal filaments, and the negatively charged ones to the bulk of disoriented water. These hypothesized coherent water domains, or CWD (which should be the areas of very low entropy) may work as a kind of electrical batteries accumulating substantial energy and discharging it if being destructed. According to Del Guidice et al. calculations, CWD diameters extend up to 100 nm (corresponding to about 10^7 molecules) and by exceeding a certain density threshold, should oscillate in a coherent way with 10^{11} Hz frequency. Due to low entropy, CWD are able to absorb non-coherent (heat) energy from the surrounding bulk water and transform it into "high grade" coherent energy. Noteworthy, CWD absorb light in the infrared and ultraviolet spectral regions. The absorbed energy may reach 12.06 eV which is only ≈0.5 eV lower than the energy of water ionization. In other words, CWD possess a substantial amount of free or almost free electrons, which results in the electrical potential difference between CWD and bulk water. In such a way, CWD should work as real machines, by producing electrical energy and the movements of charged particles. These up to now purely theoretical considerations deserve to be experimentally tested.

2.6 From Self-assembly to Self-organization: Temporal and Spatial Symmetry Breaks

What was reviewed beforehand—with a great exception of chemo-mechanical transduction in McClare and Bluemenfeld sense—relates mostly to a classical self-assembly characterized by preservation and increase rather than decrease of the symmetry order. However, for creating a complicated space-temporal organization of embryos, the reverse dynamics associated with symmetry breaks will be necessary. Let us show that even a slight structural complication (as compared to isolate supramolecular machines) just leads to symmetry breaks and other signs of self-organization, while if mostly temporal.

We start from pointing to several experimental and theoretical papers (Plaçais et al. 2009; Howard 2009; Ishiwata et al. 2010; Vogel et al. 2009; Kruse and Riveline 2011) which describe and analyze phenomenologically simple models of actomyosin contraction under loading. Even a single actin filament brought in close proximity to a substrate densely coated with heavy meromyosin molecules, when loaded by several picoNewtons elastic force, exerts rhythmic oscillations with peak frequencies from 1.5 to 14 Hz (Plaçais et al. 2009). By changing mechanical parameters, different modes of oscillations can be traced (including bimodal ones). The authors found that the oscillatory characteristics were mostly determined by the stiffness of the system, while the number of involved meromyosin molecules affected the level of the random noise. With the increase of the number of myosin molecules involved, the oscillation pattern becomes more regular, approaching that of intact muscle (Ishiwata et al. 2010).

As will be shown below, most of intracellular oscillations have several minutes periodicity, being hence enormously delayed, as compared to characteristic rates of molecular events. This alone is sufficient for ascribing these events to the feedbacks

generated in large molecular collectives. There are meanwhile also more direct arguments favoring this point of view.

Some of the oscillations and feedback reactions are based upon activity of actomyosin structures while other upon kinesin–microtubule interactions (review: Kruse and Riveline 2011). The first ones are exemplified by so different systems as moving fibroblasts exerting several pN pulling forces upon their environment with 3–4 min periodicity and hair bundles of the inner ear cells, oscillating with about 100 ms periods. Several minutes periods oscillations in large cell collectives, some of them (but not all) based on actomyosin activity, will be reviewed in the next chapter. Periodic assembly–disassembly of cortical actin was observed in microtubule-depleted cells and in cell fragments. In these cases, the actin cortex locally tears and retracts due to the action of myosin. During retraction, actin is disassembled leaving a bulge of highly tensed cortex behind; in this very place, actin is assembled again.

Another example of microtubules–kinesin-based oscillations are the movements of the meiotic prophase spindle body in fission yeasts which have 5–10 min period and last for several hours. These movements are generated by periodic pulling of spindle poles by kinesins which are attached to the cortex and are moving toward "–" ends of astral microtubules (Vogel et al. 2009). Extensive oscillations of the length and positions of mitotic spindle during the first cleavage division of *C. elegans* eggs are based upon a similar mechanism (Kruse and Riveline 2011).

All these processes definitely belong to realm of self-organization because by establishing a regular periodicity, they break temporal symmetry at the macroscopic scale (far exceeding characteristic times of individual molecular events). Obviously, the oscillation patterns require negative feedbacks between the main dynamic components (which may be supplemented also by positive feedbacks acting at shorter time periods, as mentioned in Chap. 1). What might be their origin?

As shown in several cases (Vogel et al. 2009; Kruse and Riveline 2011), such oscillations well can proceed in vitro systems, free from any chemical regulators. Thus, without denying the latter's role in intact cells, we can conclude that in the "minimal" cases, the feedbacks can be purely mechanical, provided by any loads (either natural or artificial) resisting the pulling or pushing activity of the motor proteins. More concrete models which use this assumption split into two categories. The first one (Kruse and Riveline 2011) emphasizes the existence of the bimodal velocity distribution (the modalities having the opposite signs) in the simplest, however, necessarily loaded actomyosin systems. By this model, under certain values of mechanical parameters, the elastic load/velocity (of the motors movements along actin filament) dependence becomes nonlinear, permitting the motors to switch between two velocity values which correspond to the minimal energetic potential. The model takes into consideration the translational symmetry of actin filaments which affects the strength (energetic potential) of actin motor protein binding. The second model, shared by most of authors, connects the value of elastic load with the rate of detachment of the motor proteins from the loaded actin filament. A concrete scheme suggested for the case of microtubules may be the following (Vogel et al. 2009). Suppose that an intercellular structure is pulled by the

kinesins attached to the oppositely directed microtubules, A and B (which are oriented by their "+" ends to the opposite parts of the cell membrane). The balance between both opposite forces is unstable to small differences in microtubules lengths: A slightly longer microtubule (say A) possesses more motors and exerts hence a greater pulling force to B. This promotes increased detachment rate of the motors from B, which enhances even more the pulling force of microtubule A. In other words, a positive rate/rate feedback emerges. However, because of the finite cell diameter, microtubule A should shrink losing the motors, while the tensed microtubule B, becoming free from further stretching has more chances to attach the motors again. At this moment, the movement changes its direction.

By developing this idea, Howard (2009) puts a remarkable question: "Are the individual motors and filaments micromanaged like marionettes by a small group of cellular puppeteers (signaling pathways) …? Or is there a certain degree of autonomy of action of collectives of motors and filaments that allow them to self-organize and coordinate?" Being inclined to the second version, the author develops the idea of load-accelerated motors/filaments detachment. He adds to the previous models a new assumption of negative damping meaning that with increase of the body velocity, the resisting force should be decreased, rather than increased, so that acceleration occurs. This requires additional portion of energy which should be taken "from the surroundings" (op. cit.). Another addition to the initial model is in introducing a delay (a finite time period) between the application of the load and the detachment of motor proteins from the filaments. Together, these requirements are sufficient for providing non-damped oscillations.

We describe this concept with so many details because it contains a rudiment of the feedback scheme which by our view is the leading one for the supracellular level morphogenesis, although much greater space/temporal scales are involved in the latter case (see Chap. 4). Also, one can agree with Kruse and Riveline (2011) that the biological role of the above-described oscillations may be in probing the mechanics of cell environment (stiffness and/or elastic tensions); as it will be shown later, no organized morphogenesis can proceed without such a probing.

In addition to oscillations, well-expressed space-enfolded dissipative structures consisting either of actin or of tubulin have been recently reproduced. Actin filaments, propelled in a planar geometry by immobilized molecular motors (meromyosin) when exceeding a critical density, become self-organized to form coherently moving structures which include clusters, swirls, and interconnected bands (Schaller et al. 2010). With the density increase, the disordered phase is changed first by polar nematic clusters and then by wave-like structures with enhanced directional persistency. The ordered structures in the form of swirls span up to several millimeters diameter and have lifetime up to several minutes. These structures are considered as effects of essentially cooperative interactions of many filaments "based on the balanced uptake and loss dynamics of the individual constituents" (op. cit.) which require the input of mechanical energy. In other words, they are typical dissipative events.

The same is true for streams and vortex-like structures consisting of microtubules propelled by surface-bound dyneins (Sumino et al. 2012). The streams of the

microtubules moving in both directions appear in about 5 min after ATP addition and transform into vortices of about 400 μm in diameters after next 10–15 min. Individual microtubules non-trapped within the vortex could leave it for entering a neighbor one or to travel further.

These observations are instructive, since they demonstrate the capacity of energized collectives of filaments to be involved into dissipative structures. On the other hand, their variability and large linear dimensions sharply distinguish them from any structures of a living cell. Much better approximation to the dynamic structures of the real cells is provided by experimental and theoretical analysis of the structures created in active (removed from thermodynamic equilibrium) actin gels. This will be the topic of the next section.

2.7 Metastable ("Glassy") States of the Cytoskeleton and Energy Wells

We start with reviewing in vitro studies of several mechanical parameters (elastic or stiffness modulus and maximal strain values) belonging to cross-linked or bundled actin networks (Gardel et al. 2004; Storm et al. 2005). Let us remind that in the cross-linked actin networks, the filaments are intersected at different angles, while in the bundled networks they are oriented in antiparallel fashion. While measured as functions of either actin concentration, density of cross-linkages or the amplitudes of imposed strains, the above-mentioned mechanical parameters showed a biphasic behavior: When plotted in double logarithmic coordinates, these functions were first rested at the plateau stage and after exceeding a certain threshold demonstrated almost linear increase. The biphasic behavior is associated with two thermodynamically different steps of the samples reactions: enthalpic and entropic. The first phase is the rewinding (straightening) of large loops of actin filaments. This mode dominates under relatively low actin concentrations and large distances between cross-links. Due to random arrangement of the loops, the resulted strains are oriented isotropically. In contrast, the second (entropic) phase is associated with stretching of already rectified filaments. Such a behavior is favored by increased actin concentration and high density of cross-links. The main amount of energy imposed at this stage is spent for eliminating thermal fluctuations and further stretching of the filaments. The resulted strains become anisotropically oriented along the stretch direction.

In order to describe and distinguish both types of behavior, the notions of the so-called persisting and contour lengths of actin filaments are useful (L_p and L_c correspondingly) (Storm et al. 2005; Liverpool 2006). L_c is the "absolute" length of the filament between two neighboring cross-links, while L_p is the length at which the filament loses memory of its orientation (by another expression, L_p is the characteristic length of tangential memory damping). Obviously, the greater the filament is curved and/or the densely are the loops arranged, the smaller is L_p and vice versa.

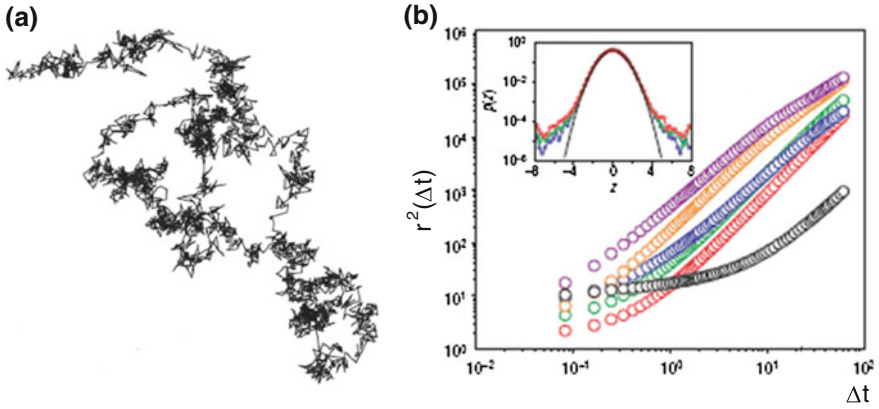

Fig. 2.2 Super-diffusive behavior and self-organized criticality in actomyosin gel. **a** A bead glued to a cell surface shows intermittent dynamics, being delayed in some locations/time moments and extensively translocated in between. **b** Statistics of spontaneous beads motions. *Horizontal axis* time lags Δt (s), *vertical axis* Areas covered during time lags ($r^2(\Delta t)(\mathrm{nm}^2)$). All the graphs except the lowest one which illustrates the effects of ATP depletion are almost linear in double log coordinates, indicating thus critical behavior. *Inset Colored lines* display deviations of beads displacements from a gaussian distribution. From Bursac et al. (2005)

Under $L_c > L_p$, the filament is considered to be flexible (such are the intermediate filaments composed of the protein vimentin), while in reverse case ($L_p > L_c$) the filament is stiff: Collagen and fibrillar actin belong to this category. Accordingly, actin filaments maintain tangential correlations over relatively large lengths, making them adequate conductors of tensile stresses.

Similar kinds of measurements have been performed on living cells with the use of ferromagnetic beads bound to the actin cytoskeleton via cell adhesion molecules (integrins) (Fabry et al. 2003; Bursac et al. 2005; Deng et al. 2006; Trepat et al. 2007). In Bursac et al. experiments, both spontaneous beads movements and those initiated by stepwise or oscillatory shear stresses were traced in several kinds of cells. In all of them, spontaneous movements of unloaded beads showed remarkable intermittent dynamics with periods of stalling (so-called "subdiffusive" behavior) and more extensive translational movements (the "super-diffusive" behavior, exceeding the limits of Gaussian distribution) (Fig. 2.2a, b). Within several seconds after application of a shear stress, the beads motility increased, but in several dozens minutes returned to a control level, indicating what is called solidification. Such a transformation requires ATP splitting energy.

This approach is remarkable, first of all, by treating the cytoskeleton as a unified dynamic system (rather than a mixture of specific components) including into it all the components which provide mechanical integrity of a cell (scaffold proteins, cell–cell and cell–matrix contacts, members of signaling cascades etc.). Such system is under permanent stress fluctuations of different degrees of randomness, which increases under diminishment of characteristic times: While under Tch < 10^{-2} s the movements are completely random, within 10^{-2}–10^{0} s range,

peculiar regime of the active non-equilibrial "stirring" is taking place, combining randomness and directionality. At the greater times, the latter dominates (Fakhri et al. 2014). The authors of the both above-mentioned papers emphasize the widespread of the power law relations between the duration of the action or the frequency of the applied forces on the one hand and the changes of mechanical parameters (stiffness, elasticity) of the sample on the other hand. As mentioned in Chap. 1, such systems should be close to the state of self-organized criticality. Applied to actin networks, it may indicate emergence of a large number of the different depth energy wells which the system can select while moving along the relaxation pathway: The deeper the well, the less it is available (because of being presented in smaller proportion or separated by higher energy barrier). In other words, power law dependence indicates metastability of actin networks and their readiness to select one of the available states. Moreover, a notion of metastability index can be introduced "as the level of mechanical agitation (noise) present in the microenvironment relative to the depth of the energy well" (Fabry et al. 2003). This index can be also defined as the "effective temperature of the matrix" (op. cit.) which is roughly proportional to the energy pumped into the cytoskeleton. When the index is high, the element can hop randomly between wells so that the system as a whole can flow and become disordered. Under smaller index values, the system's elements become trapped in deep wells from which they are unable to escape; under these conditions, the system behaves as an elastic solid body (op. cit.).

These suggestions, hardly familiar to developmental biologists, may be important for paving a way toward essentially new approaches to morphogenesis and cell differentiation. The matter is that metastability of the cytoskeleton (in its broadest meaning) may point to the cell's maintenance in a competent, but as yet non-differentiated state. Taking into consideration the increased evidences on the role of cytoskeletal transformations in cell differentiation (see Chap. 4 for more detailed discussion), one may assume that selection between cell differentiation pathways may be close if not identical to that between different energy wells of the cytoskeleton's energy relief.

2.8 Cell-Matrix and Cell–Cell Contacts: Mechanodependent Self-organization

One of the most important but as yet not properly evaluated recent achievements in cell biology was a discovery that the active responses to mechanical signals are necessary not only for differentiation but even for the very survival of metazoans cells: In the absence of such signals or under inability to respond by self-stretching, a cell is unable to proliferate (Chiquet et al. 2009) or even switches on the apoptotic program (Chen et al. 1997). In this section, we shall look what is known about molecular devices used by cells to percept and elaborate mechanical signals. As usual, we will make an accent to their dynamics, feedbacks, and self-organizing properties.

For percepting mechanical signals from the surroundings, a given cell should be bound with another one either by direct contacts, or via components of extracellular matrix (ECM). Most of the direct cell–cell contacts belong to the so-called adherent, or cadherin-mediated junctions while cell–ECM contacts are exhibited by the so-called focal junctions. Both of them are complicated multimolecular ensembles quite far from being static fastenings. Moreover, we shall see that they are active mechanosensitive formations far from thermodynamic equilibrium.

The first fundamental property of both types of contacts is that they become strengthened under loading (increased tensile forces) and weakened with the loading (tensions) decrease. This property belongs to the class of feedback reactions which are basic for all morphogenetic processes and will be discussed in more details in the next chapter. As applied to individual cells, it was studied in most details on cell–ECM (or cell-artificial substrate) contacts. Cells' bounding to ECM is provided by proteins of the integrin family which are at the same time connected with the so-called adaptor proteins linking them with actin filaments from the cytoplasmic side. The both side linkages are mechanodependent. Among them, fibronectin fibers (the main, if not the sole ECM component in embryonic tissues) are characterized by astonishing degree of extensibility (the greatest for biological fibers): They may be stretched in 8 times and when released return to the starting length within just a few minutes (Klotzsh et al. 2009). Although the Young modulus of fibronectin is extensively increased under stretching, the cells' produced forces (of several nN range) are estimated to be enough for at least moderate fibronectin stretching. Importantly, ECM stretching increases the exposure of cryptic sites which contain some imminent component of embryonic induction (Wipff et al. 2007).

At the cytoplasmic side, integrins are bound in a tension-dependent way to vinculin through the adaptor protein talin-1. Vinculin also links to actin and is recruited in response to applied forces. Another adaptor protein is $p130^{Cas}$ which, when being phosphorylated, activates small GTPases. As a result, hundreds of proteins functionally entangled to a net of positive and negative feedbacks are recruited to adhesion sites which are passing under loading from the state of small (<1 μm diameter) and unstable contacts to much larger (several μm diameter) contact zones, called focal adhesions (FAs). FA areas were shown to be in a strict linear proportionality to the amount of applied force, keeping thus a constant stress value estimated as 5.5 $nN/\mu m^2$ (Balaban et al. 2001). This again corresponds to several pN force applied to a single integrin molecule.

Recently, several physically based models have been proposed for FA growth (Shemesh et al. 2005; Ladoux and Nicolas 2012). In the context of this book, they are of a special interest because the suggested mechanisms of recruiting protein molecules to FA sites have some similarities with the models of stress-dependent behavior on the level of cell collectives (to be discussed in the next chapter). By Shemesh et al. model, the molecular dynamics of FA is driven by the tendency to minimize total free energy of the system which includes both the pool of free protein molecules and those aggregated onto a substrate stretched by actomyosin-generated pulling forces and anchored from the other side to ECM. The main system's parameters are the energy of pulling forces and the difference of chemical potentials

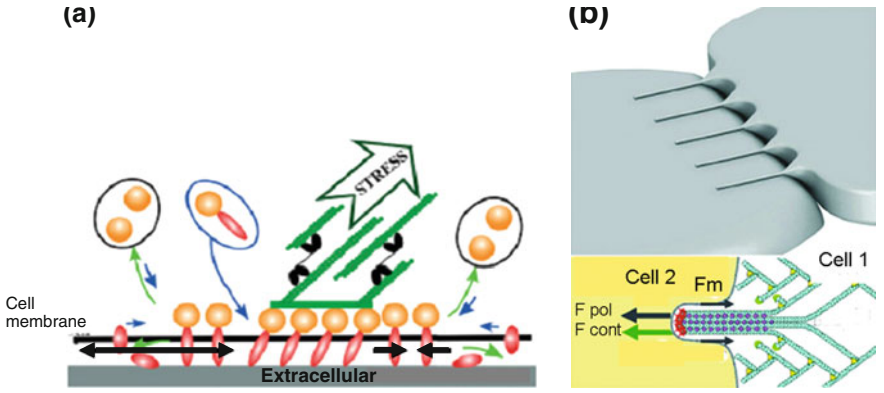

Fig. 2.3 Asymmetry in cell-substrate and cell–cell junctions. **a** Dynamics of protein turnover in focal junctions. By the action of asymetrically oriented actomyosin-generated pulling stress the leftward part of the cell membrane is stretched, while the opposite side is relaxed or slightly compressed. As a result, the protein insertion to the *left* part is expected to exceed that to the *right* one. **b** Apical junction between two epithelial cells as an asymmetric push–pull unit. Cell 1 exerts a pushing impulse generated by actin polymerization to cell 2. The latter responds by actomyosin contraction. F cont is the contractile (pulling) force and Fm is the membrane resistance of Cell 2. F pol is the pushing force of actin polymerization exerted by Cell 1. **a** From Ladoux and Nicolas (2012), modified. **b** From Brevier et al. (2008), © IOP Publishing, reproduced by permission of IOP Publishing. All rights reserved

of protein molecules in the aggregated and in the free state. Within a wide enough range of parameters, it becomes energetically favorable for free molecules to become inserted in the stretched substrate just in the direction of the pulling force because in this case, the elastic stress of the aggregated phase is relieved: This corresponds to the directed FA growth. Under relatively smaller pulling forces FA either becomes in a steady state or disassembles. If applying this model to the typical asymmetric arrangement of actomyosin bundles in relation to FA plane, one can see that the pulling bundles will be flanked by a stretched zone from the one side and by a compressed one from the other side. Under these conditions, it will be thermodynamically favorable to insert protein molecules into the stretched zone and remove them from compressed one. As a result, the molecular turnover will be accompanied by extension of the leading cell edge, that is, by crawling of the cell (Fig. 2.3a).

The local drive toward free energy decrease in no way mean that the entire mature FA is an equilibrial structure. Rather, it requires an imminent flow of directed energy being hence similar to a dissipative structure requiring tensile stress for its maintaining.

A requirement of non-dissipated portion of energy for stabilizing FA is confirmed by the properties of cell reaction known as rigidity sensing: FAs are reinforced and stabilized when establishing contacts with a rigid (non-deformable)

rather than a soft (deformable) matrix. Obviously, under the contacts with non-deformable substrate, the mechanical energy generated by actomyosin contraction is not dissipated, while in case of a relatively soft substrate, a substantial amount of energy is spent to deform the latter. This is quantified by a simple expression $W = F^2/2K$ where in our case, W is the amount of energy required by a cell to build the force F and K is the so-called spring constant, characterizing the substrate stiffness (Bischofs and Schwarz 2003). Accordingly, the greater the substrate stiffness, the smaller will be the amount of energy W spent by the cell to generate a given amount of force F and hence creating FA of a given square (which is, as mentioned above, proportional to F). In terms of time t and power N, the equivalent expression is $t = F^2/2KN$ which means that under the same power, the greater the substrate stiffness, the smaller the time period required for creating a given square FA. A widespread and morphogenetically important (but not universal) cells property to orient themselves onto anisotropic substrates along the maximal stiffness direction is explained by Bischofs and Schwarz as a tendency to minimize the energy and the time required for producing the given square FA.

On the other hand, the experiments by seeding cells onto dense arrays of pillars of a different rigidity (Saez et al. 2005) lead to somewhat other conclusions. It was found indeed that the force exerted by a cell upon each given pillar is linearly proportional to the pillar's spring constant, thus equally deforming the pillars of different stiffness. Meanwhile, according to the above-presented formula under constant energy production, the force should be proportional only to the square root of the spring constant ($F = \sqrt{2WK}$); in order to achieve a linear force/stiffness dependence, the energy produces by a cell should increase with the stiffness increase and be stored most probably in the actin cytoskeleton, making it pre-stressed. In other words, the stiffness increase should induce a positive feedback between aggregation of proteins promoting FA growth and the pulling force exerted by microfilaments. Such reactions were indeed observed. Moreover, by using ingenious single cell measuring device, the pulling force was shown to be initiated surprisingly soon ($t < 0.1$ s) after abrupt change in stiffness (Mitrossilis et al. 2010). So instead of always minimizing the energy spending, a cell behaves as an experienced stockbroker immediately increasing the investments in the projects promising greatest profits: In our case, these are the sites of greater stiffness. This emphasizes once again domination of non-equilibrium energy spending inside cells; more specifically, it points to a positive feedback between the proteins aggregation within FA and the amount of mechanical energy directed toward this FA.

Interestingly, both Bischofs and Schwarz model and Saez et al. results lead to the same qualitative conclusions about cell behavior on the substrates of regionally different stiffness: The cells will establish larger contacts with more stiff substrates and, in case of stiffness gradients move upwards the gradients, exemplifying the so-called durotaxis (Lo 2000). Coming now to unequally tensed elastic substrates and assuming that its stiffness is proportional to tension, we come to the idea of tensotaxis, that is, cell movement upwards the tension gradients. In addition, by spending its contacts-making energy in direct proportion to the local stiffness/tension of the

substrate, a cell should enhance, rather than smooth the regional differences in stiffness/tension. This will be shown to be of importance for the behavior of cell collectives.

The dynamics of cadherin-mediated cell–cell junctions share the main properties of focal adhesions in the sense that both maturation and maintenance of the first ones are also mechanodependent. These contacts transmit from one cell to another actomyosin-generated tension of pN range (Borghi et al. 2012) which promotes recruitment of vinculin to the sites of cell adhesions (Sumida et al. 2011). Another type of cell–cell contacts, hemidesmosomes of *C. elegans*, respond to muscle-generated tensions by switching on several signaling systems (Zhang et al. 2011). This may explain why muscle contraction is required for proper development of embryos of these species.

Similarly to focal junctions, cadherin-mediated ones are asymmetric, taking the shape of so-called push–pull units (Brevier et al. 2008). Their assembly starts from formation of a lamellopodia by one of the cells (called the donor cell) which exerts a pushing force (produced by actin polymerization) to the neighboring acceptor cell. As a result, the donor cell makes a protrusion, penetrating into acceptor cell. In response, this latter develops actomyosin contraction exerting thus a pulling force to the donor cell's protrusion; in the absence of this force, the protrusion fails to elongate (Fig. 2.3b).

A "push–pull" structure of the cadherin-mediated contacts indicates ones more regular lateral asymmetry of epithelial cells, which should be added to their universal apico-basal polarity. At the same time, by constantly requiring input of energy canalized by the action of actomyosin machine, these structures share non-equilibrial properties of focal junctions.

Recently, several refined fluorescent and computer imaging techniques were used for quantifying anisotropic stresses generated by mammary epithelial cells in 3D cultures (Campàs et al. 2014). Under all the reservation mentioned by the authors, this estimation seems to be the first reliable one related to the integrated tissue rather than single cells. The values obtained were 3 and 4 $nN/\mu m^2$ which is of the same order as those detected by Balaban et al. (2001) for focal junctions and twofold larger than the stresses generated by cells of embryonic tooth mesenchyme, either within cultured aggregates and in developing whole mouse mandibules.

Ingenious method for measuring forces acting across the vinculin molecules as depending upon the assembly or disassembly of the focal adhesions was elaborated by Grashoff et al. (2010). The tension sensors were constructed in which an elastic molecular domain derived from the spider silk protein was inserted between two fluorophores undergoing resonance energy transfer with wavelength changing as a function of applied force. By calibrating this device, the absolute values of forces could be measured which gave ≈2.5 pN values per vinculin molecule in stable focal contacts. Similar technique was used for evaluating the effects of the shear stress across cadherin-containing cell–cell contacts (Conway et al. 2013).

Further development of these methods opens quite new perspectives for estimating stress patterns at the level of macromorphology as well: It would be interesting to compare so-called maps of mechanical stresses based up to now upon

the local incisions techniques (see Chap. 3) with those obtained with the use of molecular sensors. This does not mean that the classical methods will lose their validity: For example, the molecular sensors hardly can detect the directions of tensions. In any case, however, the new techniques are the first ones permitting to measure the absolute values of preexisted, rather than artificially imposed stresses.

2.9 Transmission and Regulation of Mechanical Forces in Cell Cortex

As will be argued in more details in the next chapter, mechanical stresses, in most cases tensile, are transmitted in embryonic tissues over macroscopic distances, greatly exceeding individual cells diameters. Because of poor development of extracellular matrix and lack of connective tissue fibers in early embryos, the main root for transmitting tensions goes via complicated set of structures including cell (plasma) membrane proper (that is, lipid bilayer together with membrane proteins), submembrane actomyosin cytoskeleton, and membrane-to-cytoskeleton attachments linking these two components. For the sake of simplicity, we shall define this entire set of structures as cell cortex, although some authors relate this notion to submembrane components only.

The first paradox we are encountered with when speaking about tensions at the cell surface is that the lipid bilayer itself can be stretched no more than to about 2 % (Apodaca 2002), while many cells including embryonic ones, can be artificially elongated more than to 100 % of initial length, especially if the stretching is performed by several rounds separated from each other by 1–2 min intervals. It is the intervals requirement which gives the answer: During each round of stretching and immediately after it, the initial square of lipid bilayer is restored (and in some cases, restored with an overshoot) due to insertion of new portions of membrane taken from the so-called membrane reservoir. This is internalized and often folded membrane fraction, which, depending on mechanical state, may be either rapidly (within minutes or even seconds) inserted in the outer membrane plane or undergo the reverse transformation. The main part of reservoir is presented by caveolae, 60–80 nm in diameter membrane invaginations. Under physiological or experimentally induced (caused by hypotonicity) membrane stretch, the caveolae are flattened and disassembled within about 2 min in actin and ATP-independent way, considerably decreasing membrane tension. After returning to normal osmotic conditions and thus releasing membrane tension, caveolae are reassembled, now by slow actin and ATP-dependent process. As a result, cell volume becomes even smaller than it was before hypo-osmotic shock, demonstrating a certain overshoot (Sinha et al. 2011). Other sources of a membrane reservoir which are smaller than the caveolar compartment but important at some steps of cell reaction are membrane microfolds, the so-called vacuole-like dilations (spherical membrane invaginations), blebs (membrane evaginations nonsupported by actin cytoskeleton), and a pool of endomembranes undergoing exocytosis (Gauthier et al. 2012).

Tension regulation with the use of membrane reservoir is well studied and creates one of the most important morphogenetic feedbacks: Namely, cell surface stretching promotes externalization of some part of membrane pool while relaxation of cell surface tension and, the more, shrinkage of cell membrane switches on its internalization. During phagocytosis, a well-documented increase of exocytosis activation is taking place (Masters et al. 2013). Obviously, these reactions are directed toward restoring tensional homeostasis: Externalization of some part of membrane pool decreases overnormal tension, while its internalization works in the opposite way. The maintenance of membrane tension on a certain level is indispensable for polarization and directed migration of single cells (Houk et al. 2012). Let us discuss in more details the tensional dynamics during cell spreading, as studied by Gauthier et al. (2011, 2012).

After seeding a cell onto a substrate, the membrane tension is increased in 2–3 times. This is followed by unfolding of membrane reservoir, consisting at that time mostly of large membrane folds. At this stage, the tension is kept constant. Then, the next increase of membrane tension is taking place, in 2–3 min followed by a burst of exocytosis leading to extensive enlargement of membrane area and hence to its relaxation. At the same time, submembrane actomyosin network is contracted, producing membrane ruffles. As a result the tension is dropped again, now below the previous minimal level. The authors suggest that tensional dynamics is characterized by repetitive increase–decrease cycles of few dozens minutes each, each next of them occurring at lower membrane tension. As a result, cell surface becomes heterogeneous obtaining several protrusions which are anchored to the substrate and develop focal contacts associated with microfilament bundles. The latter's activity leads to another increase of tensions, now strictly localized along the protrusions. At last, due to protrusions competition, the cell acquires a single polar axis joining the leading and trailing edges. This process, also to great extent mechanically regulated, is described in more details in the next section.

At the moment, the following points from the above description are of the main interest. The first of them is that membrane tensions demonstrate a cyclic dynamics, indicating feedbacks between relaxation and strengthening; second, the feedbacks are associated with obvious overshoots; and the last point is that they drop down the cell symmetry order from almost spherical ($\infty/\infty \cdot m$) to polarized ($1 \cdot m$). This means that already at the single cell level we have a small and rudimentary, but nevertheless adequate model of morphogenesis expressed in its full scale at the level of cell collectives.

By summarizing, one may conclude that cell cortex shares both solid (elastic) and quasi-liquid properties. The elastic component is mostly coupled with submembrane actomyosin network, while the membrane proper (lipid bilayer) exhibits quasi-liquid behavior, maintaining its strain within quite narrow limits independently of preceded deformations. We use a prefix "quasi" because in the case considered the standard behavior of subsurface molecules in ordinary liquids is now reproduced on the scales of membrane vesicles and invaginations, exceeding those of single molecules in 3–4 orders at least. As we shall see later, such a dualistic

elasto-liquid behavior of cell surfaces provides a long-term maintenance of macroscopic tensile fields which are indispensable for multicellular morphogenesis.

Accordingly, as applied to cell cortex, the physical measures used traditionally both for solids and liquids can be employed. Although in most cases the estimations are of a relatively low precision, they permit to compare the values of the active forces generated within cells with those of passive resistance of cell cortex elements. As mentioned before, active forces produced by actin polymerization at the leading cell edge are enough for equilibrating resistance up to $\sim$300 nN without reducing the rate of cell advancement (Carey et al. 2011). Assuming that there are the forces generated at the leading cell edge due to actin polymerization which pull and stretch cell cortex, it will be relevant to compare them with the mechanical resistance of a lipid bilayer and submembrane actomyosin network. The elastic modulus of a lipid bilayer lays within 10^3 N/m^2 = 1 nN/μm^2 range (Diz-Muñoz et al. 2013), while that of actomyosin network extensively varies in a nonlinear fashion, depending upon its stretching (Rauzi and Lenne 2011). In the above described slightly stretched and loops-abundant enthalpic phase, actomyosin network is very soft (elastic modulus about 1 N/m^2), while under extensive stretching it passes to entropic phase with the filaments aligned in stretch direction: Now, elastic modulus can rise up to at least 10^3 N/m^2. The branched actin structures located at the leading cell edge are even stiffer: At least in vitro conditions, elastic modulus for these structures reaches 10^3 N/m^2. Suggest that the pulling force of actin polymerization is evenly spread throughout the cell membrane area having 10 nm = 10^{-2} μm thickness and several hundreds (say from 200 to 500) μm diameter (this is usual transversal cell diameter at the leading edge level). We can see that a force non-exceeding 10 nN range, that is a small part of what may be produced by actin polymerization at the leading edge, is enough for equilibrating the elastic resistance of lipid bilayer and for stretching at the same time the actomyosin network. This increases the probability of the cortical layer of an actively spreading cell to be stretched for most of the time.

Quasi-liquid properties of the cortical layer have been estimated by tension measurements giving for a nerve growth cone the value of 3×10^{-3} mN/m, for a neutrophil 3×10^{-2} nN/μm, and for erythrocyte an order greater (Hochmuth et al. 1996). Accordingly, for increasing the contour length of the cell membrane to 100 μm (and the average cell diameter to $100/\pi \approx 30$ μm), a similar force of few nanonewtons is enough. Under all reservations, these results indicate that just a small part of forces produced within a cell is enough to deform it.

2.10 Symmetry Breaks in Entire Cells

Is there anything in common in the symmetry breaks taking place at different stages of development—from its very start up to formation of specialized cells? A number of recent investigations (Munro 2006; Li and Gundersen 2008; Gucht Van der and Sykes 2009; Nance and Zallen 2011; Goehring and Grill 2013; Diz-Muñoz et al. 2013)

permitted to give a generally positive answer to this question. A brief generalized review of the main results is given below.

First, it was found that the key structural regulators of cell polarity belonged in all the cases to the family of so-called PAR (partitioning) proteins, which consist of two mutually extinct groups, displacing each other from cells cortex (mostly by phosphorylation). This already creates a negative feedback, promoting segregation of both groups. Next, extensive cross talks, mostly providing positive feedbacks, are also taking place between the members of PAR family and small GTPases Cdc-42 and Rac. It is also worth mentioning, that all the PAR proteins are highly dynamic, turning over on a timescale of tens of seconds, even if they support more stable structures.

Another member of the dynamic circuit leading to cell polarization is actomyosin network which undergoes unilateral contraction displacing the group of PAR proteins by means of so-called advection, that is, by involving them into a common flow. PAR proteins are far from being passive participants in their redistribution: For example, PAR-3 amplifies myosin activity. As a result, another positive feedback is added.

The third vectorizing member is exemplified by microtubules, the role of which largely varies in different cases of cell polarization.

One of the best studied examples of cell polarization is the establishment of antero-posterior (AP) axis in newly fertilized *C. elegans* eggs. Prior to fertilization, the entire egg cortex is occupied by one of PAR groups, the so-called Par-3/Par-6/Pkc-3 complex. The sperm marking by its entrance points the posterior pole of the future organism brings with itself the microtubule organizing center (MTOC) which relaxes the adjacent part of actomyosin network, stimulating its shift toward anterior and similarly directed advection of the above-mentioned PAR complex. Also, it stimulates the recruitment of the members of the alternative PAR proteins group to the posterior domain, possibly by its direct transportation along microtubules (Bastock and Johnston 2011). As a result, the posterior and anterior domains become sharply segregated from each other, providing strictly different fates of the blastomeres developed from each of these regions.

Either actomyosin flows or microtubules transport involving PAR proteins participate in almost all other cases of egg or cell polarization. Thus, in vertebrate oocytes (both in mouse and in *Xenopus*) the above-mentioned PAR proteins complex is involved by this flow toward the future animal pole and obviously determines the latter's position. In ascidian eggs, the oocyte polarity is first manifested by quite extensive Ca^{2+} triggered actomyosin flows displacing the so-called myoplasm, enriched by mitochondria, toward the vegetal pole. Later on a bundle of oppositely directed microtubules (their "+" ends located near the animal pole) comes into play, compressing the myoplasm at the site of the future posterior pole. The accumulation of PAR proteins complex starts from 2 blastomeres stage and goes up to 16-cell stages. Being at first microfilaments dependent, it becomes later on transported along microtubules (Sardet et al. 2007). Formation of the apico-basal polarity of mammalian epithelial cells is associated with the Par-3/Par-6/Pkc-3 loaded flows directed toward the sites of the cadherin-mediated cell–cell contacts,

while the abbreviated Par-6/Pkc complexes become bound with apical cell surfaces. In contrast, the apico-basal polarization of *Drosophila* cells is driven by the dynein-based transport of PAR-3 along microtubules toward apico-lateral cell boundaries. In reverse, PAR proteins are known to be implicated in localizing the force-generating interactions between microtubules and the cortex, being the main regulator of the polarized microtubules-based transport in *Drosophila* oocytes, *C. elegans* cleaving eggs and in both vertebrate and invertebrate epithelia (Munro 2006). By comparing the contributions of actin-based and microtubules-dependent mechanisms, it is suggested that the first ones play the key role in the initiation and rapid responses to external stimuli, while microtubules build on and stabilize the initial asymmetry (Li and Gundersen 2008).

So we see that cell polarization is always associated with a complicated network of positive and negative feedbacks between certain groups of proteins as well as between the force-generating devices—microfilaments and microtubules together with motor proteins. Taken themselves, these feedbacks are already directed toward segregating initially homogeneous cortical patterns into different domains, but are they enough to provide the global order on the single cell scale being an imminent component of cell polarization? Let us discuss this problem taking a typical polarization pattern of a crawling cell as example (Fig. 2.4). As one can learn from textbooks on the molecular biology of the cell, a polarized state is characterized by domination of the myosin II-free arborescent actin structures at the leading edge and of actomyosin contractile filaments at the rear end of a cell; this pattern is supported by negative feedbacks between the activity of two GTPases: Rac in the anterior region and Rho in the posterior one. However, this seems far from being the whole story. By casting again a glance to Fig. 2.4d–f, one can see that from the morphological point of view, the antero-posterior cell polarization means selection of a single axis out of the entire set of possible directions. This implies the competition

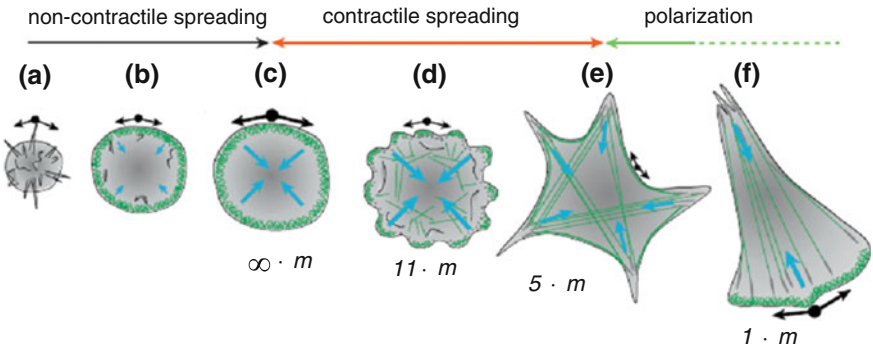

Fig. 2.4 Diagrams of mechanical stresses at successive stages of cell spreading and polarization. *Black diverged arrows* display tensions on cell surface; *blue converged arrows* display tensions generated by actomyosin contraction and maintained by newly established focal junctions. *Note* periodic ups and downs in surface tension and an overall decrease of the cell symmetry order (shown). From Gauthier et al. (2012), © Elsevier 2012, reproduced with permission from Elsevier

between several primary protrusions shown in Fig. 2.4d. Tensions look to be the best agents for making this job. Just this point of view is developed in several recent studies (Kozlov and Mogilner 2007; Houk et al. 2012; Diz-Muñoz et al. 2013). In particular, Houk et al. argued that diffusion-based mechanisms are non-sufficient for long-range interactions between frontal and rear parts of cells, while the membrane tension which by their estimations is increased twofold during leading edge protrusion may exert long-range inhibition of actin assembly going within a cell in antero-posterior direction. Within such a framework, the role of chemical attractants which are known to orient antero-posterior axes of several types of cells (from yeasts to lymphocytes) may be in triggering the internal mechanically based regulatory contour which in the second turn recruits the above-mentioned GTPases to their proper localizations.

A bold attempt to interpret the factors of cell polarity maintenance in mechanical terms without the use of chemical feedbacks has been performed by Kozlov and Mogilner (2007) employing keratinocyte fragments as a model. The fragments exhibit two most ubiquitous shapes, round and crescent-like. In the first case, just two mutually balanced forces are present: the passive tangential tension and the pushing force produced by the actin polymerization; in crescent-like forms, the contractile force of the active myosin-powered tension in the rear (concave) area is added. By the authors calculations, the free mechanical energy of the sample regarded as a function of the crescent's opening angle θ has two minima: the first one at $\theta = 0$ (corresponding to the round shape) and the other one laying between 100° and 150°. The height of the energy barrier between them depends on the ratio between the myosin-powered tension at the rear edge and the pushing force of actin polymerization at the frontal edge: The greater the latter force is, the easier is the transition from the non-polarized (round) to the polarized (crescent-like) form. The authors suggest that the main polarizing factor is just the drive toward energy minimum, while the role of more detailed chemical signaling is restricted in regulating the rate of this drive.

The next question related to symmetry breaks on the single cells level is to whether they require strong external cues or instead can go "spontaneously," that is, under infinitesimal perturbations. As far as many of symmetry breaks are started from disrupting the cortical actomyosin network, let us look for potential possibilities of such a net to be fractured "spontaneously."

In this respect, it is worth reminding a topological Brouwer theorem (for a biologically oriented review see Isaeva et al. 2012) which states that any vector field mapped onto three-dimensional surface (but not onto two- or one-dimensional ones) must have at least one singularity, that is, a point where a field continuity is broken. Just such a field is exemplified by actin network deposited on the cortex of three-dimensional egg cells: Thus, egg cortex should necessarily have at least one point of potential rupture. The demand of singularity may be the most fundamental cause for what we call cell polarization; certainly, this trend should be properly located and amplified by a set of regulatory factors.

As the first step toward more concrete models, we may consider the behavior of actin gel surrounding microscopic beads (Van der Gucht and Sykes 2009). Due to

actin polymerization, new monomers are incorporated at the bead surface underneath the preexisting gel, producing stresses and making the entire actin shell tensed. Thus, after some time the shell breaks, releasing the accumulated elastic energy. This may be an adequate model for a spectacular formation of the comet-like actin tails by a bacteria *Listeria* and to some extent for the break of actomyosin network in *C. elegans*, although in the latter case the site of the break is predetermined by the male centrosome. In any case, the value of tensile stress required for actin shell break was found to be of the same order (10^3–10^4 Pa) as for the cortical layer of most cells. By these estimations, cell cortex may be close to the break threshold, requiring no more than about 10 % of additional stress to be disrupted. The distance between the amount of the cortical tension and the instability threshold may regulate the number of ruptures to be performed: If the tension is far from threshold, the break requires a strong external influence: In this case, a single rupture is expected. Meanwhile, by approaching to the verge of stability, the appearance of numerous ruptures is more probable.

Coming back to cell polarization, we have to remind first of all that egg cells may acquire animal–vegetal polarity and, in particular, dorso-ventrality, either being induced from outside or spontaneously (see Chap. 4 for more detailed discussion). Same dualism holds true for other cases of cell polarization. For example, although by many evidences the establishment and maintenance of apico-basal polarity of an epithelial cell requires such external cues as contacts with neighboring cells and ECM, a spatially smoothed ectopic activation of the kinase LKB1 (related to the activation of myosin II based contractility) induces spontaneous symmetry breaking and establishes well-defined apical and baso-lateral domains in the absence of cell–cell contacts (Li and Gundersen 2008).

In the case of the planar cell polarity, the situation is similar. In a number of cases, it requires distinct dissymmetrizers. According to the above-presented calculations of Van der Gucht and Sykes, the moderate mechanical forces, able to overcome the energetic barrier of actomyosin net rupture, may play such a role. In this respect, some novel data on the effects of mechanical tensions on planar cell polarity may be of interest. Aigouy et al. (2010) proposed that the tensions exerted from the proximal part of *Drosophila* wing provide planar polarity of the distal part cells. In our laboratory, Evstifeeva (2013) demonstrated that in artificially stretched double explants of ventral ectoderm taken from early gastrula *Xenopus* embryos, the streams caused by ciliary beating are oriented in most cases perpendicular to stretch directions and in the intact embryos they orient at right angles to the tensions produced by gastrulation and neurulation movements. Meanwhile, in non-stretched explants, the streams are oriented much more randomly, although if tending to be grouped into several small uniformly oriented regions. So far as the direction of ciliary beating marks planar cell polarity, this indicates that the latter may be affected by mechanical force in vertebrate embryos as well.

By concluding, we may suggest that such an important and esthetically beautiful event as cell polarity is based upon a complicated and up to now not completely untangled web of negative and positive feedbacks related to different levels; among them, mechanical feedbacks seem to play the leading role in a large-scale

integration of lower levels ones. For these feedbacks to be effective, the entire cell should be either in an unstable state, or on the verge of stability: In both cases, it behaves as a nonlinear system. Being still rudimentary on the levels of cytoskeleton and single molecular machines, nonlinear properties are expressed in full scale at the upper structural levels of cell organization.

References

Aigouy B, Farhadifar R, Staple DB et al (2010) Cell flow reorients the axis of planar polarity in the wing epithelium of Drosophila. Cell 142(5):773–786

Alberts B, Bray D, Lewis J, Raff M, Roberts K, Watson JD (2003) Molecular biology of the cell. Garland Publishing Inc, New York

Apodaca G (2002) Modulation of membrane traffic by mechanical stimuli. Am J Physiol Renal Physiol 282:F179–F190

Balaban NQ et al (2001) Force and focal adhesion assembly: a close relationship studied using elastic micropatterned substrates. Nature Cell Biol 3:466–472

Bastock R, Johnston D (2011) Going with the flow: an elegant model for symmetry breaking. Devel Cell 21:981–982

Bishofs IB, Schwarz US (2003) Cell organization in soft media due to active mechanosensing. PNAS 100:9274–9279

Bluemenfeld LA (1983) Physics of bioenergetic processes. Springer, Berlin

Borghi N, Sorokina M, Sherbakova OG, Weis WL, Pruitt DL, Nelson WJ, Dunn AB (2012) E-cadherin is under constitutive actomyosin-generated tension that is increased at cell-cell contacts upon externally applied stretch. PNAS 109:12568–12573

Brevier J, Montero D, Svitkina T, Riveline D (2008) The asymmetric self-assembly mechanism of adherent junctions: a cellular push-pull unit. Phys Biol 5(1):016005

Bursac P, Lenormand G, Fabry B, Oliver M, Weitz DA, Viasnoff V, Butler JP, Fredberg JJ (2005) Cytoskeletal remodelling and slow dynamics in the living cell. Nat Mater 4:557–561

Campàs O, Mammoto T, Hasso S, Sperling RA, O'Connell D, Bischof AG, Maas R, Weitz DA, Mahadevan L, Ingber DE (2014) Quantifying cell-generated mechanical forces within living embryonic tissues. Nat Methods 11:183–189

Carey SP, Charest JM, Reinhart-King CA (2011) Forces during cell adhesion and spreading: implications for cellular homeostasis. Stud Mechanobiol Tissue Eng Biomatter 4:29–69

Chen CS, Mrksich M, Huang S, Whitesides GM, Ingber DE (1997) Geometric control of cell life and death. Science 276:1425–1428

Chernavskii DS, Chernavskaia NM (1999) Protein-machine. Biological macromolecular constructions. Moscow University Printing House, Moskva

Chiquet M, Gelman L, Lutz R, Maier S (2009) From mechanotransduction to extracellular matrix gene expression in fibroblasts. Bioch Biophys Acta 1793:911–920

Conway DE, Breckenridge MT, Hinde E, Gratton E, Chen CS, Schwarts MA (2013) Fluid shear stress on endothelial cells modulate mechanical tension across VE-cadherin and PECAM-1. Curr Biol 23:1024–1030

Danilchik MV, Brown EE, Riegert K (2006) Intrinsic chiral properties of the Xenopus egg cortex: an early indication of left-right asymmetry? Development 133:4517–4526

Del Giudice E et al (2005) Coherent quantum electrodynamics in living matter. Electromagnetic Biol Med 24:199–210

Del Giudice E, Stefanini P, Tedeschi A, Vitiello G (2011) The interplay of biomolecules and water at the origin of active behavior of living organisms. J Phys Conf Ser 329:012001

Deng L, Trepat X, Butler JP, Millet E, Morgan KG, Weitz DA, Fredberg JJ (2006) Fast and slow dynamics of the cytoskeleton. Nat Mater 5:636–640

Diz-Muñoz A, Fletcher DA, Weiner OD (2013) Use the force: membrane tension as an organizer of cell shape and motility. Trends Cell Biol 23:47–53

Evstifeeva AJu (2013) Topology and planar polarity of Xenopus embryonic ciliary epithelium. Izvestia Russ Acad Sci Ser Bio 40(6):661–667 (in Russian)

Fabry B, Maksym GN, Butler JP, Glogauer M, Navajas D, Taback NA, Millet EJ, Fredberg JJ (2003) Time-scale and other invariants of integrative mechanical behavior of the living cell. Phys Rev E 68:041914

Fakhri N, Wessel AD, Willms C, Pasquali M, Klopfenstein DR, MacKintosh FC, Schmidt CF (2014) High-resolution mapping of intracellular fluctuations using carbon nanotubes. Science 344:1031–1034

Forgacs G (1995) On the possible role of cytoskeletal filamentous networks in intracellular signaling: an approach based on percolation. J Cell Sci 108:2131–2143

Gardel ML, Shin JH, MacKintosh FC, Mahadevan L, Matsudaira P, Weitz DA (2004) Elastic behavior of cross-linked and bundled actin networks. Science 304:1301–1305

Gauthier NC, Fardin MA, Roca-Cusachs P, Sheetz MP (2011) Temporary increase in plasma membrane tension coordinates the activation of exocytosis and contraction during cell spreading. PNAS 108:11467–11472

Gauthier NC, Masters TA, Sheetz MP (2012) Mechanical feedback between membrane tension and dynamics. Trends Cell Biol 22:527–536

Goehring NW, Grill SW (2013) Cell polarity: mechanochemical patterning. Trends Cell Biol 23:72–80

Goodwin BC, Trainor LEH (1985) Tip and whorl morphogenesis in Acetabularia by calcium-regulated strain fields. J Theor Biol 117:79–106

Grashoff C, Hoffman BD, Brenner MD, Zhou R, Parsons M, Yang MT, McLean MA, Sligar SG, Chen CS, Ha T, Schwartz MA (2010) Measuring mechanical tension across vinculin reveals regulation of focal adhesion dynamics. Nature 466:263–266

Gurwitsch AG (1944) A theory of biological field (in Russian). Nauka, Moskva

Hochmuth F-M, Shao J-Y, Dai J, Sheetz MP (1996) Deformation and flow of membrane into tethers extracted from neuronal growth cones. Biophys J 70:358–369

Houk AR, Jilkine A, Mejean CO, Boltyansky R, Dufresne ER, Angenent SB, Altshuler SJ, Wu LF, Weiner OD (2012) Membrane tension maintains cell polarity by confining signals to the leading edge during neutrophil migration. Cell 148:175–188

Howard J (2009) Mechanical signaling in networks of motor and cytoskeletal proteins. Ann Rev Biophys 28:217–234

Igamberdiev AU (2012) Physics and logic of life. Nova Science Publishers, New York

Isaeva VV, Kasyanov NV, Presnov EV (2012) Topological singularities and symmetry breaking in development. BioSystems 109:280–298

Ishiwata S, Shimamoto Yuta, Suzuki Madoka (2010) Molecular motors as an auto-oscillator. HFSP J 4:100–104

Klotzsh E, Smith ML, Kubow KE, Muntwyler S, Little WC, Beyeler F, Gourdon D, Nelson BJ, Vogel V (2009) Fibronectin forms the most extensible biological fibers displaying switchable force-exposed cryptic binding sites. PNAS 106:18267–18272

Kozlov MM, Mogilner A (2007) Model of polarization and bistability of cell fragments. Biophys J 93:3811–3819

Kruse K, Riveline D (2011) Spontaneous mechanical oscillations: implications for developing organisms. Curr Top Devel Biol 95:67–91

Ladoux B, Nicolas A (2012) Physically based principles of cell adhesion mechanosensitivity in tissues. Rep Prog Phys 75:116601 (25 p)

Li R, Gundersen GG (2008) Beyond polymer polarity: how the cytoskeleton builds a polarized cell. Nat Rev Mol Cell Biol 9:860–873

Lindemann ChB, Lesich KA (2010) Flagellar and ciliary beating: the proven and the possible. J Cell Sci 123:519–528

Liverpool T (2006) Active gels: where polymer physics meets cytoskeletal dynamics. Phil Trans R Soc A 364:3335–3355

Lo C (2000) Cell movement is guided by the rigidity of the substrate. Biophys J 79(1):144–152
Masters TA, Viasnoff V, Gauthier N (2013) Plasma membrane tension orchestrates membrane trafficking, cytoskeletal remodeling, and biochemical signaling during phagocytosis. Proc Natl Acad Sci USA 110:11875–11880
Matsuno K (2006) Forming and maintaining a heat engine for quantum biology. BioSystems 85:23–29
McClare CWF (1971) Chemical machines, Maxwell's demon and living organisms. J Theor Biol 30:1–34
Mitrossilis D, Fouchard J, Pereira D, Postic F, Richert A, Saint-Jean M, Asnacios A (2010) Real-time single cell response to stiffness. PNAS 107:16518–16523
Munro EM (2006) PAR proteins and the cytoskeleton: a marriage of equals. Curr Opin Cell Biol 18:86–94
Nance J, Zallen JA (2011) Elaborating polarity: PAR proteins and the cytoskelenon. Development 138:799–809
Odell GM, Oster G, Alberch P, Burnside B (1981) The mechanical basis of morphogenesis. I Epithelial folding and invagination. Dev Biol 85:446–462
Plaçais P-Y, Balland M, Guerin T, Joanny J-F, Martin P (2009) Spontaneous oscillations of a minimal actomyosin system under elastic loading. Phys Rev Lett 103:158102
Pohl C, Bao Z (2010) Chiral forces organize left-right patterning in *C. elegans* by uncoupling midline and antero-posterior axis. Dev Cell 19(3):402–412
Pollack GH (2001) Cells, gels and the engines of life: a new, unifying approach to cell function. Ebner, Seattle
Rauzi M, Lenne P-F (2011) Cortical forces in cell shape changes and tissue morphogenesis. Curr Topics Dev Biol 95:93–121
Roh-Johnson M, Shemer G, Higgins CD, McClellan JH, Werts AD, Tulu US, Gao L, Betzig E, Kiehart DP, Goldstein B (2012) Triggering a cell shape change by exploiting pre-existing actomyosin contractions. Science 335(6073):1232–1235
Saez A, Buguin A, Silberzan P, Ladoux B (2005) Is the mechanical activity of epithelial cells controlled by deformations or forces? Biophys J: Biophys Lett 89:L52–L54
Samuel MS, Lopez JI, McGhee EJ, Croft DR, Strachan D, Timpson P, Munro J, Schröder E, Zhou J, Brunton VG, Barker N, Clevers H, Sansom OJ, Anderson KI, Weaver VM, Olson MF (2011) Actomyosin-mediated cellular tension drives increased tissue stiffness and β-catenin activation to induce epidermal hyperplasia and tumor growth. Cancer Cell 19:776–791
Sardet C, Paix A, Prodon F, Dru P, Chenevert J (2007) From oocyte to 16-cell stage: cytoplasmic and cortical reorganizations that pattern the ascidian embryo. Dev Dyn 236:1716–1731
Schaller V, Weber Chr, Semmrich Chr, Frey E, Bausch AR (2010) Polar patterns of driven filaments. Nature 467:73–77
Shemesh T, Geiger B, Bershadsky AD, Kozlov MM (2005) Focal adhesions as mechansors: a physical mechanism. PNAS 102:12383–12388
Schroedinger E (1944) What is life? The physical aspect of the living cell. Cambridge University Press, Cambridge
Sinha B et al. (2011) Cells respond to mechanical stress by rapid disassembly of caveolae. Cell 144:402–413
Speder P, Noselli S (2007) Left-right asymmetry: class I myosins show the direction. Curr Opin Cell Biol 19:82–87
Stern CD (1984) A simple model for early morphogenesis. J Theor Biol 107:229–242
Storm C, Pastore JJ, MacKintosh FC, Lubensky TC, Janmey PA (2005) Nonlinear elasticity in biological gels. Nature 435:191–194
Sumida GM, Tomita TM, Shih W, Yamada S (2011) Myosin II activity dependent and independent vinculin recruitment to the sites of E-cadherin-mediated cell-cell adhesion. BMC Cell Biol 12:48 (9 p)
Sumino Y, Nagai KH, Shitaka Y, Tanaka D, Yoshikawa K, Chate H, Oiwa K (2012) Large-scale vortex lattice emerging from collectively moving microtubules. Nature 483:448–452

Tsikolia N, Schroeder S, Schwartz P, Viebahn C (2012) Paraxial left-sided nodal expression and the start of left-right patterning in the early chick embryo. Differentiation 84:380–391

Trepat X, Deng L, An SS, Navajas D, Tschumperlin DJ, Gerthoffer WT, Butler JP, Fredberg JJ (2007) Universal physical responses to stretch in the living cell. Nature 447:592–595

Vandenberg LN, Levine M (2013) A unified model for left-right asymmetry? Comparison and synthesis of molecular models of embryonic laterality. Dev Biol 379:1–15

Van der Gucht J, Sykes C (2009) Physical model of cellular symmetry breaking. Cold Spring Harb Perspect Biol 1:a001909

Vogel SK, Pavin N, Maghelli N, Julicher F, Tolic-Nerrelykke IM (2009) Microtubules and motor proteins: mechanically regulated self-organization in vitro. Eur Phys J Spec Topics 178:57–69

Weiser DC, Row RH, Kimelman D (2007) Rho-regulated Myosin phosphatase establishes the level of protrusive activity required for cell movements during zebrafish gastrulation. Development 136:2375–2384

Wilson PA, Oster G, Keller R (1989) Cell rearrangements and segmentation in Xenopus: direct observations of cultured explants. Development 105:155–166

Wipff P-I, Rifkin DB, Meister J-J, B.Hinz (2007) Myofibroblast contraction activates latent TGF-beta from the extracellular matrix. J Cell Biol 179:1311–1323

Zhang H, Landmann F, Zahreddine H, Rodriguez D, Koch M, Labouesse M (2011) Tension-induced mechanotransduction pathway promotes epithelial morphogenesis. Nature 471:99–103

Chapter 3
Morphogenesis on the Multicellular Level: Patterns of Mechanical Stresses and Main Modes of Collective Cell Behavior

Abstract Regular patterns of mechanical stresses are perfectly expressed on the macromorphological level in the embryos of all taxonomic groups studied in this respect. Stress patterns are characterized by the topological invariability retained during prolonged time periods and drastically changing in between. After explanting small pieces of embryonic tissues, they are restored within several dozens minutes. Disturbance of stress patterns in developing embryos irreversibly breaks the long-range order of subsequent development. Morphogenetically important stress patterns are established by three geometrically different modes of cell alignment: parallel, perpendicular, and oblique. The first of them creates prolonged files of actively elongated cells. The second is responsible for segregation of an epithelial layer to the domains of columnar and flattened cells. The model of this process, demonstrating its scaling capacities, is described. The third mode which follows the previous one is responsible for making the curvatures. It is associated with formation of "cell fans," the universal devices for shapes formation due to slow relaxation of the stored elastic energy.

3.1 Introductory Remarks

After completing our review of the structures formation on subcellular levels, we come to morphogenesis in its classical sense—as a set of coordinated cell activities leading to creation of multicellular embryonic rudiments. Although most of these processes are believed to be perfectly explored, actually, they are quite far from being properly understood. To a great extent, this is because a usual focusing on what is called the specific causes of this or that organ formation shadows the general properties which should be common to almost all cases of multicellular morphogenesis.

In this chapter, we shall review the main morphogenetical processes separately from each other, leaving for the next chapter the problem of their space–temporal arrangement. Our immediate aim will be to outline some general properties of morphogenetical processes and to distinguish their main modes.

L.V. Beloussov, *Morphomechanics of Development*,
DOI 10.1007/978-3-319-13990-6_3

So far as we could see from the preceding chapters, the most plausible models of morphogenesis imply the existence of long-lived mechanical stresses. Accordingly, we will start from exploring whether more or less coherent and stable stress patterns can be traced on a macromorphological level. This task is not trivial: A priori the stressed states taking place on the supramolecular and the single-cell levels could be dissipated at the higher levels. We shall demonstrate however that this is not the case.

Next, we will deviate from developmental chronology for describing the main modes of collective cell processes which create, at any stages, the mechanically stressed multicellular communities. We shall see that in the most cases, they are emerged as relays of cell transformations which start from a single of few center(s) and involve dozens of cells. In this way, using the chains of short-range interactions, they bind together the different level processes.

3.2 Patterns of Mechanical Stresses (MS) in Developing Embryos

3.2.1 MS Patterns in Amphibian Embryos: Methods of Detection and Mapping

The most straightforward way for checking whether a piece of matter is stressed or not, borrowed from inorganic mechanics, is to firmly fix the samples ends, make a cut somewhere in between, and trace whether and when the cut edges will be shifted from their initial positions: If they are shifted apart, so to say, "immediately" (within fractions of a second), we have to conclude that before cutting, the sample was elastically stretched (see 1.2.4); if instead they are drawn together and overlapped at a similar rate, we conclude that the sample has been elastically compressed. In both cases, the sample is concluded to be prestressed. In case of ideally elastic (Hookean) behavior, the width of the gap may be considered as an adequate measure of preexisted elastic stress. However, in real cases, such estimations are aggravated by the differences in border conditions, which may be quite complicated. In the simplest cases, the distance of the gap from the edge of the cut should be taken into account: Obviously, under the same stress values, the laterally located gaps should be smaller than centrally located ones.

Additional difficulties in interpreting post-incision deformations in biological samples arise when the gap formation or other post-incision deformations cannot be qualified as "instant." While in non-biological materials any retardations of the deformation rates can be ascribed to their viscous properties and do not hence violate the general conclusions about a prestressed state, this is not so in the active living samples. In the latter cases, the delayed responses well may be associated with newly generated energy-consuming reactions triggered by the incisions themselves and telling nothing about preincisions state. As far as a distinction between the "instant" and "delayed" responses is to a great extent arbitrary, some additional criteria for

discerning pre- and post-incision events are desirable. Happily, in *Rana temporaria* embryos which we used for a primary MS evaluation (Beloussov et al. 1975), such criteria are provided by their ability to survive close to 0 °C, although the development and all the contractile tissue reactions under this temperature are arrested. By comparing post-incision reactions close to zero and under optimal temperatures, we could trace in the first case nothing more than the fast ($t \leq 1$ s) deformations in their full scale, while under optimal temperatures they were invariably followed by the delayed deformations going as a rule in the opposite directions. We conclude that only the cold-resistive fast deformations ("mechanical jumps" by Hutson 2003) can be considered as the reliable indices of preexisted quasi-elastic MS. Meanwhile, the delayed deformations are of their own interest. They were shown to be associated with de novo assembly and contraction of actin microfilaments under the naked surface of explants (Beloussov and Louchinskaia 1983) and illustrate the capacities of embryonic explants to the regular shape changes taking no more than few dozens minutes.

Among the incisions used for detecting fast deformations, the unilateral Π-shaped or bilateral H-shaped ones followed by detachment of ectoderm from the underlined tissues turned out to be most of all informative. While performed in certain definite locations, they immediately produced acute folds with their outer surfaces looking to each other (Fig. 3.1, rows 1, 2, 4 red pointers; see in particular row 4, a_2). The immediately arisen folds were too deep and acute for being the results of the apical cell constrictions only: In addition, the cells on the fold basis had to be pulled inside indicating the existence of some internal tensed structures relaxed just after separation. This suggestion was proved by the mechanically inverse methods based upon the condition of force balance (see Chap. 2). In these estimations, we took cell walls (identified with the cortical cell layers) as tensed cables and cell apexes as tension nodules. The main idea was to start from a nodule 1 (Fig. 3.2a, blue area), ascribing to one of cell walls a referent force a; then by knowing α and β angles, we can express other forces (x and y) belonging to the same nodule in a units. Then, we pass from one adjacent nodule to another (say from 1 to 2) repeating the same procedure and always expressing the forces in a units. In extreme case, we can make a round trip through some number of nodules (Fig. 3.2a, red curved arrow) returning to nodule 1 and measuring again the force along a wall. If the discrepancy of this measurement from the referent one is small, we conclude that practically all the forces affecting the given plane cells are located in this very plane (the sum of forces coming from other planes is close to zero) and vice versa. In fact, we found that the deviation from the reference value did not exceed 10 % even if the trip included more than 400 intermediate nodules (Beloussov and Lakirev 1988).

These measurements permitted to make two main conclusions. First, it turned out that the distribution of the relative tension values in cell walls was markedly bimodal: they were distinctly split into weak and strong ones, with only few intermediates (Fig. 3.2b). This permitted to take into consideration no more than these two classes of tensions. Next, this method confirmed the existence of the files and networks of strongly tensed cells which cross embryonic tissues in quite definite locations; the exit points of these cell files exactly coincide with the apexes

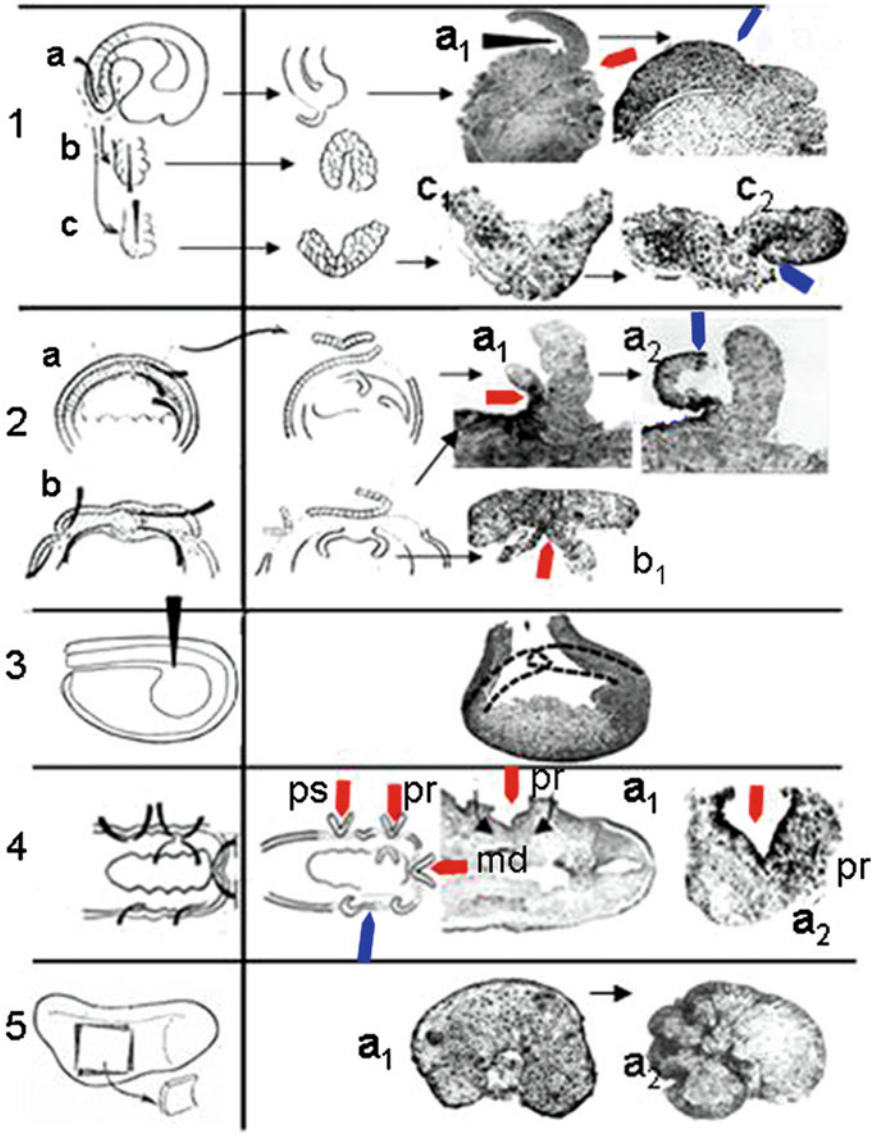

Fig. 3.1 Localizing main mechanical stresses in early gastrula—tail bud stages of Rana temporaria embryos (*rows 1–4*) by local incisions (*black wedges*). *Left column* schemes of operations. Next frames to the *right*, in succession: sketches and shots of fast deformations (*red pointers*); shots of the delayed (active) deformations (*blue pointers*). Successive steps of deformations are connected by *arrows*. *Row 5* active delayed deformations of extirpated fragments of lateral ectoderm with underlined mesoderm. From Beloussov et al. (1975), modified

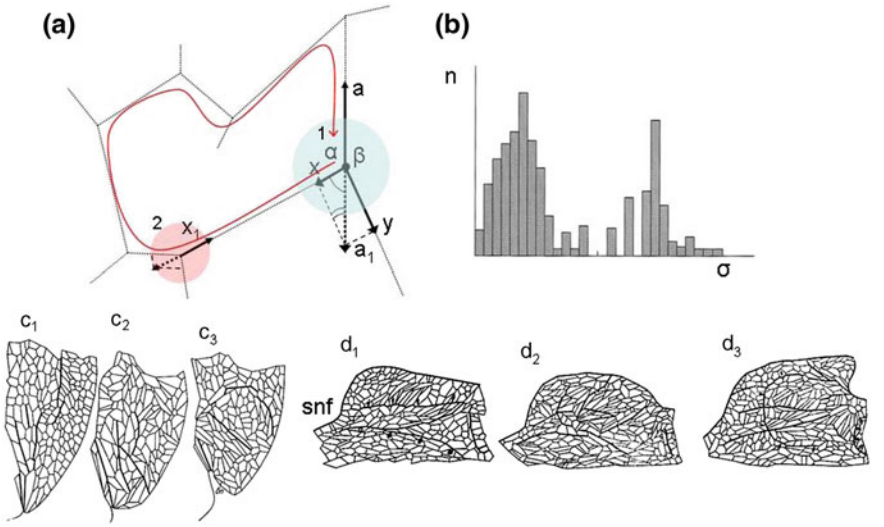

Fig. 3.2 Some results of the mechanical inverse methods. **a** Scheme of measurements. *Colored* are cell nodules 1, 2 measured in succession. *Red line* depicts measurements pathways ending in the initial point. **b** A markedly bimodal tensions distribution in a representative area of embryonic tissue. $\mathbf{c_1}$–$\mathbf{c_3}$ Evolution of tensile patterns in the dorsal blastoporal lip during gastrulation. $\mathbf{d_1}$–$\mathbf{d_3}$ Same in the *left* part of neural plate during neurulation. Dense lines are those of maximal tensions. Subneural fold *Snf*. **b**–**d** Are from Beloussov and Lakirev (1988)

of the incision-made folds. We define these structures as the cross-lines (although it may be better to call them cross-webs). The presence and arrangement of the cross-lines are the main criteria of MS patterns topology (Fig. 3.2c_1–c_3, d_1–d_3).

By combining the results of incision experiments and the mechanical inverse method, we can construct the *maps of tensile stresses* for amphibian embryos covering the developmental period from late blastula to tail bud stage (Fig. 3.3). In these, we plot three main categories of tensed structures: the outer ectodermal layer (more precisely, cells' apical cortical areas), cross-lines, and the tension nodules. By constructing the whole embryo maps, we neglect microscopic (single cells) nodules taking into consideration only macroscopic ones, which are the meeting points of cross-lines with the outer ectodermal cells. In fact, most of macroscopic nodules are extended along embryonic surfaces and can be better defined as seams. In our subsequent account, we shall use both terms.

Worth mentioning, the tensed structures are balanced by inside pressure (not shown), which may be either isotropic (up to gastrula stage exerted by turgor pressure within blastocoel and later by pressure within endodermal compartments) or anisotropic (produced by actively elongated notochord and probably by neural tube).

One of the main findings was that within a substantial developmental period from blastula to tail bud stage, the topology of tensions (i.e., the number and mutual

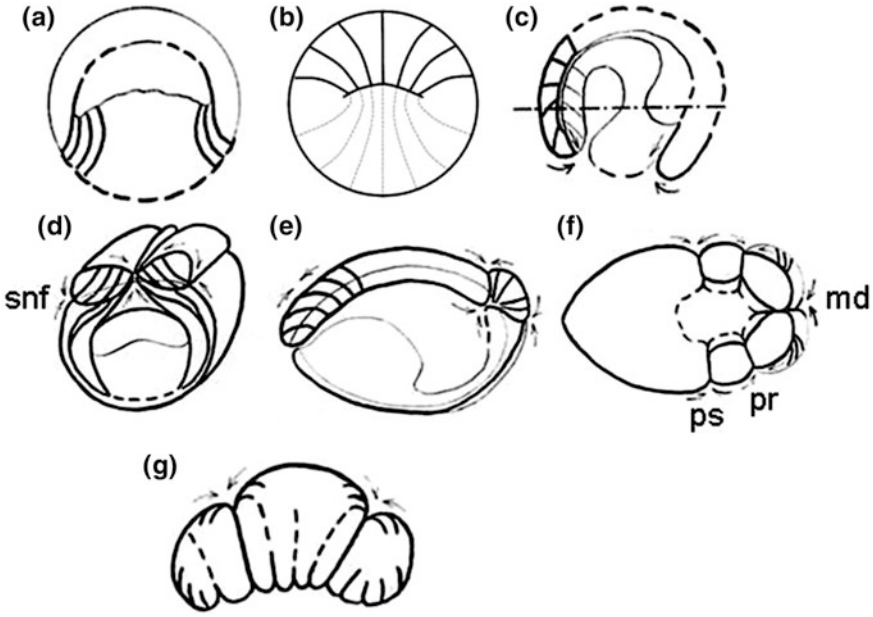

Fig. 3.3 Maps of mechanical stresses at successive developmental periods of amphibian embryos. **a** Late blastula stage, cross section. **b** Early gastrula stage, surface view from vegetal pole. *Dotted curves* display largely dispersed parts of tension lines. **c** Mid-blastula stage, cross section. **d** Early neurula stage, cross section of the trunk part. **e** Early tail bud, saggital section. **f** Advanced tail bud stage, frontal section. **g** Ectomesodermal fragment, 15 min after extirpation from a tail bud stage embryo. Dense contours depict lines of extensive tensions. *Arrows* are converging toward tension nodules

arrangement of cross-lines and nodules) is changed for few times only. The changes take no more than few dozens minutes each and exactly fit the transitions between periods outlined already by classical embryologists: blastulation, gastrulation, neurulation, and tail bud formation. Correspondingly, the number of successive maps is also small.

In particular, the incisions made at the blastula stage indicate nothing more than circular cross-lines created by moderately tensed cells which link embryonic surfaces with the ventral angles of the blastocoel and coincide with the so-called marginal zone (the one located between ecto- and endodermal areas) (Fig. 3.3a). Since the start of gastrulation, a new powerful tensile field appears associated with the formation and further evolution of the blastopore adjacent area. As seen from the surface, the field includes two new components: the circular tensions of the blastoporal lip and the radial tension lines spread from the blastopore and covering most of embryonic surface. The lines are most of all condensed in the dorsal vicinity of the blastoporal arch (this is so-called supra-blastoporal area, SBA) and gradually disperse toward ventral (Fig. 3.3b, solid and dashed lines, respectively). Circular tensions are detected by a fast pulling apart of transversely dissected parts

of the blastoporal lip and the radial tensions by even more fast (≤1 s) acute folding of SBA while being separated from underlying tissues in the blastopore direction (Fig. 3.1, row 1, a, a_1 red pointer). The divergence of the radial tensions lines by moving off the gradually contracted blastopore creates a *gradient of tensions* (or the gradient of "tensions concentration") which will be shown (see Chap. 4) to play an important morphogenetic role. Similar gradients, though not so pronounced, are taking place in the vicinity of several other nodules.

A longitudinal tip-directed (but in no way the oppositely directed one) cut through the isolated dorsal blastoporal lip leads to the immediate opening of the lip (Fig. 3.1, row 1, c, c_1, c.f. b), pointing to considerable preexisted tension on its surface. Interestingly, the opening is prolonged *actively* (more slowly and only under room temperatures) during next several dozen minutes, reversing the initial lip curvature by forming a small indentation on its former tip (same row, c_2, blue pointer). This unique property of the blastoporal lip will be discussed elsewhere. As the gastrulation proceeds, new cross-lines appear (schematically presented in Fig. 3.3c and displayed in more details in Fig. 3.2c_1–c_3). However, they do not violate the general topology.

A next drastic switching toward more complicated topology is adjusted to the very start of neurulation. This is the formation of a prolonged seam, located just along the dorsal midline and manifested by strictly localized fast bending of both outer and inner neuroectodermal layers, separated from the underlain tissues in the seam's direction (but not oppositely) (Fig. 3.1, row 2 a_1). Under normal development, the dorso-medial seam in few dozens minutes becomes connected with so-called subneural fold (snf, Figs. 3.2d_1 and 3.3d) by a powerful bundle of cross-lines easily detected by mechanical inverse method (Fig. 3.2d_1–d_3, dense contours). Another longitudinal seam also located along the dorso-medial line is detected by incising the dorsal roof of the gastrocoel (Fig. 3.1, row 2, b_1). In addition, during the entire neurulation period, the dorsal embryo region exhibits the Poissonian combination of longitudinal extension and transversal contraction generated by the actively elongated notochord. Its longitudinal compression is revealed by fast overlapping of transversal cut edges (Fig. 3.1, row 3). An overall scheme of the early neurula tensile fields is given in Fig. 3.3d.

The transition toward tail bud stage is characterized by the addition of several other seams, both in anterior and hind embryo regions. They are oriented in most cases perpendicularly to antero-posterior body axis and traced by strictly localized fast folding of separated tissues (Fig. 3.1, row 4, red pointers; Fig. 3.3e, f). The anterior region seams fit so-called post- and prebranchial folds and the mouth depression (Fig. 3.1, row 4 ps, pr, md). Notably, the invagination of otic vesicle is taking place just in the intersection point of subneural and prebranchial folds.

Active (delayed and temperature sensitive) deformations of embryonic tissues are marked by blue pointers (Fig. 3.1, rows 1, 2, 4) and shown in more details in row 5. With the exception of that observed on the blastoporal lip (row 1, c_2), they curl opposite to that observed in fast deformations: that is, the external surfaces of separated tissues become convex and exposed to outside. Most pronounced are the active deformations of the ecto-mesodermal explants prepared from the lateral areas

of advanced embryos: Already in few dozen minutes, they create rather complicated shapes containing extensively tensed cross-lines (Figs. 3.1, row 5 a_1–a_2 and 3.3g). This is one of the most spectacular evidences of a morphological self-organization.

The main conclusion from the above data is that the mechanical stresses in amphibian embryos are perfectly ordered at the macromorphological level and keep topological invariability during rather prolonged time periods, characterized by extensive morphogenetic movements. A more detailed analysis of the latter ones will be given below. Now, we shall review more or less scattered data on mechanical stresses in the samples of different age related to different taxonomic groups.

3.2.2 *Mechanical Stresses in the Embryos of Other Taxonomic Groups*

Although in a more fragmentary way, incision tests (either by knife cuts or laser ablation) were used for checking tissue tensions in embryos of quite different taxonomic groups: hydroid polyps, Drosophila, sea urchins, bony fishes, and chicken embryos. While not in all these cases the truly passive responses (indicating preexisted stresses) could be reliably distinguished from active ones, the tests unequivocally demonstrated that mechanical (mostly tensile) stresses are the imminent components of morphogenesis of virtually all the studied species.

Tensile stresses are clearly correlated with morphogenesis in the developing buds of hydroid polyps from Thecate subfamily, *Obelia loveni* and *Dynamena pumila*, but it will be more suitable to discuss the related data in the next section. Going up along taxonomic scale, one should pay attention to the cleaving eggs of Spiralia which owing to a definite geometry of the blastomeres arrangement are expected to possess some non-trivial tensile patterns. Up to now, however, these objects remained unexplored from a morphomechanical point of view.

On the contrary, the Drosophila development was extensively studied. This relates first of all to the closure of the so-called amnioserosa, investigated with the use of laser ablations technique (Peralta et al. 2007). In particular, the authors conclude "that the vector sum of… applied forces… is only a small fraction of any one of the individual forces." This unequivocally means that the native tissues are mechanically stressed and keep the force balance. With the use of the same techniques, the ventral furrow of Drosophila embryo (a site of mesoderm formation) was shown to be stretched in antero-posterior direction from its very initiation (Martin et al. 2009). On the contrary, its anterior region (a rudiment of stomodeum) is under pressure (Farge 2003). Taking all these observations together, a coherent map of mechanical stresses for the entire Drosophila embryo can be constructed. However, by the authors' knowledge, this was not done yet.

Several incision experiments have been made in sea urchin embryos. In the pioneer study (Moore 1941), no precise temporal protocol of the observed post-incision deformations was given, so that the passive ones, which might detect preexisted

stresses, could not been reliably distinguished from the active reactions. In a subsequent study (Beloussov and Bogdanovsky 1980), the incisions made through animal or lateral parts of late blastula stage *Strongylocentrotus drobachiensis* embryos were shown to be immediately ($t \ll 1$ s) followed by extensive pulling apart of the cut edges; meanwhile, similar incisions through vegetal parts produced much smaller gaps. No considerable gaps were produced by any incisions performed on the early blastula embryos. The active reactions expressed by extensive bending of some embryo regions started no earlier than 1–2 h after operations, being thus clearly distinguished from the passive ones.

These data permit to conclude that in sea urchin embryos starting from the advanced blastula stage, the tension gradient is established with its upper pole located in the vegetal-most region (that one extensively relaxed by the animal cut). The gradient seems to be the main element of sea urchin embryo tensile field at the late blastula–gastrula stages. Probably, in later development, the tensile field acquires a dorsoventral asymmetry, but this was not yet tested.

On the other hand, as shown by time-lapse observations (Gustafson and Wolpert 1967) and laser ablation experiments (Hardin and Cheng 1986), the filopodia which establish contacts between the tip of embryonic gut and blastocoel roof are also under tension. As such, they may be regarded as rudimentary cross-lines connecting the different germ layers (archenteron and the animal ectoderm). Accordingly, the tension field of sea urchin embryos can be regarded as a primitive topological equivalent of much more complicated tensile patterns of vertebrate embryos.

In Teleostei, a necessity to maintain a highly tensed state of entire blastoderm for the progress of its epiboly has been discovered long ago (Trinkaus 1969). Meanwhile, in addition to these generalized patterns, more local ones could be traced, specifying dorsoventral embryo axis well before it became expressed on the level of embryo morphology. As shown by Cherdantzeva and Cherdantzev (2006), already at the onset of epiboly, the edge angle formed by the tangents to the blastoderm and yolk surface at their dorsal meeting point is significantly smaller than a similar ventrally located angle (Fig. 3.4a, b). In addition, after symmetric frontal incisions, the dissected dorsal part has been immediately bent much more extensively than the ventrally located one (Fig. 3.4c). All of this indicates that close to the saggital plane, the tensions on the dorsal margin of epiboly area are greater than on the ventral one. Under these conditions, the only possibility to retain mechanical equilibrium (zero vector sum of all the tensions) within blastoderm–yolk border plane is to assume that the dorsal tensions are applied to a narrower area (are more concentrated) than the ventral ones (Fig. 3.4d). In other words, a dorsoventral tension gradient (the gradient of tensions concentration) is taking place, regarded by the authors as a prime factor of dorsoventral embryo polarity: If reversing the gradient with the help of incisions, the dorsoventral polarity has been correspondingly reoriented (op. cit.). In Chap. 4, we shall discuss a similar situation as applied to amphibian embryos.

In chicken embryos, at the very beginning of incubation, the blastoderm should be tensed by a peripheral microfilaments ring in order the development to be continued (Kucera and Monnet-Tschudi 1987). During subsequent development, the tensile patterns are specialized in a way similar to that in amphibian embryos.

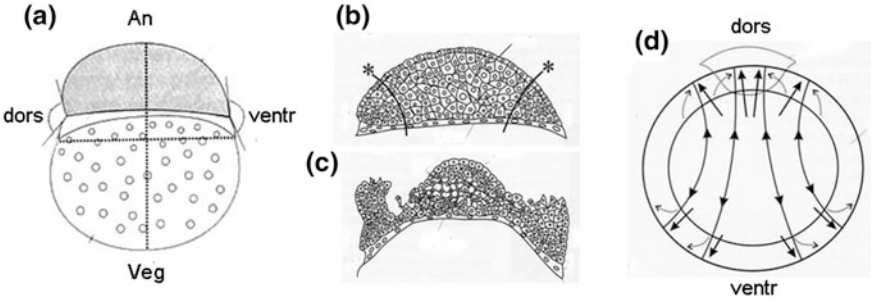

Fig. 3.4 Dorsoventral tensions asymmetry in early development of bony fishes. **a** Inequality of the edge angles on the dorsal and ventral margins at the blastoderm/yolk border is visible already soon after fertilization. **b**, **c** Saggital sections of blastoderm before and immediately after making vertical cuts along the directions shown in **b**. **d** In order to maintain mechanical equilibrium, tension lines (*solid arrows*) are converged dorsally and diverged ventrally. *Light arrows* depict mass cell movements directed toward restoring the tension balance by "diluting" dorsal side tensions and concentrating ventral side ones. From Cherdantzeva and Cherdantzev (2006) with the authors' permission

Thus, the transverse dissection of the head process (early notochord rudiment) leads to immediate overlapping of the cut edges (indicating longitudinal pressure), while a similar dissection of presomitic axial mesoderm produces instead a substantial gap pointing to preexisted tensions. The main difference from amphibian embryos was that these reactions took place under the normal incubation temperature only (Naumidi and Beloussov 1977).

3.2.3 Mechanical Stresses in Post-embryonic Epithelia

A study of mechanical stresses in tissues, organs, and cavities of the adults is an important and extensively developed affiliation of physiology and medicine (see for example Liem 2006). However, this topic is out of this book scope: We will restrict ourselves by a brief review of most typical properties of stress patterns in epithelial layers just starting to differentiate but not still losing the capacity to shape changes. Surprisingly, two taxonomically far removed kinds of epithelia—ectoderm of the vegetal generation of hydroid polyps and neuroectoderm of amphibian embryos—share quite similar mechanical properties. In brief, this is the combination of the apically located tangential tensions (common for all epithelia) with very strong radial stresses, both tensile and compressive, taking place within the depth of cell layers. We start from considering the growing tip of a hydroid, *Dynamena pumila,* at the stage of the still flat tip (Fig. 3.5a) to be in several hours subdivided into three sections by two vertical furrows. In a few seconds after the accurate detachment of the ectodermal part of the tip roof from underlining endoderm, the detached area is bent at the level of its separation and, most remarkably, creates two vertical folds,

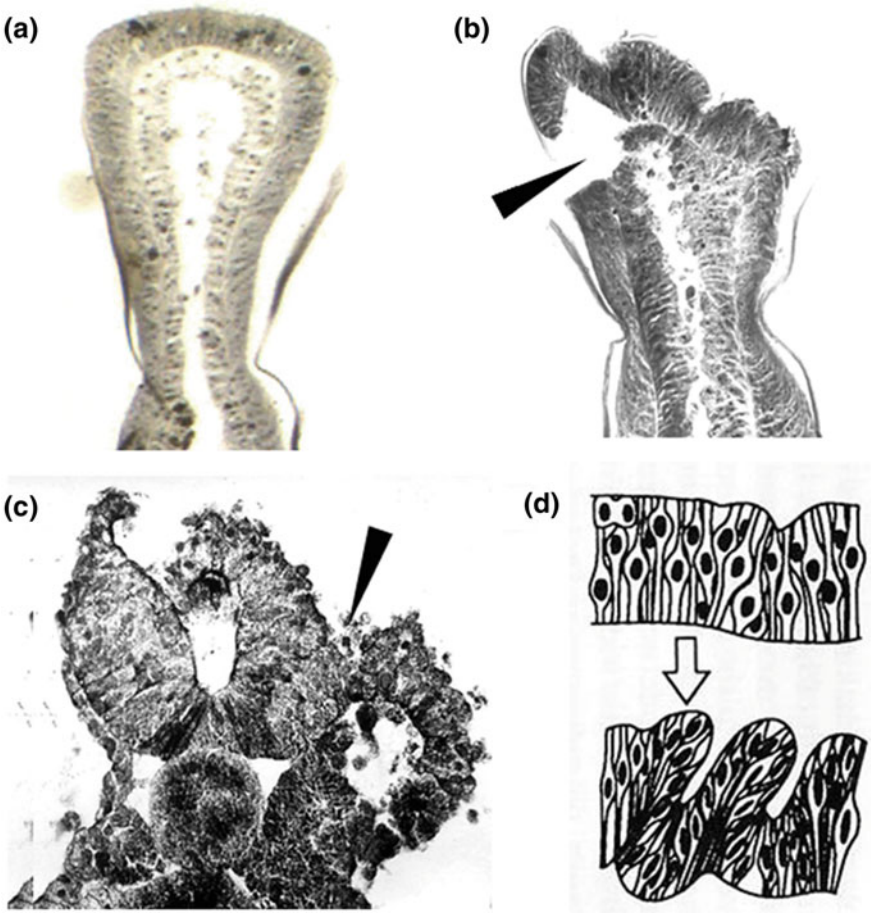

Fig. 3.5 Mechanical stresses in post-embryonic epithelia. **a** Intact growing tip of a hydroid, *Dynamena pumila*, with still flat roof. **b** Same stage sample, 1 min after incision. Two distinct grooves are seen on the roof corresponding to segregation of a tip into three parts taking place in normal development few hours later. **c** Immediate (≤1 s) creation of a gap and a curling of dissected parts of Xenopus neural tube soon after its closure. **d** extensive folding of a Urodela tail bud stage neuroectoderm starting immediately after excision and lasting for several next minutes. In **b**, **c** Incisions are indicated by *pointers*. **a**–**c** Original. **d** From Saveliev (1988), with the author's permission

exactly imitating its further morphogenesis (Fig. 3.5b). While the bending indicates standard apical tangential contraction, the rapid folds formation points to release of the *radial* tensile stresses accumulated at the sites of future ingressions well before they become visible. In addition, other roof cells become rapidly elongated demonstrating the release of the radial compression stresses.

Even more complicated, although in the long run, similar combination of stresses can be detected in the neuroectoderm of amphibian embryos. If incising

dorsoventrally a wall of just closed neural tube, the dissected parts immediately curl in the opposite directions and the cells which were initially transversely elongated are contracted up to spherical shapes (Fig. 3.5c) (Beloussov et al. 1975). These deformations indicate the release of both dorsoventral tensions on the surface and transversal (apico-basal) tensions inside the neuroectodermal layer. Saveliev (1988) confirms the presence of extensive dorsoventral surface tensions in just closed neural tubes of Urodela embryos, describing in addition less extensive but more prolonged saggital tensions provided by the neural tube bending in the saggital plane. Moreover, he describes cells' elongation perpendicularly to neural tube surfaces starting immediately after tensions release and lasting for next several minutes; this is associated with the oppositely directed transversal shifts of the central nuclei containing parts of adjacent areas. As a result, slight neuroepithelial folds are extensively reinforced in a way similar to hydroids (Fig. 3.5d). Obviously, these shifts are directed toward releasing cell–cell compression which is the greatest when nuclei-containing parts are arranged along the same line. Similarly to what took place in the dissected blastoporal lip (see Fig. 3.1, upper row c_2), the relaxation movements have been prolonged by the active ones of a similar direction.

More postponed neuroectodermal cell reactions to stretch release are also interesting and unexpected. Thus, if simultaneously releasing the transversal and the saggital tensions, the cells within several minutes become reoriented longitudinally; this never takes place in normal morphogenesis. In the next few hours, cells become completely disoriented and later on undergo apoptosis (Saveliev and Besova 1990).

3.2.4 Tensile Patterns and Developmental Order

Are the above-described tensile fields indispensable for maintaining the dynamic order of development? To explore this possibility, several kinds of experiments were performed. First, a generalized relaxation of the tensions on the embryo surface was performed by inserting ventrally a wedge of endoderm, pushing apart the surrounding tissues (Beloussov et al. 1994, 2006) (Fig. 3.6a, b, e, pointers). Using the classical "edge angles" method (Thompson 2000), we have found that less than in a minute after operation, the tensile force applied to the apical cell walls of the outer ectodermal layer (the main tension bearer) dropped sevenfold, becoming equal to that of the same cells' transversal walls. Within the next 4 h, the apical tensions slowly increased still not reaching however normal values. If performed at the blastula stage, the operations completely disturbed embryo morphology (Fig. 3.6b–d). When made at the early gastrula stage (Fig. 3.6e), they produced more local however substantial effects associated with suppression of ventro-dorsal migration of mesodermal and neuroectodermal cells. As a result, the neural rudiments were enlarged in transversal directions and duplicated or triplicated (Fig. 3.6f, g). Most important in further context was an essential and irregular increase of the areas occupied by extensively columnarized cells on the dorsal embryo areas (Fig. 3.6h). Obviously, such a reaction is directed toward restoring the relaxed tensions.

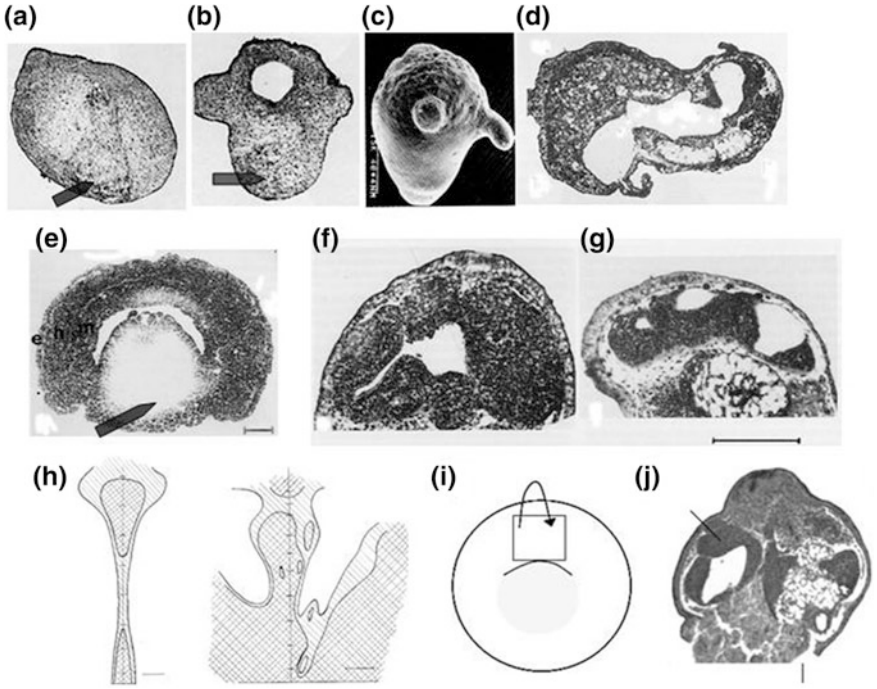

Fig. 3.6 Relaxation-induced loss of morphological order in *Xenopus* embryos. **a** A wedge of ventral tissue (*pointer* in **a** and **b**) is inserted into a blastula stage embryo, 1 h after operation. **b–d** Operated embryos 5, 24, and 48 h after wedge insertion, correspondingly. *Note* abnormal protuberances in **b**, **c** and a complete loss of order in **d**. **e** A similar wedge (*pointer*) inserted in the early gastrula stage embryo (**e**) produces more local disturbances, namely abnormal transversal extension (**f**) or multiplication (**g**) of neural tubes. **h** Two-dimensional maps of cells height/width (H/W) ratios in the dorsal ectoderm of an intact neurula stage *Xenopus* embryo (*left*) and the same stage relaxed embryo (*right*). *Vertical axis* is the dorsal midline, and lower margin fits the blastopore level. *Cross-hatched area* H/W > 2; *hatched area* 1.5 < H/W < 2; *empty area* H/W < 1.5. **i** A scheme of the "remove–replace" operation. **j** Chaotic arrangement of axial organs in the operated region, 48 h later as seen on cross section. From Beloussov et al. (1990, 2006) and Kornikova et al. (2009)

In another series of experiments (Kornikova et al. 2009), a small piece of SBA tissue extirpated from an early gastrula stage embryo within about a minute was transplanted back at the same place and in the same orientation (Fig. 3.6i). This time period was enough for the piece to be released from the tensions exerted by surrounding tissues and for becoming extensively contract without being able to restore its initial tensile pattern (because of losing the lateral contacts with the pulled apart adjacent tissues). Such "remove–replace" procedures permitted to affect tensile patterns without changing the material content and arrangement of embryonic tissues. The results were similar to those obtained by wedge-inserting experiments in the sense that the long-range order of the axial rudiments was broken. At the same time, the individual rudiments, although if deformed, could be easily recognized (Fig. 3.6j): Hence, a short-range order has been preserved.

Taken together, these data indicate that permanently maintained normal tensile patterns are indispensable for providing a long-range morphological order: Even a brief abolishment of normal patterns leads to irreparable abnormalities in the rudiments arrangement. Note at the same time that in the above experiments, almost all the cells (except those arranged along the wedges borders) do not change their mutual positions; thus, if the fate of cells would be really governed by such a factor as "positional information," the observed developmental disorder could not be expected. We have to conclude that these are the tensile patterns rather than the mutual cell positions taken per se which play the role of the ordering parameter. And so far as in the normal development, any momentary tensile patterns are created by a set of previous morphogenetic movements we can see that the ordering factors have a certain "temporal depth" or, in other words, are based upon some recent developmental history. We shall return to this suggestion in the next chapter.

3.3 Main Modes of Collective Cell Behavior

As mentioned above, practically all the morphogenetic processes are collective in the sense of involving a substantial amount of similar units into uniform transformations, as a rule propagating from small centers. These events may be either periodic or unique, leading in the latter cases to irreversible cell differentiation. It is suggested that the property to propagate is among the main tools providing a robustness and structural stability of morphogenesis (Cherdantzev 2003)

However, before coming directly to propagating processes, we will analyze the morphogenetic capacities of non-propagating collective events, implying only local interactions between the system's units. As an example, we take a densely packed cell network, neglecting (as the starting point of the analysis) any propagating processes. This part of our analysis will be mostly based on the papers by Farhadifar et al. (2007) and Aegerter-Wilmsen et al. (2010). In both ones, the modeling approach is dominated, compared to empirical data just in a few points.

3.3.1 Homeostatic Cell Reactions

Farhadifar et al. (2007) (see also Rauzi and Lenne 2011) consider densely packed two-dimensional cell networks with third-order nodules (meeting points of cell edges). The authors assume that mechanical forces applied to cell edges depend on three parameters: elasticity of the cell surface (A), linear tensions at the junctions between individual cells, and the active contractility of the cell perimeter caused by the action of actomyosin rings. Importantly, for defining the area elasticity A_a of a given cell A, a notion of this cell preferred area $A_a^{(0)}$ is introduced. The resulted cell elasticity is proportional to the difference $(A_a - A_a^{(0)})$. Thus, both positive and negative line tensions ("linear pressures") are employed. The main driving force tending

to modify any initial network pattern is identified with a tendency to reach the balance of all the above-mentioned forces in each nodule of the network (i.e., zero vectors sums). These force balances are described as local minima of the energy function. If taking all the cells of the network identical, two ground states (the most relaxed network configurations) can be identified within the space of tensions/contractility parameters. The first of them, defined as a manifold of soft networks, is compatible with negative tensions (i.e., pressures) only. It includes many cell geometries, all of them with the same minimal energy. That makes the system behave more like a liquid, the cells easily changing their neighbors. The other ground state is that of a uniform hexagonal network. It corresponds to positive tensions, is favored by relatively high contractility, and shares properties of a solid body.

Besides the ground states, which should be considered as the reference points rather than some realistic network configurations, the system possesses indefinite number of the so-called local energy minima (stable cell packing geometries) which depend upon the parameter values. By modeling the network topology which corresponds to the local minima, the authors concluded that only in a very narrow interval of arbitrary selected parameter values (small positive tensions and small contractility), it satisfies real patterns taking place in the intact or locally dissected *Drosophila* wing epithelium.

While this model does not tell us much about real morphogenesis, its very inability to do this is rather instructive. We can see that even if all the model units are endowed with rather realistic biomechanical characteristics but are not involved in any kinds of spatial feedbacks, the model's behavior is extremely non-robust (structurally unstable), which is in contrast with high robustness of most morphogenetic processes. One of the first attempts to introduce spatial feedbacks in cells packing patterns was made by Aegerter-Wilmsen et al. (2010). The authors suggested that the stress applied to a given polygonal cell by its neighbors depends upon the polygon number: A cell with a low polygon number tends to be more compressed by its neighbors, while that with a high polygon number tends to be more stretched. By assuming that a cell responds to stretch by its division which releases at least part of applied tension, the authors obtained more realistic patterns of cell packing than without making such an assumption. The idea of stress dependence of cell packing has been extended by Sugimura and Ishihara (2013). They observed that the longitudinal tensions dominating in the developing Drosophila wing are crucial for increase of the proportion of hexagonal cells and for their rearrangement in a way which orients local cells tensions along the main direction of tissue stretching. In such a way, the mechanical load on each cell contact surface is decreased and the resulted tissue tensions become more isotropic. The resulted cell packing pattern corresponds to the surface energy minimum; thus, one might expect that even if not being influenced by tensions, it will be sooner or later reached by the cell population. However, the rate of rearrangements and the relation of the final cells orientation to the axes of the entire organ (in this case, a wing) may be crucial, and the role of tension-mediated mechanisms is to reach these goals. In our subsequent account, we shall describe several stress-dependent cell reactions at least partly directed toward a less energy state but playing nevertheless

a creative role by specifying positions and shapes of multicellular structures. For doing this, we have now to pass from homeostatic cell reactions to those associated with progressive complication of embryonic bodies. We shall start from simplified in vitro models for coming later to those involving several structural levels.

3.3.2 Modes of Cell Alignment

As it was already mentioned in two preceding chapters, the tendency of densely packed structural units to align parallel to each other is as a rule energetically (entropically) favorable and hence widely spread on the supramolecular level. The same tendency, also based upon short-range interactions between units, is preserved in much greater scale structures, including multicellular communities. Although if being per se a smoothing agent (leading to increase in uniformity), the alignment trends are in fact accompanied with numerous symmetry breaks some of which are of a primary morphogenetic significance. This is because in multicellular tissues in addition to short-range interactions, the long-range ones inevitably appear, associated in many cases with generations of tensile forces by cooperatively aligned cells. In this section, we shall start the analysis of the long-range effects and will continue it in the next chapter.

In general, three main cell alignment modes can be distinguished, differing from each other by the mutual orientations of the individual cell alignments and the propagation of alignment.

First, when the both directions are coinciding with each other, the prolonged files of elongated cells are produced: This mode we define as a parallel alignment. The above-described cross-lines are originated just by this way. Another—and highly important—morphogenetic process related to this category is so-called cell intercalation.

The next type of aligning processes is characterized by mutually perpendicular orientations of the propagation tendencies and cell alignment: In this case, the coherent domains of columnar cells are created. In this context, we shall discuss one of the most instructive models of morphogenesis which describes the relations between the short- and long-range processes on the mechanical basis.

At last, we consider the case when the longitudinal cell axes are oriented obliquely to the propagating direction and monotonously increase their inclinations while shifted apart from the starting point of the cells transformation relay. We shall see that this mode is closely connected with the number of most important morphogenetic events.

3.3.2.1 Parallel Cell Alignment

We start from an exotic example demonstrating deep evolutionary roots of this reaction: the formation of the nodules and cables in the films of cyanobacteria,

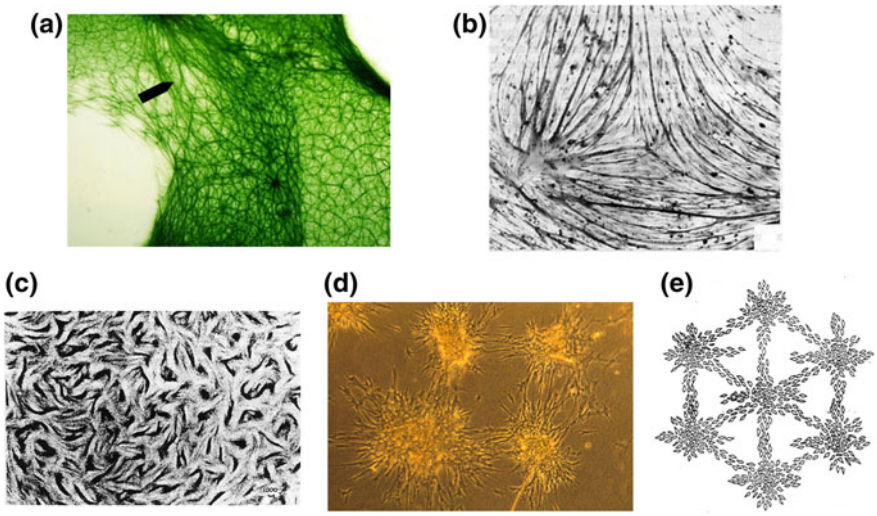

Fig. 3.7 Patterns of cell alignment, with an accent to symmetry breaks. **a** Formation of tensed ropes (*pointer*) out of a network in a cyanobacteria colony. **b** Myogenic cell cultures combining linear arrays with singularities in the meeting points. **c** Clusters of fibroblasts in collagen-containing cell cultures. **d** Segregation of chick heart fibroblasts seeded on silicon substrates to the clusters of mutually adhered and files of extensively elongated and rarefied cells. **e** A similar multicellular pattern in the site of feathers formation (planar view of a part of chicken embryo skin). **a** From Sumina and Sumin (2013). **b** From Isaeva et al. (2012). **c** From Elsdale (1972). **d**, **e** From Harris et al. (1984). **a**, **b**, **d**, **e** With the author's permission. **c** With the publishers permission

Oscillatoria terebriformis. As described by Sumina and Sumin (2013), within several dozens minutes of a strong illumination, a homogeneous bacterial net is transformed into a bunch of prolonged mechanically tensed cables (Fig. 3.7a, pointer) which again disaggregate in darkness. Thus, even protokaryots are able to create macroscopic aligned structures. As a next example, the alignment of myogenic cells can be taken (Isaeva et al. 2012). This model shows that the uniform orientation of entire cell population may be occasionally disturbed by the appearance of topological singularities which separate neighboring domains and hence break the initial overall translational symmetry (Fig. 3.7b). A step toward more regular inhomogeneities is presented by Elsdale (1972) experiments which differ from those described in Chap. 1 by the presence of collagen: Under these conditions, a common cell array is broken into single clusters (Fig. 3.7c). Even more regular patterns composed of cell clusters separated by about 10^{-4} m distances and connected by the files of aligned cells were obtained in seminal Harris et al. (1980, 1984) experiments by seeding fibroblasts onto elastic substrates stretchable by crawling cells (Fig. 3.7d).

The authors properly understood that de novo arisen macroscopic order is owed to interactions between the positive short-range and the negative long-range interactions. The first ones are based upon the tendency of the seeded cells to

establish mutual contacts, creating thus condensed cell clusters; their enlargement increases the probability of new cells to be adhered. On the other hand, same cell clusters by being enlarged stretch the surrounding elastic substrate to increased distances, creating zones of cells rarefaction and preventing thus the formation of the next cluster in the immediate neighborhood of the previous one: This is a long-range negative feedback. The authors suggest that the same sequence of events is taking place in other mesenchymal morphogenesis, for example, during feathers formation in subepidermal part of a skin (Fig. 3.7e).

By our knowledge, Harris et al. works were the first to demonstrate that the new, not preexisted scale (manifested by regular distances between cell clusters) can emerge within initially homogeneous tissue by self-generated mechanical forces. This model paved a way for several others; for approaching them, we have to pay attention to the internal activity of the aligning cells and to heterogeneity of stresses which they produce.

As shown by recent evidences, cell alignment, even if looking as a smooth equilibrial process, may be in fact associated with formation of essentially complicated stress patterns. By tracing the displacements of cells seeded onto a collagen matrix, Tambe et al. (2011) constructed maps of tangential stresses and measured the correlation between stresses and cell orientations. Stress landscape was found to be rugged: The regions of rather high tensile stresses involving groups of 10–15 cells were alternated with shorter regions of weakly compressive stresses; in the maximally tensed regions, cells were oriented and migrating along the main stress directions. The authors compare this fluctuating behavior with a glassy dynamics of cytoskeleton (see Chap. 2) by pointing that both are characterized by a local (short-range) cooperativity: In both cases, the size of cooperative clusters increased parallel to that of a system's density, but too large systems become "frozen," that is, immobile.

Similar conclusions could be derived from Vedula et al. (2012) observations of collective cell migrations within microfabricated strips of the different widths. The authors describe large-scale vortices over tens of cell lengths appeared in wide strips, whereas in narrow strips a directed contraction–relaxation behavior with much smaller correlation lengths was dominated. Thus, cell populations demonstrated migration modes with alternative pulling and/or pushing mechanisms. Cell behavior was crucially dependent upon force transmission from one cell to another: If disrupting the force transmitting cell contacts, the directed cell migration and its geometry dependence was lost. Interestingly, the force values produced by cells were of nN range, well familiar to us.

Thus, along with quite obvious manifestations of short-range correlations, somehow irregular but nevertheless correlated behavior of entire cell groups (though rather small ones) and the presence of extensive stress inequalities (varying from pulling to pushing regimes) have been demonstrated. One of the main lessons from these in vitro studies was that such irregularities could not be derived from any prepatterns: Rather, they arise each time de novo, due to spontaneously emerging instabilities within the cell population.

Now, we pass from endogenous stress patterns born within aligned cells themselves to those triggered by outside applied forces. If stretching an explant of

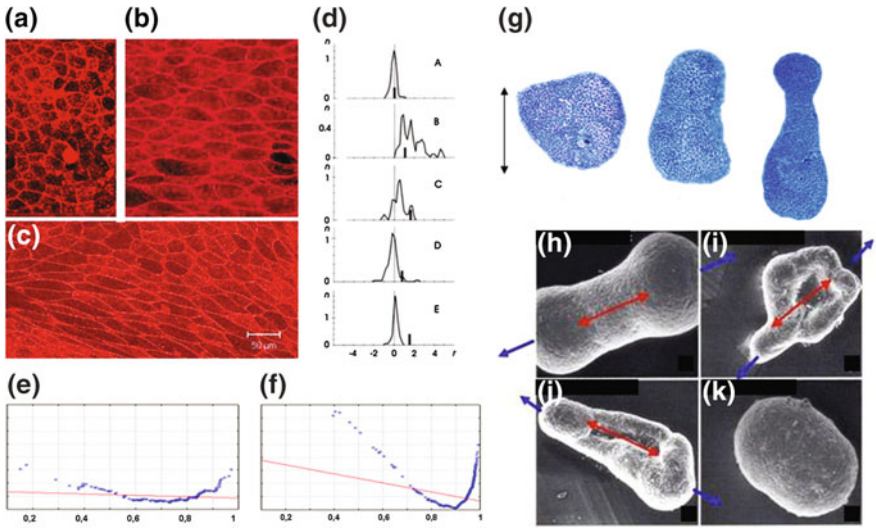

Fig. 3.8 Active reinforcing responses of Xenopus embryonic ectoderm explants to the action of stretching forces. **a**–**c** Confocal images of actin-stained ventral ectoderm explants. **a** Prior to stretching, **b** 5 min and **c** 15 min after the end of ≈160 % stretching. *Note* progressive elongation of the large cell fraction in the stretch direction, largely exceeding the amount of stretch. **d** From *top* to *bottom* the histograms of cell eccentricities prior to stretch and 30, 60, 120, and 300 min later, compared with those of entire samples (*thick vertical bars*). **e**, **f** Distribution plots of individual cell eccentricities (plotted along horizontal axes) in non-stretched and 5 min stretched samples correspondingly, as compared with linearized normal distributions (*red lines*). **g** Planar sections of SBA explants 1, 2, and 3 h after cessation of stretching in the direction shown by *double-head arrow*. **h**–**j** Scan views of the ventral ectoderm explants 6 h after the end of the stretch (*blue arrows*) as opposed to a non-stretched explant (**k**). *Red arrows* indicate active extension leading to bulges formation

Xenopus early gastrula ventral ectoderm by arbitrary directed external force and comparing the so-called eccentricities[1] of the entire sample with those of its individual cells, one can notice a fraction of cells whose eccentricities significantly exceed those of entire samples (Beloussov et al. 2000 and unpublished data) (Fig. 3.8a–d). To compensate this excess, another cell fraction should have eccentricities smaller than those of entire samples. As a result, the sets of cell eccentricities, while presented as linearized plots of Gaussian distributions, are essentially bimodal, being shifted towards higher values already after 5 min stretching (Fig. 3.8e–f). Obviously, super-eccentric cells generate compression stresses oriented in stretch direction and balanced by contraction of under-eccentric cells: As a result, we get a rise of stress inhomogeneity within a uniformly stretched explant.

[1] The **eccentricity**, denoted e or ε, is a measure of how much any conic section deviates from being circular. For our purposes, it is enough to know that the eccentricity of a circle is zero and the eccentricity of an ellipse which is not a circle is greater than zero but less than 1.

Super-eccentric cells did not live longer than about half an hour after the sample's stretching; however, they are exchanged by those producing similarly directed and even greater compression force. The latter becomes generated by cooperative cell convergence toward the axis of stretching, accompanied by cells insertion between each other. In such a way, one of the most powerful and widely spread morphogenetic processes, called convergent cell intercalation (CCI), is initiated. CCI has been traced in quite different taxonomic groups: Cnidaria (Otto and Campbell 1977; Hofmann and Gottlieb 1991), nematodes (Chisholm and Hardin 2005), Drosophila (Osterfield et al. 2013), sea urchin embryos (Hardin and Cheng 1986) and, the last but in no way the least, the vertebrates (Keller and Tibbetts 1989; Shih and Keller 1992). CCI generates the basic forces providing elongation of entire embryonic bodies or their parts (tracheal branches and respiratory appendages in Drosophila eggs, embryonic gut in sea urchin embryos, etc.). In amphibian embryos, two geometrically different CCI categories can be traced: (1) *radial* intercalation of deep ectodermal cells of the blastocoel roof providing *isotropic* planar roof extension and (2) *planar* convergence–intercalation of SBA cells toward embryo midline which extend the axial organs in antero-posterior direction.

By continuing the line traced in preceding chapters, it will be instructive to compare the CCI-involved cells with the particles of nematic liquid crystals which are arranged parallel to each other and are able to shift parallel to their long axes. Similarly to nematic crystals, the number of freedom degrees in the population of intercalating cells is increased as compared with that of non-intercalating ones and so does the entropy. The gain in entropy should facilitate a huge mechanical work performed by intercalating cells by pushing the surrounding tissues.

CCI is regulated by a complicated molecular machinery which includes specific signaling pathways (Marsden and DeSimone 2003; Kinoshita et al. 2003; Davidson et al. 2006; Wallingford et al. 2002) and expression of specific genes (Darken et al. 2002; Goto and Keller 2002). Giving a lot of new information, a knowledge of these details will not bring us however toward answering the eternal embryological questions—"why here, at that time and in this direction?" For making a step forward in getting the responses, we have to explore whether the very presence and the orientation of CCI depends upon external mechanical forces.

As mentioned before, the ventral ectoderm is incapable of anisotropic (convergent) CI without being triggered by mechanical force, but at the first glance looks capable to spontaneous radial CCI. However, actually the latter also is not completely spontaneous: At the blastula stage, the radial CCI is not only hampered, but even replaced by reverse cell movements, increasing the thickness of a cell layer, if decreasing tensions on the embryo surface either by wedge insertion (see Fig. 3.6a, b) or by reducing osmotic pressure within blastocoel (Beloussov et al. 2006). Therefore, isotropic (radial) CI requires an external stretching force.

Now what about anisotropic CCI taking place within SBA? At first glance, its perfect reproduction in relaxed SBA explants argues against a necessity of any

external tension (normally provided by involution of chordomesodermal material). However, it is easy to see that the longitudinal tensions start to restore already in a few minutes after SBA explanting due to the inward curling of posterior regions. If such a curling is prevented (as in the above-described "remove–replace" experiments), anisotropic CCI is completely abolished.

Moreover, in spite of a strong SBA bias toward medio-lateral CCI (within an entire embryo coordinates), its direction can be rotated to 90° by rather moderate (30–70 % of initial length) transversal stretching lasted for several hours (Fig. 3.8g). All of this taken together indicates that all kinds of CI should be triggered by external tensile forces oriented parallel to CI-generated extension. We define this response as tension-induced active extension (TIAE).

One of the most spectacular evidences of TIAE is the formation of bulges in the polar regions of stretched ventral ectoderm explants, making their shapes similar to those of entire embryos segregated to the head and trunk regions (Fig. 3.8h–j, c.f. k): Such structures definitely require compressive forces oriented in stretch direction. More detailed TIAE analysis will be performed in the next chapter.

3.3.2.2 Perpendicular Cell Alignment: Combination of Short- and Long-Range Interactions and a Way Toward Scaling

Epithelial layers consisting of columnar cells are widely presented in developing embryos: Some of them are depicted in Fig. 3.9a–d. Most ubiquitous examples are the early rudiments of the primary gut (Fig. 3.9a, b), the neural plate (Fig. 3.9c, np), and the placodes of sensory organs (Fig. 3.9d). A set of similar structures is however much larger: Practically, all the epithelial rudiments, including those transforming later into the mesenchyme, start to develop from coherent groups (domains) of columnar cells sharply segregated from surrounding tissues (see below in this chapter). In many cases, segregation of an early embryo into columnar and flattened cell domains is the first step in establishing morphological polarity. In particular, this is true for mammalian blastocysts. It is not occasional therefore that the most adequate term for describing the formation of columnar cell domains—contact cell polarization (CCP)—has been coined (Johnson 1981) for describing just this transformation.

Traditionally, CCP was regarded as a result of specific induction of a competent epithelial layer by the underlining rudiment: A classical example is the induction of a lens placode by eye vesicle. Without denying these irrefutable data, it is worth to remind that the inducing factor well can be quite non-specific: In Cnidarians, the formation of placode-like early buds rudiments can be triggered by simply pricking ectodermal cell layer (Plickert 1980) and in chicken embryos by apposing miniature silver rings on the surface of embryonic epithelia (Steding 1967); obviously, the only thing which could be done by the latter procedure is to prevent tangential tissue spreading. Within this book context, the most important thing is that formation of columnar cell domains is a universal reaction of embryonic tissues to relaxation of tensions on the layer surfaces. The above-described extension of

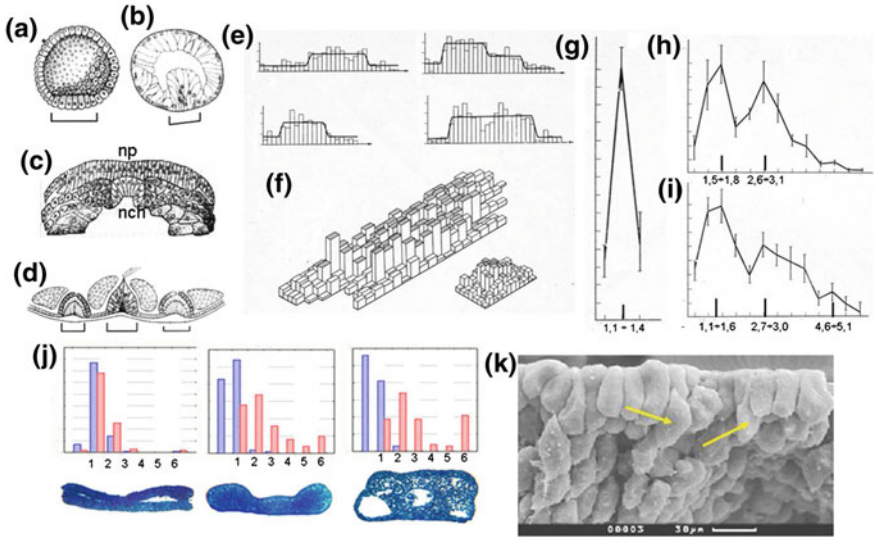

Fig. 3.9 Columnarized cell domains and contact cell polarization (*CCP*). **a**, **b** Vegetal plate (rudiment of a gut) in sea urchin and in shrimp blastulae, correspondingly. **c** Neural plate (*np*) and notochordal anlage (*nch*) in amphibian embryos. **d** Eye rudiments in spider embryos. **e**, **f** One- and two-dimensional profiles of 3 h explants from *Xenopus* early gastrula embryos showing files of columnar cells. *Vertical axis* height–width (H/W) ratios. **g–i** Histograms showing emergence of bistability in *Xenopus* embryonic tissues. *Horizontal axes* H–W differences, *vertical axes* numbers of cells. **g** Belongs to intact sample, H and I to 1 and 3 h explants correspondingly. **j** Emergence of bistability in *Xenopus* ventral embryonic ectoderm sandwiches (displayed below). From *left* to *right* 5, 60, and 120 min after explantation. *Horizontal axes* H/W ratios, *vertical axes* cell numbers. **k** A scan profile of 120 min explant. Note groups of columnar cells, some of them (*arrows*) undergoing epithelio-mesenchyme transformation. **a**, **c** From Petrov and Beloussov (1984. **b** From Beloussov et al. (1994). **d** Courtesy of S. Kremnyov

columnar cell areas caused by wedge-inserting relaxation (see Fig. 3.6 and corresponding comments) is just one example of this easily reproduced event (Beloussov 1988). In explants of embryonic tissues, CCP starts in a few dozen minutes after the extirpation and associated relaxation (Fig. 3.9f, j); noteworthy, in ventral ectodermal explants contrary to dorsal ones, the columnarized cells rapidly immigrate, undergoing epithelio-mesenchymal transition (Evstifeeva et al. 2010).

By tracing CCP in amphibian embryonic tissues, one can see that the transformation of more or less isodiametric cell shapes to the columnar ones goes in a relay fashion from one adjacent cell to another, taking about 5 min for each next cell (which is small, comparing to the lifetime of columnar cells). Most important for further modeling is that quite sharp unimodal distributions of height/width cell ratios typical for intact cell layers (Fig. 3.9g) are exchanged to bimodal ones in a few dozen minutes after explantation (and associated relaxation) (Fig. 3.9h, i). This permits to qualify a cell layer competent to CCP as a third-order nonlinear dynamic system.

The availability of quantitative data and the important role of the columnar cell domains in embryonic patterning stimulated construction of a model aiming to present this process as a result of mechanically based feedbacks similar to those suggested by Harris et al. (1984). We shall call the below presented model by the name of its first author, a prematurely died theoretical physicist Belintzev (1953–1988), Belintzev's model (BM) (Belintzev et al. 1987; see also Belintzev 1988).

In its simplest form, the Belintzev' model (BM) is expressed by a differential equation describing the rate of columnarization (dp_i/dt) of i cell belonging to one-dimensional (extended along x axis) epithelial layer. Here, $p = h - w$ (h is the cell height and w is its width in the layer plane):

$$dp_i/dt = f(p_i) + D(\delta^2 p/\delta x^2) - kT \tag{3.7}$$

The first right part member [$f(p_i)$] is a nonlinear (third order) function describing the so-called point bistability, that is, a postulated existence of two morphologically different stable states for each cell taken separately. In accordance with empirical distributions (Fig. 3.9h, i), one of the states corresponds to roughly isotropic shape and the one to extensively columnar shape. The second member describes short-range interactions between neighboring cells, exemplified by CCP relay. The relay is considered in the first approximation to be a diffusion-like process proportional to the second derivative of p along x axis. This does not necessarily mean that CCP is linked with a real diffusion of any chemical substance; most probably, it is based upon a complicated set of cytoskeletal and cell membrane transformations. In any case, however, the borders of polarized and non-polarized zones (Fig. 3.9e, f) are sharp enough for justifying the introduction of second derivatives. The third member expresses inhibition of CCP by the viscoelastic tangential tension T (k is the coefficient of viscoelasticity) of as yet non-specified origin.

Until now, BM does not differ considerably from traditional models of pattern formation. Its originality starts from considering the model cell layer as a *mechanically closed self-organizing system*, rather than experiencing external forces of unknown origin. Now, the tangential tension within the layer is assumed to be created exclusively by its cell columnarization (for this, the layer's edges should be firmly fixed, which is true for practically all embryonic samples). Under these conditions, $T \sim \langle p \rangle$ where $\langle p \rangle$ is the arithmetic average of all individual $p_i - s$:

$$\langle p \rangle = \frac{\sum_{i=1}^{n} p_i}{n}$$

By introducing $\langle p \rangle$, we get a *non-local* member, related to the indivisible "whole": This is the main BM novelty. The next step is to write $T = q \langle p \rangle$, where q is the measure of the tangential stress produced by the cell deformation (either columnarization or flattening). Now, we are interested to know how this force affects further columnarization of individual cells. It is reasonable to assume that the effect will be negative for the cells with p_i less than $\langle p \rangle$ and positive for the cells with p_i greater than $\langle p \rangle$. As a result, we get a final form of BM equation for a

mechanically closed system (a cell layer with fixed ends in the absence of external forces):

$$dp_i/dt = f(p_i) + \delta^2 p/\delta x^2 - kq(\langle p \rangle - p_i) \tag{3.8a}$$

where the contribution of the third member is negative for the cells with $p_i < (\langle p \rangle)$ (more flattened as the average) and positive for the cells exceeding average columnarization. It means that an initially homogeneous epithelial layer will be segregated into two cell populations, their p values differing from each other to a greater extent than that predicted by the point function alone. One may qualify the increase of differences as the influence of a "whole" upon the final states of individual cells (see for more details Beloussov 2013).

In general, BM brings two important results. First, it reproduces the "spontaneous" (i.e., coming from inherent instability of the system) break of translational symmetry, manifested by the segregation of initially homogeneous cell layer into sharply distinct domains of columnar and flattened cells. Note that a stable segregation (rather than a mobile front of cell columnarization, Fig. 3.10b) is possible only under fixed layer's

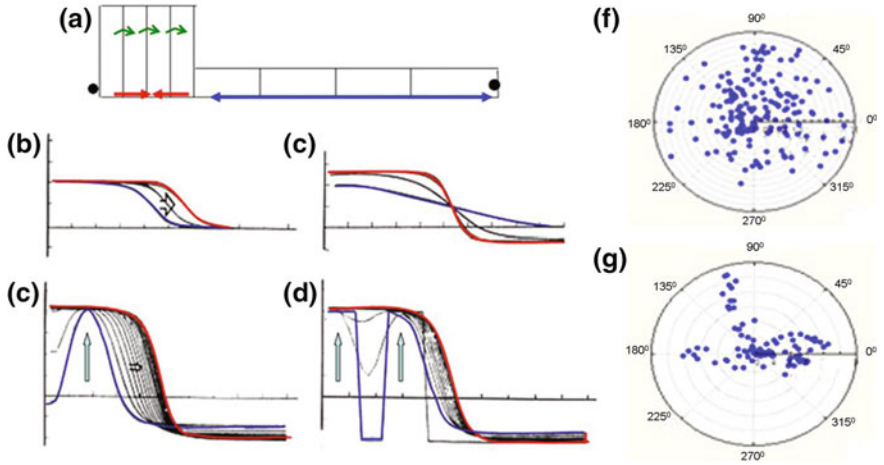

Fig. 3.10 Belintzev's model (*BM*) (**a**–**e**) and evidences for cell random search (**f**, **g**). **a** Mechanical forces within epithelial layer with fixed edges (*black dots*). *Red converged arrows* depict cells tangential contraction. *Green arrows* its transmission from one cell to another (contact cell polarization, *CCP*). Double-head *blue arrow* passive extension of the rest of the layer. **b**–**e** Model results *horizontal axes* linear coordinates within one-dimensional layers. *Vertical axes* cells height–width differences. **b** Unrestricted CCP under non-fixed layer's edges. **c**–**e** Stable and scale-invariable segregation of layers with fixed edges under different initial conditions: smooth gradient of cell columnarization in **c**, a single peak in **d** and two closely arranged peaks in **e** (*blue vertical arrows*). *Red lines* depict final patterns. **f** and **g** Angular distributions of slow (≤2.8 μm/min) and relatively fast (≈10 μm/min) cell movements in stretched explants of *Xenopus* embryonic ectoderm, correspondingly. *Note* a stochastic orientation of slow cell movements and sharp segregation of fast ones into those oriented along stretch direction (*horizontal axis*) and those close to transversal (c.f. Fig. 3.11b)

edges, supporting tensions. The final cell polarization pattern is robust enough in the sense being non-affected by the shape of initial perturbation: The result will be the same whether it is arranged in a gradient fashion (Fig. 3.10c) or consists of a single or two closely arranged perturbations (Fig. 3.10d, f). Meanwhile, if two perturbations are extensively removed from each other, each of them triggers its own columnar domain; however, the total lengths of the both domains are equal to that of the single domain under same parameters values.

The second conclusion from BM is about embryonic regulations. In terms of histology, most (if not all) of them are based upon the proportional (scale invariant) segregation of embryonic epithelial layer into columnar and flattened cell domains. As being such, they can be interpreted by BM without any additional assumptions. Indeed, let us write a phenomenological equation a cell layer of L length completely segregated into two domains of l and $L - l$ lengths, with the final p values of their cells P_1 and P_2 correspondingly:

$$\langle p \rangle = \frac{P_1 l + P_2 (L - l)}{L}$$

By transforming it into

$$\frac{l}{L} = \frac{\langle p \rangle - P_2}{P_1 - P_2}$$

one can see that the right part does not contain any values containing linear dimensions. This means that the domain proportions (expressed by the left part) should be kept intact under infinite range of embryo dimensions. In other words, from BM viewpoint, the proportional segregation of embryonic body remains the same under any absolute dimensions.

So we see that BM is able to interpret such fundamental properties of morphogenesis as the regular breaks of translational symmetry and scaling capacity, completely avoiding presumptions of a coordinate grid, positional dependence, and other notions bound with local commands. Instead, any cell is suggested to permanently sense the averaged mechanical stress of a cell layer to which it belongs and to which it gives its own small contribution. Thus, the "whole" becomes identified with delocalized stress and is for the first time untied from the "feeling of position." The positions taken by cells should look now as the consequences of morphogenetic processes, rather than their causes.

Are there any evidences for mechanosensing on the level of embryonic cells populations? By tracing movements of several hundreds of the outer ectodermal cells belonging to artificially stretched explants of embryonic ectoderm, we could distinguish two sharply separated modes of cell movements: One of them having a characteristic rate of about 10–12 μm/min was oriented stretch direction while the other one containing randomly oriented movements with the rates non-exceeding 2–5 μm/min (Fig. 3.10j, i) (Troshina et al. 2011). Noteworthy, the latter value was greater in the stretched rather than non-stretched samples, permitting to exclude its artifact

origin. We suggest that the function of random movements is to "scan" mechanic microenvironment of each individual cell.

In spite of its advantages, BM is unable to describe the morphogenesis of epithelial layers in its full scale: The matter is that the stretched cells are assumed to be "frozen" in their deformed state, producing no active responses. However, TIAE effects (discovered after the BM was formulated) showed that this is not the case: The stretched cells undergo active elongation and intercalation movements. Taking TIAE into consideration, the scheme displayed in Fig. 3.10a should be exchanged by that shown in Fig. 3.11a, b. To what extent will it modify the BM results? In particular, will the scale invariance be preserved?

This problem was explored by assuming (Beloussov and Grabovsky 2005) that TIAE is switched on after exceeding certain tension threshold *Tthr* (normalized in the range $0 < Tthr < 1$).

It turned out that within a range of high enough *Tthr* values (i.e., when TIAE effect is small), a typical segregation of a model cell layer into two domains has

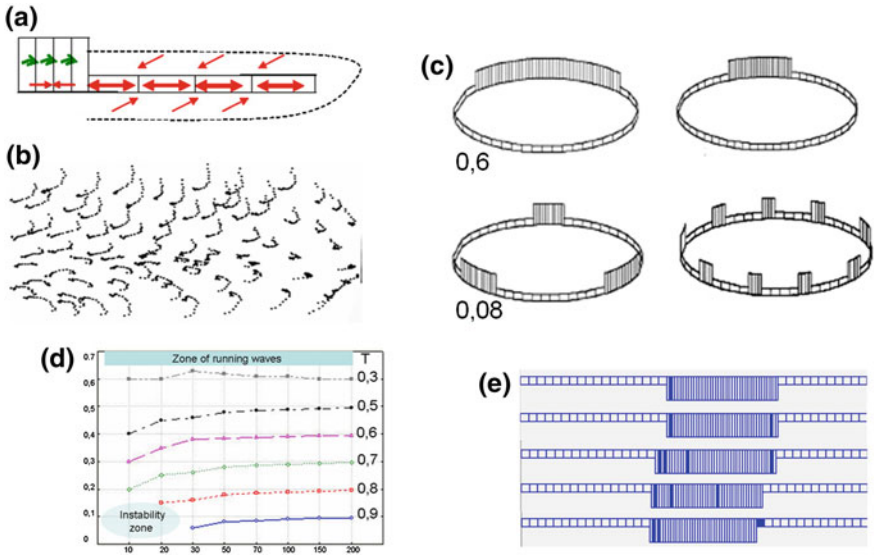

Fig. 3.11 A model of tension-induced active extension (*TIAE*). **a** active extension (instead of passive stretching, c.f. Fig. 3.10a) in response to tangential contraction of a *left* part of cell layer. **b** A map of planar convergent extension cell movements in the outer ectodermal layer of a stretched piece of Xenopus embryonic ectoderm, 30 min post-stretching period. **c** Segregation of a circular cell layer into columnar and flattened cell domains under different *Tch* values (figures) according to TIAE model. **d** TIAE model provides rather good scaling properties under realistic (not too small) number of cells (*horizontal axis*) and *Tch* values (given in *right* column). *Vertical axis* ratios of columnarized to the total cell numbers. Areas of instability and running waves (no stationary domains) are shown. **e** Stability of a layer's segregation under different numbers and arrangement of initially perturbed (columnarized) cells (*dense bars*) in terms of TIAE model. When being too far removed from other perturbed cells, a cell will come back to a flattened state (*lower row*, *right* dense cell)

been preserved (Fig. 3.11c, two upper frames). However, under further *Tthr* decrease, new effects appeared which could be understood in the following way. Suggest that a columnar domain stretches the flanking cells to the extent enough for overriding the threshold and hence for exerting a tangential pressure to more peripheral areas. As a result, the latter will be relaxed to the extent permitting their cells to create the next columnar domain and so on. In this way, a single local perturbation will be sufficient for subdividing an initially homogeneous cell layer into a number of flattened and columnar segments, whose numbers will increase as *Tthr* decreases (Fig. 3.11c, two lower frames). As shown by simulations, under even smaller *Tch* values, stationary structures disappear and are exchanged by running waves of cell columnarization. Therefore, the introduction of *Tch* parameter largely extends the repertoire of the modeled structures when compared to the BM proper. At the same time, although the absolute scaling capacities were lost, within a large enough range of *Tthr* values (embracing the entire area of stationary domains), deviations from the ideal scaling were found to be negligible (Fig. 3.11d). The modified BM model showed also substantial robustness in the sense that the columnar domains of almost the same size could be produced under rather different numbers and arrangements of initial perturbations (Fig. 3.11e).

Similarly to CCI, the formation of columnar cell domains can be compared with liquid crystallization, exemplified now by the row-aligned crystals of smectic type. In the given case, the newly arisen degrees of freedom are associated with the columnar cell capacities to *cooperative inclinations* which are of a primary morphogenetic importance and will be described below under the name of "cell fans." Thus, similarly to CCI, the formation of columnar cell domains out of a flat epithelium (whose cells are almost unable to incline) can be associated with the rise of entropy. As in the previous case, this will facilitate the performance of mechanical work by stretching a flattened part of a layer (if the latter's lateral edges are fixed). Note that the segregation of a layer with the fixed edges to the columnar and flattened parts should be qualified as a *meta*stable state: A passage to more stable one (exemplified by cell columnarization throughout the entire layer) is now prevented by mechanical resistance of the stretched layer's part. The advantage of metastable states, so widely presented in morphogenesis, is in storing elastic energy. In the section about "cell fans," we shall see how it is spent.

3.3.2.3 Periodic Patterns of Cell Alignment

The aim of this section is to demonstrate that cell transformations similar to the above-described ones can proceed in a periodic fashion, repeating for many times rather than being unique. In full scale, this is taking place in one taxonomic group only—hydroid polyps from Thecate subdivision. Its specific feature is in using so-called growth pulsations (GPs) as the main tool for stems growth and buds formation. Here, we review only those aspects of GP-based morphogenesis which are related to so-called "fans strategy," described in the next section. Other aspects of GP-based morphogenesis will be discussed in Chap. 4.

The living tissue of hydroid polyps, the so-called coenosarc, consists of two adjacent cell layers, the ecto- and endoderm, separated by the mesoglea. The main structural elements of both layers are epithelio-muscular cells. In addition, in the ectodermal layer, there are glandular cells secreting the components of chitinous exoskeleton, the perisarc, which is deposited as a soft substance on the tips of growing rudiments and is gradually hardened in the proximal direction (toward the base of a stem). Several dozens of ectodermal epithelio-muscular cells located in the distal-most regions are firmly attached to mesoglea by their basal surfaces and closely adhere to perisarc by their apical surfaces. Further to proximal similar cells are detached from the perisarc and become spread along mesoglea. Nevertheless, the hardened perisarc of the proximal zones perfectly "memorizes" the shapes molded earlier by distally located cells.

GPs are periodic rotations from oblique to transversal positions and back again exerted by both ecto- and endodermal distally located cells (Fig. 3.12a–d); these rotations are most obvious in the distal-most ectodermal cells closely adhered to the internal perisarc surface. In *Obelia loveni* species from White Sea, to which the following account is related, the GP period is about 5 min. During the so-called extension phase which takes the main part of each GP, cells change their orientations from oblique to more transversal ones (Fig. 3.12a–d). These reorientations are spread as a continuous distally directed wave with 40–90 μm/min rates. During

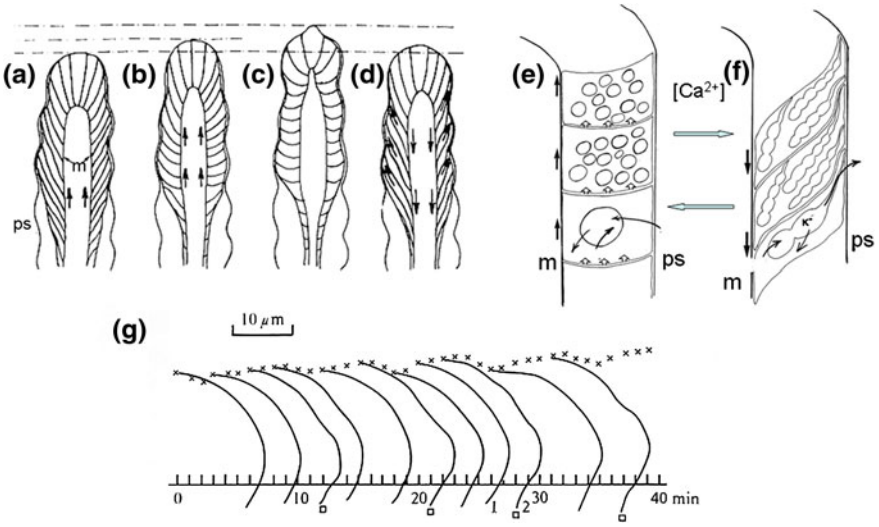

Fig. 3.12 Growth pulsations (*GP*) in Thecate hydroid polyps. **a–d** Schematic presentation of shifts and reorientations of growing tip cells during single GP. Horizontal lines at the *top* indicate distal levels reached by the tip at different GP phases. Only ectoderm is showed. **e**, **f** Sketches of intercellular chemo-osmotical events and their regulation. Frame **e** corresponds to extension and frame **f** to retraction phase. **m** Mesoglea. Perisarc *ps* (from Beloussov 1998). **g** Pulsations of a hydranth bud shapes. The contours with most relief coincide with the heights of extension phases. From Beloussov et al. (1972)

rotations, the apical cell walls remain to be firmly fixed to the inner perisarc surface, while their basal poles are shifted distally to 25–35 μm, pulling mesoglea (to which a prolonged file of proximally located ecto- and endodermal cells is attached), in the distal direction. By the same movement, the rotating cells push distalward the upper arch of the rudiment covered by still soft uppermost perisarc, lifting it up to 5–10 μm per each GP. So far as the amplitude of the mesoglea pulling in 3–5 times exceeds the length of the upper perisarc lifting, the latter during each next extension phase experiences a pressure from below. Such compression pulses are of primary morphogenetic importance as increasing the curvature of the distal part (Fig. 3.12g): These periodic increases will be "frozen" by the hardened perisarc.

In about 1 min after a round of transverse rotations is completed, the cells almost instantly return to their initial oblique positions ceasing to stretch the uppermost perisarc. The outgrowth is rapidly shortened, preserving however a part of the previously achieved growth advance due to rapid hardening of the perisarc and the "constructive rigidity" of the cusp-like shape of the growing tip. This is the retraction GP phase (Fig. 3.12d).

The most remarkable property of this phase is rapid (about 1 μm/s) and almost synchronous distalward sliding of the disto-apical cell poles along the inner surface of the perisarc: The sliding is associated with formation of prolonged distally oriented cell protrusions. The crucial role of sliding is in translocating the cells' fixation points on the inner perisarc surface toward distal. This permits them to start each next GP from the upper position providing thus a progressive growth.

According to the data available (Beloussov et al. 1989; Labas et al. 1992; Kazakova et al. 1994), the above-described events are based upon osmotic–contractile mechanisms, leading to periodic swelling–deswelling of intercellular vacuoles (Fig. 3.12e, f). At the height of the extension phase, the cells oriented close to transversal positions are full of isolated swelled vacuoles containing potassium ions in the concentration abundant to that in seawater (Fig. 3.12e). During the retraction phase, the vacuoles are fused together into prolonged channels opened in external space (as indicated by equalization of their ionic content with that of external water) (Fig. 3.12f). This concept is confirmed by GP arrest at the height of extension phase under hypotonicity of external medium or under increase of intercellular sodium transport; accordingly, GPs are arrested at the retraction phase if the opposite factors are employed (for details see Labas et al. 1992). By recent data (Nikishin and Kremnyov, in press), the proximo-distal wave of the upward cell rotations (vacuoles swelling) is arrested by blocking intercellular gap junctions, indicating thus that cell–cell contact interactions are necessary for this relay to go on. On the other hand, by blocking mechanosensitive ion channels, the retraction phase is abolished. By preliminary data, intracellular [Ca^{2+}] is increased just at this GP phase. Taken together, this permits to create the following tentative scheme. At the height of extension phase, due to the vacuoles swelling, the cell membranes become stretched and mechanosensitive channels (including Ca^{2+} ones) are activated. In its turn, Ca^{2+} inflow triggers vacuoles fusion and exocytosis, promoting thus vacuoles deswelling and release of cell–cell tangential pressure. Being pulled by elastically contracted mesoglea, the cells become under anisotropic stretch to which they

responding by actin polymerization in cell protrusions which are pushed toward distal, shifting the fixation points on the inner perisarc surface. Then, the next cycle of ion transport within the vacuoles and their osmotically driven swelling is started.

> By their functional geometry, GPs remarkably resemble the actomyosin interactions: Cell bodies which change periodically their orientations and shift distally their fixation points during each next GP perfectly imitate a myosin molecule, while perisarc and mesoglea take the role of actin filaments (mesoglea simulating the loaded filament). This is a spectacular example (next to the tensional homeostasis of cell membrane) of a literal transmission of the same working scheme for molecular to macromorphological level.

GPs are closely associated with the segregation of Thecate growing stems into columnar and flattened cell domains. The pulsatorial dynamics is exhibited only by columnar cells. Also, they are involved into fan-like multicellular configurations, to be described in the next section.

3.3.2.4 "Cell Fans": Transitory Multicellular Constructions for Slow Relaxations

Only rarely, the columnar cell domains remain flat for a long enough time period. In most cases, they start to bend inward by their apical surfaces in a few dozen minutes after their formation. This is the universal way for making epithelial folds, used by representatives of practically all the taxonomic groups, from Cnidaria to vertebrates: The list of examples includes so different events as budding in hydroid polyps, ascidians and other groups, gastrulation, neurulation, formation of lens and otic vesicles, curling of embryonic explants, and to some extent also somitogenesis. Usually, epithelial folding is considered to be an immediate consequence of apical cell contractions—but this view is imprecise and misses the real mechanisms. The crucial point is that the apical cell contractions in most cases essentially precede the bending of the entire layer. As a result, the columnar domains are first transformed into coherent groups of progressively inclined and apically converged cells which we call "cell fans." Their main feature is that the contour drawn perpendicularly to the transverse walls of the fan's cells exactly fits the future outlines of the arisen rudiment (Fig. 3.13a–k).

Worth mentioning, this property was first noticed, properly evaluated, and defined as "prognostic cell orientation" as far as 100 years ago in a study of brain development in shark embryos (Gurwitsch 1914) (Fig. 3.13a). However, because of using histological dyes selectively staining the chromatin, the author ascribed "prognostic" inclinations to cell nuclei only. This led him to suggest that a "field of forces" ("Kraftfelde") which he intuitively searched for in developing embryos did not affect other cell components. Probably, this accident delayed the development of morphomechanics for several decades.

Now, we perfectly know that "prognostic cell orientation" is based on the deformations of cell membrane and cytoskeleton and that the future bending of a layer consisting of inclined and hence mechanically stressed cells can be considered

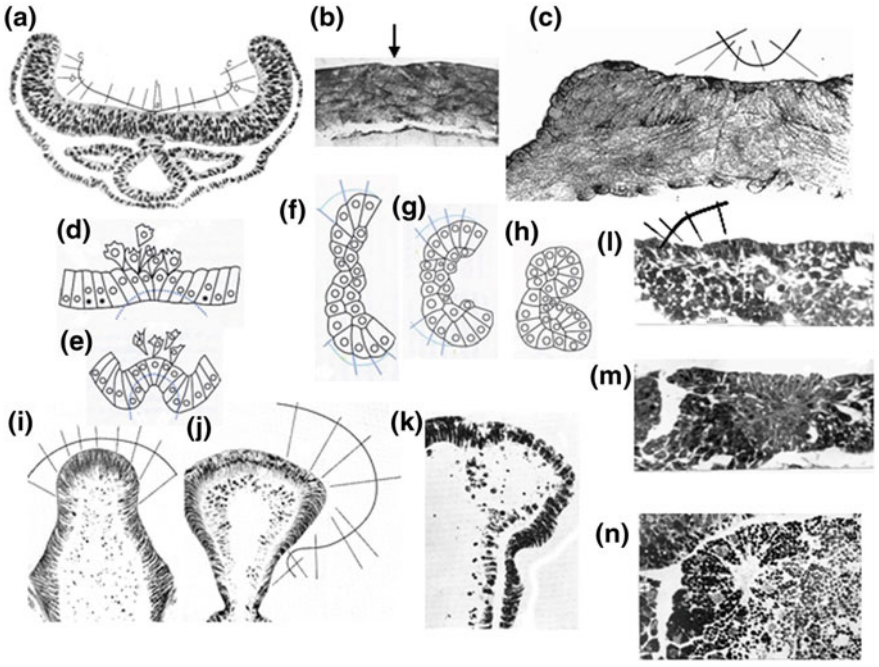

Fig. 3.13 Cell fans everywhere. Fine *curved lines* in **a**, **c**–**g**, **i**, **j** and **l** depict future contours of the anlagen plotted perpendicular to the given stage radial cell axes (prolonged in **a**, **c**, **f**, **g**, **i**, **j**, **l**). **a** The first shot of a "prognosic" cell fan in shark neurula. From Gurwitsch (1914). **b**, **c** Two successive stages of cell fan development at the early neurula stage of frog embryos (transversal sections). *Arrow* in **b** points to dorsal midline. **d**, **e** Prognostic cell arrangement at two successive stages of sea urchin gastrulation. **f**–**h** Successive stages of curling of frog embryonic ectoderm piece, 5–15 min after explantation. **i**–**k** Successive developmental stages of a growing tip of a hydroid polyp, *Dynamena pumila*. **l**–**m** Successive steps of the posterior wall formation in a chicken embryo somite (posterior to the *left*). **d**–**h** is from Cherdantzev (2006), by the author's permission

as a result of these cell relaxations toward more symmetric configurations. This suggestion is proved by immediate bending of a still flat epithelial layer consisting of such cells after being detached from underlined tissues: The rapidly bent layers are taking exactly "prognostic" shapes, closely imitating those acquired by the same rudiments in normal development several dozen minutes later (see Fig. 3.1 row 2 a_1, a_2; Fig. 3.5b).

"Prognostic" cell fans are quite ubiquitous cell constructions. The neurulation in vertebrate embryos starts from a small dorso-medially located cell fan (Fig. 3.13b) which soon extends involving not only all the neural plate layers but also the underlying axial mesoderm (Fig. 3.13c). Cell fans are indispensable components of gastrulation in all taxonomic groups (Fig. 3.13d, e) and can be easily traced in the edge regions of curling explants of embryonic tissues (Fig. 3.13f–h). Accordingly, most of what proceeds during the periods of topological invariability in amphibian

embryos are just relaxations of cell fans formed at the beginning of these periods. Same successions of events are taking place in other species as well. Thus, in the growing tip of a hydroid polyp, *Dynamena pumila*, the orientation of cell axes of the early tip predicts its subsequent transversal extension (Fig. 3.13 c.f. i, j). Similarly, the inclination of the apical parts of transversal cell axes (Fig. 3.13g) predicts further bending of cell layer (Fig. 3.13k).

Peculiar is the role of transitory cell fans formed along the median walls of somites in chicken embryo (Fig. 3.13l–n): They "predict" contours of a posterior wall of just formed somite. The mechanics of this process will be discussed further in this section and in Chap. 4.

Cell fans are formed in a relay fashion from the initiation point outward: That is, the cell inclination is increased as the relay proceeds. Therefore, each next cell added to the fan's periphery behaves in the active way rather than being affected by a common contractile force which might be located in the fan's center. As shown by electron microscopy, each next cell exerts a finger-like protrusion containing a microfilament bundle into the subapical area of its medial neighbor (Luchinskaia and Beloussov 1983). This is quite similar if not identical to the "push-pull" structures described by Brevier et al. 2008 (see Chap. 2). All of this permits to qualify a fan as a multicellular laterally directed vector.

During cell fan formation, TIAE- and BM-described dynamics are combined. The first one is obvious if observing each next pair of neighboring cells: Among them, a more peripheral cell (just added to the fan) uses its medial neighbor as a spreading substrate, demonstrating at the same time the additional (i.e., active) extension. On the other hand, each next cell involvement into a fan increases the tangential tension of entire cell layer in the BM fashion, that is, up to a limit when further involvement becomes hampered due to elastic resistance. Accordingly, the entire lengths of cell fans can be determined by BM mechanisms. Thus, they obey scaling properties.

Although on the individual cell level the relaxations toward more isodiametric shapes look quite similar, the results of the entire fans relaxations may be quite different, depending on the passive and/or active mechanics of the fan surroundings. Two main modes may be outlined here, acting either alone or in combination with each other. The first one is the already mentioned tendency to transform a cell fan into a curved surface (Fig. 3.14a, dotted contour). This is the universal way for making folds which is associated with an exchange of translational symmetry orders between single cells and cell layer as a whole. Let us indeed compare two successive stages: (1) A cell fan is already formed, but the layer as a whole is still flat: At this time, if neglecting the cells, the layer can be matched with itself under any linear shifts while if taking into consideration the individual cell shapes, no matching translations at all are taking place. (2) The individual cells become relaxed toward isodiametric shapes, while the entire layer is bent. Now, the situation is reversed: The cell shapes become almost identical, while the layer becomes curved losing thus translational symmetry. Hence, the beforehand reduced symmetry order of the parts has been transposed to the upper structural level. As mentioned in Chap. 1, such transformation corresponds to the trend toward the equilibrium state of solid bodies.

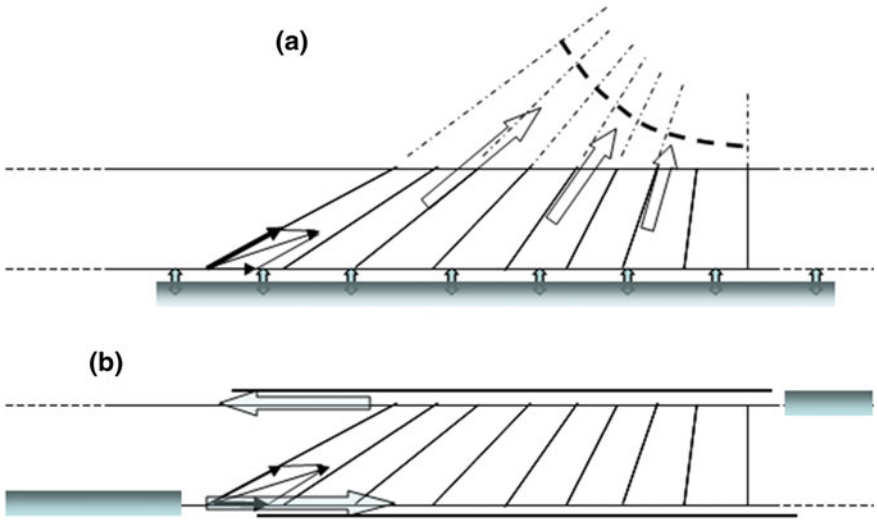

Fig. 3.14 **a**, **b** Two different modes of cell fans relaxations. *Shadowed bars* depict the resistive areas shifted by fan's relaxation in the directions shown by large empty *arrows*. Parallelograms of forces directed toward straightening the oblique cells are shown. **a** The bending mode. **b** The parallel shift mode. For detailed explanations see text

The above-described mode can be defined as the senior one, because it does not demand any specific initial (border) conditions. If however introducing such conditions by mechanically preventing the bending response, the "junior" mode will come into play, providing the cell shifts which do not change the layer's shape (Fig. 3.14b). This takes place in just described pulsatorial growth of hydroid polyps: The extension GP phase is based upon the cell transformations from inclined to rectangular shapes (i.e., to the relaxation of the fan), while the retraction phase can be interpreted as a formation of a new fan. The bending tendency is now mechanically prevented by the hard perisarc, while the direction of cell relaxation is canalized by the stretchable mesoglea. As a result, the "fan strategy" provides now the linear growth.

The advantages of the "fan strategy" for epithelial folding are clear, if comparing the bending mode with a hypothetical "step-by-step" processing consisting in the apical contraction of each next cell separately. Obviously, the latter demands finely detailed and non-robust regulation which in no way is scaled (i.e., adjusted to the dimensions of entire embryo). On the contrary, the "fan strategy" permits to make the folds scale invariant even before they take the required curvature. In addition, within the fan strategy framework, gradients of cell inclinations as well as the lag periods between their inclinations and subsequent relaxations can well be parametrically regulated, adjusting thus the curvature gradient of the resulting fold. In short, the fan strategy sets up the main characters of epithelial folds within a layer which is still flat but already mechanically stressed.

The role played by the fan strategy in the parallel shift mode is similar: First, it effectively integrates single-cell activities; next, by determining the inclination gradient, the amounts of tangential cell–cell pressure can be finely regulated. As will be shown in Chap. 4, this is of a particular morphogenetic importance, especially in the case of pulsatorial growth. Let us note meanwhile that the role of surrounding tissues in regulating this morphogenetic mode is up to now far from being properly explored.

In the broadest aspect, cell fans can be considered as the universal multicellular devices for making shapes and providing linear growth *by slowly relaxing the elastic energy stored in the inclined cells*. If comparing the times taken by mechanical jumps of separated tissues (<1 s) with the total time of the normal development, say, of amphibian neural tube (several hours), we can check indeed the retardation reaching 3–4 decimal orders. Meanwhile, as mentioned before, the immediately created shapes are amazingly similar to normal ones. Again, we see that the nature is rather scanty of inventing new principles: Same ones are used in chemomechanical transduction and in embryonic morphogenesis.

References

Aegerter-Wilmsen T, Smith AC, Christen AJ, Aegerter CM, Hafen E, Basler K (2010) Exploring the effects of mechanical feedback on epithelial topology. Development 137:499–506

Belintzev BN, Beloussov LV, Zaraiskii AG (1987) Model of pattern formation in epithelial morphogenesis. J Theor Biol 129:369–394

Belintzev BN (1988) Physical foundations of biological morphogenesis. Nauka, Moskva (in Russian)

Beloussov LV (1988) Contact polarization of *Xenopus laevis* cells during gastrulation. Ontogenez (Sov J Devel Biol) 19:405–413

Beloussov LV (1998) The dynamic architecture of a developing organism. Kluwer Academic Publishers, Dordrecht/Boston/London

Beloussov LV (2013) Morphogenesis can be driven by properly parametrised mechanical feedback. Eur Phys J E 36:132–147

Beloussov LV, Badenko LA, Katchurin AL, Kurilo LF (1972) Cell movements in morphogenesis of hydroid polyps. J Embr Exp Morphol 27:317–337

Beloussov LV, Bogdanovsky SB (1980) Cellular mechanisms of embryonic regulations in sea urchin embryos. Ontogenez (Sov J Devel Biol) 11:467–475

Beloussov LV, Dorfman JG, Cherdantzev VG (1975) Mechanical stresses and morphological patterns in amphibian embryos. J Embr Exp Morphol 34:559–574

Beloussov LV, Grabovsky VI (2005) A common biomechanical model for the formation of stationary cell domains and propagating waves in the developing organisms. Comput Methods Biomech Biomed Eng 8:381–391

Beloussov LV, Labas JA, Kazakova NI, Zaraisky AG (1989) Cytophysiology of growth pulsations in hydroid polyps. J Exp Zool 249:258–270

Beloussov LV, Lakirev AV (1988) Self-organization of biological morphogenesis: general approaches and topo-geometrical models. In: Thermodynamics and pattern formation in biology (I. Lamprecht, A.I. Zotineds). Walter de Gruyter, Berlin, pp 321–336

Beloussov LV, Lakirev AV, Naumidi II, Novoselov VV (1990) Effects of relaxation of mechanical tensions upon the early morphogenesis of *Xenopuslaevis* embryos. Int J Dev Biol 34:409–419

Beloussov LV, Luchinskaia NN (1983) A study of relay cell interactions in the explants of amphibian embryonic tissues. Tsitologia 25:939–944 (in Russian)
Beloussov LV, Luchinskaia NN, Ermakov AS, Glagoleva NS (2006) Gastrulation in amphibian embryos, regarded as a succession of biomechanical feedback events. Int J Dev Biol 50:113–122
Beloussov LV, Luchinskaia NN, Stein AA (2000) Tension-dependent collective cell movements in the early gastrula ectoderm of *Xenopus laevis* embryos. Dev Genes Evol 210:92–104
Beloussov LV, Saveliev SV, Naumidi II, Novoselov VV (1994) Mechanical stresses in embryonic tissues: patterns, morphogenetic role and involvement in regulatory feedback. Int Rev Cytol 150:1–34
Brevier J, Montero D, Svitkina T, Riveline D (2008) The asymmetric self-assembly mechanism of adherent junctions: a cellular push-pull unit. Phys Biol 5(1):016005
Cherdantzev VG (2003) Morphogenesis and evolution. KMK, Moskva (in Russian)
Cherdantzev VG (2006) The dynamic geometry of mass cell movements in animal morphogenesis. Int J Dev Biol 50:169–182
Cherdantzeva EM, Cherdantzev VG (2006) Geometry and mechanics of teleost gastrulation and the formation of primary embryonic axes. Int J Dev Biol 50:157–168
Chisholm AD, Hardin J (2005) Epidermal morphogenesis. WormBook 1–22
Darken RS, Scola AM, Rakeman AS, Das G, Mlodzik M, Wilson PA (2002) The planar polarity gene strabismus regulates convergent extension movements in Xenopus. EMBO J 21 (5):976–985
Davidson LA, Marsden M, Keller R, Desimone DW (2006) Integrin alpha5beta1 and fibronectin regulate polarized cell protrusions required for Xenopus convergence and extension. Curr Biol 16(9):833–844
Elsdale T (1972) Pattern formation in fibroblast cultures: an inherently precise morphogenetic process. In: Waddington CH (ed) Towards a theoretical biology 4: essays. Edinburgh Univ Press, Edinburgh, pp 95–108
Evstifeeva AJ, Kremnyov SV, Beloussov LV (2010) Topological and geometrical changes in *Xenopus laevis* embryonic epithelia under relaxation of mechanical tensions. Ontogenez (Russ J Dev Biol) 41:190–198
Farge E (2003) Mechanical induction of twist in the drosophila foregut/stomodeal primordium. Curr Biol 13:1365–1377
Farhadifar R, Röper J-C, Algouy B, Eaton S, Jülicher F (2007) The influence of cell mechanics, cell-cell interactions and proliferation on epithelial packing. Curr Biol 17:2095–2104
Goto T, Keller R (2002) The planar cell polarity gene strabismus regulates convergence and extension and neural fold closure in Xenopus. Dev Biol 247(1):165–181
Gurwitsch AG (1914) Der Vererbungsmechanismus der form. Arch Entw-Mech 39:516–577
Gustafson T, Wolpert L (1967) Cellular movements and contacts in sea urchin morphogenesis. Biol Rev 42:442–498
Hardin JD, Cheng LY (1986) The mechanisms and mechanics of archenteron elongation during sea urchin gastrulation. Dev Biol 115:490–501
Harris AK, Stopak D, Warner P (1984) Generation of spatially periodic patterns by a mechanical instability: a mechanical alternative to the Turing model. J Embryol Exp Morphol 80:1–20
Harris AK, Wild P, Stopak D (1980) Silicone rubber substrate: a new wrinkle in the study of cell locomotion. Science 208:177–179
Hofmann DK, Gottlieb M (1991) Bud formation in the scyphozoan *Cassiopea andromeda:* epithelial dynamics and fate map. Hydrobiologia 216(217):53–59
Hutson MS (2003) Forces for morphogenesis investigated with laser microsurgery and quantitative modeling. Science 300:145–149
Isaeva VV, Kasyanov NV, Presnov EV (2012) Topological singularities and symmetry breaking in development. BioSystems 109:280–298
Johnson MH (1981) Membrane events associated with the generation of a blastocyst. Int Rev Cytol Suppl 12:1–37

Kazakova NI, Zierold K, Plickert G, Labas JA, Beloussov LV (1994) X-ray microanalysis of ion contents in vacuoles and cytoplasm of the growing tips of a hydroid polyp as related to osmotic changes and growth pulsations. Tissue Cell 26:687–697

Keller R, Tibbetts P (1989) Mediolateral cell intercalation in the dorsal, axial mesoderm of *Xenopus laevis*. Dev Biol 131(2):539–549

Kinoshita N, Iioka H, Miyakoshi A, Ueno N (2003) PKC delta is essential for Dishevelled function in a noncanonical Wnt pathway that regulates Xenopus convergent extension movements. Genes Dev 17(13):1663–1676

Kornikova ES, Korvin-Pavlovskaya EG, Beloussov LV (2009) Relocations of cell convergence sites and formation of pharyngula-like shapes in mechanically relaxed Xenopus embryos. Dev Genes Evol 219:1–10

Kucera P, Monnet-Tschudi F (1987) Early functional differentiation in the chick embryonic disc: interactions between mechanical activity and extracellular matrix. J Cell Sci Suppl 8:415–432

Labas YA, Beloussov LV, Kazakova NI (1992) Kinematics, biological role and cytophysiology of growth pulsations in hydroid polyps. Tsitologia 34:5–23

Liem T (2006) Morphodynamik in der Osteopathie. Hippokrates Verlag, Stuttgart

Marsden M, DeSimone DW (2003) Integrin-ECM interactions regulate cadherin-dependent cell adhesion and are required for convergent extension in Xenopus. Curr Biol 13(14):1182–1191

Martin AC, Kashube M, Wieshaus EF (2009) Pulsed contractions of an actomyosin network drive apical constriction. Nature 457:495–499

Moore AR (1941) On the mechanisms of gastrulation in Dendraster excentricus. J Exp Zool 87:101–111

Naumidi II, Beloussov LV (1977) Contractility and epithelization of the axial mesoderm in the chick embryo. Ontogenez (Sov J Dev Biol) 8:517–520 (in Russian)

Osterfeld M, Du XX, Schüpbach T, Wieschaus E, Shwartsman SY (2013) Three-dimensional epithelial morphogenesis in the developing Drosophila egg. Dev Cell 24:400–410

Otto JJ, Campbell RD (1977) Budding in hydra attenuate: bud stages and fate map. J Exp Zool 200:417–428

Peralta XG, Noyama Y, Hutson MS, Montague R, Vernakides S, Kiehart DP, Edwards GS (2007) Upregulation of forces and morphogenic asymmetries in dorsal closure during Drosophila development. Biophys J 92:2583–2596

Petrov KV, Beloussov LV (1984) The kinetics of contact polarization of the cells in the induced tissues of amphibian embryos. Ontogenez (Sov J Dev Biol) 15:643–648

Plickert G (1980) Mechanically induced stolon branching in Eirene viridula (Thecata, Campanulinidae). In: Tardent P, Tardent R (eds) Developmental and cellular biology of coelenterates. Elsevier, North Holland, pp 185–193

Rauzi M, Lenne P-F (2011) Cortical forces in cell shape changes and tissue morphogenesis. Curr Top Dev Biol 95:93–121

Saveliev SV (1988) Experimental studies of mechanical tensions in neuroepithelial brain layers. Ontogenez (Sov J Dev Biol) 19:165–174

Saveliev SV, Besova NV (1990) Polarization of neuroepithelial cells after introduction of a portion of the neural tube into the neural cavity in amphibian embryos. Ontogenez (Sov J Dev Biol) 21:298–302

Shih J, Keller R (1992) Cell motility driving mediolateral intercalation in explants of *Xenopus laevis*. Development 116(4):901–914

Steding G (1967) Ursachen der embryonalen Epithelverdickungen. Acta Anat 68:37–67

Sugimura K, Ishihara Shuji (2013) The mechanical anisotropy in a tissue promotes ordering in hexagonal cell packing. Development 140:4091–4101

Sumina EL, Sumin DL (2013) Morphogenesis in the aggregates of filamentous Cyanobacteria. Ontogenez (Russ J Dev Biol 44:203–220

Tambe DT et al (2011) Collective cell guidance by cooperative intercellular forces. Nat Mater 10 (6):469–475

Thompson DA (1942, 2000) On growth and form. Cambridge University Press, Cambridge

Trinkaus JP (1969) Cells into organs. The forces that shape the embryo. Prentice Hall, New Jersey

Troshina TG, Glagoleva NS, Beloussov LV (2011) Statistical study of rapid mechanodependent cell movements in deformed explants in *Xenopus laevis* embryonic tissues. Ontogenez (Russ J Dev Biol) 42:301–310

Vedula RK, Leong BC, Lai TL, Hersen P, Kabla AJ, Lim CT, Ladoux B (2012) Emerging modes of collective cell migration induced by geometrical constraints. PNAS 109:12974–12979

Wallingford JB, Fraser SE, Harland RM (2002) Convergent extension: the molecular control of polarized cell movement during embryonic development. Dev Cell 2(6):695–706

Chapter 4
Morphomechanical Feedbacks

Abstract An attempt is made to reconstruct the natural successions of the developmental events on the basis of a common mechanically based trend. It is formulated in terms of a hyper-restoration (HR) hypothesis claiming that embryonic tissue responds to any external deforming force by generating its own one, directed toward the restoration of the initial stress value, but as a rule overshooting it in the opposite side. We give a mathematical formulation of this model, present a number of supporting evidences, and describe several HR-driven feedbacks which may drive forth morphogenesis. We use this approach for reconstructing in greater detail the gastrulation of the embryos from different taxonomic groups. Also, we discuss the application of this model to cytotomy, ooplasmic segregation, and shape complication of tubular rudiments (taking hydroid polyps as examples). In addition, we review the perspectives for applying morphomechanical approach to the problem of cell differentiation.

4.1 General Comments

Now, we approach the main goal of this book which is to suggest a scheme of more or less universal morphomechanically based feedbacks able to drive forth the development of metazoans. Up to recently, for most investigators, such a task looked impracticable and illusory due to an overall belief that the onset of each next stage is determined either by its own specific cause, or by a strictly defined portion of genetic information, read at certain time and at certain space location, or by both together. Only few authors noticed contradictions of this viewpoint (discussed in Chap. 1) and made attempts to pave another way. Among these, one of the most ambitious was the last version of the "cellular field theory" (Gurwitsch 1944; posthumous edition 1991) briefly mentioned in Chap. 2: Here, the task to derive a next stage embryonic shape from that of the preceded one (rather than from any specific cause or genetic information) was overtly formulated. It is but natural that this theory, which was created well before than intracellular mechanics has been

L.V. Beloussov, *Morphomechanics of Development*,
DOI 10.1007/978-3-319-13990-6_4

explored even in most general outlines, cannot be today accepted. However, the very purpose to follow this way as well as several incident authors' findings should be highly estimated. In any way, the following statement can be taken as a motto for all the subsequent enterprises of this kind: "According to our viewpoint, different from the dominating one, out of a really adequate description of any momentary state of a living system its transition to the next one should inevitably follow" (Gurwitsch 1991). In these terms, the task for the next generations of researchers will be no more but also no less than to reach such an "adequate description."

This aim got for the first time a firm background about half a century ago when the self-organizational "way of thinking" (reviewed in Chap. 1) started to penetrate developmental biology and demonstrated principal possibility to provide structural self-complication of embryonic body. As mentioned before, in biology this viewpoint was at the beginning introduced in the context of chemo-kinetic models and specified in terms of short-range positive and long-range negative feedbacks.

The next step in elaborating the concept of morphogenetic feedbacks was associated with the first generation of mechanically based SOT models (Odell et al. 1981; Harris et al. 1984; Belintzev et al. 1987). All of them, either overtly or in a hidden form, introduced the fundamental distinction between passive and active deformations of embryonic tissues. In other respects, however, they were essentially different. Let us survey the corresponding dynamic schemes, omitting specific details.

Odell et al. (1981) model was based on a common property of excitable tissues (from heart muscle to slime mold strands: Wohlfarth-Bottermann 1987) to contract in respond to stretch. Applying this reaction to embryonic tissues, the authors created a model of stretch–contraction relay within a cell layer. According to it, if a part of a layer is actively contracted, it will stretch the neighboring part triggering its contraction and so on. In this way, a chain of feedforward relations (without any feedbacks) will pass along the model layer. If assuming that both opposite layer edges are immobile, the system acquires feedbacks and is transformed into a stationary oscillator. Such devices may play a great role in morphogenesis (growth pulsations in hydroid polyps are an example) but cannot alone create macroscopic stationary structures.

For reproducing the latter's formation, long-range negative feedbacks (combined with short-range positive ones) seem indispensable. We know already that they were introduced at least in two mechanochemical models (Harris et al. 1984; Belintzev et al. 1987) being in both cases identified with self-generated tensions. At the same time, positive feedbacks were associated with contact cell interactions. However, in spite of making a great step forward, both models, while taken isolated, stopped to work after reproducing segregation of an initially homogeneous tissue into a number of similar domains. In particular, taken alone, they are unable to model curvature. Something else should be introduced for driving forth morphogenesis without inserting at each next step taken ad hoc initial conditions.

The lacking link is prompted by TIAE events. To make morphogenesis non-arrested after the end of a layer's segregation, a structural component assumed beforehand to be passively deformed should acquire its own activity. In terms of

stresses and in the context of TIAE model, this means that the tension imposed by external force, after passing a certain threshold, should trigger the oppositely directed active compression stress. If indeed the deformations produced by the stress will not only compensate but even overshoot those exerted by outside force, new symmetry breaks (shape complications) can be produced. One of them—formation of several columnar domains instead of one—has been already described (see Fig. 3.11 and the corresponding comments). Another expected consequence of extensive compression stress is to produce Eulerian instabilities and hence formation of curvatures. This brings us to the idea that actively generated stresses directed oppositely to those imposed by external forces (compression in response to stretching and contraction in response to relaxation/compression) and overshooting them (by the deformation criteria) may drive forth morphogenesis. We call this hypothesis the model of a hyper-restoration (HR) of mechanical stresses. In the following sections, we explore the evidences supporting the following basic suggestions of HR model (1) that passive and active stresses are oppositely directed and (2) that active responses of a given embryo part (estimated in terms of deformations) overshoot the passive ones (imposed by another part, that is, from outside). We start from the events of molecular–supramolecular levels (using data reviewed in Chap. 2) and then come to the upper structural levels.

4.2 Evidences for Hyper-restoration of Mechanical Stresses

4.2.1 Molecular–Supramolecular Levels

In Chap. 2, we gave a number of examples demonstrating a wide presentation of biphasic charging–discharging energy loops using the discharging (relaxing) branch as the working stroke. This was true not only for the elementary molecular machines (including, in the first turn, actomyosin-based contractility) but also for the supramolecular mechanochemical devices—cytoskeleton, cell membrane, and cell contacts. Remind, for example, the dynamics of the focal contacts and associated multimolecular complex under the action of a pulling force (see Fig. 2.3 and the corresponding comments): The imposed tension is released up to its initial value due to active increase in the contact areas. Correspondingly, if the tensions are relaxed, the contact areas are diminished in order to restore the tensional homeostasis. Similarly, stretched cell membranes restore their homeostatic stress values with the use of exocytosis, while relaxed cell membranes employ endocytosis for the same purpose. Several homeostatic reactions to external mechanical stresses have been registered at the level of individual cell, for example, in fibroblasts (Mizutani et al. 2004). All of these indicate that the active outputs are directed opposite to the inputs. But are the subcellular level responses accompanied by overshoots? Howard's (2009) concept of negative damping in actomyosin oscillations (see Sect. 2.6) supports this idea by implying the absorption of additional

energy just at the phase of stress release. As seen from Gautier (2011, 2012) protocols, the insertion of new portions of cell membrane in artificially or self-stretched samples is also accompanied by some overshoot.

Distinct transformation of the applied tension to a similarly directed active pressure, as well as the reverse reaction, was observed in the artificially stretched axons (Dennerly et al. 1989). The axons, while responding to moderate stretching as passive viscoelastic bodies, after exceeding 100^{-6} dyn force threshold, became actively elongated and their tension markedly reduced. On the other hand, after sudden diminution of tension, the axons contracted, sometimes doubling pre-experimental steady-state tension. Thus, the overshoots took place in both directions.

An interesting example of the overshoot reaction to stress changes tested by the shapes of cell nuclei was described by Filas et al. (2011). The authors measured responses of brain tissue to altered mechanical loads and found that both the reduction and the increase in tensions produced responses opposite to inputs. Thus, the establishment of low tensions was followed by actomyosin contraction which increased tensions and the heights of neuroepithelial cells, while stretching by external force triggered actomyosin disaggregation, relaxation, and cell flattening. After any of these interventions, the deformed nuclei did not return exactly to their intact shapes: Under tension decrease, they became more elongated while after tension increase less elongated than the control ones. By the authors' view, these deviations indicate overshoots. This may be of a special interest because, as will be shown below (Sect. 4.6.5.3), in certain cases, the shapes and the mechanical properties of cell nuclei play decisive role in cell differentiation.

4.2.2 Cellular–Supracellular Levels

4.2.2.1 Experimental Indications of Overshoots

At this level, active cell reactions to relaxations and tension increase are widely presented. Some of them have been already described in Chap. 3. Thus, cell columnarization was shown to be a usual reaction to the relaxation of tensions (see Figs. 3.6 and 3.9 and the corresponding comments). To reveal the overshoot components of this reaction, special measurements are required, to be accounted below. Overshoot responses of individual cells and cell collectives to stretching are more obvious: Such are excesses of the individual cell eccentricities over those of entire stretched samples (Fig. 3.8e, f) and formation of polar bulges (Fig. 3.8g–j). These results could not be produced in the absence of compression stresses following tensile ones.

Pronounced overshoots can be traced in experimentally bent double explants (sandwiches) prepared either from a suprablastoporal area (SBA) of early gastrula *Xenopus* embryos (Kornikova et al. 2010) or from the ventral ectoderm of the same stage embryos (Kremnyov et al. 2012). So far as under the action of external force, the concave side of a bent sandwich should be shrunk and the convex side

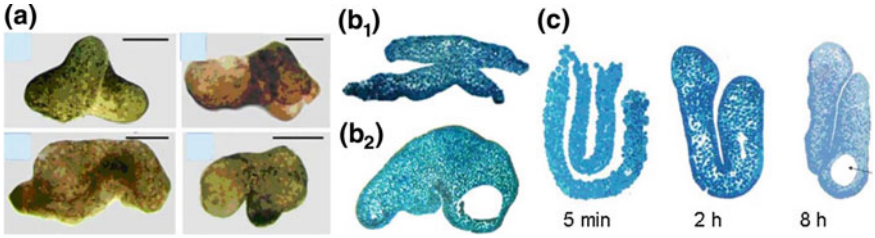

Fig. 4.1 Autonomous deepening of the artificially produced folds. **a** Two representative sandwiches prepared from *Xenopus* early gastrula suprablastoporal area, total views. *Upper row* samples in few minutes after being inserted into slightly bent grooves. *Lower row* same samples 8 h later. Indentations become much more acute (from Kornikova et al. 2010). **b_1–b_2** Cross sections of similar samples few minutes and 3 h after bending. **c** A gradual narrowing of artificially imposed fold in the sandwiches prepared from *Xenopus* early gastrula *ventral* ectoderm (from Kremnyov et al. 2012)

extended, the overshoots should be manifested by active contraction of the concave surfaces and active extension of the convex ones. Just this was taking place indeed (Fig. 4.1a–c). The active contraction of the concave surfaces was associated with the rise of so-called apical cell indexes (AI) (those are the ratios of the maximal cell heights to their apical diameters) which in Kornikova et al. experiments shifted from 3.4 ± 1.2 in the intact samples to 5.9 ± 2.8 already in 30 min after start of bending. At the same time, AI of the convex-side SBA cells decreased from 2.6 ± 1.0 to 1.1 ± 0.3, confirming tangential extension of these cells. AI increase and the rise of the curvature have been observed also in the ventral ectoderm sandwiches prepared from ventral ectoderm (Fig. 4.1c). Profound effects of these manipulations to the patterns of cell differentiation will be described later.

Now, we would like to present several semi-quantitative estimations of the overshoots (measured in terms of deformations, rather than stresses). Two first examples relate to the active contractile responses which "hyper-restore" the previously relaxed tensions under the fixed edges of the cell layer. The next two exemplify the opposite reaction: emergence of the compression stress after stretching a sample by an external force.

Our first example is based on the above-described (see Fig. 3.1, upper row, c_1, c_2) biphasic "opening" of a transversely dissected dorsal blastoporal lip, first passive and then active. As shown by the corresponding measurements, the fast cold-resisted relaxation of pre-existed tensions gives about 20 % diminishment of the sagittal length of the lip: This is the measure of its passive shrinkage. Meanwhile, the next, slow, and temperature-dependent active phase brings (under fixed edges) no less than 40 % contraction—a measure of the active restoration of tensions. As a result, we get roughly 100 % tension overshoot.

The next, rather peculiar example of the tension overshoot is associated with experimentally perturbed apical growth of a hydroid polyp, *Dynamena pumila* (Fig. 4.2). Its growing apex is periodically subdivided into three rudiments (one central and two lateral). The adjacent walls of the rudiments were shown to pulsate

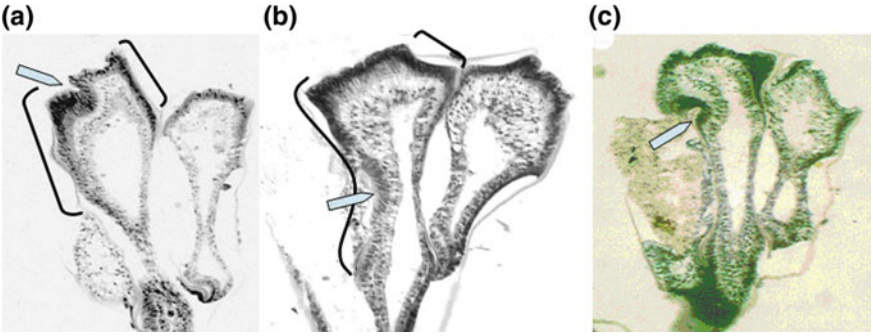

Fig. 4.2 a–c Tension overshoots in the relatively relaxed left walls in the apical region of a hydroid, *Dynamena pumila*. *Brackets* outline the columnar cells domains. *Pointers* indicate abnormal folds

in antiphase, promoting thus each other elongation (for details, see Beloussov 1998). If the lateral rudiment is removed, the adjacent wall of the central one (Fig. 4.2a–c, left walls) will retard its longitudinal growth and hence become under-stretched (relatively relaxed) as compared with the opposite wall of the same rudiment which retained normal contacts with its lateral neighbor (Fig. 4.2a–c, right walls). One can show that the relative relaxation (under-stretching) of the left walls is hypercompensated by columnarization (tangential contraction) of their cells and by formation of abnormal folds (pointers). This becomes obvious if comparing the total length ratios of the under-stretched to the normally stretched opposite wall lengths to the length ratios of the columnar cell domains in the same walls. It turned out that in the under-stretched walls, the columnar cell domains always occupied non-proportionally large territories (compare the lengths outlined by brackets in the left and right walls of the left rudiments in Fig. 4.2a, b). So far as each columnar cell is at least 3-fold tangentially contracted as a non-columnar one, this gives a considerable contraction overshoot of the under-stretched walls. To this one should add the contractions promoted by abnormal folds (Fig. 4.2a–c, pointers).

The next example is related to the double-step overshoot initiated by a slight transversal stretching of the partly labeled SBA in *Xenopus* early gastrula embryos (Fig. 4.3a, upper row, double-head arrows). This intervention releases the normal dorso-medial contraction which is dominating at this stage, arrests the dorsalward cell flow and hence relatively relaxes the ventral blastoporal lip area. The latter responds by contraction which is initiated already in few minutes after the abnormal transversal fold formation (Fig. 4.3a, upper row, pointers). The fold is extensively involuted (Fig. 4.3a, lower row), demonstrating the first overshoot. However, we will be concentrated on the second response, associated with the dorsoventral flow of labeled cells (opposite to normal one) going upward to the newly established tension gradient. We compare the increase in the flow length (ΔL) with the increase in the ventral fold perimeter (Δf) in the same successive time periods. If the cell flow was a linear consequence of the fold growth and no overshoot took place, both values would be equal (Fig. 4.3b, dotted line). It was found, however, that $\Delta L \gg \Delta f$

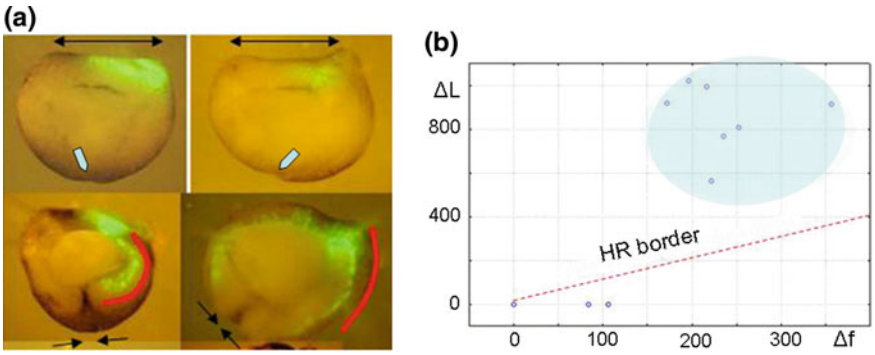

Fig. 4.3 Overshoots triggered by slight transversal stretching of *Xenopus* early gastrula suprablastoporal zone. **a** *Upper frames* display two different partly labeled embryos in 10 min after stretching (shown by *double-head arrows*). *Pointers* are directed toward just initiated ventral fold. *Lower frames* same embryos 12 later. *Note* considerable ventral shifts of the labeled material (marked by *red*) and extensive deepening of the fold (converging arrows). **b** Relations between the fold's perimeter increase (Δf) and the length increase in the ventralward cell flows (Δ*L*), arbitrary units. *Light blue area* embraces extensive overshoots of Δ*L* as compared with Δf (experiments by Tatjana Troshina)

(see extensively populated upper left region in Fig. 4.3b). The excess over the dotted line is a quantitative measure of the overshoot (in terms of deformations). Interestingly, if the folds are small (the involvement less than ∼10 % of the lateral lip area), no overshoot is taking place (left part of the plot). Therefore, for producing the overshoot, some deformation threshold should be overridden.

The latter example of the overshoot reaction is given by experiments on sucking the gastrula stage *Xenopus* embryos into a tube with the 2-fold smaller diameter (Mansurov et al. 2012). The sucking device was constructed in such a manner that after a small part of embryo was involved into the tube, the sucking force came to zero value and under further penetration took reverse sign. In spite of this, the non-inserted part of embryo actively narrowed (due to transversal contraction–longitudinal extension of its cells) and moved into the tube till to complete penetration. Then, it immediately stopped and if pushed out took a normal spherical shape in few minutes (Fig. 4.4). The embryo penetration into the sucking device was arrested by cytoskeletal drugs and by the destruction of non-penetrated part. The reaction was independent upon embryo orientation but did not take place after the end of gastrulation.

In principle, the observed reaction, as demonstrating cells convergence–extension in response to external stretching force, may be considered as the particular case of TIAE. Its peculiarity is in being spread throughout an entire embryonic body and being directed toward equalizing stresses (abolishing the imposed tension gradient) up to a limit permitted by mechanical restrictions. The "active insertion" reaction to a large extent exceeds those taking place during normal development. This shows that the active mechanical reactions of embryonic tissues are not strictly dosed but have a substantial reserve for confronting unexpected conditions.

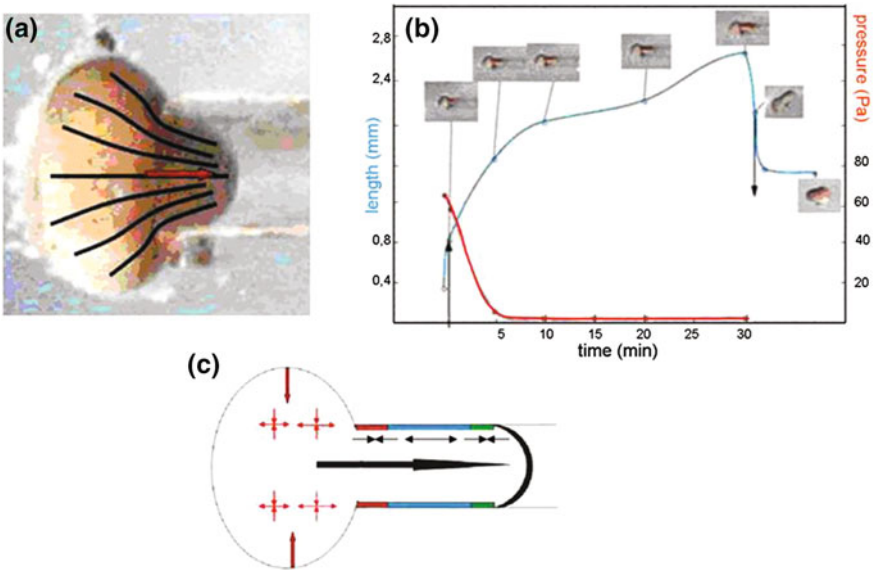

Fig. 4.4 The active intrusion of an early gastrula stage *Xenopus* embryo into a tube half the embryo in diameter triggered by an initial suction force. **a** Start of the active intrusion. *Black lines* display converged cell trajectories. **b** A protocol of an intrusion experiment. *Red curves* show the suction force (Pascals, right scale) and the *blue line* the distance from the embryo tip to the tube opening (mm, *left* scale). *Horizontal axis* time (min) elapsed from the start of the experiment. *Upward arrow* indicates the time of force application and *downward arrow* the time of embryo pushing out from the tube. **c** A sketch of cells' convergence–extension deformations in non-intruded embryo part (to the *left*) leading to its overall transversal contraction (*vertical arrows*) and alternated irregularly contracting–extending zones in the intruded part promoting a tip shift in the direction shown by *black arrow* (from Mansurov et al. 2012)

4.2.2.2 From Overshoots to Morphogenesis: Playing with the Curvatures

In the previous section, we described some experiments on deformation of embryonic rudiments and showed that these interventions were followed by what we called the stress HR (the restorations with overshoots). Now, we would like to follow this line by demonstrating that the overshoots themselves lead to further shape changes. By doing this, we shall combine episodes of normal morphogenesis with another portion of experiments. Most of all, we shall be interested in the evolution of the curvatures.

Let us first consider tubular rudiments which are slightly bent at the beginning of development. To these belong the stems of hydroid polyps, archenterons of Echinodermata embryos, anterior parts of vertebrate neural tubes, and many others. By tracing their morphology in more detail, we can see that (a) the opposite tube walls are never parallel: In undifferentiated state, the curvature of the convex walls is

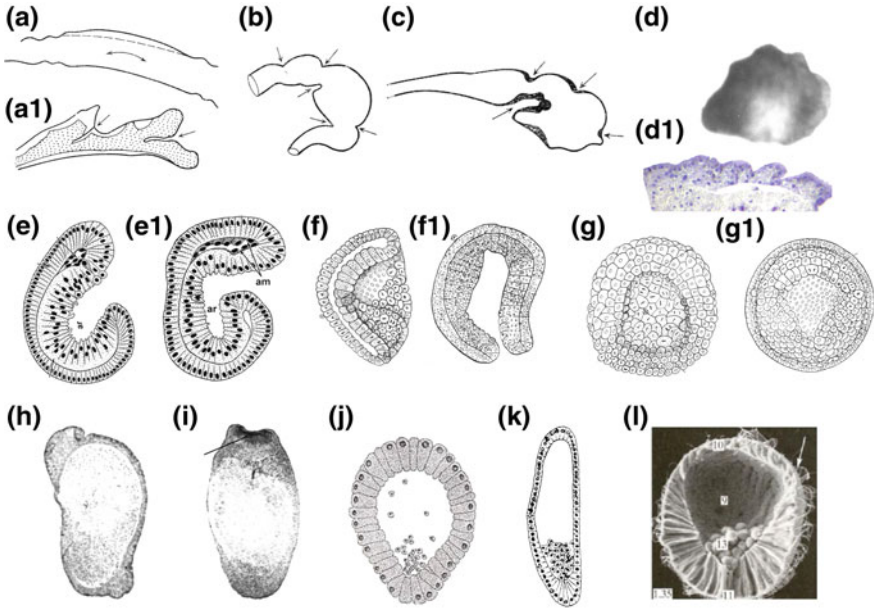

Fig. 4.5 Segregation of the curvatures. **a**–**d** Maximal curvatures and most extensive evaginations are adjusted to the convex sides of curved rudiments; invaginations are always narrower. **a** Stem of hydroid, *Obelia*. **a1** Branch of hydroid *Dynamena* with hydrant buds on the convex side. **b** Differentiation of the gut in sea urchin larva. **c** The anterior part of vertebrate neural tube. **d** Moderately stretched *Xenopus* ventral ectoderm sandwich with extensive folding on the convex side (**d1** is a cross section indicating that the folds are formed from *right* to *left*). **e**, **e1** Concentration of initially smoothed curvatures in few points of *Phoronis* embryonic cell layers. **f**, **f1**; **g**, **g1** Same in *Amphioxus* embryos. In **g**, **g1,** the curvature focusing is associated with flattening of the curved layer part and folding of the flattened one. **h**, **i** Formation of tangentially contracted (*bent arrows*) columnar cell domains in the vicinity of the maximal curvature areas in moderately stretched *Xenopus* ventral ectoderm sandwiches. **j**–**l** Immigration of cells from the mostly curved areas of cell layers. **j** Cnidaria, Hydrozoa; **k** sponges, Calcinea; **l** sea urchin embryo

always greater than that of the concave ones (Fig. 4.5a: this was checked in several dozen samples without any exception); (b) in all the observed cases of either normal (Fig. 4.5a_1–c) or experimentally induced (Fig. 4.5d, d_1) morphogenesis, convex surfaces were folded much more extensively than flat or concave ones. In particular, the buds of hydroid polyps were always formed on the convex sides even if the stem curvature has been reversed experimentally (Kossevich 2002). Obviously, these events confirm our expectations of the active hyperextension of the convex surfaces because of being initially stretched to a greater extent than the opposite ones.

Another remarkable and by all the evidences universal tendency of curved embryonic surfaces is that the smooth curvature gradients established in early development are later segregated to almost flat areas and sites of high curvature which separate them (Fig. 4.5, cf. e and e_1, f and f_1, g and g_1). Similarly, the ovoid

bodies are segregated into almost flat lateral regions and the polar regions of a high curvature: They can be either produced experimentally (Fig. 4.5h, i) or develop normally (Fig. 4.5j–l). The opposite poles are as a rule of unequal curvatures.

Remembering the Laplace law (see 1.2.4) which claims that the tensions within a given area are inversely proportional to the local curvatures, one can see that "segregations of the curvatures" are the natural consequences of HR tendencies. For proving this, let us suggest that the rudiments of uniform curvature (i.e., spherical or flat) are shifted out of uniformity under the action of some external forces. By tending to hyper-restore the initial stress values, the mostly tensed (more flat) areas should actively extend (producing forces of tangential pressure), while the less tensed (mostly curved) ones should actively contract. Both reactions can be realized by different ways and on different levels. In particular, the tangential pressure can be produced by exocytosis, by radial cell contraction, or by a kind of planar cell intercalation. Similarly, the tangential contraction can take place due to endocytosis, by tangential cell contraction (cell columnarization) (Fig. 4.5h, i), or by emigration of some cells out of the mostly curved region (Fig. 4.5j–l). Whatever the real mechanisms are, both oppositely directed reactions enhance each other. The rise of tangential pressure promotes the increase in tangential tension in the neighboring area and vice versa. As a result, the output is non-trivial: Instead of bringing the body back to its initial shape, the combination of HR reactions increases the curvature differences and transforms smooth curvature gradients into sharply segregated curvature patterns. This is the first evidence that these reactions in spite of looking conservative can in fact drive forth morphogenesis. Several other arguments favoring this suggestion will be presented below.

4.2.2.3 HR Reactions in Toroid Bodies

Among three-dimensional shapes the inflated (internally pressurized) toruses or parts of them (circular folds or their sectors) are mostly spread. All the animals with through intestines are indeed axially elongated toruses (Isaeva et al. 2012). Such a conclusion is far from being formal and reflects some deep inherent tendencies of embryonic tissues. Toroid and semi-toroid configurations (holes surrounded by circular folds) are indeed typical for embryonic bodies of quite different species (from cnidarians to vertebrates). They arise due to epithelial layers' tendencies to curl around free margins and to minimize the surfaces of the arisen folds by making them circular: The most known example is the lip of the blastopore. A universal property of inflated toroid bodies with stretchable envelopes is inequality of tensions in different directions. As it is known from mechanics (Landau and Lifshitz 1976), the transversal (meridian or circular) surface tensions in such bodies are twice as great as the equatorial ones. Suggest now that a toroid body is developed under the action of external forces out of an isotropically stressed one (in the simplest case, from a sphere or its part), tending at the same time to hyper-restore stress isotropy. This means that the meridian tensions, being the greatest, will be first of all diminished and then exchanged by compressive stresses; on the other

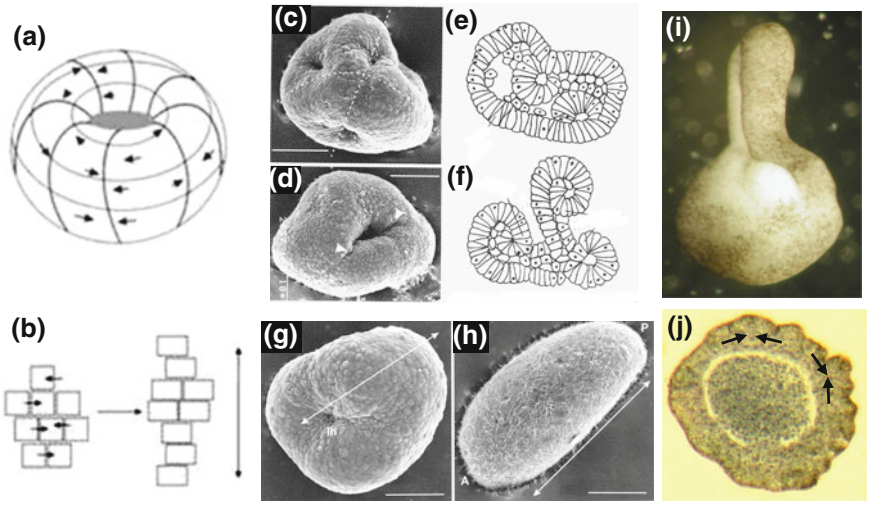

Fig. 4.6 Morphogenesis of toroid surfaces. **a**, **b** Convergent cell intercalation toward torus meridians driven toward minimization of the maximal tensions with an overshoot producing meridian pressure. **c**–**h** Variable toroid configurations and their transformations into elongated larval bodies in a hydroid, *Dynamena pumila.* From Kraus (2006), with the author's permission. **i**, **j** Transformation of a toroid circle cut from *Xenopus* early gastrula. The *folds* indicate circular compression due to the cells convergence toward meridians (*arrows*)

hand, the equatorial stresses should increase. Accordingly, one can expect convergent cell intercalation toward the meridians in combination with equatorial contraction (Fig. 4.6a, b). As a result, the torus (or its part) is expected to contract in latitudinal direction and extend along the meridians. Although the meridian and equatorial tensions will be equilibrated when the torus takes a spheroid shape, in the case of overshoot, it will continue to elongate in meridian direction (perpendicularly to the torus plane). It may be just this antero-posterior elongation which creates architectonic basis of all the animals with actively contracted blastopore, confirming thus pertinence of Isaeva et al. (2012) scheme.

Morphogenesis of toroid surfaces has been traced in embryos of two taxonomically largely removed groups—hydroid polyps and amphibians.

By Kraus (2006) observations, an embryo of a hydroid polyp, *Dynamena pumila*, at the late cleavage stage consists of several randomly oriented multicellular toruses (Fig. 4.6c–f). During subsequent development, single toruses are fused together, creating finally a single torus, which is closed from one side, elongated in meridian direction, and forms the entire larval body. A single torus hole (to be later on also closed) fits the anterior larval pole (Fig. 4.6g, h). Thus, the last torus surpasses spheroid shape when the meridian and equatorial tensions are equal to each other and demonstrates a distinct overshoot. Even more spectacular overshoot reaction is observed in *Xenopus* embryos. An entire circular blastoporal lip, or a transversal tissue ring taken from a suprablastoporal area, if isolated, transforms in several hours into a narrow tube elongated parallel to the main torus axis (Fig. 4.6i).

Extensive folding observed in transversal sections points to the equatorial cell convergence (Fig. 4.6j).

As will be shown later, dynamics of toroid bodies is crucial for gastrulation and may be regarded as the best example of highly coordinated cell movements which may be driven by mechanogeometry alone.

Now, let us come to the general formulation of the HR model.

4.3 General Premises and Formulation of HR Model

By the author's knowledge, an important role of energetic overshoots was first emphasized by the Russian physiologist Arshavsky (1974) who claimed that during the fertile period of the living cycle of an organism, any act of motile activity of striated muscles is accompanied by a gain of energy, overriding its spending. Certainly, the excessive energy should be borrowed from internal sources.

In Chap. 1, we suggested that shape formation may be in its essence a side effect of the general trend to minimize free energy when it takes place in nonlinear systems with metastable energy wells. HR hypothesis can be regarded as further specification of this idea. The first part of HR reaction (until the start of the overshoot per se) is indeed identical to the universal Le Chatelier response ("Any change in status quo prompts an opposing reaction in the responding system": Wikipedia) directed toward thermodynamic equilibrium. The very overshoot can be regarded as a prolongation of the Le Chatelier trend which can take place in non-equilibrium systems with permanent energy inflow. Note in this respect (as demonstrated by the above examples), that the *direction of the overshoot deformation* always *coincides* with that of the perturbation triggering the entire HR reaction, while the *stress changes* in these two phases are directed *oppositely* to each other. Thus, a sample is actively extended in the same direction in which it was passively stretched, but from the beginning of active reaction, the stress is changed from the positive tensile to the negative compressive.

Let us present now the verbal formulation (first used by Beloussov et al. 1994), a diagram and a suggested phase portrait of HR model:

> Whenever a change is produced in the amount of local stress applied to a cell or local region of tissue (regardless of whether this change comes from a neighboring part of the embryo or has been exerted by an experimenter), the cells or tissue region will respond by actively generating forces directed toward the restoration of the initial stress value, but as a rule overshooting it. Whenever such changes in stress are unevenly distributed (stronger one place than another), or are anisotropic (stronger in one direction) then the responses induced will be directed toward reducing (with an overshoot) whichever deviations were greatest.[1]

[1] The author is grateful to Prof. A. Harris for polishing the style of this formulation.

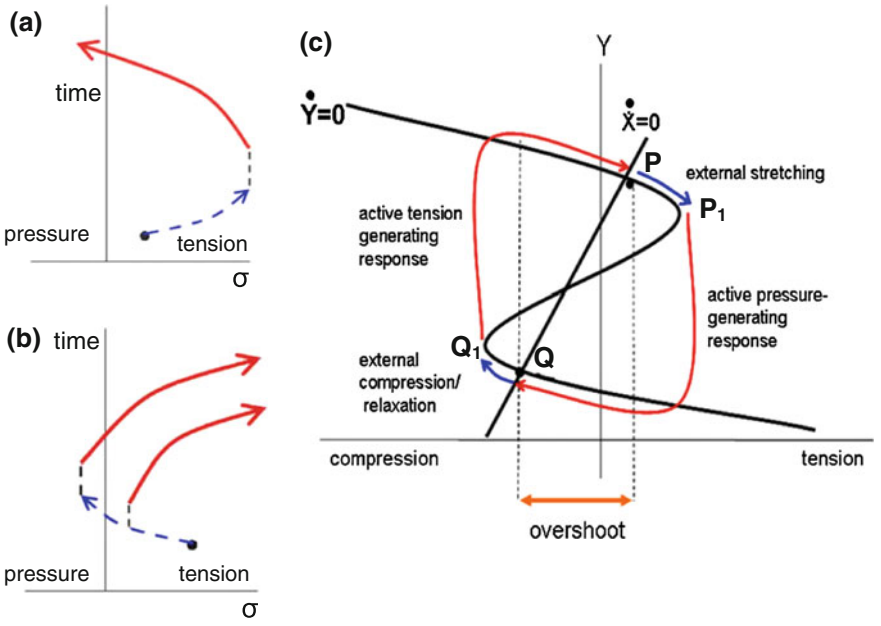

Fig. 4.7 Model of a stress hyper-restoration (*HR*). **a** A response to externally applied tension. **b** Same for tension's relaxation/pressure. In both frames, external perturbations are displayed by *blue dashed lines*, active responses by *red solid lines,* and lag periods by *black dashed lines*. *Horizontal axes* stress, *vertical axes* time. **c** Interpretation of HR response in terms of Van der Pol equations phase portrait. For explications, see text

The diagrams illustrating HR model are presented in Fig. 4.7a, b. In both frames, the stresses are plotted along horizontal axes (tension to the right and compression to the left), while the vertical axes exemplify time. The stresses imposed onto the sample from the outside are shown in hatched blue, whereas those generated as a response within the affected sample in solid red. The first phase of the reaction (action of an outside force) will be qualified as passive while that generated as a response within the given sample as active. The active response develops as a rule more slowly than the passive phase. Both of them can be separated from each other by a certain temporal delay (hatched vertical lines).

4.4 Some Basic Properties of HR Responses

1. *HR reactions are closely associated with auto-oscillations.* In the most adequate way, they may be described by the Van der Pol equations (see Chap. 1) taken in the trigger version:

$$dx/dt = y - kx - b \tag{4.1a}$$

$$\varepsilon dy/dt = -\left(y^3 + ay + x\right) \tag{4.1b}$$

Under proper (not too small) k values, the system has two stable nodules, P and Q (Fig. 4.7c). We associate the slow variable x with mechanical stresses (which are indeed slowly changed during normal development) and the fast variable y with relatively fast phase transitions of the cytoskeletal machinery determining the directions of HR responses. Accordingly, the shifts PP_1 and QQ_1 exemplify external perturbations of mechanical stresses, while the loops P_1Q and Q_1P display the oppositely directed active responses to these perturbations. One can also see that the trajectory going in a clockwise direction from Q_1 to P corresponds to the Belintzev's model in its authentic form (increase in tangential tension in response to relaxation/compression), while the right part of the entire cycle going in the same direction from P_1 to Q corresponds to TIAE. We shall define the first trajectory as the BM loop and the second one as the TIAE loop.

One can easily see that in the two-nodule system, the inclination of x-zero isocline from lower left to upper right is necessary and sufficient for achieving just *hyper*-restoration, that is, the excess of the response over perturbation. Remarkably, such an inclination is also necessary and sufficient for providing stability of the nodules themselves: Under reverse slope, the nodules become unstable so that the system does not exist at all. Thus, the capacity for overshoots is embedded in the very structure of Van der Pol model.

2. *A specific property of HR model is its temporal depth.* All the concepts aiming to "explain" morphogenesis, from Driesch' law to chemo-kinetic and mechano-chemical models, are based on deriving, in this or that way, the next *momentary* state of an embryo from a preceded, also *momentary,* one. On the contrary, HR model operates with the *finite segments of time* [small pieces of "embryonic history" or "metamoments" (Anisov 1991)] to which *the changes* in stress values triggering the oppositely directed overshooting inputs are attributed. Accordingly, HR model is dealing with the first derivatives of stresses, rather than the absolute values.

   These properties are most of all clear if taking for comparison the concept of positional information (PI): while PI associates the "information" about further development with static positions of embryonic structures, HR model ascribes it to their shifts and deformations, modulating stress patterns.

3. *Overshoots may be the properties of the upper structural levels and may be manifested within a restricted range of characteristic times.* As mentioned above, at the molecular–supramolecular events, most of the responses are directed toward restoring homeostasis, while the overshoots are not so pronounced or are lacking at all. Probably, the amplification of responses is a specific property of the upper structural levels. Another disputable question is whether the overshoots are linked with a certain range of characteristic times.

Taber (2009) suggests that they are taking place only within a restricted range of characteristic times typical for morphogenesis in sensu stricto. By his view, the slowest processes associated with growth are characterized by the undershoots, while the fastest contractile processes, contrary to HR model, are going (in terms of stresses) non-oppositely to the inputs. In any case, these considerations do not contradict the morphogenetic role of the mechanisms described by HR model but invite further investigations.

4. *HR responses to stretch and relaxation/compression lead to morphogenetically asymmetric results.* Indeed, the first ones, by producing active compression stresses in response to externally imposed tensions, generate Eulerian instabilities leading to the buckling, folding, etc., of initially flat surfaces, that is, to the increase in dimensionality. On the other hand, the active contractile reactions to the relaxation/compression inputs tend to straighten the samples, to eliminate geometric errors and to provide a long-range mechanosensing. A regular morphogenesis demands perpetual interaction of both components. The first of them can be qualified as creative while the second one as ordering.
5. *The overshoot responses are opened for regulations in many points.* It is but trivial to remind that all the physical forces acting within the living organisms are the matter of detailed multistep regulations. The latter, even if affecting nothing except the rates of certain processes, are enough for providing all the amazing diversity of the living beings.

This should be true for HR responses as well. The factors that might affect them can be divided into two categories: those derived from the model itself and those coming from the outside. The first category relates to parametric regulation. Among these, the most important will be the changes of k and b parameters from the linear Eq. (4.1a). It is easy to see that by changing the inclination of x-zero isocline (by modulating k parameter) or by shifting it in vertical direction (affecting b parameter), one changes the perturbation values required for triggering the next (either BM or TIAE) loop. In the context of TIAE model, this means to change Tch parameter value which is known to determine the number and the lengths of columnar domains. In addition, nothing prevents us to assume that x-zero isocline is itself nonlinear and thus somehow curved; under these conditions, the rates of movement along the lower and the upper slow branches will be different. Modulations of a parameter from Eq. (4.1b) not only provide the very existence or, in the opposite, the absence of oscillations but determines also their amplitudes, that is, the distances between maximally tensed and relaxed/compressed states.

In addition to these possibilities coming from the very nature of HR-involved feedbacks, we may assume an indefinite set of alien factors (resided either within the given organism or coming from the outside) which also affect HR; in the model terms, they should be qualified as introducing new initial conditions. They well may act in quite a robust manner, just arresting the responses in some points of the loop. At the end of this chapter, we shall discuss this problem in more detail as related to cell differentiation.

4.5 Main HR-Based Morphomechanical Feedbacks

Now, we would like to attract the reader's attention to the following remarkable property of HR responses: They are coupled with each other in few standard self-perpetuated modes constructed in such a manner that an active reaction of the part A perturbs a mechanically bound part B in a way providing the next active A response. We call these constructions the morphomechanical feedbacks. Some of these reactions have been already described but still deserve to be represented in the generalized form.

4.5.1 Contraction–Extension Feedback (CEF)

This is a feedback triggered either by contraction or by extension of a certain part (A) of a cell layer with fixed edges (Fig. 4.8A_1–A_4). Under these easily reproduced conditions, the rest part (B) of the layer is deformed in the opposite way (e.g., extends in response to A part contraction: Fig. 4.8B_1) and generates the active stress of the same sign, shrinking part a (Fig. 4.8A_2). As a result, after a number of such

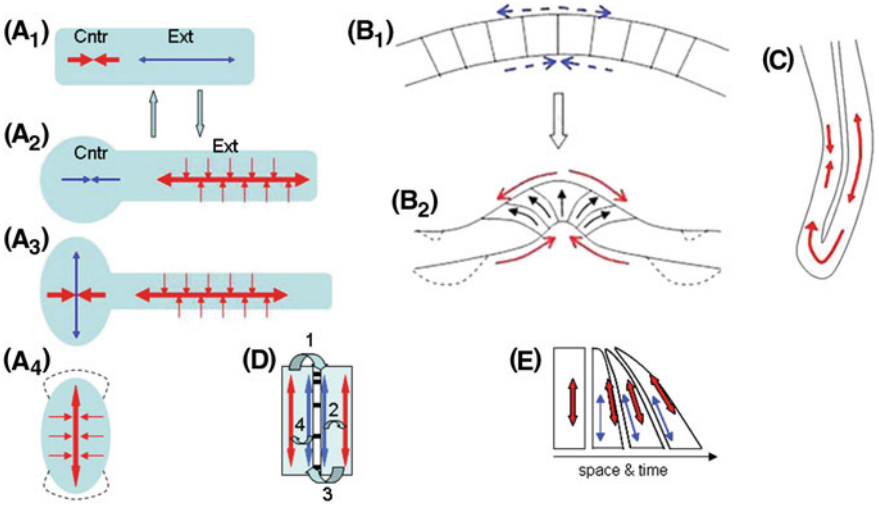

Fig. 4.8 Main morphomechanical feedbacks. $\mathbf{A_1}$–$\mathbf{A_4}$ Expected tissue deformations under the action of a contraction–extension (*CE*) feedback. $\mathbf{B_1}$–$\mathbf{B_2}$ A curvature-increasing (*CI*) feedback. **C** Same feedback acting upon a lip. **D** Extension–extension (*EE*) feedback. *Blue bent arrows* indicate a succession of the unit actions upon each other. **E** Same feedback producing a cell fan with increased inclination of structural elements. *Blue arrows* depict passive deformations and *red arrows* active ones. *Dotted lines* in $\mathbf{A_4}$ and $\mathbf{B_2}$ outline subsequent deformations. *Curved black arrows* in $\mathbf{B_2}$ show the expected flow of cell material from concave to convex side of an arisen curvature

iterations, the cell layer will be stably segregated into two domains, one of them (Fig. 4.8A_1, A_2 Ext) longitudinally extended and the other one (same frames, Cntr) contracted. The latter domain should be passively extended in the transversal direction due to tissue incompressibility (Fig. 4.8A_3). This may switch on a similarly directed active extension which under some mechanical resistance will produce bulges on the opposite poles (Fig. 4.8A_4). In principle, these orthogonal contraction–extension patterns may repeat many times, although in real cases the number of successive steps is almost never greater than two.

The just described Contraction–Extension Feedback (*CEF*) can be defined as the senior mode so far as it is of the greatest wavelength and requires no special perturbations. As mentioned above, the number of domains can increase in the presence of additional local perturbations and/or at small enough values of threshold parameter (Tch). In any case, *CEF* breaks the initial translational symmetry of the cell layer.

A characteristic *CEF* property making it universal is its capacity to act under quite different scales and in different locations, from regular to random. One of the smaller scales where *CEF* is taking place is exemplified by the above-described "push–pull" units of several micrometers' dimensions (Chap. 2 Fig. 2.3(b)), while one of the largest is manifested by segregation of vertebrates' neural system into trunk and head parts (extended to about a mm). As described above (see Fig. 3.8 and the corresponding comments) in stretched explants, *CEF* acts in a sequence on two different levels: first at the single cell level and then on the level of cell collectives: these two rounds amplify each other. Later on, some evidences will be presented supporting *CEF* participation in ooplasmic segregation.

4.5.2 Curvature-Increasing Feedback (CIF)

This beforehand-described reaction can be considered as a modulation of *CEF* for the case when the actively contracted and extended areas are arranged one above the other, rather than in a linear succession (Fig. 4.8B). Curvature-Increasing Feedback (*CIF*) is based upon instability of flat cell layers: It is triggered by slight bending and directed toward its enhancement. Moreover, *CIF* predicts the formation of the opposite sign curvatures on the flanks of a primary fold (Fig. 4.8B_2, dotted contours), that is, the lateral spreading of the folded patterns (see Fig. 4.5 and the corresponding comments). A special case of *CIF* action is exemplified by the dynamics of the so-called lips, that is, densely pleated cell layers possessing a slight common curvature (Fig. 4.8C). Clearly, the combination of active extension of the convex layer with contraction of the concave one will lead to the involution of the tissue via the fold from the convex to the concave side of a lip. By this suggestion, one of the most important morphogenetic processes, the involution of cell material around the blastoporal lip, should be regarded as a direct function of the lip's geometry.

4.5.3 Extension–Extension Feedback (EEF)

This feedback is also a generalization of a number of beforehand-exposed examples (related to perpendicular spreading of cell alignment). However, it deserves to be overtly formulated. Take two adjacent mechanically active structural units (not necessarily single cells) and suggest that one of them (Fig. 4.8D, 1, red arrow) is actively elongated. Then, the neighboring unit will be stretched at first passively (Fig. 4.8D, 2, blue arrow) and then (according to HR model) actively (same frame, red arrow), supporting and even increasing the extension of unit 1. In this way, both units will be actively extended. Next, suggest that instead of two, we have an entire row of units, in which the left one starts to actively extend (Fig. 4.8E). This event will switch on the passive–active extension, spread toward the next units (blue and red double-head arrows), creating the already described dynamic structure, a cell fan. Interestingly, in this case, the spatial and temporal axes coincide with each other, permitting to "read" the temporal history of each individual cell deformation by tracing spatial cell succession from the left to the right. Cherdantzev and Cherdantzeva (2006) suggest that such spatial–temporal coincidence (based upon relaylike cell recruitment into the same morphological transformation) is the main condition of structurally stable morphogenesis.

4.6 Reconstructing Developmental Successions in Terms of HR Model

Now, we want to show that the HR reactions described beforehand separately from each other can be combined into prolonged developmental successions without introducing ad hoc any new initial conditions in each next moment. This is not to say that the latter should not appear at all, but we hope to demonstrate that most of them merely intensify the tendencies that could be derived, even if in a rudimentary form, from HR-associated feedbacks. In other words, our aim will be to present developmental pathways as HR-driven successions of relaxations from an unstable dynamic state toward a structurally stable one (as a rule, with diminished symmetry order) which in some moment becomes in its turn unstable and so on.

Coming now to the developmental events in their chronological succession, we have to notice that at the present time, more or less complete morphomechanical description is reliable only for a period extending roughly from blastula to neurula stages of vertebrate embryos: Our knowledge of active mechanics of both preceding and succeeding events is still quite fragmentary. Nevertheless, we cannot avoid discussing the latter ones, even if in single points only. This section will also include some suggestions on the morphomechanics and evolutionary origin of the main metazoan body plans known as proto- and Deuterostomia. In addition, we shall trace in more detail the morphogenesis of hydroid polyps as a suitable example of the curvature formation. In the end, we review some modern data on the morphomechanical component of cell differentiation.

4.6.1 Morphomechanics of Zygote

The early development of fertilized eggs is associated with a series of quite obvious but still poorly explored mechanical events. One of the most important ones, which can be even regarded as a trigger for the entire subsequent development, is Ca^{2+}-dependent exocytosis of cortical alveoli. Being shadowed by its role in creating perivitelline space, the participation of exocytosis in extensive relaxation of cortical cell layer is usually omitted. Meanwhile, according to HR model, it is this relaxation which should provide the subsequent extensive contraction of the egg surface; in its turn, the contraction is the main driving force of a large set of cooperative events defined as ooplasmic segregation (already discussed to some extent in Chap. 2).

Now, we are interested to explore whether the ooplasmic segregation is somehow associated with morphomechanically based feedbacks. One of up to now few evidences supporting this idea is a spectacular textbook example of ooplasmic segregation—formation of the polar lobe at the vegetal egg pole of several mollusk species. At least in one of them (*Dentalium*), studied more than a century ago by Wilson (1925)—this process exhibits scaling capacities: If deleting an animal egg's fragment, the volume of the vegetal polar lobe will be correspondingly reduced. Hence, the polar lobe proportions are regulated by an integrated system embracing the entire egg. So far as the lobe formation is preceded by a sharp segregation of the egg surface into two domains—the folded one producing the lobe and the rest of the surface remaining smooth (Dohmen and Verdonk 1974), the scaling machinery may be not so different from that described by Belintzev's model for the case of multicellular formations.

The elements of self-organization are even more obvious in ooplasmic movements associated with the formation of dorsoventrality. It is well known that this kind of dissymmetry can be settled not only in the hard regime, requiring specific perturbations, but also in the soft one, under small non-specific fluctuations (Cherdantzev 2003). Let us look what might be the contribution of HR reactions to these events.

In amphibian, egg-specific perturbations are exemplified by the formation of microtubule array spread toward future dorsal side from the oppositely located sperm entrance site (Cha and Gard 1999). In addition to "+" end-directed transport of signaling molecules, the growing microtubules inevitably compress (or at least relax) the future gray crescent area (Fig. 4.9a). The latter's response expected by HR model would be the active animal–vegetal tangential contraction. Owing to this, the central region of the animal surface will be passively stretched and the tension lines gradually dispersed in the ventral direction (Fig. 4.9b, c). As a result, the tension gradient will emerge, going downhill in dorsoventral direction as it takes place in bony fish eggs (see Fig. 3.4d). Its existence is confirmed by the regional curvature differences of the newly fertilized egg surface, as seen in sagittal projection (Fig. 4.9b). Contrary to ubiquitous believing, the egg surface is quite far from being spherical: Its animal part is flattened (indicating the highest tension),

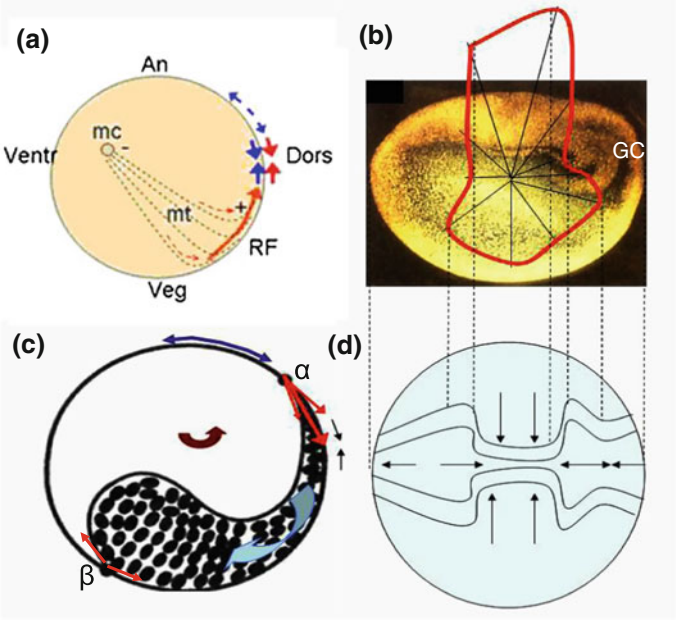

Fig. 4.9 The suggested patterns of mechanical stresses in the cortical layer of newly fertilized amphibian egg. **a** The stress-producing cortical shifts based on +end-oriented vesicle transport along the microtubules (*mt*). *mc* male centrosome. **b** The real (essentially deviated from spherical) shape of an egg in the sagittal projection and a polar diagram of its curvature radii. *GC* gray crescent area. **c** An experimental counterclockwise egg rotation in the gravity field (*brown central arrow*) leads to a clockwise downward leakage of the yolk (*blue arrow*) taking a cometlike configuration due to immiscibility with the endoplasm. Assuming the existence of interfacial tension on the yolk (*black dots*)–endoplasm border, we get an effective summation of the cortical and interfacial tensions in the nodule α (contrary to β), making α similar to the dorsal area of a normal egg. **d** Animal view of an egg depicted in **b** illustrating regional "concentrations" of the tension lines taken reversely proportional to the curvature radii shown in (**b**). *Arrows* display expected movements of the cortical components uphill the tension gradients

while the surrounding dorsal and ventral areas are curved that is less tensed (see diagram apposed to Fig. 4.9b). This indicates the existence of two opposite tension gradients: the animal–dorsal one caused by microtubule pressure and the animal–ventral one just corresponding to that detected in bony fish eggs. Thus, one can suggest the latter to be the primary bearer of dorsoventral polarity not only in fish, but also in amphibian eggs. Assume now, in accordance with HR model, that the mostly tensed animal egg surface tends to hyper-relax by inserting new particles and thus actively extending, while the vegetal (and in particular the gray crescent) surface areas tend to increase tension by internalizing some part of their material. This pattern exactly fits the main tendencies of further development which include not only ooplasmic segregation but also the later events up to gastrulation.

Let us remind now that it is possible to establish dorsoventral polarity in quite unusual location of the amphibian eggs by such non-specific intervention as

rotation in the gravity field. Under these conditions, a new dorsal pole is formed in the rotation plane due to the flow of a heavy subcortical yolk downward: This takes place even if the microtubules have been destructed by irradiation (Gerhart et al. 1981). Hence, the normal mechanism of DV establishment can be completely replaced by the yolk flow. This may be explained by the emergence of a new tensile field including interphase tensions on the borders between yolk-enriched and yolk-devoid compartments in addition to the tensions on the surface. As shown in Fig. 4.9c, due to cometlike shape of yolk-enriched compartment replaced by gravity force, the opposite force nodules are extensively asymmetric, the upper one (α) having much greater tangential component than the opposite (β). As mentioned before, for balancing the tension inequality on the egg surface, the tension lines should be dispersed in $\alpha\beta$ direction, creating thus the tension gradient with the upper pole coinciding with α nodule: This looks to be enough for the latter to acquire the properties of the dorsal embryo pole. We can see that the tension gradients, whatever being their material constituents, are the only elements which are necessary and sufficient for establishing dorsoventral polarity.

4.6.2 Morphomechanics of Cytotomy

Cytotomy is a division of cell body into two parts at the anaphase–telophase stage of mitotic division. From the very beginning of its regular study (performed in most cases in the large blastomeres of cleaving eggs), cytotomy was treated as a mechanical problem: The main aim of the researchers was to detect the force creating the properly located division furrow. Most researchers agree that this force is created by actomyosin ring positioned in the furrow plane by the polar microtubules participating in mitotic cell division. Actually, however, this is but a part of a complicated dynamics involving the entire cortical layer of the dividing cell. The factors coordinating the processes within the entire dividing cell are far from being clear. We want to show that HR model may be of some help here; moreover, we hope to demonstrate that cytotomy and gastrulation share a similar set of morphomechanical feedbacks.

In terms of HR model, the cytotomy can be treated as a drive of initially spherical elastic shell, becoming deformed toward elliptic shape, back to HR of the uniformly spread stresses. The main deforming force is exerted by kinesin-promoted divergent sliding of polar microtubules (Fig. 4.10a, solid red arrows) and is assisted by the insertion of the tubulin subunits to "+" ends of the kinetochore microtubules (same frame, curved arrows). As a result, cell cortex is stretched and centrosomes pulled apart (blue arrows). According to the Laplace law, the tension in the most curved polar cortex regions is decreased while in the flattened equatorial regions increased: This also fits experimental data (Schroeder 1990; White 1990). As a result, a bipolar tension gradient is emerged, going uphill toward equator from both sides. Similarly to above-presented examples, the expected HR response will be in creating the converging flows of cortical material (containing actomyosin

subunits) uphill the gradient, that is, from the poles toward equator (Fig. 4.10b, solid bent arrows). These flows have been indeed observed (Cao and Wang 1990). Being met in the equatorial plane, the flows provide circular contraction (same frame, vertical converging arrows), that is, create the cleavage furrow. Interestingly, in artificially prepared toroid eggs (Rappaport 1961; see also Harris 1990), numerous converging flows are emerged, all of them oriented similarly to those shown in Fig. 4.6j.

While in most cases the cleavage furrows are circular, in cnidarian eggs they are formed as unipolar ingressions and look quite similar to the blastopores. Such a resemblance is far from being superficial: As will be shown later, the gastrulation looks to be driven by the same kind of contraction–extension feedbacks, the blastopore becoming the contraction zone and the suprablastoporal area the extension one.

Importantly, early determination of the blastomere fates taking place in several taxonomic groups (Nematodes, Spiralia) is associated with active spreading of the blastomere surfaces over each other, indicating overshoots in the surface extension in one (Fig. 4.10d) or both (Fig. 4.10e) sister blastomeres. Accordingly, the rotational

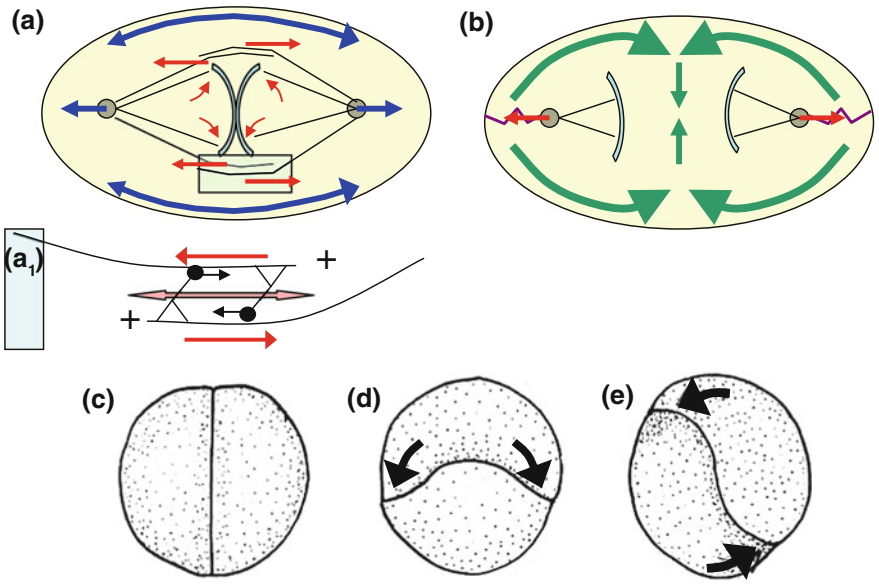

Fig. 4.10 Morphomechanics of cytotomy, applied to early cleavage. **a** Deformation of the cortical layer by kinesin-mediated pulling apart of the polar microtubules. **a$_1$** Detailed presentation of the pulling apart mechanisms. *Mt* microtubules, *k* kinesins moving to +ends of antiparallel microtubules. *Red arrows* depict active events, and blue ones depict passive shifts. **b** Convergent flows of cortical material (*green*) suggested to move uphill the tension gradients born by curvature inequalities. Dynein-mediated shifts of centrioles are shown. **c–e** Radial, bilateral, and spiral patterns of the first cleavage divisions correspondingly as functions of the cortical flows (*dense arrows*). From Cherdantzev (2003) with the author's permission

symmetry order $2 \cdot m$ typical for the radial cleavage (Fig. 4.10c) changes either to $1 \cdot m$ (bilateral cleavage, Fig. 4.10d) or even to 1 (spiral cleavage, Fig. 4.10d). In the latter cases, the mirror symmetry is broken and the egg becomes either right- or left-handed. Although symmetry breaks are regulated in each case by specific factors (up to now not completely understood, see Freeman 1983), the executive mechanisms in each case are associated with membrane flows and unequal spreading of the blastomere surfaces. Noteworthy, these events are lacking when no early blastomere specification is taking place.

4.6.3 Morphomechanics of Blastulation and Gastrulation

4.6.3.1 Evidences for Self-Organization

Most common embryonic shape resuming the cleavage period is that of blastula—a quasi-spherical body with the pressurized cavity (blastocoel) inside. It is of primary importance that for continuing its development, blastula should deviate, at least slightly, from the precisely spherical shape either by its surface curvature, or by eccentric blastocoel position, or (what is the most usual) by both criteria: Precisely spherical blastulae (which can be experimentally produced in sea urchin embryos) are incapable to develop further. It is widely believed that the deviations from spherical symmetry, oriented along animal–vegetal (AV) egg axis, are irreversibly established already during early oogenesis. A simple experiment shows, however, that the morphological asymmetry quite similar to the normal one can be established much later: Perfect "miniblastulae" (their diameters being about 20-folds smaller than the normal ones) with eccentrically located cavities can be obtained from small single- or double-layered explants of the blastocoel roof extirpated from the late blastula or early gastrula embryos (Fig. 4.11a, b). Such "miniblastulae" are so small that cannot capture any traces of the whole egg AV polarity: Their morphological polarity is formed de novo, being a clear-cut example of self-organization. In addition, small invaginations imitating the start of gastrulation but unable to develop further appear sometimes in the multilayered "bottoms" of these formations (Fig. 4.11a, b, pointers). In contrast, the artificially folded explants (Fig. 4.11c) prepared from the same material (see Fig. 4.1c and the corresponding comments) exhibit another kind of asymmetry: Their opposite sides are always unequal, resembling the dorsal and ventral blastoporal lips of amphioxus gastrulae (see Fig. 4.5f_1). Thus, the artificial deformation is enough for changing completely the acquired asymmetry.

By our suggestion, the starting point for morphological differentiation of miniblastulae is the loss of stability of a precisely centered position of the pressurized blastocoel. If indeed the blastocoel or some part of it deviates from concentric position even slightly, its walls will become segregated into the parts of unequal thickness: The smaller the local diameter, the greater will be the stretching stress produced by the pressurized cavity. Accordingly, the mostly stretched part is expected to be most actively extended (either by cells flattening or by their radial

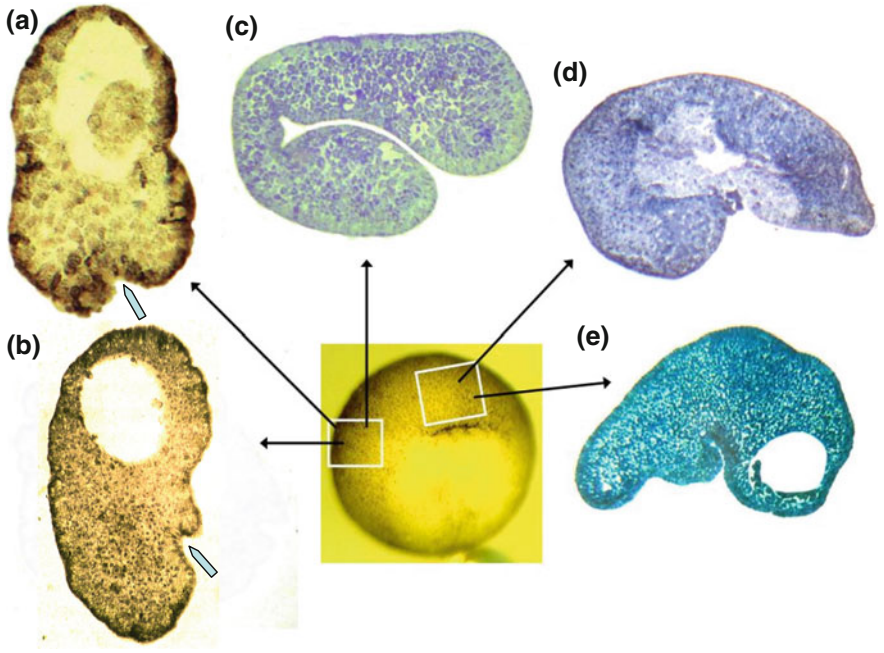

Fig. 4.11 Self-organizing tissue fragments extirpated from the ventral ectoderm (**a**–**c**) or from suprablastoporal areas (**d**, **e**) of *Xenopus* early gastrula embryos. *Pointers* in **a**, **b** are rudimentary blastopores. Fragment **c** was folded after explantation (cf. Fig. 4.1c)

intercalation). In doing this, it will relax/compress the less stretched parts, promoting cell condensation and formation of invaginations within the latter. In other words, a typical *CEF* embracing the entire miniblastula body will be established. Meanwhile, in the folded explants, the same feedback will be established between both sides of the fold, making one of them contracted and the other one (the upper one, Fig. 4.11c) extended. Again, the initial mirror symmetry turns out to be unstable.

And what about inability of miniblastula to proceed a full-scale gastrulation? Does it mean that the latter can take place nowhere except its standard location?

Experiments show that it is not the case: The capacity for far-going invaginations is more or less evenly smoothed throughout the entire SBA: Small explants from any SBA part are easily transformed into "minigastrulae" (Fig. 4.11d, e), some of which produce also the blastocoels, becoming copies of the entire embryos (Fig. 4.11e). This confirms once more the classical results (see Sect. 1.1.2) demonstrating extended self-organizing capacities of induced tissue. Obviously, the role of so extensively studied SBA located inductive centers (De Robertis 2009) is quite far from establishing strict prepatterns. Rather, their action may be described in terms of parameters, increasing the number of permitted pathways without determining their localization.

After demonstrating that both blastulation and gastrulation can proceed under experimental conditions in a self-organizing manner, we may come to a more detailed analysis of normal gastrulation. Our aim will be to present it as a succession of HR reactions, the outcome of each one serving as initial conditions for the next. By taking a broad taxonomic view, we shall divide almost all the types of gastrulation (except those occurred in Cnidaria) into two main classes. The first of them, dominating in Deuterostomia subreign, is characterized by the leading role of the blastopore dynamics, while in that typical for Protostomia, the forces located outside the blastopore play the main role. We define the first way of gastrulation as the active and the second as the passive blastopore mode.

4.6.3.2 The Active Blastopore Mode

For exploring this mode, we take amphibian embryos as the main example and shall analyze the morphomechanics of the blastula–neurula period. To these, we shall add just a few comments as concerning Amniota embryos.

As a starting event, we take the just accounted scenario of miniblastula formation, applying it now to the normal gastrulation (Fig. 4.12a). Our next step will be to consider the rudimentary invagination emerged in the relaxed/compressed area as mechanically active, that is, reacting to the deformation by tangential contraction. The mechanogeometric consequences will be the following. First, because the diameter of the contracted blastopore is much smaller than that of the entire embryo, the blastopore will play the role of a tension nodule, establishing the gradient of tensions around. As argued before (and confirmed, besides all, by sucking experiments, see Fig. 4.4 and corresponding comments), such gradient will promote the blastopore-directed flow of cells. Next, the blastoporal margin will be transformed into a semi-toroid lip, obtaining the intrinsic tendency for equatorial contraction and cells involution (see Fig. 4.8c and the corresponding comments).

The blastoporal lip is never a circularly symmetric body: Its asymmetry, just slightly expressed in lower Deuterostomia, becomes pronounced in most Anamnia species. It is a textbook view that the blastopore asymmetry is in a hard manner specified soon after fertilization. However, as shown in the preceded section, this is not precisely the case: The dorsoventral blastopore asymmetry can be initiated by such a non-specific factor as the gravity force. Similarly, in Teleostei embryos, non-specific mechanogeometry is involved in this specification (Sect. 3.1.2). By following this line, it is easy to demonstrate that the circular symmetry of the blastoporal lip in the presence of mechanical stresses is inherently unstable. The origin of instability is the same as in spherical blastula: Under any local deviation from the uniform circular contraction, the *CEF* will be established along the blastopore circumference, enhancing any small contraction inequalities. The resulted senior mode will be the establishment of a mirror symmetry ($1 \cdot m$) which is identical to the acquisition of dorsoventrality, the site of the main contraction belonging to the dorsal side. Meanwhile, a family of junior modes corresponding to

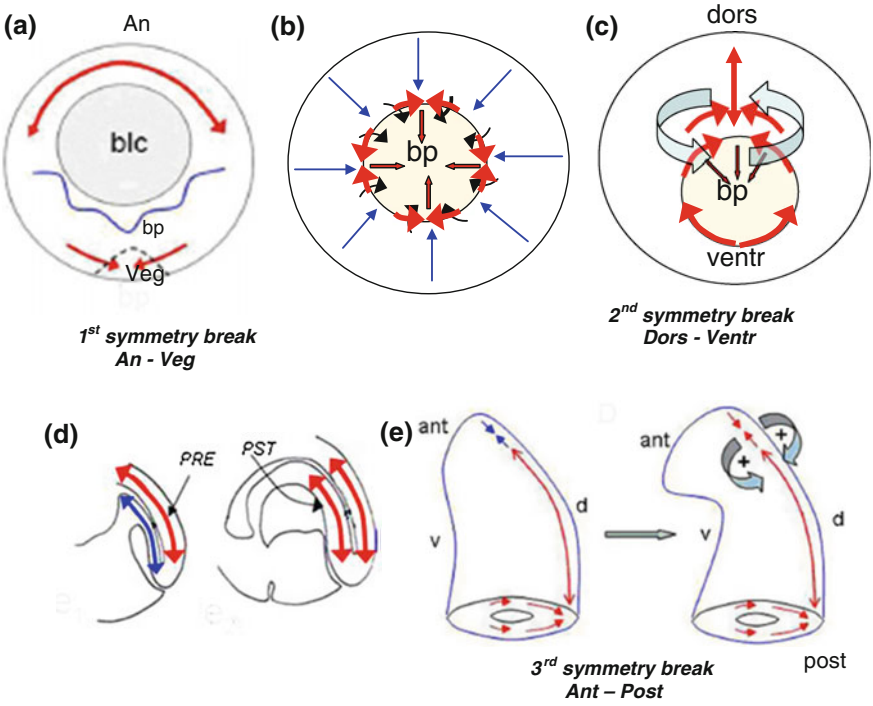

Fig. 4.12 Morphomechanics of gastrulation and trunk–head segregation, as exemplified by amphibian embryos. **a** and **e** Lateral views; **b**, **c** views from the blastopore; **d** sagittal sections. Three successive symmetry breaks creating animal–vegetal, dorsoventral, and antero-posterior axes are outlined. *Blue bent arrows* in frame **c** depict feedbacks between SBA and blastopore areas. In **d**, *PRE* are the preinvoluted and *PST* are the post-involuted parts. For detailed explanations, see text

multi-radial symmetries is also allowed. These ones are exemplified by tentacle whorls (cnidarians and other sedentary invertebrates).

This symmetry break triggers what may be qualified as the main engine of gastrulation: This is *CEF* established between the contracting blastopore and the longitudinally extending (mostly due to convergent cell intercalation) SBA (Fig. 4.12c). The feedback is at work until the gastrulation is completed and provides at the same time axial elongation of the embryo.

Our next aim will be to explore morphomechanical relations established between the pre- and post-involuted parts of the cell material during invagination of the latter. There are good evidences to suggest that these parts are involved in the common extension–extension (*EE*) feedback (see Fig. 4.8d). If indeed the post- and preinvoluted cell layers are detached from each other just after the start of involution, the first of them immediately shrinks, indicating that it was *passively* extended by the apposed part of preinvoluted layer. However, if making this operation somewhat later, the post-involuted layer expands in the longitudinal direction in few seconds, demonstrating thus *active* extension (Beloussov et al. 2006). This succession is just

what is to be expected by the action of *EE* feedback (Fig. 4.12d). This interpretation has been supported by recent experiments (Hara et al. 2013), demonstrating that the leading edge of involuted mesoderm exerts a pulling force of several dozens nN range. Further extensive spreading of post-involuted layer along the inner surface of the blastocoel roof can be interpreted as an overshoot response to its previous passive stretching. In general, extensive inequalities in the simultaneous movement rates between several mechanically bound areas of gastrulating embryos—SBA, post-involuted part, blastoporal surface (Keller 1978; Ignatieva 1979)—should unambiguously produce transitory mechanical stresses indispensable for regulating the entire process of gastrulation.

Gastrulation movements in vertebrate embryos smoothly pass to those usually attributed to neurulation: Just mentioned axial SBA extension will trigger a new *CEF* contour along the dorsal midline with the foremost (future head) region at first passively shrunk and then actively contracted in mid-dorsal direction: This is the third symmetry break, establishing now antero-posterior embryo polarity (Fig. 4.12e).

It is worth mentioning that the second and the third symmetry breaks demarcate two successive periods of development characterized by topologically invariable tensile fields (see Fig. 3.3 and the corresponding comments). Thus, the period between the second and the third breaks is what we call the gastrulation, while the period after the third break relates to neurulation.

Let us summarize now the main experiments supporting the "active blastopore" scenario:

1. Requirement of tangential stretching for the radial cell intercalation in the blastocoel roof is supported by previously (see Sects. 3.2.4 and 3.3.2.1) described experiments on decreasing osmotic pressure within the blastocoel or on relaxing tangential tensions by wedge insertion: Under these conditions, cell intercalation is replaced by reverse cell movements, leading to cell clusterization instead of spreading.
2. Gastrulation movements (both latero-medial cell convergence in suprablastoporal area and involution) immediately stop after relaxing tensions in the suprablastoporal area (Beloussov 1988; Beloussov et al. 2006; Kornikova et al. 2009) although from the viewpoint of "passive" mechanics, the relaxation should instead facilitate involution.
3. Under normal conditions, the bottle-shaped cells forming the early blastoporal lip are flattened in transverse direction, while if being isolated, they flatten isotropically (Hardin and Keller 1988; our observations). This confirms *CEF*-based suggestion that normally the shape of the bottle cells is molded by meridian compression exerted by the latero-medially converged cells of the suprablastoporal area.
4. Isolated semi-toroid blastoporal lip is autonomously contracted in equatorial direction and elongated in meridian one, imitating thus the blastopore narrowing.

4.6.3.3 Morphomechanics of Early Amniota Development

As mentioned before (Sect. 3.1.2), a chicken embryo blastoderm, in order to develop further, should be contracted around its periphery from the very beginning of incubation. The ovoid shape of embryonic shield indicates that the site of its maximal contraction is adjusted to posterior pole. Its positioning is known to be affected by gravity force (Kochav and Eyal-Giladi 1971) and hence by yolk redistribution, probably in a way similar to that taking place in rotated amphibian eggs (see Fig. 4.9c and related comments). In any case, the existence of a single tension nodule at the edge of embryonic shield is enough for triggering *CEF* quite similar to that depicted in Fig. 4.12a; the only differences are that the animal and vegetal poles should be now replaced by the anterior and posterior ones correspondingly and all the cell movements and corresponding stresses will be arranged onto a flat, rather than spherical surface. This change in geometry abolishes a competition between converging cell streams moving now in-plane, rather than along the spherical meridians; this promotes more extensive cell condensation at the posterior pole where the primitive streak is originated (Fig. 4.13a). Due to this, the streak exerts longitudinal compression, visualized by its slightly bent shape (Fig. 4.13b). The area immediately anterior to the streak (Hensen's node) responds to compression by the contraction and immigration of cells, stretching thus (at first passively: Fig. 4.13b, blue double-head arrow) the anteriormost region of the blastoderm (so-called head process). As usually, the stretching triggers the latter's active extension (mediated by convergent cell intercalation) which pushes now backward the primitive streak leading to its contraction and gradual degeneration (Fig. 4.13c). At this stage, the *CEF* contour fully homologous to that shown in Fig. 4.12c is established between the (primitive

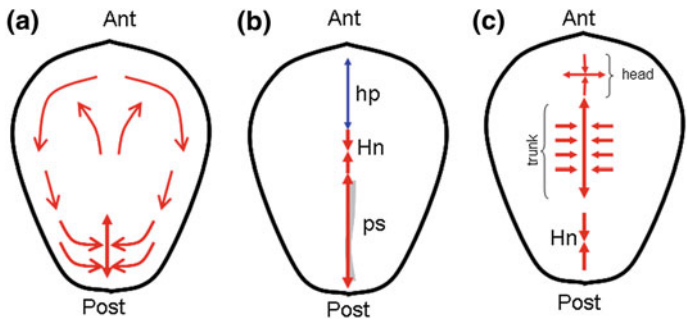

Fig. 4.13 Morphomechanics of early development in Amniota. **a** "Polonaise" cell movements during primitive streak formation, closely resembling those during blastulation of Anamnia embryos (cf. Fig. 4.12a) but arranged now onto a flat surface. **b** Primitive streak (*ps*) exerting a longitudinal pressure indicated by its slight bending (*thick gray line*). *Hn* Hensen's node developing the active contraction response. *hp* head process, being now under passive stretching. **c** Standard active responses in the trunk and head regions (cf. Fig. 4.12e). Hensen's node area and reduced primitive streak (not shown) under pressure. *Ant* anterior pole, *Post* posterior pole

streak + Hensen's node) and the head process. It is amazing to see how the identical morphomechanical feedback contours are retained in so different taxonomic groups in spite of extensive transformations of their visible morphology.

4.6.3.4 Experimentally Induced Deviations from the «Active Blastopore» Chreod

Here, we describe unusual developmental transformations embracing the entire amphibian embryonic body but triggered by quite local disturbance described above as a "remove–replace" operation (Fig. 3.6i; see for details Kornikova et al. 2009). As mentioned, this operation arrests the gastrulation at the stage of the still opened blastopore which then extends abnormally in ventral–dorsal direction. This is, however, far from being the whole story: Under subsequent development, the operated *Xenopus* embryos are transformed into strange tail-bearing bodies with pronounced gill arches much more resembling Amniota embryos at so-called "pharyngula" stage than any stages of Anura development (Fig. 4.14a, b cf. c).

The succession of events triggered by these interventions may look as the following (Fig. 4.14d). The "remove–replace" procedure blocks the medio-lateral convergence–longitudinal extension of SBA, breaking thus *CEF* between this area and the dorsal blastoporal lip. Accordingly, the blastopore ceases to contract actively becoming instead passively shrunk toward the midline due to the lateral pressure exerted by continuing radial cell intercalation in the surrounding ectoderm. This makes the blastopore slitlike and exerts transversal pressure to the ventral blastoporal lip area. As a result, the ventral lip and its surroundings uptake to some extent the role normally played by the dorsal lip and establish somehow abortive but nevertheless distinct *CEF* acting now along the ventral, rather than dorsal embryo midline. Formation of a tail on the ventral embryo midline can be

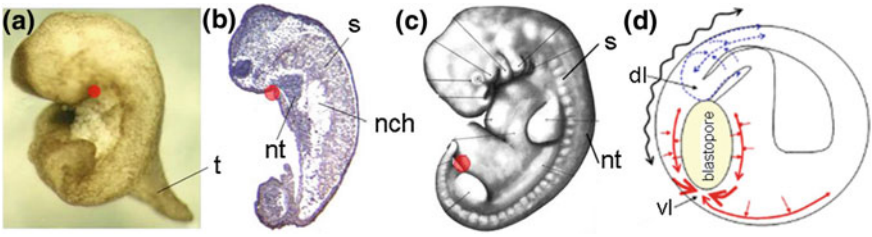

Fig. 4.14 Pharyngula-like monsters (**a** is the total view, **b** is the sagittal section) developed from Xenopus embryos as a result of "remove–replace" procedure, as compared with a textbook image of Amniotes pharyngula (**c**). *Red disks* in (**b**), (**c**) depict positions of the dorsal blastoporal lips. *Nch* notochord; *Nt* neural tissue; *S* somites; *t* tail-like protrusion. *Note* a close resemblance of the overall shapes in spite of largely non-homologous positions of the dorsal blastoporal lips and the main axial rudiments. **d** A draft of RRP-caused stress redistributions. Relaxed stresses are shown by *dotted blue* and those newly emerged by *solid red*. *Wavy line* symbolizes relaxation. *Dl* dorsal lip, *vl* ventral lip of the blastopore

considered as a peculiar result of the overshoot response (a local super-extension) of the mostly extended ventral embryo surface.

So we see that a minimally damaging block of one of the mechanical feedbacks is enough for replacing the normal gastrulation with a strange mixture of developmental tendencies, each of them being separately expressed in another taxonomic group: The formation of pharyngula-like bodies is a property of amniotes, while a passive slitlike blastopore is typical for Protostomia (see below for more details). Note also that in spite of an overall resemblance of the abnormal *Xenopus* embryos and classical pharyngulae, the homologous embryonic structures (dorsal blastoporal lips marked by red circles; neural tissue; somites) are located in quite different positions if measured in the entire body coordinates (Fig. 4.14 cf. a, b and c); hence, the maps of embryonic rudiments and the overall morphology are not strictly bound together. What can be concluded from all of this is that both within the individual and super-individual (taxonomic) scale, the development consists of a restricted number of structurally stable pathways (Waddington's chreods) which can be variously combined and changed by each other due to relatively simple perturbations of tensile fields.

4.6.3.5 Passive Blastopores and Their Evolutionary Predecessors

Try to crumple a sheet of paper for making a round ingression in it: You will see that it is practically impossible. On the other hand, it will be very easy to fold the sheet straightly. This shows us what kind of blastopores can be made by the forces located outside of them: They should be definitely slitlike. Just this way of gastrulation was taken by no less than a half of the animal kingdom, belonging to the Protostomia subreign: They create slitlike blastopores under the action of pushing forces exerted by the multiplied and tangentially spread neighboring blastomeres (Fig. 4.15a).

As compared with the active blastopore mode, such a strategy will result in considerable reduction of long-range tensile fields at the expense of compressive ones. Although the transversal blastopore compression is expected to promote, as usually, its active contraction, the latter will proceed only in transverse directions and to a small extent. At the same time, the antero-posterior elongation of transversely contracted slitlike blastopore will be caused by Poissonian effect (see Box) which is relatively small and produces nothing more than rapidly damped compression forces applied only to the tissues surrounding the blastopore poles (future stomo- and proctodeum) (Fig. 4.15b, cf. c). As a result, the architectonics of the Protostomia embryos very much deviates from that of the embryos with active blastopores. While the latter develop long-range tensile field permitting to create independent (located outside the blastopore) antero-posterior body axis with all of its derivatives, Protostomia embryos are lacking the fields integrating the entire body and have no possibilities to create their main axis anywhere out of the elongated blastopore. A well-known reversion of the dorsoventral Protostomia polarity as related to Deuterostomia is just a consequence of these fundamental morphomechanical differences.

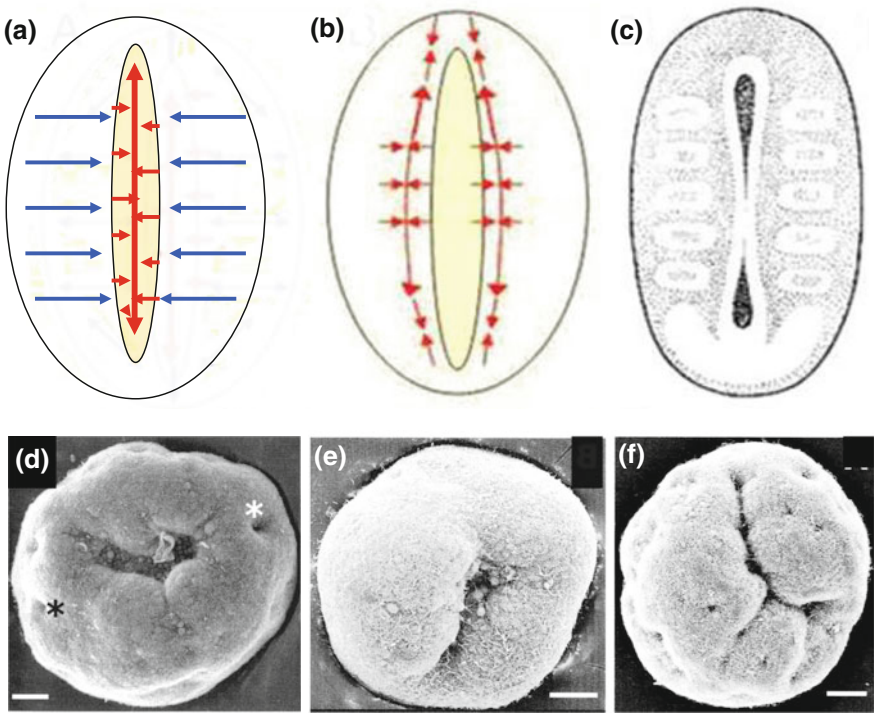

Fig. 4.15 Slitlike blastopores. **a**, **b** Associated morphomechanics (for detailed explanations, see text). **b** A well-developed slitlike blastopore of Peripatus embryo creating antero-posterior embryo axis. **d**, **f** Irregular slitlike blastopores in Anthozoa (*Nematostella*) embryos. *Asterisks* in **d** point to independent ingression of solitary *bottle-shaped cells*. **d–f** Courtesy of J. Kraus

Moving downward along evolutionary scale toward cnidarians (class Anthozoa), we can see quite irregular and variable blastopores consisting nevertheless of several slits (Fig. 4.15d–f). In addition, some solitary sites of the bottle-shaped cell ingressions can be traced (Fig. 4.15d, asterisks). Therefore, in this taxonomic group, some initial attempts to combine both passive and active forms of gastrulation can be traced. By comparing these shapes with the perfect slitlike blastopores of advanced Protostomia, we can see that a proper regulation of the forces located outside the blastopore also was not an easy evolutionary task.

At last, some remarks should be made concerning the polarized larvae of sponges, cnidarians, and some other invertebrates: There are good reasons to suggest that their, in most cases, ovoid shapes are acquired due to the above-described HR reactions leading to increase in the local curvature differences (see Fig. 4.5j–l and the corresponding comments).

4.6.4 Morphomechanics of the Post-gastrulation Events

4.6.4.1 Morphogenesis of the Tubular Anlagen

Formation and further shape complication of tubular anlagen molded from epithelial layers of a uniform curvature belong to the most finely regulated and at the same time widely spread morphogenetic processes. These anlagen are quite various: Some of them, like the heart or the brain, in spite of deformations, retain more or less recognizable tubular shapes; others, remaining tubular, are split in a number of branches—such are glands, lungs, and kidneys; next ones, such as eyes or inner ears of vertebrates, lose in their accomplished state any similarity with tubes. All of them are quite attractive for morphomechanical research, and a number of important results specifying the sources and the distribution of deforming forces have been up to now obtained, in particular as related to heart development (Taber 2006, 2014; Männer 2013). However, the main principles of these force coordination in space and time remain unclear. Is the morphogenesis of tubular anlagen stress dependent? Can HR model be somehow applied to their formation? Our knowledge is still too fragmentary for giving definite responses to these questions, although some hopeful suggestions have been made.

Thus, as argued by Huang and Ingber (1999) and Ingber (2006), a necessary precondition for the epithelial branching during gland formation is the local degradation of the basement membrane which causes pulling apart of membrane edges and hence stretching of the naked part of the cell layer which then forms a fold. By the authors' idea, the stretching facilitates penetration of the mitogens and other fold-promoting factors in the given area. Without denying the role of these particular regulators, we would like to remind that the stretch-promoted active extension is much more general reaction leading to folding even in the absence of any specific factors in the incubation medium. This situation iterates a number of times, each next rupture of the basement membrane assuming to be adjusted to a mostly stretched site (that of the greatest convexity). In this way, a mechanogeometric feedback is established, very similar to that deduced from HR model.

In this and other cases characterized by the complication of the curvature patterns, the main problem is to derive characteristic wavelengths of the arisen folds from non-spatial parameters which can be reduced in the long run to genetic factors (note that the folding patterns in many cases belong to species-specific characters). In a way, this is one of the most fundamental problems of morphogenesis. Let us analyze this situation taking as example the shape changes during bud formation in thecate hydroids. Although, as accounted before, their mode of development is rather specific and in some relations almost unique, the arisen shapes are amazingly similar to mostly ubiquitous ones: For example, a tri-lobe differentiation of *Obelia* hydranth very much resembles the differentiation of embryonic brain into three primary vesicles. This could not take place if the principles of shape formation in thecate were completely different from those in other taxonomic groups.

As mentioned before (Sect. 3.3.2.3), in thecate hydroids, slight successive increases in the curvature relief are strictly adjusted to the extension phases of each next growth pulsation. This means that the tangential cell–cell pressure taking place just at this phase is a direct cause of the curvature increase. But why the characteristic curvature wavelength equals to no less than several dozen cell diameters while almost each individual myoepithelial cell is able to shift radially independently from its neighbors, producing thus much narrower fold? Let us introduce the notion of bending rigidity defined as the minimal distance R separating structural units which are kinematically independent from each other, that is, they are capable of independent radial shifts. Now, our question will be why the wavelengths of the arisen folds always exceed R-s? Note that in the cases considered, the folds are not preceded in one-to-one manner by some prepatterns, for example, by the columnar cell domains of a definite length.

This problem was explored with the use of the model approach (Beloussov and Grabovsky 2003). For achieving generality (because the problem relates to much wider set of species than those belonging to Thecata), the initial shapes were taken as simple as possible, having U-shaped longitudinal projections (Fig. 4.16a) and circular transversal ones. We assumed that each model object consisted of a constant number N of kinematically independent units. The curvature increase was modeled by ascribing to each unit a centrifugal displacement proportional to the vector sum of the lateral pressure forces coming from two neighboring units. In this way, each unit displacement was roughly proportional to the local curvature of the group consisting of three neighboring units.

In general, three categories of parameters were used, taken constant for all of the points of the model sample and for the entire modeling time:

1. Elasticity parameter W defined within the range $0 < W < 1$. It was taken as a measure of the backward (centripetal) shifts of imaging points occurring after each next extension GP phase and ascribed to elastic retractions of the previously deformed mesoglea (Fig. 4.15a, blue inward arrows). It describes the passive component of the process.
2. A group of parameters regulating time–amplitude GP patterns (briefly *GP* parameters) taken as the temporal successions of the extensions and retractions within each GP. They are written as 5-figure sets (e.g., −2, 3, 8, 10, 7), where the positive values display extensions and the negative ones retractions proceeded within each next GP. This group of parameters describes active deformations.
3. Bending rigidity parameter R taken proportional to the distance between two neighboring points able to shift radially independently from each other. Hence, $R \sim 1/N$, where N is the number of kinematically independent units (imaging points).

   The assumed uniform space/time distribution of these parameters permits, in principle, to bind them directly with some genetic factors.

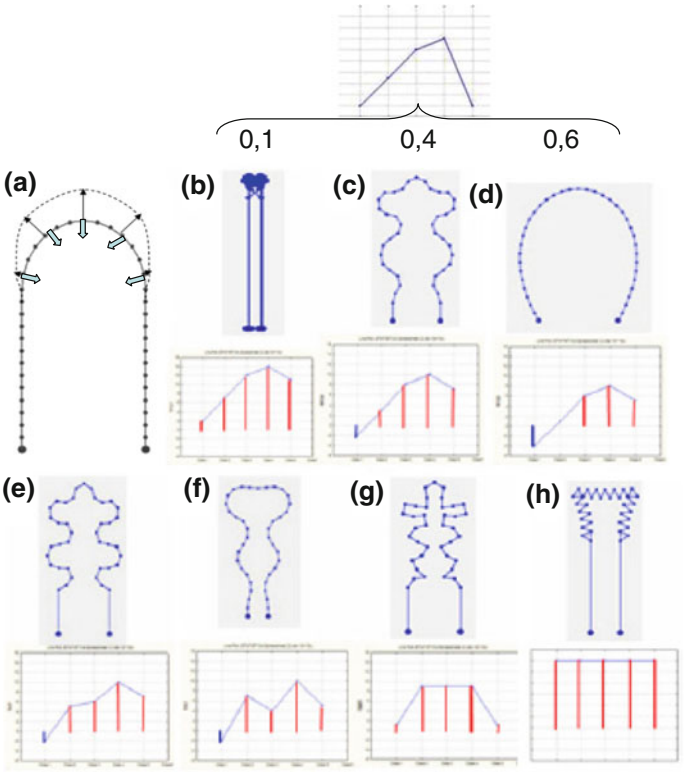

Fig. 4.16 Modeling morphogenesis of *U-shaped* rudiments at different values of *W* and GP parameters. **a** is the starting shape. *Points* are kinematically independent elements. *Dotted contour* is that achieved by the curvature-dependent extensions (*black arrows*). Inward-directed *blue arrows* display elastic retractions described by *W* parameter. Shapes **b**–**d** are generated either under the above-displayed GP pattern and different W values (shown) or under constant $W = 0.4$ and different GP patterns (displayed in the *lower* parts of **b**–**h** frames; *red bars* depict extensions and *blue bars* retractions). Shapes **e**–**g** are also generated under $W = 0.4$ and GP patterns shown below

The most important and unexpected result of modeling was a crucial dependence of the long-range order upon the relative proportions of retractions and extensions, described either by *W* or by *GP* parameters. In both cases, if the retractions were too small, the initial shape was collapsed into a tightly packed bundle of imaging points (Fig. 4.16b). On the contrary, under too great retractions, smoothed contours without any folds were produced (Fig. 4.16d).

Meanwhile, within intermediate range of *W* values (at about $0.35 < W < 0.55$) and GP parameters compatible with moderate retractions, a set of biomorphic shapes (resembling hydroid buds, archenterons with coelomic sacs, brain vesicles of vertebrate embryos, etc., at the same time) could be reproduced (Fig. 4.16c, e–g). Importantly, under non-pulsating regimes (constant lateral pressure), nothing more than quite primitive shapes without long-range order appeared (Fig. 4.16h).

The diminishments of the bending rigidity parameters gave more trivial results, namely a proportional decrease in the folds wavelengths which, however, always remained greater than R values.

It is also worth mentioning that all the shapes depicted in Fig. 4.16 are stable in the sense of remaining unchanged under any number of further iterations. Thus, some shapes remain constant due to their geometry irrespectively of any regulatory agents coming from the outside.

The same kind of modeling was performed with circular configurations, imitating transversal sections of cylindrical bodies. In these cases, also W-dependent properties have been revealed. Within the biomorphic zone of W values, the rudiments segregated into several lobes, their number decreasing with W increase. Notably, the constant numbers of lobes were retained within relatively large zones of W values flanked by the areas of structural instability (Fig. 4.17). Thus, the symmetric 5-lobe patterns reproduced within $0.385 \leq W \leq 0.414 \approx 3 \times 10^{-2}$ W units were flanked from both sides by the intervals $0.381 \leq W \leq 0.384$ and $0.415 \leq W \leq 0.425$ where these shapes were irregularly alternated with asymmetric ones and those with another lobe number (compare perfect 4-lobe shapes at $W = 0.415$ and 0.420 with 5-lobe shapes returning at $W = 0.381$, 0.418 and 0.425). Interestingly, similar successions were reproduced at 10-fold diminished W ranges, indicating scale-free properties (Fig. 4.16, upper line).

We can see that shape formation, even when modeled according to simple rules, setting nothing but mechanical coherency of the rudiments, lateral pressure, and alternation of the forward and backward steps, possesses some non-trivial self-organizing capacities: the alternations of the structurally stable and unstable zones and scale-free (fractal) properties. Another conclusion from the above-presented models is that a coupling of invariable rules of shape formation with dimensionless parameters may be quite constructive. This permits to formulate an approach to the genes–morphogenesis relations inverse to the usual one: to start from formulating shape formation rules, then to explore (by modeling) what kind of dimensionless factors should be taken as parameters for obtaining realistic shapes, and only then to search for concrete genetic factors which may provide the required parameter values.

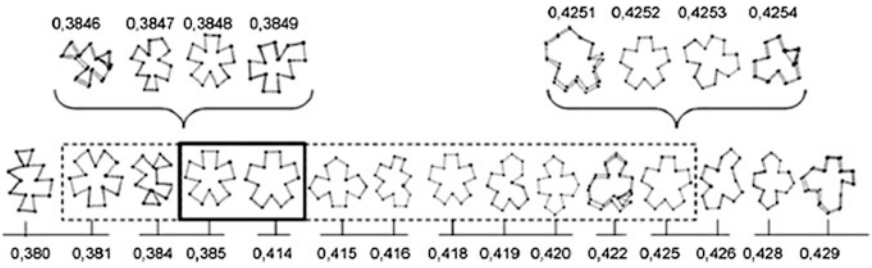

Fig. 4.17 A detailed evolution of a 5-lobe shape under smooth changes in W values. While a stable 5 m shape is permanently reproduced only within the densely outlined W range, it also emerges from time to time within a larger range (*dashed contour*), for example, under $W = 0.418$ and $W = 0.381$. On the other hand, 4-lobe shapes also appear within this range

Non-expected effects of periodic retractions upon the emergence of long-range order in shape formation are of a special interest. It seems plausible that the role of retractions in the mechanosensitive systems is similar to that ascribed to diffusion in chemo-kinetic models. Both agents, each one in its own context, spread local activities over larger spaces, increasing thus the characteristic dimensions of arisen structures. Contrary to diffusion however, which coefficients are as a rule taken ad hoc, the retractions are perfectly measurable entities. Note that we introduce two kinds of retractions: While the passive ones, exemplified by W values, are related to mechanical properties of deformed material, those participating in GPs are active and are assumed to be finely regulated.

Now, what about the role of HR component? True, the above-presented model does not use it overtly, although the auto-oscillating regime employed by GPs is based upon the same Eqs. (4.1a, b) and differs from HR regime only by k parameter values. However, actually HR component is at work at two different characteristic times. At Tch typical for growth pulsations, it is manifested by the rapid active distalward elongation of each cell at the retraction GP phase: This elongation is the active response to the passive cell stretching by the downward-shifted mesoglea and is indispensable for progressive growth and hence perisarc molding. Next, at much greater Tch, it is involved in the regular fluctuations of the longitudinal growth activity between the ectoderm and the endoderm. Namely, at the beginning of each next stem formation, the longitudinal pressure exerted by the ectoderm exceeds that of the endoderm, so that the latter is passively stretched. At the beginning of hydranth formation, the situation is reversed: The greatest pressure is produced by the endoderm. Since the start of hydranth differentiation, the next reversion is taking place: Ectodermal cells are extensively extended in the longitudinal direction, indicating the next round of overlapping activity. Obviously, each next round implies transformation of passive stretching into active extension—a typical HR-involving process. Characteristic times of these rounds are in the scale of hours. These events justify Taber's (2009) suggestion that HR reactions may be bound to specific characteristic times.

4.6.4.2 Metamerization (Segmentation)

Metamerization (also named segmentation) is one of the most ubiquitous but still poorly understood morphogenetic processes consisting in a progressive splitting of embryonic tissues into a number of similar or slightly dissimilar units. Although formally the emergence of iterated zones of gene expression within a syncytial layer of insect eggs may be also attributed to this class of events, we miss it for concentrating on the "classical" cases, exemplified by the formation of somites within the axial mesoderm and of the cartilages in the vertebrate limbs. While in the first case, metamerization gives rise to similar multicellular units, the formation of limb cartilages is characterized by amazing complexity and diversity of the achieved configurations.

In recent studies, mostly dealing with somite formation, the dominating role is played by the so-called clock and wave front model suggested first by Cooke and Zeeman (1976). Taken isolated, this is one of the most refined and "physicalized" embryological concepts. Referring the reader to several comprehensive papers (Pourque 2003), we shall outline here only the main conclusions of the theory. They are in suggesting the existence of a pacemaker (acting on the level of gene expression) sending periodic signals for separating each next (posteriormost) somite from the still non-segmented part of the mesoderm.

The corresponding empirical evidences are somehow controversial: While many of them clearly indicate the presence of periodic signals fitting the times of each next somite separation, recent data have shown that segmentation may well go without any clocks (Dias et al. 2014). Our critique of the clock and wave front model is focused onto its simplifying view of segmentation as a sequential "cutting" of a passive ensemble of mesodermal cells dictated by periodic external signals. As it was briefly mentioned above (see Fig. 3.13l–n and the corresponding comments; for the detailed account, see Beloussov and Naumidi 1983), the cells located to posterior from the last somite are quite far from being passive. Instead, they create transitory bent groups (cell fans) which, while being transversely restricted by surrounding anlagen, can determine the somite lengths without any additional signals: The latter, if present, may only contribute in synchronizing the development of the opposite somite series.

Moreover, laterally fused mesodermal sheets slightly shifted in the longitudinal direction and starting thus to form "out-of-phase" segments were shown to gradually readjust their segmentation patterns, molding, after a period of randomness, perfect common somites (Beloussov and Ivanov 1970). Thus, even if existing, the "clocks" should be able to readjust their rates for providing a proper morphology. This points again to the coordinated (rather than commanded from outside) activity of the cells located behind each last somite. A still lacking theory of segmentation should be based, most probably, on the tendency of a tissue roomed within a compartment of a definite geometry and deformed by external stretching forces to minimize its surface energy. Accordingly, the old models of the liquid column splitting into single drops (Thompson 1942) even if looking at the first glance naïve and crudely mechanistic may imitate some fundamental properties of embryonic segmentation. An interesting attempt to prolong the mechanistic line in somite formation has been recently performed by Truskinovsky et al. (2014). In any case, however, the main problem for somitogenesis as well as for other organs' formation is to reveal the feedbacks connecting externally imposed tensile stresses with the active forces generated within the involved tissues.

As to the formation of limb cartilages, some interesting suggestions were made by Harris and Murray (personal communication). Taking as initial point Harris et al. (1984) experiments on self-clustering of cells seeded onto elastic substrates, the authors regard the increase in the cartilage numbers in the proximo-distal limb direction—one proximally located cartilage (humerus or femur), two cartilages (radius and ulna) in the next to distal part, and many cartilages in the distalmost parts—as indispensable result of progressive flattening of the limb rudiment in the

proximo-distal direction (the flattening itself requires a special explanation[2]). The model elegantly predicts discontinuity of the cartilages (the existence of joints) between the limb parts with different cartilage numbers: The joints correspond to the sites of instability which should necessarily being located between the sites corresponding to different numbers of stable modes. This research trend deserves to be continued.

4.6.5 Morphomechanical Approaches to Cell Differentiation

Even a decade or so ago, the suggestion that cell differentiation pathways can be somehow affected by mechanical forces or cell deformations would sound absurd: How can such refined molecular processes as those involved in the proper transcription of genetic code be dependent upon so crude and essentially non-specific agents as macroscopic mechanical forces? In spite of this prejudice, however, some pioneering works indicating such a possibility appeared still in premolecular era. For example, Lopashov and Stroeva (1964) demonstrated that a flat spreading of the eye vesicle cells triggers their differentiation to the pigment epithelium, while tight packing into the balls of columnar cells shifted their differentiation pathways toward retina. Hence, in this case, the mechanics paves a direct bridge between morphogenesis and cell differentiation. In recent years, a number of influential works appeared describing the role of mechanical factors in cell differentiation in much greater detail. Some of them are briefly reviewed below.

4.6.5.1 Gene Expression Depends upon Deformations of Embryonic Tissues

This line of investigations started from Farge (2003) report that a brief localized pressure applied to the stomodeum area of the mutant Drosophila embryos unable to develop this rudiment was sufficient to remove the developmental block by activating *twist* gene and possibly some others. The activation was achieved by stimulating a regulatory protein, β-catenin, otherwise stored in a subcortical depot, to be transported into cell nuclei. Next, Desprat et al. (2008) showed that the deformation (indentation) of the mesodermal rudiment in Drosophila embryos lacking *snail* gene was enough to restore the normal mesoderm-forming capacities in these defective embryos. Addressing to the representatives of quite other phylum, zebra fish embryos, Brunet et al. (2013) showed that if the expression of a gene *ntl*,

[2] The limb flattening is identical to its surface/volume (i.e., ectoderm/mesoderm) ratio increase, which within the HR framework can be explained in the following way: The proliferating and swelled inner mesoderm exerts the pressure which stretches the overlain ectoderm; it is the latter's overshoot response which provides the increase in the surface–volume ration as well as formation of the apical ridge at the distal cusp.

a homolog of an early mesodermal marker *brachyuri*, is blocked by the arrest of epiboly movements, it can be still renewed by magnetic force stretching the arrested cells. A key link stimulated by exogenous mechanical forces appeared to be the same in all these events: This was phosphorylation of β-catenin by a tyrosine residue. As a result, the interactions between β-catenin and E-cadherins of cell–cell junctions were repressed, permitting thus β-catenin release from junctions to cell nuclei where it activates mesodermal genes.

The role of tissue deformations in positioning different kinds of embryonic tissues was shown also in Kornikova et al. (2010) experiments by bending double SBA explants (sandwiches) extirpated from early gastrula *Xenopus* embryos. In addition to the above-described active curvature enhancement (see Fig. 4.1 and the related comments), the authors observed quite regular geometry-dependent arrangement of cell domains differentiated along either muscular or neural pathways. In non-deformed explants, these domains were arranged in a polar fashion, the neural rudiments shifted toward anterior, while poorly expressed mesodermal ones located posteriorly (Fig. 4.18a–c). At the same time, spherical rudiments were characterized by random patterns (Fig. 4.18d–f), while in the artificially bent ones (irrespectively of the bending direction), somite tissues were arranged as extended arches on the convex (and hence mostly stretched) sides of explants, whereas the compact bulges of neural tissues on the opposite (concave) sides (Fig. 4.18g–k). Taking into consideration that in the explants of a sandwich type, both longitudinal halves are identical, the observed regional distinctions in differentiation pathways can be ascribed only to the differences in local deformations: More stretched areas produce muscular tissue, while the relaxed-compressed ones are biased toward neural fate. Interestingly, in a few spherical explants producing coherent muscular

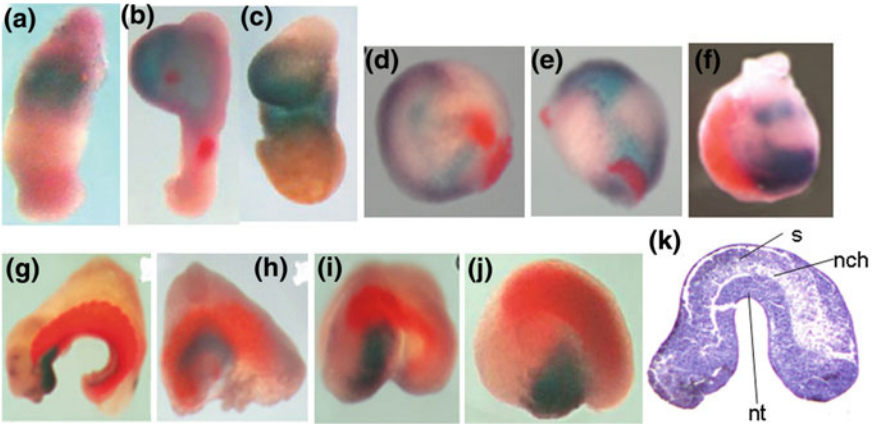

Fig. 4.18 Neuromesodermal patterns depend on the geometry of the suprablastoporal (*SBA*) tissue sandwiches. **a–j** In situ-hybridized samples. *Deep blue* Sox3 (neural marker) expression sites; *Red* sites of muscular actin gene expression, **a–c** non-deformed, **d–f** spherical, **g–j** bent in different directions SBA sandwiches. **k** Histological section of a bent SBA sandwich. *S* somites, *nch* notochord, *nt* neural tissue. **a–j** from Kornikova et al. (2010)

domains, the latter also became arch-shaped and arranged along the periphery, that is, in the most stretched region (Fig. 4.18f). On the other hand, the anteriormost positions of the neural tissue domains in straight explants (Fig. 4.18a–c) are those where the tissue is compressed from behind by the longitudinally extended regions (similarly to what is taking place in normal embryos).

In the context of Brunet et al. (2013) conclusions on the necessity of gastrulation-promoted stretching for differentiation of mesoderm, it would be interesting to know what happens if the gastrulation in *Xenopus* embryos is arrested. A series of previously described experiments (see Fig. 4.14 and the related comments) give the answer: Somite mesoderm is developed in quite unusual locations which are again the most stretched of all (Fig. 4.14b). Similarly, the neural tissue takes most compressed (or at least less stretched) sites. So far as in experimental situations, both stretching and compression stress values definitely deviate from the normal ones, it is worth to suggest that the cells react in a robust manner to the changes in the relative rather than absolute stress values.

4.6.5.2 Effects of the Substrate Geometry and Rigidity

Now, we come to the role of substrate geometry in regulating cell differentiation (McBeath et al. 2004; Hyun et al. 2006; Kilian et al. 2010). The most far-going conclusion from these studies was that "cell shape itself (is) a driving factor in development" (McBeath et al. 2004). True, the links between cell shape (which can be microfabricated by a proper preparation of the substrate) and its differentiation pathway became revealed up to now only in most general outlines. It was stated, however, that for osteogenesis, a proper cell shape is an irreplaceable factor, while soluble agents can be supplanted by stimulating RhoA signaling. The shape may act by modulating localization of GTPase family members, focal adhesion assembly, and cytoskeletal contractility. Recently, a new group of mechanosensing pathways controlling cell geometry has been described (Low et al. 2014). All of this paves a firm bridge between morphogenesis and cell differentiation.

Another related approach is exemplified by a seminal work of Engler et al. (2006) exploring the role of substrate stiffness for cell differentiation. By these data, human mesenchymal stem cells produced neural cells while seeded onto the most soft substrates (0.1–1 kPa stiffness), gave myoblasts when seeded onto substrates of intermediate stiffness (8–17 kPa), and developed into osteocytes while seeded onto most stiff substrates (25–40 kPa). In all these cases, the primary differentiation events were associated with drastic changes in cell morphology: Presumptive neural cells exerted single prolonged protrusions (axons), myoblasts became bipolar, and osteocytes were transformed into flattened disks. These data can be tentatively interpreted if employing the beforehand-discussed model of cell polarization (Sect. 2.10) and taking into consideration that just seeded cells were initially relaxed and tend to self-stretch. By doing this, they exert in different directions the protrusions which compete with each other. Those seeded on the softest (easily deformed) substrates require the longest protrusions for restoring normal tensions;

on the other hand, already their first attempt has more chances to be successful and hence able to inhibit all the others. Accordingly, these cells acquire unipolar symmetry, typical for the nerve cells. With the rise of stiffness, the protrusions' growth rate decreases; so the chances to produce at the same time two opposite ones (i.e., less of all competing with each other) are increased, promoting cell bipolarity specific for myoblasts. At last, for the cells seeded on the stiffest substrate, it is enough to produce, for being properly self-stretched just short protrusions which slightly compete with each other: Accordingly, the number of protrusions can be large, and the cells spread as disks. In any case, we see that acquaintance by the cell a proper shape precedes its differentiation. A recently discovered dependence of stem cell fates on a spatial organization of the niche where they develop (Rompolas et al. 2013) can be interpreted in a similar manner.

4.6.5.3 Mechanical Stresses in Cell Nuclei

Other promising trend has been initiated by the discovery of the prestressed state of cell nuclei (Mazumder and Shivashankar 2010; Chalut et al. 2012). Such state is owed to the activity of the cytoskeleton and is transmitted via nuclear envelope to chromatin (including heterochromatin regions). The centromeric heterochromatin seems to be the primary nuclear load bearer for the microtubule-based forces. As a result, the effective shape of cell nuclei is based upon the balance of external forces exerted by microfilaments and microtubules and intrinsic forces caused by entropic nature of DNA polymers. That permits to regard cell nucleus as a mechanosensor. Most important, the nuclei stiffness was shown to be the smallest and fluidity of lamin scaffold the greatest in non-differentiated cells as compared with those involved in differentiation. By specifying this suggestion, Chalut et al. (2012) distinguish a naïve or totipotent state of stem cells from the primed or predifferentiation one. It is the latter period which corresponds to the maximally decondensed state of chromatin and the greatest softness of cell nuclei. Accordingly, the genome is maximally opened to the action of mechanical forces just in this state.

In tune with these findings, Hersen and Ladoux (2011) suggest that the differences in cell differentiation pathways cultured on soft and stiff substrates may be also based on deformations of cell nuclei: The nuclei of cells placed onto soft substrates are less deformable (more round) than those of flattened cells living onto stiff substrates.

No doubt, today, we are at the very beginning of understanding the role of mechanogeometry in cell differentiation. What however seems to be clear is that differentiation cannot be regarded as a single-step transmission of specific "information" to embryonic cell treated as tabula rasa. Rather, recent data enforce us to accept a SOT view on cell differentiation as consisting of at least two different steps: the parametrically regulated acquiring of competence (i.e., of nonlinear potential relief with a restricted number of stable states) and the dynamically regulated final selection of one of these states. What we know about mechanogeometric events inclines us to attribute them to dynamic factors acting at the second step when the

potential relief is already formed. Under these circumstances, their low specificity may not be a fatal obstacle from achieving a proper final decision, while their close connection with morphogenesis will be of a great value for establishing a proper positioning for each type of differentiated cells. On the other hand, the factors of competence, according to their parametric nature, may well be spatially smoothed and their origin deeply rooted into the developmental history of the given cell or tissue region and supported by a complicated genetic background. Anyway, to elucidate, at least in most general outlines, the relations between morphomechanical feedbacks and gene expression becomes one of the most important but still slightly touched problems of developmental biology. Some of preliminary approaches to this task will be discussed in the concluding chapter of this book.

References

Anisov AM (1991) Time and computer. A non-geometric image of time. Nauka, Moskva (in Russian)

Arshavsky IA (1974) Focus for development: the energy rule of skeletal muscles. Dev Phychobiol 7:291–295

Belintzev BN, Beloussov LV, Zaraiskii AG (1987) Model of pattern formation in epithelial morphogenesis. J Theor Biol 129:369–394

Beloussov LV (1988) Contact polarization of *Xenopus laevis* cells during gastrulation. Ontogenez (Sov J Dev Biol) 19:405–413

Beloussov LV (1998) The dynamic architecture of a developing organism. Kluwer Academic Publishers, Dordrecht

Beloussov LV, Grabovsky VI (2003) A geometro-mechanical model for pulsatile morphogenesis. Comput Methods Biomech Biomed Eng 6:53–63

Beloussov LV, Ivanov EA (1970) Interactions and regulations during segmentation of mesoderm in amphibian embryos. Zh Obsch Biol 31:469–480

Beloussov LV, Luchinskaia NN, Ermakov AS, Glagoleva NS (2006) Gastrulation in amphibian embryos, regarded as a succession of biomechanical feedback events. Int J Dev Biol 50:113–122

Beloussov LV, Naumidi II (1983) Cell contacts and rearrangements preceding somitogenesis in chick embryo. Cell Diff 12:191–204

Beloussov LV, Saveliev SV, Naumidi II, Novoselov VV (1994) Mechanical stresses in embryonic tissues: patterns, morphogenetic role and involvement in regulatory feedback. Int Rev Cytol 150:1–34

Brunet T, Farge E et al (2013) Evolutionary conservation of early mesoderm specification by mechanotransduction in Bilateria. Nat Commun 4:2821. doi:10.1038/ncomms3821

Cha BJ, Gard DL (1999) XMAP230 is required for the organization of cortical microtubules and patterning of the dorsoventral axis in fertilized *Xenopus eggs*. Dev Biol 205:275–286

Chalut KJ, Guck J et al (2012) Chromatin decondensation and nuclear softening accompany Nanog downregulation in embryonic stem cells. Biophys J 103:2060–2070

Cao LG, Wang YL (1990) Mechanism of the formation of contractile ring in dividing cultured animal cells. II. Cortical movement of microinjected actin filaments. J Cell Biol 111:1905–1911

Cherdantzev VG (2003) Morphogenesis and evolution. KMK, Moskva (in Russian)

Cherdantzeva EM, Cherdantzev VG (2006) Geometry and mechanics of teleost gastrulation and the formation of primary embryonic axes. Int J Dev Biol 50:157–168

Cooke J, Zeeman EC (1976) A clock and wavefront model for control of the number of repeated structures during animal morphogenesis. J Theor Biol 58:455–476
Dennerly TJ, Lamoureux P, Buxbaum RE, Heidemann SR (1989) The cytomechanics of axonal elongation and retraction. J Cell Biol 109:3073–3083
De Robertis EM (2009) Spemann's organizer and the self-regulation of embryonic fields. Mech Dev 126:925–941
Desprat N, Supatto W, Poille P-A, Beaurepaire E, Farge E (2008) Tissue deformation modulates twist expression to determine anterior midgut differentiation in Drosophila embryos. Dev Cell 15:470–477
Dias A, Almeida I, Belmonte JM, Glazier JA, Stern CD (2014) Somites without a clock. Science 343:791–994
Dohmen MR, Verdonk NH (1974) The structure of a morphogenetic cytoplasm, present in the polar lobe of *Bithynia tentaculata* (Gastropoda, Prosobranchia). J Embryol Exp Morphol 31:423–433
Engler AJ, Sen S, Sweeney HL, Discher DE (2006) Matrix elasticity directs stem cell lineage specification. Cell 126:677–689
Farge E (2003) Mechanical induction of twist in the Drosophila foregut/stomodeal primordium. Curr Biol 13:1365–1377
Filas BA, Bayly PV, Taber LA (2011) Mechanical stress as a regulator of cytoskeletal contractility and nuclear shape in embryonic epithelia. Ann Biomed Eng 39:443–454
Freeman G (1983) The role of egg organization in the generation of cleavage patterns. In: Alan R (eds) Time, space and patterns in embryonic development. Liss Inc, NY, pp 171–186
Gauthier NC, Fardin MA, Roca-Cusachs P, Sheetz MP (2011) Temporary increase in plasma membrane tension coordinates the activation of exocytosis and contraction during cell spreading. PNAS 108:11467–11472
Gauthier NC, Masters TA, Sheetz MP (2012) Mechanical feedback between membrane tension and dynamics. Trends in Cell Biol 22:527–536
Gerhart J, Ubbels G, Black S, Hara K, Kirschner M (1981) A reinvestigation of the role of the grey crescent in axis formation in *Xenopus laevis*. Nature 292:511–516
Gurwitsch AG (1944, 1991) A theory of biological field. Nauka, Moskva (in Russian)
Hara Y, Nagayama K, Yamamoto TS, Magtsumoto T, Suzuki M, Ueno N (2013) Directional migration of leading-edge mesoderm generates physical forces: implication in Xenopus notochord formation during gastrulation. Dev Biol 382:482–495
Hardin J, Keller R (1988) The behavior and function of bottle cells in gastrulation of *Xenopus laevis*. Development 103:211–230
Harris AK (1990) Testing cleavage mechanisms by comparing computer simulations to actual experimental results. Ann NY Acad Sci 582:60–77
Harris AK, Stopak D, Warner P (1984) Generation of spatially periodic patterns by a mechanical instability: a mechanical alternative to the turing model. J Embryol Exp Morphol 80:1–20
Hersen P, Ladoux B (2011) Push it, pull it. Nature 470:340–341
Howard J (2009) Mechanical signaling in networks of motor and cytoskeletal proteins. Ann Rev Biophys 28:217–234
Huang S, Ingber DE (1999) The structural and mechanical complexity of cell-growth control. Nat Cell Biol 1:E131–E138
Hyun J, Chen J, Setton LA, Chilkoti A (2006) Patterning cells in highly deformable microstructures: effect of plastic deformation of substrate on cellular phenotype and gene expression. Biomaterials 27:1444–1451
Ignatieva GM (1979) Early embryogenesis of fishes and amphibians. Nauka, Moskva (in Russian)
Ingber DE (2006) Mechanical control of tissue morphogenesis during embryological development. Int J Dev Biol 50:255–266
Isaeva VV, Kasyanov NV, Presnov EV (2012) Topological singularities and symmetry breaking in development. BioSystems 109:280–298
Keller R (1978) Time-lapse cinematographic analysis of superficial cell behavior during and prior to gastrulation in *Xenopus laevis*. J Morphol 157:223–247

Kilian KA, Bugarija B, Lahn BT, Mrkisich M (2010) Geometric cues for directing the differentiation of mesenchymal stem cells. PNAS:4872–4877
Kochav S, Eyal-Giladi H (1971) Bilateral symmetry in chick embryo determination by gravity. Science 171:1027–1029
Kornikova ES, Korvin-Pavlovskaya EG, Beloussov LV (2009) Relocations of cell convergence sites and formation of pharyngula-like shapes in mechanically relaxed *Xenopus embryos*. Dev Genes Evol 219:1–10
Kornikova ES, Troshina TG, Kremnyov SV, Beloussov LV (2010) Neuro-mesodermal patterns in artificially deformed embryonic explants: a role for mechanogeometry in tissue differentiation. Dev Dyn 239:885–896
Kossevich IA (2002) Role of the skeleton in determination of branching points in hydroid colonies. Zh Obsch Biol 63:40–49 (in Russian)
Kraus YuA (2006) Morphomechanical programming of morphogenesis in Cnidarian embryos. Int J Dev Biol 50:267–276
Kremnyov SV, Troshina TG, Beloussov LV (2012) Active reinforcement of externally imposed folding in amphibian embryonic tissues. Mech Dev 129:51–60
Landau LD, Lifshitz EM (1976) Mechanics, 3rd edn (Course of theoretical physics S). Pergamon Press, Oxford
Lopashov GV, Stroeva OG (1964) Development of the eye; experimental studies. Israel Program for Scientific Translations, Jerusalem
Low BC, Pan CQ, Shivashankar CV, Bershadsky A, Sudol M, Sheetz M (2014) YAP/TAZ as mechanosensors and mechanotransducers in regulating organ size and tumor growth. FEBS lett 588:2663–2670
Männer J (2013) On the form problem of embryonic heart loops, its geometrical solutions, and a new biophysical concept of cardiac looping. Ann Anat 195:312–323
Mansurov AN, Stein AA, Beloussov LV (2012) A simple model for estimating the active reactions of embryonic tissues top a deforming mechanical force. Biomech Mod Mech biol 11:1123–1136
Mazumder A, Shivashankar GV (2010) Emergence of a prestressed eukaryotic nucleus during cellular differentiation and development. J R Soc Interface 7:S321–S330
McBeath R, Pirone DM, Nelson CM, Bhadriraju K, Chen CS (2004) Cell shape, cytoskeletal tension and RhoA regulate stem cell lineage commitment. Dev Cell 6:483–495
Mizutani T, Haga H, Kawabata K (2004) Cellular stiffness response to external deformation: tensional homeostasis in a single fibroblast. Cell Motil Cytoskelet 59:242–248
Odell GM, Oster G, Alberch P, Burnside B (1981) The mechanical basis of morphogenesis. I. Epithelial folding and invagination. Dev Biol 85:446–462
Pourque O (2003) The segmentation clock: converting embryonic time into spatial pattern. Science 301:328–330
Rappaport R (1961) Experiments concerning the cleavage stimulus in sand dollar eggs. J Exp Zool 148:81–89
Rompolas P, Mesa KR, Greco V (2013) Spatial organization within a niche as a determinant of stem-cell fate. Nature 502:513–518
Schroeder TE (1990) The contractile ring and furrowing in dividing cells. Ann NY Acad Sci 582:78–87
Taber LA (2006) Biophysical mechanisms of cardiac looping. Int J Dev Biol 50:323–332
Taber LA (2009) Towards a unified theory for morphomechanics. Philos Trans R Soc 367:3555–3583
Taber LA (2014) Morphomechanics: transforming tubes into organs. Curr Op Gen Devel 27:7–13
Thompson D'Arcy (1942, 2000) On growth and form. Cambridge University Press, Cambridge
Truskinovsky L, Vitale G, Smit TH (2014) A mechanical perspective on vertebral segmentation. Int J Eng Sci 83:124–137
Wilson EB (1925) The cell in development and inheritance. Macmillan, New York
Wohlfarth-Bottermann K-E (1987) Dynamic organization and force in cytoplasmic strands. In: Bereiter-Hahn J, Anderson OR, Reif W-E (eds) Cytomechanics. Springer, Berlin, pp 154–168

Chapter 5
Morphomechanics of Plants

Andrei Lipchinsky

Abstract Plants operate with tensional and compressive stresses that are extreme by animal standards. These stresses vary sharply on sub- and supracellular scales, but are orchestrated at the organismal level and evolve in a well-defined way during morphogenetic events. Plant morphogenesis is accomplished by localized and anisotropic yielding of cell walls that accommodate turgor-driven extension without losing mechanical integrity. Plant cell walls are connected cohesively into a stress-allocating network enabling mechanical forces to be efficiently transmitted and serve as a long-distance messenger that plays an important integrative and regulatory role. Mechanical forces control the dynamics of both cortical microtubules and phytohormone auxin transporters, the two key players in guiding plant morphogenesis. The onset of organogenetic events in shoots and roots is associated with stereotypical changes in the pattern of tissue stresses. Initiation of leaves, lateral roots, and root hairs can be rationalized within the framework of the concept of stress hyperrestoration.

5.1 An Outline Survey of Self-stressed Plant Architecture and Its Implications for Plant Mechanobiology

It may seem paradoxical that plants with their walled sedentary cells and solid tissue texture generally exhibit greater phenotypic plasticity, the ability more rapidly and profoundly change their development and morphology in response to environmental cues than do mechanically more compliant animals. A clue to this conundrum may reside in the mechanical design of plants whose rigidity comes not just from intrinsic material properties of their elemental constituents, but from the whole structure balancing tremendous tensional and compressive forces internally

A. Lipchinsky (✉)
Department of Plant Physiology and Biochemistry,
St. Petersburg State University, St. Petersburg, Russia
e-mail: alipchinsky@gmail.com

L.V. Beloussov, *Morphomechanics of Development*,
DOI 10.1007/978-3-319-13990-6_5

Fig. 5.1 The phenomenon of tissue tension. On sectioning a turgid dandelion flower stalk lengthwise, the split halves curl outward due to spontaneous elastic extension of the inner tissues and shrinkage of the epidermis. The effect is especially pronounced when the stalk is placed in water. *Left* from Gager (1916); *right* courtesy of Jürgen Köller

generated and orchestrated within the plant body. The outer tissue of many growing plant organs such as coleoptiles, hypocotyls, and young stems is held in a state of longitudinal tension by inner tissues maintained in net longitudinal compression. These stresses can be readily demonstrated by sectioning a turgid axial organ lengthwise, whereupon the split halves curl outward due to spontaneous extension of the inner tissues and shrinkage of the epidermis (Fig. 5.1). The significance of the mutual tension between outer and inner tissues for plant mechanical stability can be appreciated from the fact that upon peeling, many turgid organs lost most of their rigidity and buckle under their own weight; the phenomenon mentioned as early as 1848 by Brücke and explained by Sachs in (1875): "We have here the case of an elastic stiff body consisting of two parts, each in a high degree flexible and by no means stiff; only in their natural connection do the epidermal tissue and internal tissues together form an elastic rigid body" (cit. after Vandiver and Goriely 2008).

In an intact above-ground plant organ, the tensile stress reaches a maximum value near the organ surface and was estimated to be as high as 40 MPa in the outer walls of epidermal cells (Hohl and Shopfer 1992). This stress is equivalent (although opposite in sign) to the pressure on the bottom of a 4,000 m water column. It is therefore clear that to change their form, growing plant organs could just relax—locally take the edge off epidermal tension, allowing the restrained inner tissues to perform passive mechanical work. A body of evidence suggests that this mechanism does underlie the plant morphogenetic machinery, and it is established that a number of environmental and endogenous stimuli can, within minutes, induce metabolically controlled localized and anisotropic yielding of epidermal cell walls. Apart from the rapid changes in plant form, this process has another inevitable, but perhaps not fully appreciated consequence—the change in the pattern of tissue stresses. The tissue stresses are known to play an instructive role in determining the directions of cell growth and the plane of cell division by orienting the microtubule network and by polarizing hormone auxin transport. Therefore, local softening of the epidermal cell walls can result not only in rapid changes in plant morphology

due to passive expansion of inner tissues but can also provoke long-term active growth responses leading to time-dependent progression of shape.

At first glance, high internally generated stresses could compromise plant sensitivity to external mechanical stimuli. In fact, the situation appears to be the reverse. Mechanical stresses, varying sharply on subcellular scales, integrated over the tissues and dynamically orchestrated at the organismal level, imply that the whole plant can be thought of as a far-from-equilibrium hierarchical system with continuous mechanical coupling (Kasprowicz et al. 2011). Such systems are known to exhibit complex mechanical behavior and are very sensitive to external influences, in particular, due to signal-amplifying force transfer through specific mechanically prestressed pathways (Ingber 2003). The ability of plants to perceive extremely weak mechanical stimuli astonished Darwin (1860) who would determine the minimum force required to cause movement of the hair-like tentacles on the leaves of the sundew: "I measured with micrometer several bits of woman's hair … which caused movement and found that under 150th of inch amply sufficed. Of same hair I sent 6 in. to be weighed in London by best balance." The result puzzled Darwin so much that over the next 15 years, from time to time, the great Englishman diligently ascertained its validity, raising the issue only in his correspondence, and first published it only in 1875: "It is an extraordinary fact that … a human hair, 8/1000 of an inch in length and weighing only 1/78740 of a grain (0.000822 mg) … after resting for a short time on a gland, should induce some change in its cells, exciting them to transmit a motor impulse throughout the whole length of the pedicel, consisting of about twenty cells, to near its base, causing this part to bend, and the tentacle to sweep through an angle of above 180° … The pressure exerted by the particle of hair, weighing only 1/78740 of a grain and supported by a dense fluid,[1] must have been inconceivably slight. We may conjecture that it could hardly have equaled the millionth of a grain … A bit of hair, 1/50 of an inch in length, and therefore much larger than those used in the above experiments, was not perceived when placed on my tongue; and it is extremely doubtful whether any nerve in the human body, even if in an inflamed condition, would be in any way affected by such a particle" (Darwin 1875). Darwin also described as intriguing facts that neither water droplets nor heavy rains triggered movement of sundew tentacles, and when a human hair was dragged uninterruptedly across a sundew leaf surface it also excited no movement in the plant, yet resistance from the viscous mucilage was significant. The opposite behavior Darwin found in the closely related to sundew Venus flytrap, in which case only dynamic, but not static loading exerted by a human hair caused the leaf trap to close. In fact, Venus flytrap captures moving insects by an active trapping mechanism, while sundew fastens a prey by gluing it by sticky mucilage.

Now, 150 years after Darwin's seminal experiments, we know that the ability to sense and differentially respond to extremely weak mechanical forces is a common feature of all plants. Specific mechanical sensing underlies perception of gravity,

[1] Sugary mucilage secreted on the sundew's leaf surface in order to attract and glue insects.

one of the most important directional environmental cues that plays a pivotal role in morphogenesis of all plants by providing, in general, the upward growth of their above-ground organs and the downward growth of the roots. Gravity is a unique environmental factor: it is pervasive and acts on all molecules, but its perception cannot occur at the molecular scales since the acceleration of atoms and molecules due to gravity is many orders of magnitude lower than their acceleration due to thermal motion. Gravity sensing must involve large mechanically integrated structures whose gravity-driven displacement is discernible on the background of thermal fluctuations and cytoplasmic streaming. In plants, gravity sensing is explained primarily by the starch–statolith hypothesis, which posits that the sedimentation of dense starch-filled plastids (amyloplasts) activates mechanosensitive ion channels in the endoplasmic reticulum and the plasma membrane, and subsequent ion fluxes trigger a cascade of downstream signaling events leading to differential organ growth. Although there is a large body of evidence supporting this hypothesis, it is instructive to indicate how short the duration of stimulus presentation and how low the threshold acceleration for gravity perception can be. The amyloplast sedimentation rate was determined to be several μm/min (Sack et al. 1986; Massa and Gilroy 2003), while the gravity perception time was estimated to be shorter than 1 s, and within a few seconds after changing the plant's orientation with respect to gravity vector, the cell membrane potential and the cytoplasmic Ca^{2+} concentration can change (Hejnowicz et al. 1998; Behrens et al. 1985; Toyota et al. 2013). What seems even more remarkable is the threshold acceleration perceived by plants in a microgravity environment, estimated to be as low as 1.4×10^{-5} g (Driss-Ecole et al. 2008). Energetic considerations show that in this case, the work done by the gravity force on a sedimenting statolith is about 10^{-23} J, that is two orders of magnitude below the thermal noise ($1/2\ kT = 2 \times 10^{-21}$ J). This suggests that amyloplasts can affect mechanosensitive ion channels in the endoplasmic reticulum and/or the plasma membrane only indirectly, apparently via cytoskeletal network, which probably can integrate forces transduced from all organelles within the cell and amplify these forces in expense of the mechanical energy stored in this prestressed network. In other words, it is not statoliths but the whole cell with its self-stressed architecture appears to be the elemental gravity-susceptible structure (Baluška and Volkmann 2011).

The foregoing data indicate that plants can generate considerable mechanical stresses, and yet are able to sense, interpret, and differentially respond to very small mechanical perturbations. These features and the mechanical design of plants, which allows the forces to be efficiently transmitted at both the cellular and organismal levels, suggest that the mechanical stress can serve as a long-distance messenger and play an important integrative and regulatory role in plant growth and development. Furthermore, since "the form … is a diagram of forces" (Thompson 1917), the mechanical stress cannot be considered just as the regulator of plant development but is also the ultimate driving force for all morphogenetic events. Turning this relationship around, one can see the feedback circuit: The growth changes the pattern of tissue stresses, which provoke further growth response, and so on. This circuit implies that certain morphogenetic patterns can be derived solely

from a mechanogeometrical deterministic cycle without direct reference to genetic and biochemical underpinnings. As a matter of fact, since the time of Johannes Kepler, the greatest minds of humanity have been fascinated and intrigued by geometrical regularities in the arrangement of leaves and other reiterative plant organs (florets, scales, seeds) adopted venerable Fibonacci sequence-related patterns and tried to explain this phenomenon by a simple mechanogeometrical imperative. Currently, the corpus of evidence supporting this tantalizing perspective is rapidly growing, as discussed below.

5.2 Organogenetic and Proliferative Events at the Shoot Apex Are Correlated, but not Coupled, and Are Under Control by a Non-local Master Field

In plants, most morphogenesis takes place post-embryonically as a result of indeterminate growth ensured by self-renewing stem cell populations residing in discrete niches termed meristems. Three basic types of meristems, apical, intercalary, and cambial, are generally recognized. Apical meristems are established at opposite poles of the embryo axis and maintained at the growing tips of shoots and roots throughout a plant's life. The shoot apical meristem (SAM) gives rise to a series of regularly spaced primordia that develop into leaves and axillary buds during vegetative growth and into floral organs during reproductive period. The SAM is a dome-shaped structure consisting of a few hundred relatively small cells organized around two principles: stratification into clonally isolated layers and zonation into histologically and functionally distinct regions (Fig. 5.2).

The characteristic feature of outer layers of the SAM is anticlinal pattern of cell divisions (Fig. 5.2a). This means that as cells divide, new partition walls are formed almost exclusively perpendicular to the meristem surface. As a result, daughter cells remain in their original layer, and the cells within a particular layer are usually clonally related. The layers of the SAM showing this pattern are collectively called the tunica. In most dicots, the tunica consists of two cell layers: The outermost layer (L1) develops into the epidermis; the underlying layer (L2) produces most of the ground tissues and usually gives rise to germ cells. Beneath the tunica lies inner pool of meristematic cells referred to as the corpus (L3). These cells divide in various planes and therefore constitute a three-dimensional cluster of cells rather than a cell monolayer. They initiate the vasculature and adjacent internal tissues. All three layers contribute to the formation of the lateral organs and growth of the stem.

Superimposed on these layers are three zones with different functions and cytohistological traits (Fig. 5.2b). The central zone (CZ) at the summit of SAM harbors several moderately large and vacuolated cells that divide very slowly and take no part in organogenesis. This inert region comprises the most apical cells from each of the clonal layers, so that all shoot tissues can be considered as being ultimately derived from it. The CZ is flanked laterally by the peripheral zone (PZ) and subtended at the base by the rib zone (Rib). Cells of the PZ are small, densely

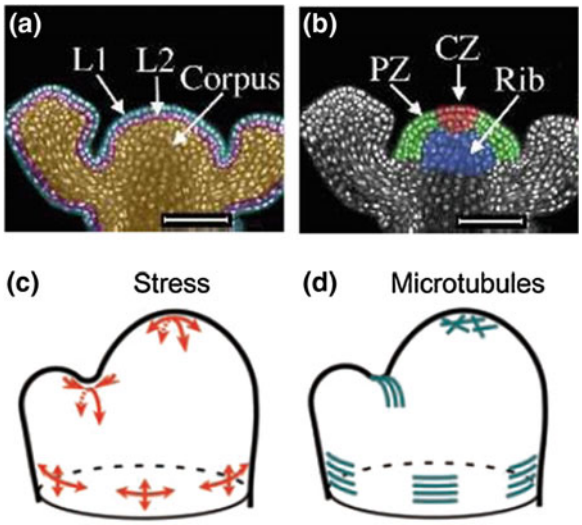

Fig. 5.2 Patterns in the shoot apical meristem. **a** Stratification into three clonally distinct cell layers. Cell divisions in the outer two layers (*L*1 and *L*2) are oriented almost exclusively perpendicular to the meristem surface, giving rise to the neat cell tiers. The remaining cells divide in all planes, making up the bulk of the meristem (Corpus). **b** Three developmental zones. The *CZ* at the summit of the meristem harbors moderately large infrequently dividing initials feeding their derivatives into the *PZ*, where cells are small and divide rapidly, initiating lateral organ primordia. Subjacent to the *CZ* and *PZ* is the rib zone (Rib) characterized by relatively large cells and an intermediate proliferative activity. *Scale bars* correspond to 50 μm. **c** The predicted force fields at the meristem surface. **d** The orientation of microtubules beneath the outermost epidermal cell walls. **a**, **b** courtesy of Elliot Meyerowitz **c**, **d** from Hamant et al. (2008), reprinted with permission from AAAS

cytoplasmic, and divide very rapidly. Periodically, at the proximal (lower) end of this zone, a subset of cells in the inner tunica layer (L2) starts to divide periclinally (parallel to the organ surface) to initiate lateral organ primordia. The rib zone, located beneath the CZ and encircled by the PZ, is characterized by highly vacuolated cells undergoing a dramatic, disproportionate increase in their size preceding each cell division. These cells give rise to the pith of the stem.

The mechanism underlying the stereotyped pattern of cell divisions in the SAM and the significance of this pattern for shoot morphogenesis are unclear. The embryonic allocation of cells into separate clonal layers that form different tissues might give the impression of early lineage commitments of meristematic cells and a causal relationship between the pattern of cell division and proper organ formation. Investigations of cell layer invasion events, however, provided the evidence that the final position of a cell in the SAM, not its clonal origin determines the cell fate; once a cell is displaced from its original layer, it and all its descendants adopt the division pattern typical for the cells in the receiving layer (Sagawa and Mehlquist 1957; Stewart and Dermen 1975; Pohlheim and Kaufhold 1985). A growing body of other evidence indicates that the stereotyped sequence of cell divisions neither dictate nor explain morphogenesis in the SAM. Although usually the appearance of

periclinal divisions in the inner tunica layer provide a way for a primordia bulge to arise and extend in a lateral direction, the mutants in which cell division orientation is randomized due to lacking of preprophase band can still generate leaves at the correct relative position (Traas et al. 1995). In cases where cell division was blocked by γ-radiation (Foard 1971) or with spindle toxin oryzalin (Hamant et al. 2008), leaf initiation proceeded through cell expansion alone. The SAM retains its ability to generate lateral organs in correct spatiotemporal patterns even despite local disruption of cell division patterns by micro-induction of key genes affecting cell-cycle progression: cyclin and cyclin-dependent kinase (Wyrzykowska et al. 2002), phragmoplastin (Wyrzykowska and Fleming 2003), cyclin-dependent kinase inhibitors (Bemis and Torii 2007).

Above data suggest that proliferative and organogenetic events in the SAM are not directly linked to each other. Instead, they may arise independently as a manifestation of a common pattern-imposing field. The involvement of mechanical signals in the putative field seems highly plausible considering the strong dependence of the orientation of cell divisions on the vector of mechanical forces (Linthilac and Vescky 1984; Lynch and Lintilhac 1997). Because cells in the tunica start to divide periclinally often concomitantly with (or just before) the emergence of a new primordium (Cunninghame and Lyndon 1986; Reddy et al. 2004), the local change in the stress may precede and therefore be responsible for correct lateral organ establishment. When cell divisions are prevented, the organ initiation occurs by cell expansion alone, which is under strict mechanical control too (Wymer et al. 1996; Fisher and Cyr 2000; Zhou et al. 2007).

Since the proper positioning of lateral organ primordia can persist despite an abnormal pattern of cell division, the mechanical forces can play an instructive morphogenetic role only if the stress distribution in the SAM is relatively independent of the pattern of cell division. Several aspects of plant architecture and growth physiology suggest that this abstraction can be valid. Plant cells are encased by cell walls connected cohesively into a stress-allocating scaffold allowing more rigid elements to accept more load and the whole system to deform in a coordinated fashion. In the SAM and subtending stem the cell walls of the outer cell layers have the highest load-bearing capacity owing to their high thickness, specific chemical composition, and complex multilayered texture. Therefore, the peripherally located walls can accept most of the stress generated by cell turgor in the bulk of the SAM. Furthermore, the cells located deeply in the rib zone are typically several times larger than cells in the tunica and therefore under similar turgor tend to expand in many times faster. These variations in cell size scaling down from inner to outer cell layers are an additional factor ensuring outward transferring of wall tension. It seems plausible that turgor pressure does not vary significantly between the cells in the SAM since these cells are interconnected by plasmodesmata, plasma membrane-lined channels that pass through cell walls and allow direct cell-to-cell transfer of signals and solutes (Imaichi and Hiratsuka 2007). However, the geometric characterization of cell surfaces in the SAM suggests that cell turgor probably negatively correlate with cell size (Corson et al. 2009). This correlation can hardly affect the strong general trend of outward wall tension transferring. Instead,

the turgor adjustment could be thought of as a homeostatic loop serving to smooth out the local variations in growth rate and supracellular stress distribution that can arise from the disordered nature of proliferating plant tissues (Corson et al. 2009).

5.3 Stress Pattern, Cortical Microtubule Dynamics, and the Orientation of Nascent Cellulose Microfibrils Are Wired into the Circuitry Modulating Plant Morphogenesis

Cellulose microfibrils are major load-bearing components of plant cell walls and their ordered deposition plays a pivotal role in establishing wall mechanical anisotropy. In an elongating cell, the microfibrils are typically deposed perpendicularly to the longitudinal axis, reinforcing the wall in girth and allowing directional growth to proceed under isotropic turgor pressure. Half a century ago, Green (1962) showed that the internodal cells of the green alga *Nitella*, normally reaching several centimeters in length and only a millimeter in width, after treatment with colchicine lose their hoop-like cellulose reinforcement and swells into spheres. At that time colchicine was known as a drug to disassemble mitotic spindle, and Green proposed that similar filaments lie in the cortical cytoplasm of interphase plant cells and affect orientation of newly deposed cellulose microfibrils. The next year Ledbetter and Porter (1963) published the first electron microscopy images of plant mitotic spindle fibers and observed similar tubular structures in interphase cells just beneath the plasma membrane. The observed slender hollow fibers, aptly termed by the authors as microtubules, were arranged in cortical cytoplasm parallel to each other and mirror the orientation of the cellulose microfibrils in the adjacent cell wall. Soon afterward, the correlative alignment between cortical microtubules and newly deposed cellulose microfibrils was observed in many rapidly growing plant cells (Newcomb 1969), and Green's idea that microtubules direct cellulose orientation was entrenched as a central tenet of plant morphogenesis.

After visualization of putative cellulose synthesizing complexes at the plasma membrane (Robinson and Preston 1972) and advent of the fluid mosaic model for biological membranes (Singer and Nicolson 1972), it was hypothesized that microtubules act as molecular rails guiding cellulose synthesizing complexes in the plasma membrane as they extrude cellulose microfibrils into the wall (Heath 1974). Ample evidence supporting this hypothesis has been accumulated over the next decades, although contradictory results have been also obtained (Sugimoto et al. 2003; Himmelspach et al. 2003). The current understanding of the relationship between microtubule orientation and cellulose deposition includes recognition that under normal conditions in most, if not all, rapidly growing plant cells microtubules does provide a spatial template for the movement of cellulose synthase complex, yet some self-organization processes between nascent microfibrils can also occur in parallel in the walls (Baskin 2001). Live cell fluorescent imaging convincingly

showed that cellulose synthase complexes move along linear trajectories that are coincident with the underlying microtubules, and a change in orientation of fluorescently tagged microtubule arrays by light excitation or by application of a drug oryzalin results in a correlated shift in cellulose synthase tracks (Paredez et al. 2006). Recent identification of a linker protein between cellulose synthase complexes and microtubules (Bringmann et al. 2012; Li et al. 2012) has further substantiated Heath (1974) hypothesis that microtubules act as rails on which cellulose synthase complexes move leaving a "trace" of crystallising cellulose behind.

The pivotal role of microtubules in the orientation of cellulose deposition and, thereby, in the establishment of cell growth polarity suggests that plant morphogenesis can be mediated by reorganization of microtubule arrays. Paul Green and colleagues (Hardham et al. 1980) provided the first evidence that one of the earliest events in leaf primordia initiation is a reorientation of cortical microtubules beneath the outer epidermal cell walls, and Hamant et al. (2008) found strong indications that a feedback loop encompassing tissue morphology, stress patterns, and microtubule-mediated cellular properties plays an essential role in shoot apical morphogenesis. Given the dominant contribution of outer cell walls in combating the stress generated in the meristem bulk, the mechanical structure of the SAM is often represented as a shell inflated by uniform pressure from inside (Selker et al. 1992; Hamant et al. 2008; Burian et al. 2013). The stress anisotropy at the shell surface can be deduced from the anisotropy of the surface curvature. Stress is predicted to be isotropic in the axisymmetric summit of the apical dome, but with distance from this singular point it is expected to become anisotropic with maximal tensile stress in the circumferential direction, i.e., orthoradial with respect to the meristem pith (Fig. 5.2c). Using live fluorescent imaging, Hamant et al. (2008) showed that alignment of cortical microtubules beneath the outer cell walls of the SAM generally corresponds to the direction of maximal tensional stress (Fig. 5.2d). At the meristem summit, where stress is predicted to be isotropic, microtubules do not show any preferential orientation and constantly change their arrangement at 1–2 h intervals. At the periphery of the meristem, microtubules align predominantly in circumferential arrays excepting the sites where primordia start to grow up. At the sites of incipient primordia microtubules undergo massive reorientation following transient stress field and reach a new stable alignment in supracellular arrays along the boundary of the primordium protrusion.

To test whether microtubule orientation will follow the direction of maximal tension when the stress field is modified experimentally, Hamant et al. (2008) designed cell ablation assays. Mechanical simulations predict that after ablation of a small patch of the epidermal layer the lines of maximal tension would arc around the wound. In the first series of ablation assays, the target cells were located within the CZ of the meristem, where cell wall mechanical properties and tensile stress were initially nearly isotropic. Within several hours after ablation, microtubules in cells surrounding the ablation site aligned circumferentially with respect to the wound. This result is consistent with the hypothesis that microtubules respond to mechanical stress by reorienting themselves parallel to the direction of maximal tension, although it does not rule out the alternative explanation that the observed

microtubule rearrangement is induced by a biochemical wound signal. To test the latter scenario, Hamant et al. (2008) proceeded the experiments with cell ablations in the boundary domain between the meristem and the growing primordia, where initial stress was predicted to be strongly anisotropic due to saddle-shaped tissue geometry. In contrast to CZ ablations, the ablations in the boundary region resulted in a lack of microtubule reorientation in neighboring cells, or in a delay of reorientation lasting 7.5 h or more. This weak response is difficult to explain by a biochemical wound signal which should trigger a similar response irrespectively of whether the ablation affected the boundary domain or the CZ of the SAM. On the other hand, the observed weak response matches the predictions based on the assumption of stress-dependent microtubule rearrangement since the stress field generated by the ablation in the boundary region along the primordium protrusion should be in competition with the strong stress normally occurring in this saddle-shaped domain. As a final approach, the authors applied force to the meristem directly by squeezing it with two Teflon blades. After this manipulation, compressed cells reoriented their microtubules along the blades, in parallel to new maximum stress direction.

The above results consolidate the idea that microtubule dynamics, microfibril orientation and stress pattern can be coupled in a regulatory loop modulating plant morphogenesis. This loop provides a positive feedback for differential growth (Hamant et al. 2008; Uyttewaal et al. 2012). A positive type of growth feedback implies that although this regulatory loop cannot directly account for the primary events underlying primordia initiation, it can promote the subsequent progression of primordia shape. Assume, for example, that a group of cells in some region of the SAM exhibits an enhanced growth leading to the formation of an incipient bulging. This bulging solely due to its geometry would result in the generation of extra tension along the contour encircling the bulging. This tension would reorient the microtubules arrays to arc around the bulging, and congruent realignment of cellulose microfibrils would induce anisotropic cell expansion, amplifying initial growth-rate gradients. This would increase the slope of protrusion curvature that would induce the next round of stress-mediated microtubule reorganization with further strengthening of the local outgrowth. This speculative scenario is consistent with the decreased growth heterogeneity observed at the SAM after oryzalin-induced depolymerization of microtubules (Hamant et al. 2008) and in mutants impaired in the microtubule-severing protein katanin (Uyttewaal et al. 2012). In both cases, the spatiotemporal pattern of primordia initiation did not seem to be affected, yet the differential growth was attenuated and the crease between the meristem and primordia did not formed.

The fact that depolymerization of microtubules did not prevent proper primordia initiation indicates that the feedback loop involving stress-dependent microtubule reorientation is only one of the regulatory mechanisms incorporated into the robust machinery of plant morphogenesis. The spatiotemporal regulation of organ initiation is thought to depend largely on the polar transport of the plant hormone auxin (Reinhardt et al. 2003a; Traas 2013). When auxin transport is disturbed, organ initiation is often severely affected or even arrested. Importantly, recent studies outlined below suggest that mechanical forces act as principal directional cues to control not only microtubule orientation but also auxin transport.

5.4 Stress-Dependent Polarization of Auxin Transporters Is Pivotal in Spatiotemporal Patterning of Organ Initiation at the Shoot Apex

Auxin is a versatile regulator of plant development, the hormone with strong context- and dose-dependent morphogen character that affects nearly all aspects of plant life. Derived from tryptophan, auxin is reminiscent of serotonin, and some parallels between auxin and serotonin functions have been noted (Esser et al. 2006; Baluška and Mancuso 2013). In growing plant tissues, the auxin concentration field is shaped by the unique transport system which provides auxin movement from cell to cell in a polar manner, often against its concentration gradient. The weakly acidic nature of auxin (pK 4.75) implies that at moderately low pH (<5.0) characteristic of growing cell walls, a certain fraction of auxin exists in the protonated lipophilic form that can readily diffuse through the cell membrane into the cell. In addition to simple diffusion, in some tissues auxin influx is facilitated by the AUX/LAX family of membrane proteins. Inside the cell, owing to the neutral cytosolic pH (pH $\sim$ 7.0), auxin appears effectively "trapped" in the form of negatively charged polar ion that is unable to freely cross the lipid bilayer. Two groups of transmembrane transporters mediate auxin efflux: (1) the PIN-FORMED (PIN) protein family and (2) members of multidrug resistant/P-glycoproteins subfamily of ABC (ATP-binding cassette) proteins. Although in certain types of cells all transporters mentioned above show asymmetric distribution within the cell membrane, it is only in the case of the PIN proteins that polar targeting is a typical feature, and these proteins are regarded as the major determinants of the directionality of cell-to-cell auxin flow (Grunewald and Friml 2010).

The polar cellular localization of PIN proteins is a dynamic outcome of their constitutive cycling between the plasma membrane and endosomal compartments. This process is profoundly influenced by various endogenous and environmental directional cues, among which the preexisting pattern of auxin concentration plays a prominent role. However, how the supracellular landscape of auxin distribution can modulate the allocation of PIN proteins within the boundaries of a given cell is largely unclear. Heisler et al. (2010) proposed that the intracellular trafficking of PIN proteins is navigated according to the stress field perceived by the membrane of a responding cell and generated due to auxin-mediated differential growth of neighboring cells. Auxin promotes plant growth primarily by activating loosening of cell walls. Therefore, the walls of a cell with a higher auxin concentration yield more readily, transferring turgor-induced stresses onto the walls of adjacent cells. Given the fact that an increase in membrane tension stimulates exocytosis, while a decrease in cell surface stress promotes membrane internalization (Fricke et al. 2000; Meckel et al. 2005; Proseus and Boyer 2005; Zonia and Munnik 2008), it seems plausible that perception by a cell of the expansion of its neighbor can propel outgoing traffic of membrane constituents, causing the plasma membrane adjacent to the expanding neighbor to accumulate PIN proteins.

To explore the above hypothesis, Heisler et al. (2010) surveyed the subcellular distribution of the fluorescently tagged PIN proteins in epidermal cells of the intact SAM and in SAMs subjected to a variety of treatments that affect tissue stresses. It was observed that PIN proteins are usually concentrated on cell sides that are parallel to the predicted direction of maximal tension. As the first treatment to affect tissue stresses, Heisler et al. (2010) used cell laser ablation, the approach similar to that used in the work of Hamant et al. (2008). It was found that in cells adjacent to ablation sites the ablation induced a subcellular relocalization of PIN proteins to the membrane domains farthest away from the wound. This response was not prevented by auxin transport inhibitor (NPA) or by auxin analog (2,4-D) that freely diffuses between the cells, indicating that the cell polarization cannot be accounted for by auxin concentration gradients. To elucidate whether the PIN relocalization was associated with microtubule rearrangement the authors examined PIN behavior in the SAM after depolymerization of the microtubules. The results showed that that ablation-induced PIN relocalization was generally maintained in the absence of microtubules, although at certain regions of the plasma membrane (particularly, near high-stressed cell vertices) PIN distribution was broader after oryzalin treatment than before. This implies that microtubules are not necessary for ablation-induced PIN relocalization, yet they can contribute to this process. This inference is consistent with the findings that cytoskeletal elements ensuring PIN trafficking are microfilaments and not microtubules (Geldner et al. 2001). The contribution of microtubules in ablation-induced PIN relocalization can be explained by the feedback loop between microtubule dynamics and mechanical stresses discussed above, which amplifies stress heterogeneity and thereby can indirectly promote the targeting of PIN proteins to the most tensed cell sides.

Interestingly, PIN proteins in epidermal cells of both intact and laser-wounded meristems are generally concentrated in membrane domains that are parallel to the predominant orientation of cortical microtubules (Heisler et al. 2010). This correlation was observed, in particular, in cells at the tip of the meristem dome where the epidermal tension is largely isotropic and microtubules rapidly change their orientation. In this respect, it is pertinent to note that at the meristem summit the tangential stress is isotropic only at supracellular scales (due to constant curvature of meristem surface), but it can be strongly anisotropic within individual cells (due to peculiarities of cell geometry).

Above data suggest that despite the dynamic behavior of both microtubules and PIN proteins in the SAM, they arrangement is under control of a common upstream regulator, presumably biomechanical in nature. To pursue this hypothesis further, Heisler et al. (2010) altered mechanical status of meristematic cells by treating them with isoxaben, an inhibitor of cellulose biosynthesis. The authors reasoned that if the addition of load-bearing cellulose to growing cell walls is prevented, the stress levels for existing wall components should increase. Consistent with this proposal, it was found that isoxaben treatment induces hyperalignment of both PIN proteins and microtubules to predicted maximal stress direction. More recently, Nakayama et al. (2012) employed an alternative strategy to modify the mechanical stress in cell walls of the SAM involving osmotic manipulations. The authors found that in

hypoosmotic environment, when cells absorb water and inflate, thereby increasing wall tension, the amount of PIN proteins in cell membranes increases, whereas in hyperosmotic conditions, when cells deflate and wall stress relieves, massive internalization of PIN proteins occurs. The authors provided the evidence that although the hyperosmotic loss of plasma membrane-localized proteins in the SAM is a common phenomenon, PIN proteins respond to osmotic perturbations particularly sensitively. In order to validate the involvement of mechanical factors in PIN relocalization, Nakayama et al. (2012) modified biophysical state of the SAM also by external force applications, membrane-interactive chemical treatments, and growth inductions. The changes in PIN intracellular distribution observed after these assays substantiate the notion that PIN turnover is under control of mechanical forces.

The polar localization of PIN proteins correlates with organogenetic events. It has been shown that in the epidermal cells of the SAM, PIN proteins orient predominantly toward the sites of primordia initiation and externally supplied auxin can induce primordia formation at the site of hormone application (Reinhardt et al. 2000, 2003a). This implies the existence of a morphogenetically relevant feedback loop between auxin distribution and its transport. The data cited above suggest that auxin can feed back on its own flux by causing differential cell growth and thereby modifying supracellular stress pattern. Computer simulations have shown that such a mechanism would be able to promote the primordia growth and generate realistic phyllotactic patterns (Heisler et al. 2010; Jönsson et al. 2012). Although at first sight this model is just a mechanistic version of numerous chemically based morphogenetic models, it is more general and allows cells to rapidly integrate information not only from their nearest neighbors, but also from more distant cells about auxin gradients, mechanical perturbations, organ geometry, and other factors that modulate growth. Nevertheless, recent analysis suggests that none of the published models can explain patterns of auxin fluxes observed in plant meristems in a self-organized manner (Van Berkel et al. 2013). This implies that there is an extra level of control of both auxin fluxes and morphogenetic events. Furthermore, the idea that some unidentified mechanism (presumably also based on the tissue mechanics) can maintain phyllotactic patterning in the absence of auxin/PIN-based regulatory loop was recently proposed on the grounds of a detailed characterization of auxin transport mutants (Guenot et al. 2012).

5.5 Expansins—Stress-to-Strain Actuators that Play a Preeminent Role in Plant Morphogenesis

The involvement of the mechanical stress as a shared element in both well-established morphogenetic circuits (encompassing PIN relocalization or microtubule reorientation) suggests that stress modulation can alter developmental program. The most convincing evidence to support this hypothesis comes from the finding that transient induction of cell wall-plasticizing proteins belonging to the expansin superfamily can

trigger unscheduled development of the leaf (Pien et al. 2001). Expansins are cell wall proteins implicated in the control of plant growth as primary agents catalyzing wall stress relaxation (McQueen-Mason et al. 1992; Cosgrove 2000). They do not interact specifically with proteins and nucleic acids and, therefore, can affect morphogenesis only through patterning the stress field. Expansins act as principal downstream effectors that terminate cascades of biochemical events initiated by auxin and other key plant growth regulators.

Although molecular mechanism of expansin action is uncertain, the weight of evidence indicates that expansins increase cell wall extensibility and relieve wall tension by loosening the hydrogen bonding between cellulose microfibrils and matrix polysaccharides that tether the microfibrils in the wall (Yennawar et al. 2006; Lipchinsky 2013). Expansin loosens the wall in a characteristic pH-dependent manner ($pH_{opt} < 4.5$). Stimulation of plasma membrane H^+-ATPase that pumps protons in the wall is the most rapid and prominent metabolic effect of auxin, which enables expansin activation and turgor-driven cell enlargement within a few minutes after hormone challenge. Not only extracellular pH but also the abundance of expansins in cell walls is a rate-limiting factor for expansin-mediated wall loosening (Link and Cosgrove 1998). Consistently, auxin induces wall relaxation and cell enlargement not only by acidifying the extracellular space, but also by enhancing expansin gene expression (Hutchison et al. 1999; Catala et al. 2000). Given the pivotal role of auxin flows in specifying the sites of leaf initiation (Reinhardt et al. 2003a), it is not surprising that accumulation of auxin-inducible expansin transcripts is predictive for the emergence of leaf primordia (Reinhardt et al. 1998). This, in turn, suggests that local administration of expansin can be used a physiologically sound tool to explore the role of mechanical stresses in spatio-temporal control of leaf initiation. In this line of inquiry, Pien et al. (2001), using an inducible promoter system, found that transient local induction of expansins in the SAM can initiate a program of development generating leaves that, at the level of overall morphology and histology, are indistinguishable from normally forming leaves. This finding corroborates earlier study of Fleming et al. (1997) demonstrating the emergence of leaf-like organs initiated by local application of expansin-loaded microbeads to the meristem surface. The organs induced in the latter case had several important morphological and gene expression characteristics of young leaves, but were devoid of vascular bundles, have indented tip and did not developed into phenotypically normal leaves. It seems that the abnormal morphology and histology of these aberrant structures provide a basis for understanding the role of mechanical forces in plant morphogenesis and deserves due attention.

The studies under consideration (Fleming et al. 1997, 1999; Pien et al. 2001) were performed on tomato plants. In tomato, as in many other plants, leaves are initiated in an orchestrated pattern, phyllotaxis, with the divergence angle between consecutively issued primordia practically indistinguishable from the golden angle ($2\pi/\varphi^2 \sim 137.5°$). The constant divergence angle means that when the positions of two most recently emerged primordia are known, the positions at which the successive primordia will normally arise can be predicted. Following Snow and Snow (1932), leaf primordia that have emerged are designated P1, P2, P3, and so on, in

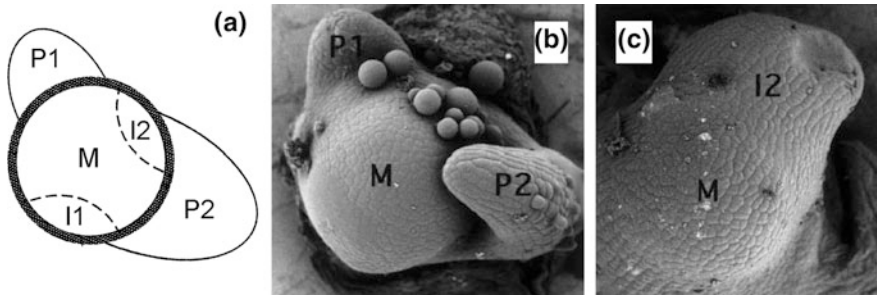

Fig. 5.3 Expansin-induced morphogenesis. **a** Schematic representation of a tomato apex with spiral phyllotaxis. The *bold circle* delimits the apical meristem (*M*). The positions of the youngest and the second youngest primordia (*P*1 and *P*2, respectively) can be used to predict the sites of next scheduled primordia emergence (*I*1 and, subsequently, *I*2). **b** Overview of a meristem after the placing of expansin-loaded microbeads onto the *I*2 position between *P*1 and *P*2. **c** Unscheduled primordium induced by topical expansin application at the *I*2 site and marked by an abnormal indented tip. From Fleming et al. (1999), with kind permission from Springer Science and Business Media

order of ascending age, while the groups of cells that are specified by location of P1 and P2 to be recruited into future primordia are designated I1, I2, and so forth, in the expected order of outgrowth (Fig. 5.3a). Fleming et al. (1997, 1999) demonstrated that local alteration in epidermal cell wall extensibility by topical application of expansin can induce out-of-sequence primordia emergence. More specifically, when expansin-coated resin microbeads were placed on the meristem surface on the I2 position, the formation of primordium-like structure occurred at that site, and the emergence of a primordium at position I1 was suppressed. The organs generated at I2 position had several essential characteristics of normal leaves: They were green, produced normal trichomes, and had intact internal tissues. Even at early stages of bulging, unscheduled organs grew without overt increase in cell size, suggesting that expansin-induced expansion was tightly coupled with cell division. The primordia expressed the Rubisco protein previously shown to be a positive marker for leaf differentiation and a negative marker for the apical meristem. Furthermore, the unscheduled organs functioned as leaves in the sense of developmental interactions: Following precocious formation of I2 primordia, the handedness of subsequent phyllotaxis was reversed, and this shift can be readily explained by the fact that the suppressed "nomogenous" I1 primordium and I2 outgrowth which appeared instead are positioned on different sides with respect to P1. Thus, after the formation of I2 structure, the positioning of the subsequent leaves was readjusted in such a way that new leaves arose in the largest available space again.

Although expansin application triggered morphogenetic events that recapitulated some essential aspects of normal leaf development, the induced primordia did not develop into phenotypically normal leaves. Some of the generated organs underwent extensive axial elongation, but none of them were able to undergo normal leaf lamina expansion. Sections through these organs showed no obvious differentiation

into vascular and mesophyll tissue; vascular bundles could be found only at the primordia base where they terminated abnormally at the adaxial surface. The aberrant cytological differentiation was further evidenced by the bizarre pattern of marker gene expression. Another and perhaps the most striking common feature of expansin-induced organs was their indented tip, a hollow terminal structure that was very distinct from peg-like apex seen in normally developing leaves (Fig. 5.3b, c).

Analysis of fluorescently labeled protein diffusion from beads onto the apical meristem indicated that externally supplied expansin was likely to affect only the epidermal cell walls (Fleming et al. 1999). This suggests that the formation of the incomplete leaf structure after expansin application might reflect a failure of the exogenous protein to penetrate beyond the outer layer of the SAM and mimic the pattern of expansin expression that occurs during normal leaf initiation. To overcome the penetration problem, Pien et al. (2001) generated transgenic tomato plants bearing a cucumber expansin gene under the control of a tetracycline-inducible promoter. At the same time, to validate the method used for gene induction, a series of experiments was carried out with transgenic plants engineered to express the GUS reporter gene linked to the same promoter; these assays revealed that application of anhydrotetracycline-impregnated lanoline paste to the small region of the SAM induced reporter gene expression in all cell layers beneath the area of treatment. When the inducer was manipulated onto the I2 position in the SAM of plants bearing Tet::expansin construct, morphogenesis occurred at that spot, skipping the scheduled leaf initiation at the I1 position. In contrast to the previous study (Fleming et al. 1997), these primordia developed into normal leaves that contained all expected cell types and displayed complete histological architecture indistinguishable from that of regularly formed leaves. Consistent with the previous findings, the unscheduled organs reversed the phyllotactic spiral of organs generated subsequently.

Expansins are well known to directly change only the mechanical properties of cell walls. Therefore, the above data imply that fine modulation of mechanical stresses can bypass molecular events normally preceding primordia initiation. This outcome, in conjunction with the tight interrelation between plan organ geometry and tissue stresses, suggests that progression of plant shape can be conceived as a self-sustaining phenomenon. As noted Philip Lintilhac (2013): “We need to consider the shape of the apex, meaning its surface topology, not just as the product of apical meristem behavior but also as a controlling element in a conformational feedback circuit. We need to consider shape as input as well as output.” This standpoint alluding to the seminal insights of D’Arcy Thompson and further to Goethe implies that each subsequent shape is a consequence of the previous one and any alteration of plant mechanogeometrical status would modify the development in a strictly predictable way. In this context, the question arises as to how the aberrant structure of the primordia generated after topical expansin application is to be understood. Why within a wide variety of issued leaf-like organs certain

common hallmarks—limited lamina extension, lack of vascular bundles, and indented primordia tip—are often observed?

It is well established that auxin plays an important role in vascular pattern formation (Sachs 1981; Scarpella et al. 2006; O'Connor et al. 2014). In incipient and young leaf primordia, auxin transporters of the PIN family are localized at the sides of the cells that points to primordia apex and/or center. During subsequent leaf development, the auxin carriers accumulate in a narrow cell file along the primordium midline at the basal side of the cells. This file acts as auxin sink and corresponds to the provascular strand which subsequently differentiates into leaf midvein. The gradual reorientation of PIN, first toward the top, then to the center, and later to the base of the leaf primordia, is generally explained by a positive canalization feedback: cells that experience elevated levels of auxin are induced to absorb more auxin from adjacent tissues, and to transport it downwards more efficiently than their neighbors; the strategic auxin paths thus formed become vascular bundles later. However, the findings of Heisler et al. (2010) and Nakayama et al. (2012) indicating a crucial role of mechanical forces in PIN allocation suggest that the paradigmatic version of the canalization theory taking into account only auxin concentrations and fluxes should be amended. As it follows from the studies referred to above, stress-dependent PIN allocation ensures that the net auxin flow is directed to the cells whose walls relax most rapidly. There is no doubt that external expansin application increased mainly the extensibility of epidermal cell walls. This would result in the rheological imbalance between outer and inner cell layers that can prevent PIN allocation to the cell sides that point to the center and base of the leaf primordia and thus suppress vascular bundle formation.

Referring to the perhaps most challenging feature of the expansin-induced primordia—their indented tip (Fig. 5.3c)—it is imperative to point out that this hallmark increases primordia surface-to-volume ratio and therefore can be explained as a result of the buckling-like deformation triggered by access epidermis expansion that cannot be accommodated by commensurate strain in the underlying tissue. This interpretation implies that outer cell layer can be, at least locally, under biaxial tangential compression. This is not a trivial issue since in young growing stems as well as in juvenile ephemeral plant organs (such as coleoptiles), the yield threshold for the epidermal cell wall extension exceeds the stress produced by turgor pressure in epidermal cells, implying that some extra tension transduced from the inner tissue is essential for epidermal cell growth (Hejnowicz and Sievers 1996; Hohl and Shopfer 1992). The assumption that the outer cell layer of the SAM can be under multiaxial compression is also inconsistent with the predominant model of the SAM representing the outer cell layer as an elastic shell that resists the uniform pressure exerted by the tissue underneath (Selker et al. 1992; Hamant et al. 2008; Burian et al. 2013). Nevertheless, as we shall discuss below, even during normal development, the outer cell layer of the SAM can be locally under multiaxial compression.

5.6 A More Detailed Analysis of Tissue Stresses at the Shoot Apex and Their Significance for Plant Morphogenesis

Snow and Snow (1947, 1951) first drew attention to the fact that deep cuts and surface incisions made at the SAM often immediately and widely gape open, suggesting that the outer cell layer is under tension. Usually, the gapping is most evident at some distance from the meristem summit. In the context of the above studies of expansin-induced morphogenesis carried out in the apices of tomato, it is noteworthy that the pronounced opening of the cuts was observed particularly in the SAM of tomato (Hussey 1971, 1973). In this case, quite marked gaping and, more notably, tearing opening of the tissue beneath the incised tunica occurred at the meristem flanks, especially at the sites of incipient leaf primordia. Once the leaf bulge was well formed, much less gaping took place. In the axil of the primordium, cuts immediately closed up and exuded a drop of sap, suggesting that this region is under compression.

Perhaps the most comprehensive analysis of the distribution of tissue stresses in the shoot apex was performed by Dumais and Steele (2000) for the inflorescence SAM of sunflower. The radial surface incisions that cover the whole diameter of the capitulum was found to open widely in the center of the meristem, but remained closely pressed at some distance from the meristem summit—in the annular region referred to as generative. It has been proposed that in this region, initiation of floret primordia occurs (Dumais and Steele 2000), but it is now accepted that primordia are initiated more centrally, while in this region, they just start to be morphologically apparent (Mirabet et al. 2011). Although the observed profile of gap opening suggests that the epidermis is under tension in the central region of the meristem and under circumferential compression near the generative region, the detailed pattern of tissue stresses cannot be confidently inferred from this observation since the degree of cut opening and closing at a particular point depends not merely on the local stress in this point, but also on the stress distribution in the neighboring area. Therefore, the observed gaping pattern leaves open the possibility that, the epidermis is under maximal tension not exactly at the meristem center but somewhere between the center and the boundary of the generative and central regions. This interpretation is consistent with the trajectories of cracks initiated in the generative region during its local dissection (Fig. 5.4a). Circumferential compression (or reduced circumferential tension) in the generative region was assumed to explain why cracks propagate mostly circumferentially and do not readily cross the generative region. However, the cracks also do not run into the meristem center, and it seems likely that the second factor accounting for the resultant trajectory is the lack of considerable epidermal tension at the meristem summit. The assumption of negligible tension at the meristem summit is also supported by numerical simulations performed on the basis of the cross-sectional geometry of the capitulum (Fig. 5.4b).

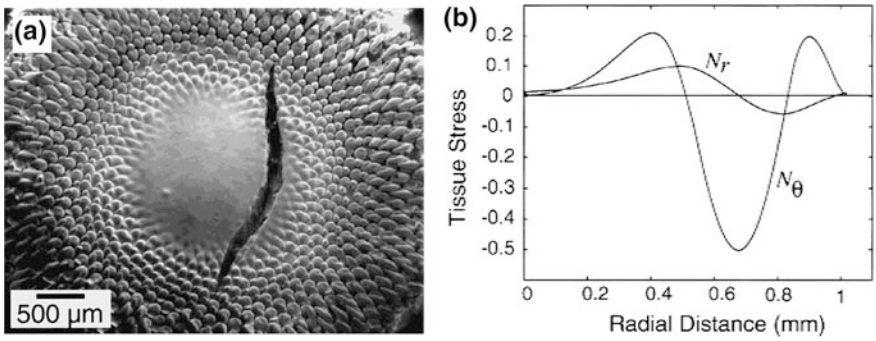

Fig. 5.4 Stress distribution on the surface of the inflorescence meristem of sunflower. **a** Fracture of the sunflower capitulum initiated in the generative region (where primordia start to be morphologically apparent) and spontaneously propagated mostly circumferentially until the opposite generative region was crossed. The crack does not run into the meristem center, indicating the lack of considerable epidermal tension in this region. The crack also does not cross the generative region at a right angle, suggesting the presence of compressive stresses in this region in the circumferential direction. **b** Plots of radial (N_r) and circumferential (N_θ) stresses at the meristem surface as a function of distance from the center of the meristem. Stress profiles were obtained from computer simulations based on the cross-sectional geometry of the capitulum. The location of the compressive zone (negative stress values) corresponds to the generative region. From Dumais and Steele (2000), with kind permission from Springer Science and Business Media

The above data (Snow and Snow 1947, 1951; Hussey 1971, 1973; Dumais and Steele 2000) indicate that epidermis in the SAM is generally under tension but do not argue that it is stretched uniformly over all the underneath. Rather, they suggest that the epidermal tension is negligible at the meristem summit and reaches a maximum in the regions that committed to give rise to primordia bulges and decreases (or even reverses) as the primordia start to grow out. The same trend in stress pattern can be deduced from a number of other circumstantial evidence. Case in point is the cell proliferation activity which often reaches a maximum beneath the sites of incipient primordia, but comes down thereafter (Hussey 1971, 1973; Lyndon 1970). The cytohistological zonation of the SAM also well correlates with the presumed changes in the pattern of tissue stress. More specifically, the cells located at the meristem summit are relatively large, vacuolated, and isodiametric. These morphological features relate these cells to those in the meristem pith but not to the epidermal cells on the meristem flanks, hinting that the apical and deep inner cells have a similar mechanical status. Furthermore, the epidermal cells at the meristem summit have rather thin walls, and if this region was under significant tension, these slowly growing cells would undergo rapid extension. Finally, the idea of the systematical variations in surface tension can also spring out from the data on the differential elastic strain-stiffening behavior in different regions of the SAM (Kierzkowski et al. 2012).

To infer the relationship between cell fate and tissue stresses, it is instructive to translate the pattern of tissue tension over meristem surface into the temporal course of the stress experienced by epidermal cells during their ontogeny. The data

presented above suggest that initially, when the cells are located at the meristem summit, they are scarcely stressed but are put under progressive tension further on as they displaces down along the meristem dome. This onset of tension can be readily explained as a natural outcome of the boundary conditions. Namely, the tension in the outer cell layer has to be generated if the following three assumptions are satisfied:

(1) Cells in the outer (L1) and inner (L2, L3) cell layers have a common developmental potential and tend to grow with similar rate;
(2) When a cell displaces down from the meristem summit, the distance that it needs to pass to achieve a given latitude increases with angular distance traversed more rapidly when it passes along L1 than when it passes along L2 or L3;
(3) The outer and inner cell layers cannot slide with respect to each other.

The first assumption is justified by the invasion events, when a cell displaced from its original layer adopts the fate and division pattern typical for the cells in the receiving layer (Stewart and Dermen 1975; Pohlheim and Kaufhold 1985; Szymkowiak and Sussex 1996). The second assumption implies an increase in the meristem surface curvature with the distance from the meristem tip; this is apparently the case for the central region of the SAM (Dumais and Steele 2000; Kwiatkowska and Dumais 2003). The third assumption reflects the normal symplastic mode of meristem growth in which relative position of adjacent cells preserves since their walls are glued together by the middle lamella.

Under the above well-established assumptions, the onset of tension in the epidermis and compression in the inner cell layers of the SAM can be thought of as a passive mechanical response of the meristematic tissue which unites the cell layers that tend to grow uniformly but forced to be curved due to geometric constriction imposed by the subtending stem. The reduction of epidermal tension in the generative region of the SAM cannot be explained in such starkly mechanistic terms and implies an active enhancement of epidermal cell growth. The emergence of regularly spaced primordia is probably associated with this growth enhancement. Due to the integrative nature of tissue stresses, the local stress relaxation on the sites of primordia initiation would lead to the concomitant relief of epidermal tension in the adjoining area where no significant growth response takes place, i.e., in the vicinity of infant lateral organs. This means that the stress experienced by a cell that enters into the generative region of the SAM would depend on its position relative to recently formed primordia. If the cell is located just above an incipient primordium, it would experience a lowest tension possible in the given latitude of the meristem dome, and as the infant organ displaces down along the meristem dome, the stress in this latitude increases until new primordium is initiated. In the issue, the cells committed to primordia formation differ from all other cells in the SAM in that they have been subjected to highest tensile stress during their drift along the meristem dome.

Turning the above relationship around one can hypothesize that it is the imposed mechanical stress that is the principal factor determining cell fate. This assumption,

however, might seem inconsistent with the data on expansin-induced leaf initiation discussed above. Since expansin application enhances the extensibility of epidermal cell walls, one might suspect that cells that are recruited into expansin-induced primordia have avoided extreme tension. This line of argument is not credible. First, none of the experiments done to date demonstrates that expansins are able to induce leaf primordia to arise de novo. Rather, the available data suggest that expansins advance the premature development of an incipient primordium that has been initiated before the protein application. Likewise, there is no conclusive evidence whether the expansin-induced precocious growth of the I2 primordium blocks the developmental program of the scheduled primordium at the I1 position. Fleming et al. (1999) noted that the I3 primordium appears in approximately the same position at which the I1 primordium was expected to arise, and it is possible that the I3 primordium is just the delayed I1. The second important point is that the relaxation of stress in cell walls inevitably involves a partial transduction of tension to the cell membrane. Since mechanical stresses are perceived, in particular, via the plasma membrane, it seems plausible that expansin-mediated wall relaxation can be interpreted by a cell as an extra tension. Therefore, the data on expansin-induced primordia do not contradict the assumption that it is the high tensile stress experienced by epidermal cells during their displacement down along the meristem dome that triggers the enhancement of cell growth and initiation of leaf primordia. Furthermore, the hypothesis under consideration can naturally explain why only the peripheral meristem zone was competent to the expansin-induced primordia initiation.

The regular spatial variations of tension over the meristem surface imply parallel variations of tissue stresses in subepidermal cell layers. Therefore, not only epidermal but also inner cells recruited into leaf primordia are likely to undergo a unique stress–strain history. Unfortunately, the above considerations regarding the distribution of surface tension cannot be used to deduce stresses in inner cell layers since the dynamics of the incisions and cracks reflects the stress pattern primarily in the tangential plane, while in the L2 and L3 layers the principal stresses would be in radial (normal to the organ surface) direction. However, the ablation experiments outlined below provide indications that the inner cell layers also respond to mechanical perturbations in the manner contemplated by the concept of stress hyperrestoration.

Reinhardt et al. (2003b) using microsurgical and laser ablation methods found that removal of patches of epidermal cells from the tomato SAM led to dramatic change in cell division pattern in the underlying cell layer. Instead of dividing anticlinally, the cells under lesion started to divide periclinally, giving rise to ordered cell stacks that grew out perpendicularly to the surface. This outcome was found to occur irrespective of whether the ablations affected only a limited area or the entire meristem surface. In any case, the periclinal divisions were commenced in a highly regular pattern that was clearly different from irregular callus-like proliferation occurring, for example, at the base of cut primordia. This implies that the observed switch in cell growth and division fashion was not a general wound response. The phenomenon under consideration can be partly explained by assuming that the removal of the L1 layer resulted in the relief of the radial stress

that had been exerted by L1 on the underlying cells and had restricted the plane of their division. However, although the relaxation of the radial stress can explain the initiation of periclinal divisions, it cannot explain why the cells in L2 ceased to divide anticlinally, especially considering that the removal of L1 would significantly increase the tangential tension in L2. Even more, after the ablation of L1, the mechanical status of L2 turned out to be similar to that of intact L1, so the question arises as to why, whereas L1 proliferates almost exclusively anticlinally, L2 under the same stress conditions started to proliferate mostly periclinally.

The above issue brings us back to the idea that it is not the mechanical stress itself but its increment that provides an overriding impetus for morphogenetic responses. The L2 layer had been under biaxial tangential tension before the ablation of L1, so this manipulation did not qualitatively change the tangential stress field in L2. In contrast, the effect of L1 removal on the radial stress is dramatic. Upon this manipulation, the stress exerted by L1 on the underlying cells vanished, allowing the cells in L2 to relax in the radial direction. This suggests that the switch in cell growth polarity and division plane orientation after L1 ablation could be considered as an active response tending to restore the original stress profile. Indeed, the growth of L2-derived cells in the direction perpendicular to the meristem surface gave rise to the supernumerary paradermal cell tiers that pressed each other and thereby generated inward pressure leading to the restoration (and overshooting) the original radial stress. On the other hand, the fact that the cells in the emerging layers had an abnormal stress–strain history offers a possible explanation of why leaf initiation was never observed at the meristem area from which the original superficial layer had been removed.

A fairly straightforward demonstration that mechanical forces can profoundly influence the pattern of meristem morphogenesis in the manner contemplated by the concept of stress hyperrestoration comes from constraint experiments (Hernández and Green 1993; Green 1999; Potocka et al. 2011). Hernández and Green (1993) found that lateral compression of a developing sunflower capitulum between two parallel clamps altered both phyllotaxy and organ identity. Instead of being spiral, the rows of primordia that were initiated after tissue compression became relatively straight and roughly paralleling the constraints. In further contrast to the normal inflorescence, in which each primordium gives rise to a bracteole subtending a floret, in the constrained capitulum, the bracteole–floret pair was often replaced by a single giant bract. In a subsequent series of experiments, Green (1999) found that the lateral constraint in the form of a frame imposed to the residual meristem of a detached *Graptopetalum* leaf led to the formation of ectopic row of leaves oriented, as in the previous case, parallel to the constraint. These results were interpreted by the authors in terms of the buckling theory that is as a passive bulging response (Hernández and Green 1993; Green 1999). However, the amplitude of the buckling-induced undulation would apparently be quite small (Dumais and Steele 2000), and the formation of primordia humps is obviously an active process that cannot be fully explained by passive buckling. On the other hand, the change in the pattern of tissue stresses induced by lateral constraint in the experiments under consideration is similar to that induced by L1 ablation in the above study of Reinhardt et al.

(2003b). In both cases, the manipulations led to an increase in lateral-to-radial stress ratio in the subepidermal cell layers. In the study of Reinhardt et al. (2003b), this shift was achieved by decreasing the radial (perpendicular to the meristem surface) stress, while in the constraint experiments (Hernández and Green 1993; Green 1999), this ratio alteration was due to lateral compression. This implies that the constraint-induced morphogenesis can be explained in the same way as suggested above, as a tendency for stress restoration. More specifically, the switch in the direction of inner cell growth from the tangential to radial would allow these cells experiencing extra lateral compression to avoid further increase in the lateral stress. The resultant extra pressure generated in the subepidermal cell layers due to mechanically prompted radial growth increases tangential tension in the epidermis, which, in order to restore the original stress field, would enhance its growth and thereby further promote primordia bulging.

5.7 Tissue Stresses and Morphogenesis in Roots

A similar response to imposed lateral compression was observed for the apical meristem of the root (Potocka et al. 2011). In contrast to the SAM, the root apical meristem (RAM) is not a strictly terminal structure, but is situated at a distance of a few millimeters from the apex surmounted by a root cap that protects the stem cell niche from the harsh soil environment. Consistently, the RAM produces cells basipetally as well as apically, giving rise to the root proper extending proximally toward the shoot, and the root cap growing downward and sloughing cells as the root penetrates the soil. Two types of RAM organization are distinguished depending on whether the cap is histologically discrete from the rest of the root or not. In the closed type of RAM organization, there is a clear root-cap boundary and the cell files can be easily traced back to their origins—a few initials in the middle of the quiescent center (Fig. 5.5a, b). In RAMs with an open organization, irregular cell files span the root cap and the root proper dissolving the boundary between them and blurring the convergence zone in the quiescent center (Fig. 5.5e). Many angiosperm families have representatives with both exclusively open and exclusively closed RAM's, while some species exhibit both types of RAM organization even in the same root at different times (Clowes and Wadekar 1989; Baum et al. 2002). In these species, after closed/open switch meristems produce completely normal uniform roots, thus revealing that cell division pattern has no essential bearing on the resultant phenotype. Furthermore, clonal analysis showed that cell divisions in one initial layer can give rise to a derivative contributing to the other layer, indicating that it is position, not lineage, that determines cell fate (Kidner et al. 2000). These findings suggest that the meristem cellular configuration is unlikely to have a functional significance and may emerge due to an intrinsic self-organization. We have addressed a similar issue above in the context of the SAM capable to generate lateral organs in a correct spatiotemporal fashion despite severe disruptions of the cell division pattern.

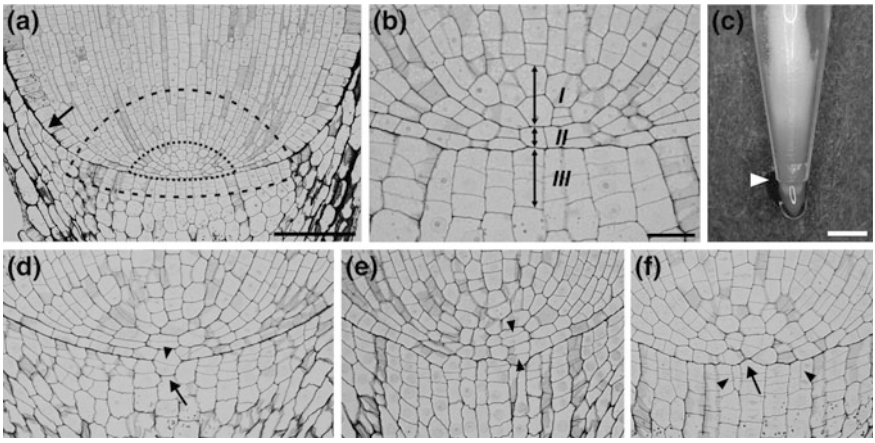

Fig. 5.5 The switch from closed to open organization of the RAM in *Zea mays* induced by lateral constraint. **a** Median longitudinal section through an unconstrained root apex. The root proper-cap boundary (*arrow*) indicates a closed RAM organization; the approximate regions of functional (*dashed line*) and structural initials (*dotted line*) are marked. **b** Magnification of the root pole region from the former section (**a**), showing three tiers of initials (*arrows*). **c** The root growing through the narrow conical tube (*arrowhead* indicates the tube end). **d** Section through a root apex just entering into the constricting zone. Meristem opening starts by breaking the root-cap boundary (*arrow*) with an atypical periclinal division (*arrowhead*) in the middle cell tier. **e** Section through a root apex in the tightest zone of the confining tube showing an open meristem organization with initials dividing periclinally (*arrowheads*) and growing toward the cap. **f** Section through a root apex leaved the narrowing. The root-cap border again recognizable (*arrow*), while atypical longitudinal cell divisions (*arrowhead*) occur in the root cap. *Scale bars* 100 μm (**a**), 20 μm (**b**), and 1 mm (**d**). From Potocka et al. (2011), with kind permission from the authors

The ontogenetic lability of RAM architecture in conjunction with the mechanical impedance normally exerted by the soil on the growing roots provides a physiologically relevant background to experimentally address the role of mechanical forces in the putative pattern-imposing field. In this line of inquiry, Potocka et al. (2011) investigated the effect of mechanical stress on RAM organization of *Zea mays*. This plant under normal conditions has the closed RAM with three clearly defined cell tires exhibiting a neat pattern of cell divisions (Fig. 5.5a, b). The upper (I) tier gives rise to cells of the vascular cylinder, the middle tier (II) initiates the cortex and epidermis, and the lower tier (III) produces the root cap. In the experiments under consideration, the maize roots were constrained to grow through a plastic conical tube and the tapering end of which had an internal diameter smaller than normal diameter of the root apex (Fig. 5.5c). As the root apices reached the constricting narrowing, the strong reorganization of the RAM architecture occurred. The first noticeable change took place in the middle tier where some initials underwent periclinal divisions which hardly ever occur in this very central region (Fig. 5.5d). Next, most distal cells of the root proper began to grow into the cap side and the root-cap boundary became more or less irregular. Finally, the border broke down and the typical closed RAM organization turned to open (Fig. 5.5e).

The above sequence of events is similar to the response of the SAM to L1 removal discussed earlier (Reinhardt et al. 2003b). In both cases, cells in the second cell layer (the L2 in the case of the SAM and the middle tier in the case of the RAM), instead of dividing anticlinally, started to divide periclinally, giving rise to ordered cell stacks that grew out perpendicularly to the layer surface. In both cases, the experimental manipulations led to an increase in lateral-to-radial stress ratio in the second cell layer. In the study of Reinhardt et al. (2003b), this shift was achieved by decreasing the radial pressure, while in the study of Potocka et al. (2011), this ratio alteration was due to lateral compression. These common points imply that the switch from the closed to open RAM organization can be explained in a way similar to that suggested above in the discussion of the ablation experiments of Reinhardt et al. (2003b) and constraint experiments of Green (Hernández and Green 1993; Green 1999), that is, as a tendency for stress restoration. More specifically, when the root tip reached the constricting narrowing, the cells in the middle cell tier that had been probably hardly, if ever, stressed (Kwiatkowska and Nakielski 2011) were exposed to the rapidly increasing lateral compression. Consistently, the observed switch in growth direction of these cells to the side of root cap would allow them to avoid further increase in the lateral stress and restore initial lateral-to-radial stress ratio.

When the root apex leaved the narrowing, the root-cap border again became recognizable, indicating that the RAM tended to revert back to the closed organization (Fig. 5.5f). However, up to the end of the experiment (24 h), the root-cap border remained irregular and the RAM did not regain the neat proliferation pattern. One of the specific features of the RAM in this intermediate state was the occurrence of longitudinal cell divisions in the root cap. These divisions enhanced cap growth in the tangential direction, and this response can be construed as a tendency to accommodate the extra tangential tension generated in the cap due to the preceding ingrowth of the root proper toward the root cap.

The above analysis suggests for the robust stereotypical character of the morphogenetic response to mechanical perturbations leading to stress hyperrestoration regardless of the experimental procedure and the type of the meristem involved: the shoot meristem in the study of Reinhardt et al. (2003b), the residual leaf meristem in the study of Green (1999), and the root meristem in the work of Potocka et al. (2011). Given this stereotypical response, it is worthwhile to contemplate whether the pattern of lateral root initiation can be construed in a way similar to that discussed above in explaining phyllotaxis. In many plants, lateral roots do emerge successively at approximately constant separation distance and divergence angle from the previous one. A simple yet poignant example can be found in *Arabidopsis* and tomato plants, whose primary roots often grow in a serpentine fashion due to regular alternation between right and left deflections of the root tip accompanied by nearly equidistant positioning of lateral roots at the convex side of each bend (Newson et al. 1993; De Smet et al. 2007). Although in the majority of plant species, the patterns of root bending and branching are not very regular, they are still tightly coupled, and lateral organs are initiated almost exclusively at the convex side of the local curvature. Artificial bending of primary roots by any methods leads

to curve-related lateral root formation. Manual bending of root for 20 s, after which the root was returned to its straight growth positioning, with no obvious asymmetry in the geometry on either side of the root was found to be sufficient to induce lateral root formation at the convex side of the transient bend (Richter et al. 2009). Double reciprocal bends produced with no reorientation of either the apical or basal parts of the root using the elegant gel-sliding technique also resulted in emergence of lateral roots at the convex of the bends (Richter et al. 2009). These findings suggest that the plasticity of root system development can be explained by the fact that unlike the shoot apex, which is shielded from external mechanical influences by ensheathing leaves, the root tip is exposed to environmental loads, which interfere with the intrinsic tissue stresses and thereby modify pattern of lateral root initiation.

Lateral roots arise at the convex side of the parental root irrespectively of whether the root bending is a passive (mechanical) or active (nastic or tropic) response. In the latter case, the differential growth of cells on opposite sides of the root can be induced, for example, by high environmental temperature (Sattelmacher et al. 1990), obstacle-touching stimuli (Goss and Russell 1980; Okada and Shimura 1990), and root reorientation with respect to the gravity vector (Lucas et al. 2008). The importance of auxin redistribution for root gravi- and thigmotropic responses (Ottenschlager et al. 2003; Band et al. 2012) gave rise to the idea that the reorientation of auxin fluxes can explain the emergence of lateral roots on the convex side of the bend (De Smet et al. 2007; Laskowski et al. 2008; Lucas et al. 2008; Lavenus et al. 2013). However, the direction of auxin net flow that underlies root tropic bending is the opposite of what one might expect if the auxin redistribution is directly responsible for bend-induced lateral root initiation. For example, when a parental root is positioned at an angle to the gravity vector, auxin is redistributed toward its lower lateral side (Band et al. 2012). Roots are much more sensitive to auxin than shoots, and the auxin flow to the lower side of the inclined root results in auxin supraoptimal concentration that locally inhibits cell growth causing the downward root curvature. Consequently, the slowly growing concave side of the graviresponding root is temporarily exposed to higher concentrations of auxin than the more rapidly growing convex side. On the other hand, it is well established that externally supplied auxin or local activation of its biosynthesis can induce lateral root formation, and, furthermore, accumulation of auxin in progenitors of root founder cells is one of the early events normally preceding lateral root development (de Smet et al. 2007; Dubrovsky et al. 2008; Sugimoto et al. 2010). This implies that root tropic bending involves, at least as an immediate first step, the establishment of the auxin gradient of the opposite direction to the gradient that would arise to provide positional cues for the emergence of lateral roots on the convex side of the bend. Consistent with this inference, it has been found that root bending can elicit lateral root formation on the convex side of the bend in the absence of tropism-associated auxin fluxes (Richter et al. 2009), and auxin signaling mutants which form no lateral roots in unstrained state retain the ability to initiate lateral roots upon bending (Ditengo et al. 2008). These findings suggest that there is a morphogenetic trigger that can specify the sites of lateral root initiation independently (e.g., upstream) of auxin-dependent events. Can mechanical stresses act as the trigger in question?

Unlike leaves that are typically initiated on flanks of the SAM, the inception of lateral roots in the majority of plant species is believed to take place outside the apical meristem in the region extending from the vicinity of the RAM up to several millimeters behind. Specification of lateral root founder cells occurs deep within the parental root in a cell layer designated as pericycle. The pericycle originates from the RAM as a continuous ring of cells encircling the root vascular tissues and is surrounded from outside by multilayered root cortex and epidermis. The differences in the onset of organogenetic events in shoots and roots—relatively late inception of lateral roots deep within parental tissue—are likely correlated with the differences between shoots and roots in the spatiotemporal pattern of tissue stresses. The seminal works of Sachs (1882) and Darwin and Acton (1894) showed that after sectioning a root tip lengthwise, the split halves curve inward. These observations led to the general assumption that the tissue stresses in growing roots are opposite to those in the above-ground organs (Kutschera 1989). However, when roots were split longitudinally so that epidermis and cortex were freed from the root "central core," the strips also bent inward (Burström 1971; Abeysekera and McCully 1994). This suggests that root innermost (vascular) tissue is of minor significance for strip incurvature, and it is the inner layer(s) of the root cortex that are under maximum tensile stress. Therefore, biomechanical status of the inner root cortex seems to be similar to that of the epidermis in shoots. Physiological data support the idea that in roots, not the epidermis, the inner cortex operates as a key tissue controlling the growth (Baskin et al. 1992; Baluška et al. 1994).

Likewise, in root apices, tissue stresses reach a maximum value not at the flanks of the meristem, as they do in shoots, but at a distance of a few millimeters behind. When epidermal surface strips are removed from the apical and subapical root zones, the strips often display marked pleating of the radial walls of epidermal cells (Abeysekera and McCully 1994). The pleating is most prominent in portions of the epidermis which overlie the transition zone between the RAM and the region of rapid cell elongation. In this transition zone, the specification of lateral root founder cells is believed to take place (Baluška and Mancuso 2013). Since the pleating of radial walls is apparently resulted from longitudinal shortening of the isolated epidermal surface due to the release of turgor pressure and tissue stresses, this observation suggests that root cortex in this zone is in a highly stressed state. The correspondence between the biomechanical states of the transition zone of roots and the flanks of the SAM is further evidenced by their similar response to hyperosmotic treatment (Burström 1971; Kierzkowski et al. 2012). It seems obvious that upon plasmolysis, when turgor pressure is lost, plant cell should shrink, which does happen in almost all cases. The root meristem also contracts during plasmolysis, as do more proximate regions of the root. Only the transition zone was found to expand in length upon hyperosmotic treatment (Burström 1971). The similar surface expansion after plasmolysis was observed for basal regions of the SAM (Kierzkowski et al. 2012). Although at present, it is hardly possible to reconstitute the stress distribution that underlies this unexpected response, the similar behavior of the transition zone of roots and the flanks of the SAM suggests the similarity in their stress patterns. Therefore, one can assume that the differences in the onset of

organogenetic events in shoots and roots—the inception of lateral roots (1) deep within parental root tissue (2) outside the apical meristem—can reflect that in roots (1) not epidermis but multilayered subepidermal cortex is under highest longitudinal tension and (2) this tension increases in proximal direction quite gradually reaching a maximum value at some distance from the RAM.

The pattern of cell divisions during lateral root initiation is highly variable. Different types of asymmetric divisions can underlay the onset of lateral root formation (Dubrovsky et al. 2001), and even if primordia were initiated due to similar formative events, they do not follow stereotypical proliferative paths passing through the same developmental stages with markedly different numbers of cells (Lucas et al. 2013). A major change in primordia shape is associated with the breaking of the Casparian strip—a lignified band of cell wall material that cements endodermis (innermost layer of the root cortex). Using casparian strip mutants as well as targeted alteration of the overlaying tissue mechanical properties, Lucas et al. (2013) showed that a stress field has a crucial impact on the primordia morphogenesis. Likewise, Vermeer et al. (2014) found that mechanical feedback between endodermis and pericycle is absolutely required for the initiation and growth of lateral roots. Collectively, the observations suggest that root primordia morphogenesis is canalized by biophysical interplay between the developing organ and overlaying tissues. From this perspective, one can explain the fact that early development of root primordia cannot proceed outside the parental root, and young primordia when cultivated in situ fail to develop further (Laskowski et al. 1995). The switch to the stage of developmental autonomism from which root primordia can properly develop when excised from the parental root coincides with the formation of primordia apical meristem that implies, inter alia, the establishment of a self-stressed structure.

Although the evidences mentioned above suggest that the sites of primordia initiation correspond to the region of the parental root where longitudinal tension in the root cortex reaches a maximum value, the stress distributions in the radial and circumferential directions at these sites can be variable. In cases when the root curvature is caused by purely mechanical factors (manual bending) or is due to one-sided growth inhibition, the convex side of the root is likely to experience radial and circumferential compression. However, when root bending is due to one-sided growth enhancement, the stresses in the pericycle tissue (where lateral roots originate) in radial and circumferential directions at the convex side of the bend would be of opposite sign. More specifically, since the rate of root growth is controlled by root cortex that located outside the pericycle, one-sided enhanced growth of the cortex impels the underlying pericycle to fill extra space extending root founder cells in all directions. Root nastic and tropic responses are usually due to both inhibition of growth at one side and activation of growth at the opposite side, resulting in variable and complicated pattern of radial and circumferential stresses. Given the strong dependence of the orientation of cell divisions on the distribution of mechanical forces (Linthilac and Vescky 1984; Lynch and Lintilhac 1997), it seems likely that the variability of proliferative events underlying lateral root formation (Dubrovsky et al. 2001; Lucas et al. 2013) reflects the variability of tissue

stresses in the circumferential and radial directions. On the other hand, the conserved longitudinal profile of tissue stresses (Burström 1971; Abeysekera and McCully 1994) together with strong mechanical feedback between the developing organ and overlaying tissues (Lucas et al. 2013; Vermeer et al. 2014) is probably able to ensure the stereotyped progression of overall primordium shape.

The spontaneous incurvature of longitudinally split root apices (Burström 1971; Abeysekera and McCully 1994), the pleating of epidermal cell walls in surface peels isolated from subapical root regions (Abeysekera and McCully 1994), and a unique response of the transition root zone to hyperosmotic treatment (Burström 1971), taken together, suggest that root inner cortex is under tension that reaches a maximum value in the regions where specification of root founder cells takes place. Since the incursion of root primordia into overlying cell layers would decrease tension of these layers, lateral root development can be rationalized in terms of stress hyperrestoration. This aspect is highlighted by the fact that lateral roots typically emerge at the convex side of local root curvature where extra tension accumulates. Interestingly, root hairs are initiated predominantly on the opposite, concave side of a bend (Goss and Russell 1980; Sattelmacher et al. 1990). Since root hairs are extensions of the epidermis that does not transverse any cell layers but greatly increase the surface area of the root, their development on the concave root surface would decrease the curve-related compression and therefore can also be contemplated in terms of stress hyperrestoration. As in the case with lateral roots, the initiation and growth of root hairs are associated with local accumulation of auxin (Jones et al. 2009). The fact that root hairs develop predominantly on the concave root surface, while lateral roots emerge on the convex root side suggests that mechanical stresses can regulate morphogenesis upstream of auxin-dependent events.

References

Abeysekera RM, McCully ME (1994) The epidermal surface of the maize root tip. III. Isolation of the surface and characterization of some of its structural and mechanical properties. New Phytol 127:321–333

Baluška F, Mancuso S (2013) Root apex transition zone as oscillatory zone. Front Plant Sci 4:354

Baluška F, Volkmann D (2011) Mechanical aspects of gravity-controlled growth, development and morphogenesis. In: Wojtaszek P (ed) Mechanical integration of plant cells and plants. Signaling and communication in plants, vol 9, pp 195–223

Baluška F, Barlow PW, Kubica Š (1994) Importance of the post-mitotic growth (PIG) region for growth and development of roots. Plant Soil 167:31–42

Band LR, Wells DM, Larrieu A, Sun J, Middleton AM et al (2012) Root gravitropism is regulated by a transient lateral auxin gradient controlled by a tipping-point mechanism. Proc Natl Acad Sci USA 109:4668–4673

Baskin TI (2001) On the alignment of cellulose microfibrils by cortical microtubules: a review and a model. Protoplasma 215:150–171

Baskin TI, Betzner AS, Hoggart R, Cork A, Williamson RE (1992) Root morphology mutants in *Arabidopsis thaliana*. Aust J Plant Physiol 19:427–437

Baum SF, Dubrovsky JG, Rost TL (2002) Apical organization and maturation of the cortex and vascular cylinder in *Arabidopsis thaliana* (Brassicaceae) roots. Am J Bot 89:908–920

Behrens HM, Gradmann D, Sievers A (1985) Membrane-potential responses following gravistimulation in roots of *Lepidium sativum* L. Planta 163:463–472

Bemis SM, Torii KU (2007) Autonomy of cell proliferation and developmental programs during *Arabidopsis* aboveground organ morphogenesis. Dev Biol 304:367–381

Bringmann M, Li E, Sampathkumar A, Kocabek T, Hauser MT, Persson S (2012) POM-POM2/cellulose synthase interacting1 is essential for the functional association of cellulose synthase and microtubules in *Arabidopsis*. Plant Cell 24:163–177

Burian A, Ludynia M, Uyttewaal M, Traas J, Boudaoud A, Hamant O, Kwiatkowska D (2013) A correlative microscopy approach relates microtubule behaviour, local organ geometry, and cell growth at the *Arabidopsis* shoot apical meristem. J Exp Bot 64:5753–5767

Burström HG (1971) Tissue tensions during cell elongation in wheat roots and a comparison with contractile roots. Physiol Plant 25:509–513

Catala C, Rose JK, Bennett AB (2000) Auxin-regulated genes encoding cell wall-modifying proteins are expressed during early tomato fruit growth. Plant Physiol 122:527–534

Clowes FAL, Wadekar R (1989) Instability in the root meristem of *Zea mays* L. during growth. New Phytol 111:19–24

Corson F, Hamant O, Bohn S, Traas J, Boudaoud A, Couder Y (2009) Turning a plant tissue into a living cell froth through isotropic growth. Proc Natl Acad Sci USA 106:8453–8458

Cosgrove DJ (2000) Loosening of plant cell walls by expansins. Nature 407:321–326

Cunninghame ME, Lyndon RF (1986) The relationship between the distribution of periclinal cell divisions in the shoot apex and leaf initiation. Ann Bot 57:737–746

Darwin CR (1860) Letter to D. Oliver (16 Nov. 1860). Darwin correspondence database. http://www.darwinproject.ac.uk/entry-2985

Darwin CR (1875) Insectivorous plants. John Murray, London

Darwin F, Acton EH (1894) Practical physiology of plants. Cambridge University Press, Cambridge

De Smet I, Tetsumura T, De Rybel B, Frei dit Frey N, Laplaze L et al (2007) Auxin-dependent regulation of lateral root positioning in the basal meristem of *Arabidopsis*. Development 134:681–690

Ditengou FA, Teale WD, Kochersperger P, Flittner KA, Kneuper I et al (2008) Mechanical induction of lateral root initiation in *Arabidopsis thaliana*. Proc Natl Acad Sci USA 105:18818–18823

Driss-Ecole D, Legue V, Carnero-Diaz E, Perbal G (2008) Gravisensitivity and automorphogenesis of lentil seedling roots grown on board the international space station. Physiol Plant 134:191–201

Dubrovsky JG, Rost TL, Colon-Carmona A, Doerner P (2001) Early primordium morphogenesis during lateral root initiation in *Arabidopsis thaliana*. Planta 214:30–36

Dubrovsky JG, Sauer M, Napsucialy-Mendivil S, Ivanchenko MG, Friml J, Shishkova S, Celenza J, Benková E (2008) Auxin acts as a local morphogenetic trigger to specify lateral root founder cells. Proc Natl Acad Sci USA 105:8790–8794

Dumais J, Steele CR (2000) New evidence for the role of mechanical forces in the shoot apical meristem. J Plant Growth Regul 19:7–18

Esser AT, Smith KC, Weaver JC, Levin M (2006) A mathematical model of morphogen electrophoresis through gap junctions. Dev Dyn 235:2144–2159

Fisher DD, Cyr RJ (2000) Mechanical forces in plant growth and development. Grav Space Biol Bull 13:67–73

Fleming AJ, McQueen-Mason S, Mandel T, Kuhlemeier C (1997) Induction of leaf primordia by the cell wall protein expansin. Science 276:1415–1418

Fleming AJ, Caderas D, Wehrli E, McQueen-Mason S, Kuhlemeier C (1999) Analysis of expansin-induced morphogenesis on the apical meristem of tomato. Planta 208:166–174

Foard DE (1971) The initial protrusion of a leaf primordium can occur without concurrent periclinal cell divisions. Can J Bot 49:1601–1603

Fricke W, Jarvis M, Brett C (2000) Turgor pressure, membrane tension and the control of exocytosis in higher plants. Plant Cell Environ 23:999–1003
Gager CS (1916) Fundamentals of botany. P. Blakiston's Son & Co, Philadelphia
Geldner N, Friml J, Stierhof YD, Jurgens G, Palme K (2001) Auxin transport inhibitors block PIN1 cycling and vesicle trafficking. Nature 413:425–428
Goss MJ, Russell RS (1980) Effects of mechanical impedance on root growth in barley (*Hordeum vulgare* L.) III Observations on the mechanism of response. J Exp Bot 31:577–588
Green PB (1962) Mechanisms for plant cellular morphogenesis. Science 138:1404–1405
Green PB (1999) Expression of pattern in plants: combining molecular and calculus-based biophysical paradigms. Am J Bot 86:1059–1076
Grunewald W, Friml J (2010) The march of the PINs: developmental plasticity by dynamic polar targeting in plant cells. EMBO J 29:2700–2714
Guenot B, Bayer E, Kierzkowski D, Smith RS, Mandel T, Žádníková P, Benková E, Kuhlemeier C (2012) PIN1-independent leaf initiation in Arabidopsis. Plant Physiol 159:1501–1510
Hamant O, Heisler MG, Jonsson H, Krupinski P, Uyttewaal M et al (2008) Developmental patterning by mechanical signals in *Arabidopsis*. Science 322:1650–1655
Hardham AR, Green PB, Lang JM (1980) Reorganization of cortical microtubules and cellulose deposition during leaf formation of *Graptopetalum paraguayense*. Planta 149:181–195
Heath IB (1974) A unified hypothesis for the role of membrane bound enzyme complexes and microtubules in plant cell wall synthesis. J Theor Biol 48:445–449
Heisler MG, Hamant O, Krupinski P, Uyttewaal M, Ohno C, Jönsson H, Traas J, Meyerowitz EM (2010) Alignment between PIN1 polarity and microtubule orientation in the shoot apical meristem reveals a tight coupling between morphogenesis and auxin transport. PLoS Biol 8: e1000516
Hejnowicz Z, Sievers A (1996) Acid-induced elongation of *Reynoutria* stems requires tissue stresses. Physiol Plant 98:345–348
Hejnowicz Z, Sondag C, Alt W, Sievers A (1998) Temporal course of graviperception in intermittently stimulated cress roots. Plant Cell Environ 21:1293–1300
Hernández LF, Green PB (1993) Transductions for the expression of structural pattern: analysis in sunflower. Plant Cell 5:1725–1738
Himmelspach R, Willamson RE, Wasteneys GO (2003) Cellulose microfibril alignment recovers from DCB-induced disruption despite microtubule disorganization. Plant J 36:565–575
Hohl M, Schopfer P (1992) Cell-wall tension of the inner tissues of the maize coleoptile and its potential contribution to auxin-mediated organ growth. Planta 188:340–344
Hussey G (1971) Cell division and expansion and resultant tissue tensions in the shoot apex during the formation of a leaf primordium in the tomato. J Exp Bot 22:702–714
Hussey G (1973) Mechanical stress in the shoot apices of *Euphorbia*, *Lycopersicon*, and *Pisum* under controlled turgor. Ann Bot 37:57–64
Hutchison KW, Singer PB, McInnis S, Diaz-Salaz C, Greenwood MS (1999) Expansins are conserved in conifers and expressed in hypocotyls in response to exogenous auxin. Plant Physiol 120:827–831
Imaichi R, Hiratsuka R (2007) Evolution of shoot apical meristem structures in vascular plants with respect to plasmodesmatal network. Am J Bot 94:1911–1921
Ingber DE (2003) Tensegrity II. How structural networks influence cellular information processing networks. J Cell Sci 116:1397–1408
Jones AR, Kramer EM, Knox K, Swarup R, Bennett MJ, Lazarus CM, Leyser HM, Grierson CS (2009) Auxin transport through non-hair cells sustains root-hair development. Nat Cell Biol 11:78–84
Jönsson H, Gruel J, Krupinski P, Troein C (2012) On evaluating models in computational morphodynamics. Curr Opin Plant Biol 15:103–110
Kasprowicz A, Smolarkiewicz M, Wierzchowiecka M, Michalak M, Wojtaszek P (2011) Introduction: tensegral world of plants. In: Wojtaszek P (ed) Mechanical integration of plant cells and plants. Signaling and communication in plants, vol 9, pp 1–25

Kidner C, Sundaresan V, Roberts K, Dolan L (2000) Clonal analysis of the *Arabidopsis* root confirms that position, not lineage, determines cell fate. Planta 211:191–199

Kierzkowski D, Nakayama N, Routier-Kierzkowska AL, Weber A, Bayer E, Schorderet M, Reinhardt D, Kuhlemeier C, Smith RS (2012) Elastic domains regulate growth and organogenesis in the plant shoot apical meristem. Science 335:1096–1099

Kutschera U (1989) Tissue stresses in growing plant organs. Physiol Plant 77:157–163

Kwiatkowska D, Dumais J (2003) Growth and morphogenesis at the vegetative shoot apex of *Anagallis arvensis* L. J Exp Bot 54:1585–1595

Kwiatkowska D, Nakielski J (2011) Mechanics of the meristems. In: Wojtaszek P (ed) Mechanical integration of plant cells and plants. Signaling and communication in plants, vol 9, pp 133–172

Laskowski MJ, Williams ME, Nusbaum HC, Sussex IM (1995) Formation of lateral root meristems is a two-stage process. Development 121:3303–3310

Laskowski MJ, Grieneisen VA, Hofhuis H, Hove CA, Hogeweg P, Marée AF, Scheres B (2008) Root system architecture from coupling cell shape to auxin transport. PLoS Biol 6:307

Lavenus J, Goh T, Roberts I, Guyomarc'h S, Lucas M, De Smet I, Fukaki H, Beeckman T, Bennett M, Laplaze L (2013) Lateral root development in *Arabidopsis*: fifty shades of auxin. Trends Plant Sci 18:450–458

Ledbetter MC, Porter KR (1963) A "microtubule" in plant cell fine structure. J Cell Biol 12:239–250

Li S, Lei L, Somerville CR, Gu Y (2012) Cellulose synthase interactive protein 1 (CSI1) links microtubules and cellulose synthase complexes. Proc Natl Acad Sci USA 109:185–190

Link BM, Cosgrove DJ (1998) Acid-growth response and alpha-expansins in suspension cultures of bright yellow 2 tobacco. Plant Physiol 118:907–916

Lintilhac PM (2013) The problem of morphogenesis: unscripted biophysical control systems in plants. Protoplasma 251:25–36

Lintilhac PM, Vesecky TB (1984) Stress-induced alignment of division plane in plant tissues grown in vitro. Nature 307:363–364

Lipchinsky A (2013) How do expansins control plant growth? A model for cell wall loosening via defect migration in cellulose microfibrils. Acta Physiol Plant 35:3277–3284

Lucas M, Godin C, Jay-Allemand C, Laplaze L (2008) Auxin fluxes in the root apex co-regulate gravitropism and lateral root initiation. J Exp Bot 59:55–66

Lucas M, Kenobi K, von Wangenheim D, Voβ U, Swarup K, De Smet I et al (2013) Lateral root morphogenesis is dependent on the mechanical properties of the overlaying tissues. Proc Natl Acad Sci USA 110:5229–5234

Lynch TM, Lintilhac PM (1997) Mechanical signals in plant development: a new method for single cell studies. Dev Biol 181:246–256

Lyndon RF (1970) Rates of cell division in the shoot apical meristem of *Pisum*. Ann Bot 34:1–17

Massa GD, Gilroy S (2003) Touch modulates gravity sensing to regulate the growth of primary roots of *Arabidopsis thaliana*. Plant J 33:435–445

McQueen-Mason SJ, Durachko DM, Cosgrove DJ (1992) Two endogenous proteins that induce cell-wall extension in plants. Plant Cell 4:1425–1433

Meckel T, Hurst AC, Thiel G, Homann U (2005) Guard cells undergo constitutive and pressure-driven membrane turnover. Protoplasma 226:23–29

Mirabet V, Das P, Boudaoud A, Hamant O (2011) The role of mechanical forces in plant morphogenesis. Annu Rev Plant Biol 62:365–385

Nakayama N, Smith RS, Mandel T, Robinson S, Kuhlemeier C, Kimura S, Boudaoud A (2012) Mechanical regulation of auxin-mediated growth. Curr Biol 22:1468–1476

Newcomb EH (1969) Plant microtubules. Ann. Rev. Plant Physiol 20:253–288

Newson RB, Parker JS, Barlow PW (1993) Are lateral roots of tomato spaced by multiples of a fundamental distance? Ann Bot 71:549–557

O'Connor DL, Runions A, Sluis A, Bragg J, Vogel JP, Prusinkiewicz P, Hake S (2014) A division in PIN-mediated auxin patterning during organ initiation in grasses. PLoS Comput Biol 10:e1003447

Okada K, Shimura Y (1990) Reversible root tip rotation in *Arabidopsis* seedlings induced by obstacle-touching stimulus. Science 250:274–276

Ottenschläger I, Wolff P, Wolverton C, Bhalerao RP, Sandberg G, Ishikawa H, Evans M, Palme K (2003) Gravity-regulated differential auxin transport from columella to lateral root cap cells. Proc Natl Acad Sci USA 100:2987–2991

Paredez AR, Somerville CR, Ehrhardt DW (2006) Visualization of cellulose synthase demonstrates functional association with microtubules. Science 312:1491–1495

Pien S, Wyrzykowska J, McQueen-Mason S, Smart C, Fleming A (2001) Local expression of expansin induces the entire process of leaf development and modifies leaf shape. Proc Natl Acad Sci USA 98:11812–11817

Pohlheim F, Kaufhold M (1985) On the formation of variegation patterns in *Filipendula ulmaria* 'Aureo-Variegata' through changes in the plane of cell division in the epidermisses of young leaves. Flora 177:167–174

Potocka IJ, Szymanowska-Pułka J, Karczewski J, Nakielski J (2011) Effect of mechanical stress on *Zea* root apex. I. Mechanical stress leads to the switch from closed to open meristem organization. J Exp Bot 62:4583–4593

Proseus TE, Boyer JS (2005) Turgor pressure moves polysaccharides into growing cell walls of *Chara corallina*. Ann Bot 95:967–979

Reddy GV, Heisler MG, Ehrhardt DW, Meyerowitz EM (2004) Real-time lineage analysis reveals oriented cell divisions associated with morphogenesis at the shoot apex of *Arabidopsis thaliana*. Development 131:4225–4237

Reinhardt D, Wittwer F, Mandel T, Kuhlemeier C (1998) Localized upregulation of a new expansin gene predicts the site of leaf formation in the tomato meristem. Plant Cell 10:1427–1437

Reinhardt D, Mandel T, Kuhlemeier C (2000) Auxin regulates the initiation and radial position of plant lateral organs. Plant Cell 12:507–518

Reinhardt D, Pesce E-R, Stieger P, Mandel T, Baltensperger K, Bennett M, Traas J, Friml J, Kuhlemeier C (2003a) Regulation of phyllotaxis by polar auxin transport. Nature 426:255–260

Reinhardt D, Frenz M, Mandel T, Kuhlemeier C (2003b) Microsurgical and laser ablation analysis of interactions between the zones and layers of the tomato shoot apical meristem. Development 130:4073–4083

Richter GL, Monshausen GB, Krol A, Gilroy S (2009) Mechanical stimuli modulate lateral root organogenesis. Plant Physiol 151:1855–1866

Robinson DG, Preston RD (1972) Plasmalemma structure in relation to microfibril biosynthesis in *Oocystis*. Planta 104:234–246

Sachs J (1875) Text-book of botany, morphological and physiological. Clarendon, Oxford

Sachs J (1882) Vorlesungen über Pflanzen-Physiologie. Verlag W Engelmann, Leipzig

Sachs T (1981) The control of the patterned differentiation of vascular tissues. Adv Bot Res 9:151–262

Sack FD, Suyemoto MM, Leopold AC (1986) Amyloplast sedimentation and organelle saltation in living corn columella cells. Am J Bot 73:1692–1698

Sagawa Y, Mehlquist GAL (1957) The mechanism responsible for some X-ray induced changes in flower color of the carnation, *Dianthus caryophyllus*. Am J Bot 44:397–403

Sattelmacher B, Marschner H, Kuhne R (1990) Effects of the temperature of the rooting zone on the growth and development of roots of potato (*Solanum tuberosum*). Ann Bot 65:27–36

Scarpella E, Marcos D, Berleth T (2006) Control of leaf vascular patterning by polar auxin transport. Genes Dev 20:1015–1027

Selker JML, Steucek GL, Green PB (1992) Biophysical mechanisms for morphogenetic progressions at the shoot apex. Dev Biol 153:29–43

Singer SJ, Nicolson GL (1972) The fluid mosaic model of the structure of cell membranes. Science 175:720–731

Snow M, Snow R (1932) Experiments on phyllotaxis. I. The effect of isolating a primordium Philos. Trans R Soc Lon B 221:1–43

Snow M, Snow R (1947) On the determination of leaves. New Phytol 46:5–19

Snow M, Snow R (1951) On the question of tissue tensions in stem apices. New Phytol 50:184–185
Stewart RN, Dermen H (1975) Flexibility in ontogeny as shown by the contribution of the shoot apical layers to leaves of periclinal chimeras. Am J Bot 62:935–947
Sugimoto K, Himmelspach R, Williamson RE, Wasteneys GO (2003) Mutation or drug-dependent microtubule disruption causes radial swelling without altering parallel cellulose microfibril deposition in *Arabidopsis* root cells. Plant Cell 15:1414–1429
Sugimoto K, Jiao Y, Meyerowitz EM (2010) Arabidopsis regeneration from multiple tissues occurs via a root development pathway. Dev Cell 18:463–471
Szymkowiak EJ, Sussex IM (1996) What chimeras can tell us about plant development. Annu Rev Plant Physiol Plant Mol Biol 47:351–376
Thompson DW (1917) On growth and form. Cambridge University Press, Cambridge
Toyota M, Furuichi T, Sokabe M, Tatsumi H (2013) Analyses of a gravistimulation-specific Ca^{2+} signature in *Arabidopsis* using parabolic flights. Plant Physiol 163:543–554
Traas J (2013) Phyllotaxis Development 140:249–253
Traas J, Bellini C, Nacry P, Kronenberger J, Bouchez D, Caboche M (1995) Normal differentiation patterns in plants lacking microtubular preprophase bands. Nature 375:676–677
Uyttewaal M, Burian A, Alim K, Landrein B, Borowska-Wykret D et al (2012) Mechanical stress acts via katanin to amplify differences in growth rate between adjacent cells in *Arabidopsis*. Cell 149:439–451
Van Berkel K, De Boer RJ, Scheres B, Ten Tusscher K (2013) Polar auxin transport: models and mechanisms. Development 140:2253–2268
Vandiver R, Goriely A (2008) Tissue tension and axial growth of cylindrical structures in plants and elastic tissues. Europhys Lett 84:58004
Vermeer JE, von Wangenheim D, Barberon M, Lee Y, Stelzer EH, Maizel A, Geldner N (2014) A spatial accommodation by neighboring cells is required for organ initiation in *Arabidopsis*. Science 343:178–183
Wymer CL, Wymer SA, Cosgrove DJ, Cyr RJ (1996) Plant cell growth responds to external forces and the response requires intact microtubules. Plant Physiol 110:425–430
Wyrzykowska J, Fleming AJ (2003) Cell division pattern influences gene expression in the shoot apical meristem. Proc Natl Acad Sci USA 100:5561–5566
Wyrzykowska J, Pien S, Shen WH, Fleming AJ (2002) Manipulation of leaf shape by modulation of cell division. Development 129:957–964
Yennawar NH, Li L-C, Dudzinski DM, Tabuchi A, Cosgrove DJ (2006) Crystal structure and activities of EXPB1 (Zea m 1), a beta-expansin and group-1 pollen allergen from maize. Proc Natl Acad Sci USA 103:14664–14671
Zhou J, Wang B, Li Y, Wang Y, Zhu L (2007) Responses of chrysanthemum cells to mechanical stimulation require intact microtubules and plasma membrane-cell wall adhesion. J Plant Growth Regul 26:55–68
Zonia L, Munnik T (2008) Vesicle trafficking dynamics and visualization of zones of exocytosis and endocytosis in tobacco pollen tubes. J Exp Bot 59:861–873

Concluding Remarks

To the authors' knowledge, the term "morphomechanics" was coined during the last decade independently by several authors. In any case this term looks appropriate for defining a rapidly grown branch of science situated somewhere in between (or inside of?) molecular, cell, and developmental biology. Its very intermediate position illustrates the tendency to search something common for different structural levels: nothing better than mechanical forces and stresses suit this purpose. At the same time, the morphomechanical approach in no way neglects the necessity to treat each level separately. For example, the forces and deformations taking place on the molecular–supramolecular level, even if affecting morphogenesis in the long run, cannot be directly translated into supracellular structures: emergence of the latter is an essentially macroscopic event, having no microscopic "homunculi" beneath. This is why in this book our main attention was directed to mechanical stresses acting onto the supracellular level where the most important morphogenetic decisions are taken.

The actual and potential applications of morphomechanics are quite diverse. Several research groups expect that it should bring important results in medicine and biotechnology (general review: Fredberg et al. 2009; applications to cancer problem and metastatic growth: Coughlin and Fredberg 2013; Huang and Ingber 2007; Samuel and Olson 2011; Ulrich et al. 2009). In fact, the "medical morphomechanics" was at work well before this branch of science was formally outlined. Among the first examples one may recall effective curing of limb abnormalities by accurately dozed stretching (Ilizarov 1984). Remarkably, the surgeon used intuitively the rates and amounts of the post-stretch relaxation (that is, the active response of the organism, directed oppositely to the applied stress) as the criteria for the treatment success. The mechanical aspects of regenerative medicine today look very promising (Levine 2011).

Meanwhile, however important may be the present-day and future practical applications of the morphomechanical approach, the main authors' aim was to explore its possible contributions to the general theory of organic development. Remarkably same were the desires of the founders of this approach. For example, D'Arcy Thompson in his historic book opposed the tendency of traditional morphologists to describe "the differences between [organisms] … point by point, and

L.V. Beloussov, *Morphomechanics of Development*,
DOI 10.1007/978-3-319-13990-6

"character" by "character" to "a proof that a comprehensive law of growth" has pervaded the whole structure in its integrity, and that some more or less simple and recognizable system of forces has been at work" (Thompson 1942, 2000, p. 275). This is just what we defined as a law-centered, or nomothetic approach.

Let us review again the supporting arguments and, on the other hand, the limitations of this method.

As it was said in the Introduction, the law-centered approach was invented in natural sciences for apprehending reiterative successions of events which were proved not to be bound with each other by a chain of specific cause–effect relations. By using this approach we "derive" each next state of the observed system from a common law, rather than from any unique properties of the preceded state. However, by doing this we cannot avoid referring to certain "initial" and/or "border" conditions which we have to take as given. This is a strong memento showing that our world cannot be fully reduced to a law-obedient continuum: there will always be place for unique, non-repeatable events which we have to describe just as they are without trying to reduce them to any embracing law. Hence, the place for ideographic approach is always left. While the classical physics and mechanics can ignore ideography either completely or at least to a great extent, for biology, as for other disciplines with historical component this is impossible.

Unique non-repeatable events may play a role not only in initial/border conditions but also in the parameters introduced within the embracing laws. Being such, they contribute so much to the specificity of the system behavior that they are often regarded as the main causes, or controllers, or whatever you call them, of the entire process. It is necessary however not to forget that the parameters per se have no definite meaning outside the context of the law to which they belong.

Anyway, all of this enforces us to briefly discuss again the places for the laws and for the ideographic factors in embryonic development and how these components interact with each other.

The main arguments for introducing the law-centered approach in embryology are the same as in physical sciences: it is the repeatability of the developmental successions combined with numerous failures to represent them as strictly specific cause–effect chains. In addition, the existence of a rich molecular background of developmental processes creates new ambiguities: to our knowledge, so far as practically any molecular signal can be "read" in different manners, we are confronted with a grave problem of its proper *interpretation* by a developing organism. Accordingly, a desired law should not only embrace large enough space-temporal domains of development, but do it in so simple and nonspecific a manner that the problem of interpretation can be passed over or at least greatly restricted. Moreover, we wish to avoid as far as possible a vague notion of "information," used in many cases for hiding our ignorance.

We hope that the HR model takes a step in this direction. Indeed, it looks rather universal, its relaxatory branch follows completely the main physical laws (most adequately formulated by Le Chatelier principle) while the ascending (energy-consuming) branch is natural for systems with perpetual energy inflow. In addition, this model operates with nothing more than mechanical stresses—the values which

together with their immediate consequences (deformations) do not require (in contrast to any chemical factors) any additional "interpretation." Let us recall also that a specific feature of the HR model distinguishing it both from the classical versions of the morphogenetic fields and the positional information concepts is its temporal depth: it is the nearest "history" of mechanical stresses rather than any static values, which is suggested to determine the next step of development.

On the other hand, we could see that any HR reaction, for bringing any specific morphogenetic results, and even any results at all, should be properly parameterized. It is also obvious that most of the developmentally important parameters—the signaling pathways and the genetic machinery—are rooted in the molecular levels events. Such parameters should be quite specific. How can they be emerged and coupled with much more robust morphomechanical processes? Can the parameters be in some way derived from the morphogenetic or some other laws? In spite of our attitude to the law-centered approach we believe that in general the answer should be in the negative. Instead, it is plausible to suggest that: (a) the parameters have been coined in the course of evolution independently and at least in some cases prior to the morphogenetic events into which they became integrated later on; (b) such integration was a unique or at least very rare evolutionary event.

The first point can be illustrated by the discovery of the genes involved in formation of such typical Metazoan attributes as the cell–cell contacts and extracellular matrix, in a unicellular flagellate, *Monosiga brevicollis*, in which they cannot fulfill their routine functions (King et al. 2008). Along with this, a substantial argument for the evolutionary uniqueness of the coupling between molecular parameters and morphogenesis was presented in the above-mentioned work of Brunet et al. (2013) on mechano-dependence of the mesodermal genes expression. As mentioned above, a highly specific molecular machinery providing this coupling (phosphorylation of β-catenin by a precisely positioned tyrosine residue) turned out to be the same in two main animals' phyla (Proto- and Deuterostomia) diverged no later than 570 millions years ago: it is highly improbable that such a specific decision could be made twice. A uniqueness of such coupling and its independency from the gastrulation itself is highlighted by the existence of the involution-mediated gastrulation in several taxonomic groups (including some Sponges: Ereskovsky 2005) having no mesoderm at all.

Being unique, such molecular transformations belong formally to ideography and should be hence taken as given. A much greater weight of ideographic component in biology in comparison to physical sciences is associated with the trivial fact that any organism has a lot of evolutionary ancestors: accordingly, nature had plenty of time for coining and/or selecting a huge amount of parameters for each next step of development.

Anyway, such a dualistic view, splitting development to the permanently acting "laws" and uniquely introduced ideographic components should help us to formulate reasonable questions for exploration and adequate modes of answers. For example, the question "why a part of embryonic brain acquires a structure of an eye" should be at first answered in terms of morphomechanical laws, by outlining the main feedbacks and showing in what way they are coupled. As a next, more

difficult and refined step of investigation, it would be desirable to explore in what way each of the feedback loops should be parametrically modulated for providing the structural specificity. Only when/if this work is fulfilled will it be reasonable to search for the genes whose expression may ensure the required parameterization. Meanwhile, a ubiquitous believing that for "explaining" the development of a given rudiment it is enough to enumerate the genes that somehow affect it, is to our view a kind of self-delusion.

The uniqueness of setting up each next parameter during the course of evolution should not deflect us from appreciating their amazing adjustment to the law-determined course of morphogenesis. Conrad Waddington (1940) was probably the first to emphasize that the epigenesis (the non-genetic component of development) "canalyzes" the action of genes instead of being their mere toy. His successor, Brian Goodwin (1994) wrote: "Genes don't control: they cooperate in producing variations on generic themes," meaning by "generic themes" the law-determined motifs.

In this book context such approach is supported by the paradoxical at first glance situation: it turns out to be possible to reconstruct rather prolonged periods of development by using nothing more than a few simple HR-based feedbacks, without even mentioning any molecular level factors known to be indispensable for the real proceeding of the reconstructed events. The success of such reconstructions can be explained only if accepting that the molecular level factors are playing in tune with what is dictated by morphogenetic laws, and not the other way round.

If returning to our postman allegory (see Introduction) the situation will look as if instead of moving from one fixed address to another the letter carrier will stubbornly follow its own standard trajectory (dictated probably by the landscape—the Waddington's allegory of invariable laws), while the addressees are learning step-by-step this situation, putting the post-office boxes along his way.

So, contrary to the still dominating views we may conclude that there are macroscopic level events, which by obeying the nomothetic laws are driving forth along a regular way not only ontogenesis, but also the evolution. On the other hand, during their phylogenetic history the organisms show an amazing capacity to assimilate and memorize the molecular level events very much enriching their potencies and non-deviating at the same time from the law-determined pathway. As written by an evolutionary biologist sharing similar views: "Each step of morphogenesis will be obviously interpreted as activation of a gene competent to a structure which should be formed at the given moment and in the given place… and each step of evolution [should be regarded] as a recognition (or emergence) of a gene which is competent to a *new* structure never formed before" (Chaikovsky 2008; italics authorized).

Thus, by following the morphomechanical approach we came unexpectedly to some general problems which looked a priori to be quite alien from mechanics and are still far from being solved. Is this the advantage or the deficiency of the suggested approach? We believe that the first is true.

References

Brunet T et al (2013) Evolutionary conservation of early mesoderm specification by mechano-transduction in Bilateria. Nat Commun 4:2821. doi:10.1038/ncomms3821

Chaikovsky JV (2008) Active bound world. KMK, Moscow (in Russian)

Coughlin MF, Fredberg JJ (2013) Changes in cytoskeletal dynamics and nonlinear rheology with metastatic ability in cancer cell lines. Phys Biol 10:065001

Ereskovsky AV (2005) Comparative embryology of Sponges (Porifera). Saint-Petersburg University Press, Russian

Fredberg JJ (2003) Time scale and other invariants of integrative mechanical behavior in living cells. Phys Rev E 68:041914

Fredberg JJ et al (2009) Biomechanics: cell research and applications for the next decade. Ann Biomed Eng 37(5):847–859

Goodwin BC (1994) How the Leopard changed its spots. Weidenfeld & Nicolson, London

Huang S, Ingber DE (2007) A non-genetic basis for cancer progression and metastasis: self-organizing attractors in cell regulatory networks. Brest Dis 26:27–54

Ilizarov GA (1984) Stretching stress as a factor exciting and supporting the regeneration and growth of the bone's and soft tissues. In: Structure and biomechanics of the skeletal-muscular and heart-vessels systems of vertebrates. Ukraine Representative Conference, Kiev, pp 38–40

King N et al (2008) The genome of the choanoflagellate Monosiga brevicollis and the origin of metazoans. Nature 451:783–788

Levine M (2011) The wisdom of the body: future techniques and approaches to morphogenetic fields in regenerative medicine, developmental biology and cancer. Regenerative Med 6:667–673

Samuel MS, Olson MF (2011) Actomyosin-mediated cellular tension drives increased tissue stiffness and β-catenin activation to induce epidermal hyperplasia and tumor growth. Cancer Cell 19:776–791

Thompson D (1942, 2000) On growth and form. Cambridge University Press, Cambridge

Ulrich TA, de Juan Pardo EM, Kumar S (2009) The mechanical rigidity of the extracellular matrix regulates the structure, motility and proliferation of glioma cells. Cancer Res 69:4167–4174

Waddington CH (1940) Organizers and Genes. Cambridge University Press, Cambridge